The Influence of Electric Vehicle Availability on Vehicle-to-Grid Provision within a Microgrid.

Author: Donovan Aguilar Dominguez

PhD Thesis

A dissertation submitted for the degree of
Doctor of Philosophy

Department of Chemical & Biological Engineering
University of Sheffield
United Kingdom

July, 2023

Declaration

I hereby declare that except where specific reference is made to the work of others, the contents of this report are original and have not been submitted in whole or in part for consideration for any other degree or qualification in this, or any other university. This dissertation is my own work and contains nothing which is the outcome of work done in collaboration with others, except as specified in the text and Acknowledgements.

"If you tell the truth you don't have to remember anything."

- Mark Twain

Abstract

By 2030, the number of electric vehicles (EVs) on the road is expected to increase to 11 million in the UK, meaning that there will be an increase in electricity demand. A potential solution to help manage this increase in demand is to use a technology called vehicle-to-grid (V2G) which is essentially a connection post that allows a bidirectional flow of energy, which means that EVs can charge and discharge when connected. Through this technology, the electrical grid can make use of the energy already stored in the battery of the EV.

This research aimed to understand the effects of EV availability on V2G technology within a microgrid and evaluated the feasibility of providing ancillary services. A predictive model, primarily trained on internal combustion engine vehicle (ICEV) trips, used the UK's historical travel data to predict the location of EVs, achieving significant understanding of travel behaviour and EV availability. Split into two tasks—predicting start and end locations—this model utilised light gradient boosting machine (LightGBM) due to its superior performance. After fine-tuning, it yielded a weighted average F1 score of 0.900 and 0.902 for tasks 1 and 2, respectively. The model, when informed by new, real-world EV data, derived travel start and end locations, which was the fed into an optimisation model.

This optimisation model use a mixed integer linear programming (MILP) approach to schedule EV battery usage at the household level and study various case studies involving V2G technology. Simulations factored in different photovoltaic (PV) penetration rates, energy tariffs, and peer-to-peer (P2P) pricing mechanisms withing a microgrid. First, the technical and economic benefits of home batteries, smart charging (V1G), and Vehicle-to-home (V2H) systems in EVs were evaluated, with an emphasis on performance and electricity bill reduction. The second case studied the potential of EVs to provide short term operation reserve (STOR) services. The third case explored a payment mechanism to optimise the state of charge (SOC) for EVs under V1G and V2H technologies for a week and estimate the energy available for restoration services.

The study reveals that both stationary home batteries and EVs, when integrated

with solar power and dynamic tariffs, can effectively reduce electricity costs, despite the fluctuating availability of EVs. Notably, EVs, when combined with P2P energy sharing and V2H systems, offer comparable performance to stationary batteries, in addition to their transportation benefit. In terms of STOR provision, EVs meet the technical requirements, with their availability significantly influencing STOR provision. Factors like energy tariffs, solar power penetration rates, and P2P mechanisms have minimal effect on the STOR energy amount, but they do affect the overall microgrid performance. The study also highlights the need to maintain a 15% surplus of EVs within the microgrid for ensured resilience. Effective strategies to maintain a high SOC in EVs include higher payment rate systems, implementation of V1G and V2H strategies, and dynamic energy tariffs. The study, however, recommends limiting users to V1G to prioritise potential energy use for restoration services. Although EV availability affects the minimum SOC, it is not more significant than other factors such as EV penetration rates, energy tariffs, and P2P price mechanisms.

The findings imply that EV availability can reduce some of the benefits that stationary home battery have, such as surplus noon charging, while V2H might match home batteries in certain situations. EVs can offer STOR services as the fulfil most of the technical requirements, but the energy amount is dependant on available EVs during STOR events. EV availability had minimal effect on maintaining minimum SOC for a week that could potentially be used for restoration services, with energy tariffs and end-of-week incentives being more influential. Different PV penetration rates, energy tariffs, and P2P price mechanisms each have varied impacts on grid performance and V2G provision depending on the scenario.

Keywords: Electric Vehicles, Smart Charging, Vehicle-to-Home, Vehicle-to-Grid, Machine Learning, Peer-to-Peer, Solar Generation, Optimisation

Acknowledgements

I would like to thank my supervisor, Dr Alan Dunbar for his support and feedback throughout this process for his understanding during difficult times. Thanks also go to my second supervisor, Prof Solomon Brown for his support and advice during this time.

Thanks to the Sheffield ESA CDT students for sharing many fun times in and out of the office. I would also like to thank Sharon Brown for her support from the very beginning of the application process, without her none of this would have been possible.

Thank you to my family for supporting me in everything, especially my mother, father and brother, who were as excited as me when I started this journey. Most importantly, I would like to thank my partner Luz, who despite the ups and downs is always there. Thank you for all your support and understanding. Also thanks to my dog Mika who came all the way just to be with us. Special thanks to Eli and Bollis, who have supported us unconditionally.

I would also like to thank all the people I have met since I first arrived in Sheffield, especially those I can call friends. Richard and Emma, the Hollingworth family, Becky, Louise, Sasha, Kim, Minki, Mina, Rinako, Omer, Lorian, Gee and the amazing group of our very first friends: Stuart, Tom, Emily, Sam, Grace, Ashleigh, Ieuan and Kirsty. Thank you for making us feel at home.

I would like to express my sincere gratitude to my boss, Dr Jennine Jonczyk, for her unwavering support since day one in my new job, which greatly contributed to the completion of my thesis.

Thank you all, I could not have done this alone... and thank you Steel City.

Contents

List of Figures

List of Tables

List of source codes

Glossary

Abbreviation	Description	Page
AI	Artificial Intelligence	36
BM	Balancing Mechanism	20
CapEx	capital expenditure	128, 129, 206
CHP	combined heat and power	215
CNN-LSTM	Convolutional Neural Network - Long Short-term Memory	36
DER	Distributed Energy Resources	31, 32, 175
DNO	Distribution Network Operator	19, 33
DSR	Demand Side Response	20
E7	Economy Seven	xviii, xxi, xxiii, 83, 106, 109, 120, 123, 124, 129, 132, 162, 165, 166, 168, 174, 193, 195–197, 201, 220, 224, 225, 231
EA	EA Technology	xvi, xxviii, 68–73, 75

Abbreviation	Description	Page
EBI	Energy Balance Index	xviii, xx, xxii, xxiv, xxv, 99, 111, 114–116, 118, 146–148, 150–152, 184, 185, 187, 219–221, 224, 226, 231, 233
EFR	Enhanced Frequency Response	19
EV	Electric Vehicle	v, vi, xv–xvii, xix–xxv, xxviii, xxxi, 1–7, 9–32, 35–44, 46, 68, 70–77, 83–91, 95–98, 101–103, 105–118, 120, 123–132, 134–136, 138–140, 142–146, 149, 151, 158–165, 167–171, 173–184, 186–188, 193, 194, 196, 199–215, 219–225, 229–231
FFR	Firm Frequency Response	20
GPRS	general packet radio service	68
ICB	intelligent control box	68
ICE	Internal Combustion Engine	46
ICEV	Internal Combustion Engine Vehicle	v, 4, 5, 12, 44, 76, 203–205, 207

Abbreviation	Description	Page
K-NN	K-nearest Neighbors	38
LightGBM	Light Gradient Boosting Machine	v, xxxi, 52, 53, 62, 64–67, 76
LP	Linear Programming	100
LR	Logistic Regression	xxxi, 52, 53, 62–65
LSTM	Long Short Term Memory	37, 38
MILP	Mixed Integer Linear Programming	v, 5, 14, 27, 77, 85, 100, 101
MIQP	Mixed Integer Quadratic Programming	100
ML	Machine Learning	xvi, xxvii, xxxi, 6, 36, 37, 41, 43, 44, 49, 58–60, 62, 76
MMR	Mid-market Rate	35, 93, 95, 126, 127, 168, 200, 213
NGESO	National Grid Electricity System Operator	19, 29, 31
NTS	National Travel Survey	xv, xvi, xxvii, xxxi, 23, 30, 45–54, 71–73, 203, 204, 206, 207
OpEx	operating expenditure	128, 129, 206

Abbreviation	Description	Page
P2P	Peer-to-peer	v, vi, xvii–xxiii, xxv, 4–7, 32–36, 40, 41, 78, 85, 89–96, 98, 99, 102, 106, 107, 109, 111–118, 120, 121, 123, 125–129, 132, 141, 143–152, 154–156, 158, 162–165, 168, 169, 171, 173, 174, 178–189, 191, 193, 195, 196, 200–202, 205, 206, 209–214, 220, 224, 225, 229–232
PHEV	plug-in hybrid electric vehicle	33
PV	Photovoltaic	v, vi, xvi–xxv, 5, 6, 9, 10, 35, 78, 80, 81, 89, 101, 106, 107, 109, 110, 112–123, 125–129, 131, 132, 141, 143–160, 162–165, 168, 169, 171, 173, 174, 178, 180–196, 200–202, 205, 206, 210–214, 219–235
QP	Quadratic Programming	100

Abbreviation	Description	Page
RF	Random Forest	52, 53, 62, 64, 65
RR	Replacement Reserve	20
SDR	Supply And Demand Ratio	35
SEL	Super Stable Export Limit	20
SOC	State Of Charge	v, vi, 3–7, 23, 25, 27, 28, 30–32, 40, 86–88, 170, 171, 173–180, 183, 186, 188, 193, 196, 199–202, 208–213, 231, 232
SSR	Self-suffiency Ratio	xviii, xx, xxii, xxiii, 98, 99, 111, 114–119, 127, 128, 146–148, 150–153, 168, 171, 183–185, 187–190, 201, 202, 212, 224, 231
STOR	Short Term Operation Reserve	v, vi, xix–xxi, xxiv, xxv, xxviii, 3, 4, 6, 7, 20, 29–31, 39–41, 91, 131–140, 142–146, 149–151, 156, 158–164, 167–171, 207–209, 212, 224–226, 229, 230

Abbreviation	Description	Page
V1G	Smart Charging	v, vi, xv, 1, 4–7, 10–12, 14–17, 36, 38, 95–97, 102, 106, 108, 109, 114, 116–118, 120, 123, 125–129, 140, 178, 179, 184, 186–189, 193, 195, 196, 200, 202–207, 209–213, 231
V2G	Vehicle-to-grid	v, vi, xv, 2–6, 11–20, 22–32, 36–44, 46, 70, 72, 77, 78, 86, 90, 91, 95–98, 101, 102, 131, 132, 134, 140, 141, 162, 168, 174, 202–205, 210, 212, 214, 215, 224

Abbreviation	Description	Page
V2H	Vehicle-to-home	v, vi, 2, 4–7, 12, 35, 46, 70, 72, 85, 95–97, 102, 106, 108, 109, 114, 116–118, 120, 123, 125–129, 132, 134, 140, 162, 165, 168, 171, 174, 178–180, 184, 186–189, 193, 195, 196, 200–207, 209–213, 220, 231, 232

Nomenclature

Sets

$t(T)$	Set of time periods
$v(V)$	Set of households with electric vehicle

Constants

M	Sufficiently large positive number
η	Bidirectional charger efficiency
$\alpha_{v,t}^{avail,home}$	Vehicle availability at home for v at t
$\alpha_{v,t}^{avail,street}$	Vehicle availability at street for v at t
$P^{max,ch}$	Bidirectional maximum charge power (kW)
$P^{max,dis}$	Bidirectional maximum discharge power (kW)
$P^{max,street}$	Street maximum charge power (kW)
dt	Time step in hours
SOC	Battery total capacity (kWh)
SOC^{min}	Battery minimum state of charge
SOC^{max}	Battery maximum state of charge
SOC^{init}	Battery initial energy stored
SOC^{final}	Battery final energy stored
$E_{v,t}^{demand,vehicle}$	Energy required for driving for v at t (kWh)
$E_{v,t}^{demand,house}$	Household load demand for v at t (kWh)
$E_{v,t}^{solar}$	Solar generation for v at t (kWh)
$E_{t}^{delta,p2p}$	Energy imbalance at t (kWh)

$Pr_{v,t}^{buy,grid}$	Price for household power import from the grid for v at t (£/kWh)
$Pr_{v,t}^{buy,p2p}$	Price for household power import from peer-to-peer for v at t (£/kWh)
$Pr_{t}^{buy,street}$	Price for charging in a street charger at t (£/kWh)
$Pr_{t}^{sell,grid}$	Price for household power export from surplus solar generation at t (£/kWh)
$Pr_{v,t}^{sell,p2p}$	Price for household power export to peer-to-peer for v at t (£/kWh)
$Pr_{v,t}^{sell,v2g}$	Price for household power export to vehicle-to-grid for v at t (£/kWh)
$Pr_{v,t}^{mid,p2p}$	Price mean value used for peer-to-peer prices for v at t (£/kWh)
$Pr^{SOC,final}$	Price for the amount of state of charge at the end of the week (£/kWh)
ST_{t}^{event}	Short term operation reserve discharge event at t
$ST^{threshold,theory}$	Theoretical maximum energy from electric vehicle for short term operation reserve

Variables

$B_{v,t}^{ch}$	Binary variable for battery charge for v at t
$B_{v,t}^{dis}$	Binary variable for battery discharge for v at t
$B_{v,t}^{exp}$	Binary variable for energy export from the house for v at t
$E_{v,t}^{charge}$	Energy for battery charge when at home for v at t (kWh)
$E_{v,t}^{charge,street}$	Energy for battery charge from street charging for v at t (kWh)
$E_{v,t}^{discharge}$	Energy from battery discharge to satisfy household load for v at t (kWh)
$E_{v,t}^{discharge,v2g}$	Energy from battery discharge towards vehicle-to-grid for v at t (kWh)
$E_{v,t}^{solar,used}$	Energy from solar generation used to satisfy household load for v at t (kWh)
$E_{v,t}^{solar,export}$	Energy from solar generation exported to the grid for v at t (kWh)

$E_{v,t}^{solar,p2p}$	Energy from solar generation exported for peer-to-peer for v at t (kWh)
$E_{v,t}^{import}$	Energy imported from the grid for v at t (kWh)
$E_{v,t}^{import,p2p}$	Energy imported from peer-to-peer for v at t (kWh)
$E_{v,t}^{import,total}$	Total energy imported for household for v at t (kWh)
$E_{v,t}^{export,total}$	Total energy exported from a household for v at t (kWh)
$E_{v,t}^{net}$	Net energy flow for household for v at t (kWh)
$E_{v,t}^{SOC}$	Current state of charge of the battery for v at t (kWh)
C_{v}^{import}	Cost from energy imported from the grid for v (£)
$C_{v}^{import,street}$	Cost from energy imported from street charging for v (£)
$C_{v}^{import,p2p}$	Cost from energy imported from peer-to-peer for v (£)
$C_{v}^{export,solar}$	Cost from energy exported from surplus solar generation to the grid for v (£)
$C_{v}^{export,v2g}$	Cost from energy exported to vehicle-to-grid for v (£)
$C_{v}^{export,p2p}$	Cost from energy exported to peer-to-peer for v (£)
$C_{v}^{SOC,final}$	Cost for the amount of energy in the battery at the end of the week for v (£)
$ST_{t}^{threshold,max}$	Maximum energy than can be provided by all vehicles for short term operation reserve at t (kWh)
$ST^{percentage}$	Maximum percentage of energy that can be provided by all vehicles for short term operation reserve
$ST_{t}^{demand,aggregated}$	Aggregated energy provided by vehicles for short term operation reserve at t (kWh)
BS^{value}	Minimum state of charge that can be held for all vehicles during a week.

Chapter 1

Introduction

At the end of 2020, the UK announced the phase out of all new petrol and diesel automobiles and vans by 2030 [1], this was another step forward towards achieving the net zero goal by 2050 established in 2019 [2]. All this means that different industries need to start looking for alternatives to reduce greenhouse gas emissions. Considering that in the UK 33% of the green house emission were from the transport sector in 2018 [3], decarbonising the transport sector will represent a significant challenge.

The electrification of transport has been recognised as a viable option to overcome this challenge; however, since the number of electric vehicles (EVs) are expected to increase to 11 million by 2030, there will be an increase in electricity demand that will require significant investment to improve the electrical grid to cope with such peak demand [4]. Therefore, understanding the nature of this increase in demand is needed to maintain the security and quality of electricity supply in the future by finding solutions to this challenge.

A potential solution to reduce the impact of charging a large number of EVs at the same time in the future and help the penetration of renewable energy is the use of smart charging (V1G), which means that consumers will charge their EVs off peak times when electricity demand is low, helping the consumer benefit from a lower price on electricity, reducing the overall cost of charging and saving additional costs that otherwise will be necessary to improve the electrical grid to handle peak demand. This technology can also help integrate renewable energy by charging when there is surplus generation, such as wind and solar energy [5].

Although the integration of EVs comes with challenges, it can also offer new opportunities for consumers and the electrical grid. Considering that most vehicles are parked 95% of the time [6], EVs can be connected to the grid and support and provide energy already stored in the EVs' battery [7], connecting millions of EVs and coordinating their charging and discharging would minimise the costs of EV charging while allowing the grid to balance the integration of high levels of variable renewable energy sources [8]. To make this possible, EVs will have to be connected to a vehicle-to-grid (V2G) enabled charger, a system that provides a bidirectional flow of energy whenever EVs are connected to a V2G enabled charge station, which effectively turns EV into a mobile battery that can provide power back to the grid or directly to a house (Vehicle-to-home (V2H)) or building [9]. This means that EVs can be considered as another type of storage capable of supporting the electrical grid; however, using EVs to support the electrical grid must be treated completely differently from other energy storage systems, such as stationary batteries, due to the availability of EVs during the day, as the main purpose is to provide travel, which means that they will not be connected to the grid at all times. Therefore, driving behaviour, availability of EVs and location of V2G chargers can have a significant impact on the potential economic value of V2G.

The use of V2G can support the grid by providing different ancillary services to balance the grid. Figure 1.1 shows the value streams accessible for V2G.

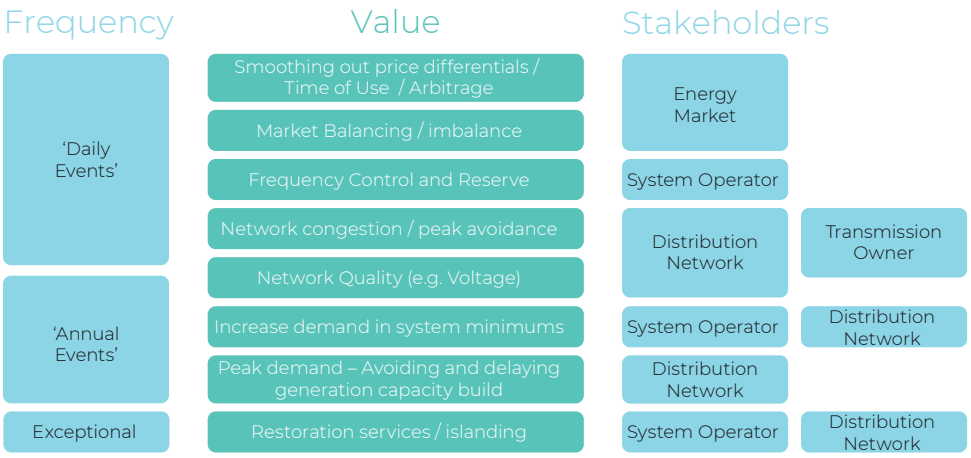

Figure 1.1: Identified services that are accessible by V2G [8].

Ancillary services such as demand side response, frequency response services,

reserve services, reactive power services, and system security services are among the services that V2G have the potential to provide to support the grid [10]. However, driving behaviour, availability of EVs and location of V2G chargers can have a significant impact on the potential economic value of V2G when providing ancillary services. In the existing literature, ancillary services, such as short term operation reserve (STOR) and restoration services, have received little attention. These services can be of significant interest to system operators and potentially generate a revenue stream for EV owners. The reasoning behind these two is that according to [8], STOR is one of the most promising ancillary services for V2G, however, a better understanding of the availability of EVs is required before looking at providing this service [11]. For restoration services, there has been an increase in interest from the National Grid to explore nontraditional technologies that could help in the provision of this service [12, 13], however, they found that there are two challenges before considering EVs, the uncertainty surrounding the EVs' availability and state of charge (SOC) during the day.

In the literature, only a handful of studies have considered the availability of EVs when studying V2G, while studies that have considered the availability of EVs as one of the key factors to evaluate the value of V2G, are limited by fixed availability times and recognised the importance of further studying the impact of availability of EVs in the delivery of ancillary services [8]. Considering that the provision of ancillary services through V2G is based on the availability of EVs and the number of those connected to the grid, it is important to study the impact of the availability of EVs to connect to the grid to measure the value of V2G in the UK.

Furthermore, the penetration of renewable technologies has continuously increased, particularly in small-scale solar generation, which can also affect the electrical grid, as some studies show that a high number of exports to the grid from local solar generation can harm the distribution network [14]. For instance, high levels of solar generation during periods of low demand can cause voltage rise in the distribution network, potentially leading to equipment damage and service interruptions [15], can cause reverse power flow which creates operational challenges [16] and can lead to overloading of distribution lines, causing accelerated ageing of infrastructure and increasing the risk of equipment failure [17]. A recent report stated that cur-

rently in the UK there are approximately one million of such installations and this number is expected to increase in the near future [18, 19]. Therefore, it is important to address the increasing number of solar generation, particularly at the community level, with alternative solutions such as the formation of local energy communities with energy traded between households, commonly known as peer-to-peer (P2P) trading, which could help address this by allowing members of the community to trade energy with their neighbours [20].

Taking into account the knowledge base explored in this chapter and the literature reviewed in chapter 2. The research planned in this work will focus on the following; to assess the impact of the availability of EVs when providing energy when connected at home through V2G and to evaluate the suitability to provide ancillary services according to a variety of criteria. The purpose of this research is to close the gap surrounding the value of V2G.

Therefore, this work aims to answer the following research questions:

- Can machine learning models be trained to predict the start and end locations of EVs trips for the purpose of optimising V2G services, including V1G and V2H? Can the travel patterns learned from mostly internal combustion engine vehicles (ICEVs) data be effectively used to predict the locations of EVs?

- What impact does the availability of EVs have on the effective implementation of V1G and V2H services services within a microgrid? How does the application of the predictive model to real-world EV data inform and optimise V1G and V2H services, and how does this technology compare to stationary batteries in terms of leveraging the predicted EV availability and location data?

- Are EVs capable of providing STOR services within a microgrid when connected at home? How does the availability of EVs impact the provision of these services and their ability to fulfil technical requirements as outlined by the National Grid in the UK?

- What strategies or mechanisms can be implemented to encourage EVs to consistently increase their SOC throughout the week? What are the impacts of V1G and V2H strategies on the minimum SOC maintained in EVs for potential

restoration services? How does the availability of EVs influence the capacity the minimum SOC that can be maintained over the course of a week?

- How do varying conditions, such as different photovoltaic (PV) penetration rates and energy tariffs, impact the implementation of V1G, V2H and V2G services within a microgrid throughout different weeks of the year? How does the P2P energy trading, and specifically the variation in P2P prices, impact the provision of V2G services within a microgrid?

The work performed in and the major contributions of this thesis are described as follows:

- An innovative predictive model that uses machine learning designed to predict the location and availability of EVs by using two separate classifiers. This model specifically predicts the start and end locations of electric vehicle EV trips, which significantly improves the understanding of EV availability and location for optimising V2G services.

- A two-dataset strategy harnessing real-world historical travel data, predominantly composed of ICEVs, for training and validation of the predictive model by capturing general travel patterns, and the applying this validated models to real-world EV data to study V2G services.

- An optimisation model using mixed integer linear programming (MILP) was developed, building upon a base model of stationary batteries to factor in the variable daily availability of EVs. This model, integrating V2G and P2P energy trading, streamlines diverse energy sources to minimise electricity costs for the participants within a microgrid. This optimisation model, significantly reduces solving times, enabling the exploration of various microgrid configurations. It demonstrates adaptability in managing multiple EVs using V2G technology and offers the potential to be modified for exploring the use of stationary batteries.

- The use of real-world datasets, including household electricity demand, PV generation, and electricity tariff prices for simulations.

- An evaluation of the technical and economic benefits of home batteries, V1G, and V2H systems in EVs, focusing on their performance and capacity to minimise consumer electricity costs. Furthermore, it analyses the efficacy of a grid-connected microgrid in reducing household electric bills, offering valuable insights into optimal energy management for homes equipped with a stationary battery or an EV with a bidirectional charger.

- An examination of the feasibility of EVs to provide STOR services when connected at home by considering the aggregated power of available EVs at home within a microgrid when energy is required for STOR. The feasibility is analysed based on the technical requirements and the six committed windows of the year outlined by the National Grid in the UK.

- A new payment mechanism designed to encourage EVs to increase the amount of SOC throughout the week. Furthermore, we compare the impacts of V1G and V2H strategies on the minimum SOC maintained in EVs for potential restoration services.

- An examination of the impact of microgrid operations under varying conditions on stationary batteries and V2G services. The impact is analysed across different PV penetration rates, energy tariffs, and P2P with two different price mechanisms, determined by the volume of energy traded within the microgrid.

The remainder of this work is structured in a sequential way starting with Chapter 2. This chapter provides a literature review on EVs and their role in providing V2G services. The aim here is to frame the context and purpose of this work, setting the stage for the subsequent discussions.

In Chapter 3, a machine learning (ML) solution is introduced, designed to predict the location and availability of EVs for V2G services. This predictive model is developed and tested on real-world historical travel data, serving as a foundation for subsequent real-world EV trip data predictions.

Chapter 4 presents an optimisation model that will be used for investigating various case studies involving V2G technology within a microgrid, including V1G and V2H application, and the provision of STOR services. It further introduces the

concept of P2P energy trading within a microgrid, describes the data that will be used for the simulations, and establishes the performance and solver metrics used in the analysis.

Chapter 5 evaluates the technical and economic benefits of home batteries, V1G, and V2H systems in EVs, with a particular focus on their performance and on minimising consumer electricity bills. This chapter also investigates the impact of EV availability on their capacity to provide V1G and V2H services, comparing these services with those of stationary batteries.

In Chapter 6, the feasibility of EVs in providing STOR services when connected at home is explored, assessing their potential to support the power grid based on the technical requirements to provide this service. The focus here is to understand the extent to which the availability of EVs affects their capacity to provide these STOR services.

Chapter 7 introduces a payment mechanism to maximise the SOC that EVs can maintain over a week under V1G and V2H technologies. This analysis provides insights into the potential of EVs and these technologies to support power restoration during outages.

The work concludes in Chapter 8, where the results of the research are discussed, evaluated and their limitations are acknowledged. Suggestions for future work in the field are also provided.

Chapter 2

Literature Review

This chapter focuses on putting the research within the framework of what has already been published in the scientific literature.

2.1 Background

In 2019, the UK became the world's first large economy to introduce laws requiring the reduction of greenhouse gas emissions to zero by 2050 [2]. According to 2018 data, the transportation industry accounted for 33% of UK greenhouse gas emissions [3]. As a result, decarbonisation of transport presents a significant challenge in achieving this goal; therefore, electrification of transport has been suggested as one of the most viable alternatives. Taking into account that, towards the end of 2020, the UK government announced a plan to restrict the sale of new petrol and diesel vehicles by 2030 and to promote the adoption of electric vehicles (EVs) throughout the country [21, 22]. However, with the electrification of transport, electricity demand is expected to increase in the future as the number of EV increases, with up to 11 million electric vehicles predicted to be registered in the UK by 2030 and 36 million by 2040 [23]. This is expected to require substantial investment to upgrade the electrical grid to accommodate the increased demand [24].

In the UK, the growth of integrated renewable generation at the community level, specifically small-scale solar photovoltaic (PV) systems, also impacts the electrical grid. With around one million installations already in place and an expected increase in the near future, these systems contribute to changes in the grid's performance. [18,

19]. Although the increase in PV solar generation will help in the decarbonisation of the electrical grid, this renewable source is a variable and non-dispatchable resource, and it is not guaranteed that the generation will correspond well with electrical demand [25]. Moreover, multiple households exporting solar energy at the same time represent a concern for distribution systems, possibly resulting in voltage violations and line overload [14].

These two technologies, PV solar generation and EVs, certainly come with challenges and opportunities, which will be discussed in the following sections.

2.2 Smart charging (V1G)

Smart charging (V1G) is a safe and practical method of charging an EV in periods when the demand for power is lower, during periods of low electricity prices or when there is a surplus of renewable energy in the grid. In other words, it is a strategy for managing EV charging in a smart way to avoid overloading or destabilising the grid [26, 5]. This method of charging is considered the best way to deal with the rapid increase in EVs, as this benefits both consumers by reducing charging costs and the electrical network by avoiding further investment to reinforce the network, where otherwise large investments would have to occur in the electrical grid in terms of operating conditions if smart charging is not implemented [27]. Therefore, smart charging has the potential to make the adoption of EVs a smooth transition towards decarbonisation of transport. Dallinger et al. [28] explored the fluctuating generation of electricity from renewable energy sources in California and Germany, and then analysed the potential benefits of connecting EVs to the grid to balance the generation of energy from renewable energy sources. While their study illustrates that EVs have the ability to charge during periods of surplus renewable generation via V1G, they assumed fixed availability times for the EVs throughout the day. This means that, despite showcasing the potential for EVs to boost the integration of renewable energy sources into the grid, their model works on the premise of predetermined charging periods.

Furthermore, studies of the impact on the distribution network when smart charging is not used have shown that voltage problems on the local grid during the

day, such an increase in demand at peak times, and recommending the use of smart charging to avoid causing problems to the network [29, 30]. Their study was predominantly focused on analysing the charging patterns of EVs during the evening, and only considered the winter season. This could potentially limit the scope of their research, as it does not account for variations in charging habits across different times of the day and seasons of the year. Mwasilu et al. [31] undertook a study of previous work and emphasised the significant economic investment that unregulated charging can cause in power system networks, citing findings that V1G can avoid up to 70% of the investment in power distribution systems. They concluded that further studies should be conducted to analyse the feasibility of using EVs more efficiently for both system operators and consumers. Schmalfuß et al. [32] found that a proper implementation of V1G requires having precise availability times and the minimum required range to cover the travel needs; however, they suggested that this might only be achieved by having this information provided directly by the EV owners. They also found that encouraging EV users to interact with the grid will most likely have an influence on their daily habits, which not all EV owners are willing to change.

Wang et al. [33] determined that price variations based on time of day can be advantageous for both the operator and the consumer due to the flexibility to charge when it is more convenient during the day. Will and Schuller [34] investigated user acceptance of V1G in Germany, finding that grid stability and improved integration of renewable energy sources were the mains drivers to include these technologies according to users. However, Tan et al. [35] raised concerns about the potential barrier to V1G and vehicle-to-grid (V2G) deployment due to insufficient charging infrastructure. Therefore, while user approval is important, the expansion of charging stations remains a critical factor to consider in the future growth of V1G and V2G systems.

Another potential advantage of using EV is the reduction of greenhouse gas emissions, as they have zero tailpipe emissions. However, due to EVs' need for electric energy, it is crucial that the energy generated comes from sources with lower environmental impact, such as renewable energies [36]. Furthermore, [37] conducted an analysis of the impact of greenhouse gas emissions from EVs and

compared it to greenhouse gas emissions among 70 different countries. They found that greenhouse gas emissions produced by EVs have less of a negative impact on the environment than internal combustion engine vehicle (ICEV) in the subcompact, compact, full-size luxury and SUV vehicle categories. As a result of the correlation between greenhouse gas emissions of EVs and the electricity generation mix of each country, they determined that countries with a large proportion of fossil fuels in their electricity generation mix, EVs were associated with more greenhouse emission emissions than ICEV.

2.3 Vehicle-to-grid (V2G)

V2G is a system that allows a bidirectional flow of energy whenever an electric vehicle is plugged into a V2G enabled charging station, effectively turning the EV into a mobile battery that can supply power back to the grid or directly to a household (Vehicle-to-home (V2H)) [9]. Figure 2.1 shows a diagram of the energy flow of V2G and how this technology operates. This type of interaction tends to occur inside what is called a smart grid, which includes the use of smart meters to monitor the energy flow. This method also has the benefits of V1G, including improved grid reliability, facilitating the integration of renewable energy sources, and providing ancillary services. V2G technology not only enables EVs to act as temporary energy storage but also contributes to the overall stability of the grid system. As the use of electric vehicles increases, the potential for V2G to support energy management at both the micro and macro levels is considerable, forming a robust solution to meet future energy demands.

Various studies have investigated the integration of EVs and how they can support the deployment of renewable energy in the grid. This has been done by demonstrating the benefits of using V2G and storing energy from renewable energy when excess generation is produced and then returning it to the grid when needed [39]. A 2016 report by the Institution of Mechanical Engineers [40] recognised the importance of integrating energy storage technologies into the grid in the UK so it can allow storing excess generation from renewable sources to return it at peak demand hours. This report highlighted the importance of promoting the adoption of new

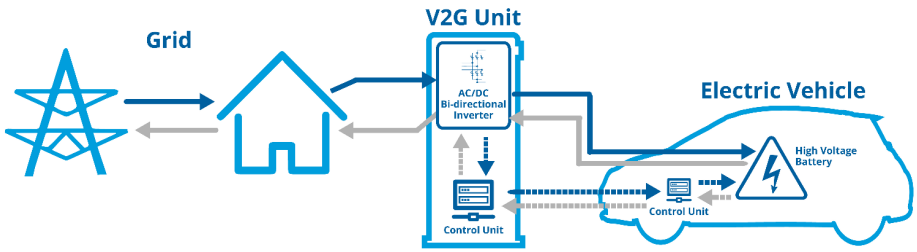

Figure 2.1: Diagram showing how V2G operates [38]. The blue line shows the flow of energy from the grid to the electric vehicle. The grey line shows the flow from the electric vehicle to the grid. The dashed lines represent the communication flow between the electric vehicle and the V2G charger.

technologies to support the grid, such as the use of energy storage technologies and the encouragement of the deployment of renewable energy sources. Mwasilu et al. [31] conducted a study of the relevant literature on the interaction of EVs with smart grids. The authors discussed the potential of EVs to support the penetration of renewable energy sources, concluding that surplus energy enables EVs owners to reduce their electricity bill and added that further studies should focus on understanding of the dynamic behaviour of the EVs is indispensable to better understand their integration in the electrical grid and the potential benefits of V2G. Moreover, the impact of EVs and V2G technologies has in the electrical grid was investigated by Gay et al. [41], particularly on developing small island states, and it was determined that the addition of V2G to the electrical grid can help to adopt renewable energy sources in isolated islands and maintain a steady electricity supply. They added that the use of fixed energy price tariffs or not implementing smart charging technologies can potentially slow down the integration and deployment of renewable energy sources.

Lund and Kempton [7] studied the impact of V2G on the Denmark energy system and how it can help integrate renewable energy sources. They found that using low-priced periods of the day and V2G can improve the electric power system by providing ancillary services such as voltage and frequency regulation. While the authors consider the availability of EVs, their approach appears quite conservative. They use predetermined fixed times of the day, divided into one-hour lots, to represent the available EVs. This may overlook the granularity required for a more

realistic assessment of EV availability. Additionally, they simplify the model by treating the entire EV fleet's batteries as one large unit, equivalent to the sum of all individual batteries. In reality, total battery capacity is not consistently accessible due to variations in vehicle usage and grid connection availability. This model also assumes EVs are fully charged when they disconnect to drive, which is not always the case. The model does not account for vehicles driving for more than an hour and the associated reduction in total charge. It also presumes all cars are grid-connected when not in use, which is impractical in some settings like workplaces or mass transit stations.

Thomas et al. [42] proposed a mixed integer linear programming (MILP) approach to simulate an energy management system for an office building to analyse the impact of providing energy to the building through V2G and the uncertainty of solar generation affects the energy management system and the sale of energy back to the grid. They reported that the addition of V2G to office buildings can increase efficiency and help integrate renewable energy sources, significantly reducing building energy consumption. The authors modelled a fleet of 30 EVs, mentioning that their behaviour mirrors work-related mobility patterns typically seen with conventional vehicles. Drawing upon the statistic that 82% of Belgium's population adheres to fixed working hours and shifts, they framed usual working hours as between 8 am and 6 pm. This model, however, may be overly simplistic for a comprehensive understanding of EV availability. While it is beneficial for creating a baseline scenario, the assumption of homogeneous mobility patterns does not necessarily reflect the complex, diverse nature of real-world EV usage. Variations in commuting distances, non-work-related vehicle use, and irregular travel patterns are all factors that could significantly affect the actual availability of EVs for grid services. This approach might oversimplify the model, potentially leading to an over- or underestimation of the actual availability of EVs for grid services.

Moreover, according to Cenex et al. [8], in the UK, the use of V1G to reduce demand peaks has been reported to have the potential to save up to £200 million in investment required to meet electricity demand from 2020 to 2030, with an additional £90 million per year in potential savings if V2G is used compared to not using either of these technologies. In general, the usage of V1G and V2G can help to reduce

congestion in distributed networks, where rewards mechanisms can be introduced for customer participation in said congestion reduction to increase the adoption of these technologies [43]. Figure 2.2 shows the potential impact of V2G on reducing the peak demand in future scenarios. This figure shows how V2G even further reduces peak demand when coupled with smart charging. V2G is expected to properly support the grid in locations where plug-in rates are high.

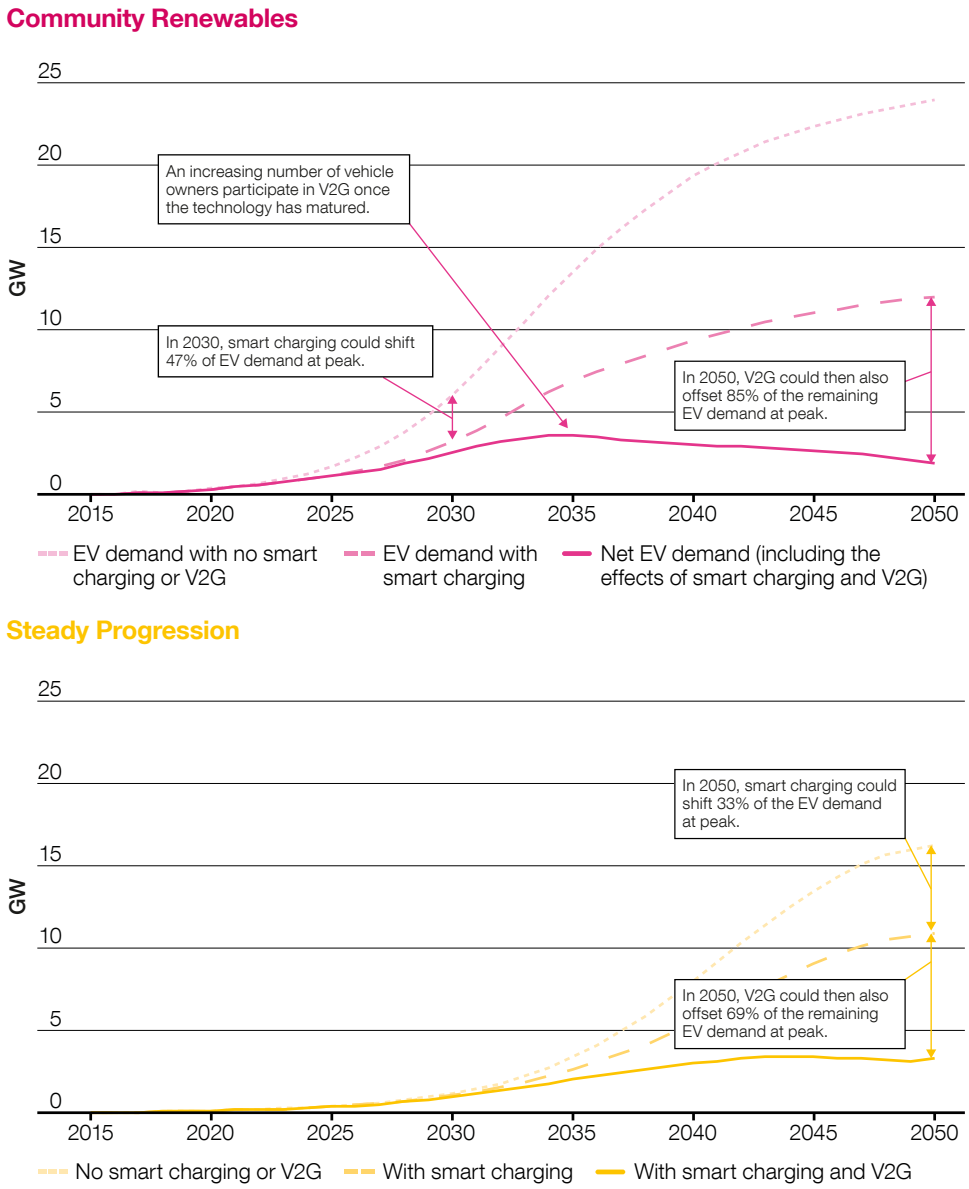

Figure 2.2: Assumptions on how much EV capacity may be available for V1G and V2G during times of peak demand [4].

Rodrigues et al. [44] examined the implementation of V2G to provide energy back to the grid using the energy already stored in the battery of EVs when idle whenever local demand exceeds local generation. They proposed combining V1G and V2G to store energy in the EVs for later used to ensure the proper operation of a microgrid. In this study, the authors also considered the availability of EVs crucial for estimating the available dispatchable power to adequately support microgrid operation. In their research, the authors focused primarily on the night hours when most EVs are typically available for charging. However, this approach might not fully account for the broader impacts of EV availability on grid stability and renewable integration. By only studying a few select night hours, they may have overlooked key aspects of EV utilisation during other periods of the day, potentially limiting the robustness of their findings.

Yilmaz and Krein [45] analysed different case studies conducted around the world, considering that V1G and discharging energy to the grid through V2G is the best option to increase the benefit and profit for both the grid operator and EV owners. In their review, they found that uncoordinated charging of EVs can potentially increase peak load issues, leading to problems such as increased power losses, reduced grid reliability, and increased costs. However, the use of V2G strategies, offer a potential solution, enhancing the use of renewable sources and reducing costs and emissions. Nevertheless, they concluded that the success of V2G strategies largely depends on the availability of EVs. Factors like vehicle usage patterns and charging infrastructure accessibility can significantly influence this availability. Therefore, understanding these patterns is crucial for maximising the potential of V2G strategies and mitigating challenges posed by uncoordinated charging operations.

Kiaee et al. [46] proposed an algorithm to make the most profit from charging and discharging EVs through V2G. This was achieved by charging the vehicle when the price of electricity is low and discharge energy to the grid when the price of electricity is high. Their results showed that by applying their proposed algorithm, a 13.6% charging cost reduction can be achieved when using V2G technologies. Here, the study acknowledges that EVs are not stationary and tend to move to different locations during the day. Particularly on weekdays, it assumes that EVs belonging

to working individuals follow a predictable driving pattern: commuting to work in the morning and returning home in the afternoon. This predictability potentially offers a consistent framework for estimating the availability of EVs for V2G services. However, the algorithm employed in this study allocates the same travel pattern to each EV for all simulation days but varies the start and duration time of their daily journey. The daily commute is modelled to occur at a random, but constant time between 7 am and 10 am, and the return journey between 4 pm and 6 pm. Despite these assumptions providing some degree of realism, they may still overlook the inherent variability in real-world EV availability, impacted by factors such as non-work-related vehicle use, such as travelling for leisure. Therefore, for a more accurate portrayal of EV availability and its consequential impact on providing V2G services, further research might need to consider these diverse aspects of EV usage.

While previous studies, such as Dubarry et al. [47], have demonstrated that V1G usage has a negligible impact on battery degradation, and the intelligent use of V2G can optimise battery conditions to minimise degradation [48], there are still concerns about the long-term effects of V2G on battery life. Although demand-side management has been shown to be beneficial for most Li-ion batteries on the market, and Uddin et al. [49] discussed various perspectives on battery degradation, it is important to consider that the viability of V2G may be affected by factors such as battery technology, usage patterns, and the efficiency of smart energy trading. Consequently, further research and advancements in battery technology and energy management systems are needed to ensure the long-term profitability and sustainability of V2G.

Loisel et al. [50] studied the penetration of EVs into Germany by 2030 and how the addition of V1G and V2G can affect the power system. They estimated the loads of EVs for the year 2030 based on the 2013 driving patterns. They concluded that incorporation of V1G will facilitate the penetration of renewable energy sources, but implementation of V2G resulted in almost negligible profit for users, advising that more incentives should be offered when participating in V2G to compensate for the high cost of EVs, which will increase EV adoption. Their study analysis of aggregated demand for electricity from potential EVs demonstrates varying driving patterns across seasons, days, and passenger car segments. Notably, over 70% of vehicles are not in use from 7:00 a.m. to 7:00 p.m., and above 90% are available

from 8:00 p.m. to 6:00 a.m., suggesting potential availability for V2G services. However, while these patterns provide a useful overview, the impact of variations in individual behaviour, non-work-related vehicle use and its impact on EV availability must also be considered for a comprehensive understanding of the potential of V2G services. Therefore, more understanding of EV availability that covers different travel patterns is necessary to fully understand the potential of V2G services.

Van der Kam and Van Sark [51] investigated solar energy generation and the usage of V2G to benefit from surplus solar energy generation. The authors concluded that the introduction of solar energy generation can benefit the grid by increasing self-consumption and reducing the demand peak when EVs are introduced. They also found that the self-consumption rate is decreased when EVs are away due to the availability of EV to provide or store energy while not connected; however, they did not consider the energy consumed by EV when travelling, which can also impact their final results. In this context, the EVs being utilised for car sharing might introduce potential downsides when considering their availability for V2G operations. Although the pseudorandom generation of trip patterns attempts to realistically represent vehicle use in a shared mobility context, it might also increase the inherent uncertainty in EV availability. Car sharing can result in unpredictable and sporadic usage patterns, making it challenging to reliably estimate when vehicles will be available for V2G operations. Furthermore, the energy consumption for driving is also a significant factor. As the EVs are consuming a certain amount of energy during their trips, there needs to be a balance between the energy used for mobility and the energy reserved for V2G services. Thus, extensive use of the vehicles might limit their potential to provide V2G services. The study states that the EVs require around 10 MWh annually for the trips, but it doesn't clarify how this energy requirement might impact their availability for V2G operations.

Mwasilu et al. [31] found that by absorbing the surplus energy production from wind or solar energy to later deliver power to the grid through V2G can potentially enable EVs to support the grid by providing different ancillary services. Tan et al. [35] reported that V2G has the potential to improve and support the electrical grid through different ancillary services with appropriate management systems and attractive incentive schemes, which will play an important role in the implementation

of V2G. In their report they mentioned that V2G technology in the power system have the potential to improve and support the electrical grid. With the implementation of appropriate management systems and attractive incentive schemes, V2G can provide a variety of ancillary services, achieving objectives such as peak load shaving, load levelling, voltage regulation, and profit maximisation, among others. Further, V2G technology can provide frequency regulation and even contribute to system recovery during blackouts, underscoring its potential in maintaining grid stability and resilience. However, the feasibility of these services highly depends on the availability of EVs to connect to the power grid. This availability aspect becomes a crucial consideration in the effective implementation of V2G strategies, emphasising the need for intelligent charging infrastructure and scheduling systems to maximise the number the amount of energy that of grid-connected EVs can provide for V2G services.

2.4 Ancillary Services

Ancillary services are a range of operations beyond energy generation and transmission that help to maintain the stability and security of the electrical grid [52]. In Great Britain, the National Grid Electricity System Operator (NGESO) is the entity that ensures that electricity is transported from different energy generators to distribution network operator (DNO) so that they can take the electricity from the grid to supply it to homes and businesses when they need it. NGESO is also in charge of system balance, ensuring that energy supply and demand are always balanced, guaranteeing the stability and security of the electrical grid. [53].

An overview of some of the ancillary services required to provide such grid balance is provided below.

- Demand Side Response (DSR): that consists of a smart use of energy from homes and businesses can turn up, turn down, or shift demand in real-time [54].

- Frequency Response Services: helps to maintain the frequency of the system at 50 hz with a range of $\pm 1\%$. This ancillary service includes enhanced frequency

response (EFR), firm frequency response (FFR) and mandatory response services [55].

- Reserve Services: that provides different sources of additional power in case of forecast electricity mismatch in supply and demand. This ancillary service includes balancing mechanism (BM) start up, demand turn up, fast reserve, replacement reserve (RR), short term operation reserve (STOR) and super stable export limit (SEL) [56].

- System Security Services: that, as the name suggests, provides different services that keep the security and quality of the electricity supply. This ancillary service includes intertrips, system operator to system operator, restoration services (formerly known as black start), transmission constraint management and maximum generation [57].

Several studies have examined how EVs can help balance electricity demand and supply by altering their charging levels to ensure correct operation of the grid. The majority of EVs, including plug-in hybrids, could provide valuable services to the grid due to the fast response of their batteries inside, which offer a rapid response time. A recent report by Statnett [58], a Norwegian state-owned enterprise, further supports this assertion. Published in 2018, the report discovered that EVs are even capable of providing FFR as their response time was found to be under 2 seconds. However, leveraging these capabilities to provide additional services via V2G will require the establishment of new market rules [8, 59]. Yilmaz and Krein [45] conducted an extensive review of different aspects of V2G, such as the possibility of providing ancillary services to support the grid. They concluded that the cost reduction benefit that V2G can offer compared to more traditional technologies can be significant enough to encourage the adoption of V2G to provide ancillary services and eventually replace traditional technologies.

2.4.1 Demand side management

As it is described by the National Grid ESO [54] “demand side response (DSR) is all about intelligent energy use. Through DSR services, businesses and consumers can increase, decrease or shift demand in real time”. DSR is one of the most important

tools that can help guarantee the security, sustainability and affordability of the grid by reducing the peaks in demand and filling in the troughs by taking advantage at times when there is excess in electricity generation, as well as at times when the electricity generated is cheaper and cleaner. In this context, EVs are capable of supporting the grid by charging and discharging when required.

A study by Octopus Energy [60] encouraged consumers to engage in a more efficient use of energy to avoid high demand peaks. They evaluated the use of a time-of-use energy tariff that presented participants with price variations throughout the day, with the goal of engaging customers with their energy use at home to analyse how particular users, including EV owners, modified their schedules to take advantage of the drop in energy prices. The trial involved allowing participants to check energy rates in advance for the next day using a mobile app, giving them the ability to plan their energy use for the following day, generally offering low energy pricing during off-peak periods and high energy prices during peak times. The study lasted 6 months and it was found that peak use was reduced by 28.19% and participants saved up to £229.00 during the test period, Participants who owned an EV were the ones who changed their habits of electricity consumption the most by charging their EV at off-peak times, which resulted in a 47% reduction in energy consumed during peak times, concluding that, with the appropriate incentives, a shift in demand is possible and reduce congestion on the grid. Guo and Chan [61] studied EV charging during a period of time. They proposed that the implementation of alternative pricing tariffs may potentially drive owners to charge at specific times of the day, as well as encourage the use of renewable energy sources during periods of excess generation. The authors found that demand side response is an important aspect that can help reduce demand peaks if incentives are offered to EV owners.

Wang et al. [33] conducted a study on how to achieve peak load reduction by scheduling EV charging behaviour, suggesting a price negotiation method that requires the consumer to participate in a bid system with the operator in which both parties compare and negotiate the pricing. This price variation is determined by various factors, such as the time of day and the amount of power generated by renewable energy sources. They concluded that their proposed approach can effec-

tively increase profits for operators, reduce costs for consumers, and balance the load on the system. Wolinetz et al. [62] studied the long-term influence of consumer behaviour on the value of vehicle-grid integration to supply backup electrical power, support load balancing and lower peak loads. They concluded that vehicle-grid integration impacts the wholesale electricity prices by reducing them to 0.7% by 2050 in the Canadian electricity market. Despite these findings, the study acknowledges several limitations. The model accounts for consumer choices affecting EV adoption and utility-controlled charging participation but does not extend this to decisions regarding home charging power or workplace charging access. The model also overlooks potential changes in consumer behaviour in response to time-of-use electricity pricing, as well as how participation in V2G could influence EV usage decisions. These considerations might, in fact, enhance the value of V2G. Furthermore, the study does not capture all potential benefits that utility-controlled charging could offer, such as second-to-second load balancing or deferral of distribution system upgrades, which occur at more granular levels. It is essential to consider these limitations when interpreting the study's results and applying them to demand-side management strategies within the broader context of V2G implementation.

Coignard et al. [63] studied the adoption of EVs and the implementation of V2G services have substantial implications for demand side management in the context of California's energy landscape. With the mandate for 1.3 GW of stationary energy storage by 2025 in California, the advent of V2G technology can offer an alternative by potentially providing up to 5.0 GW of storage. They found that this large-scale integration of EVs could enable more effective demand side management through controlled charging, smoothing out demand peaks, and improving grid stability. It can also support valley filling and ramping services, thus optimising the grid operations and enhancing the renewable energy integration. However, several challenges could hamper the effective utilisation of EVs and V2G services for demand side management. These include the lack of sufficient incentives for EV owners to participate in V2G, limited availability of EVs capable of delivering V2G services, and range anxiety, which might deter potential users. Therefore, the implementation of well-designed policies and incentives is crucial to mitigate these issues and promote widespread adoption of EVs and V2G services, thus maximising their potential in

demand side management and supporting a more resilient and sustainable grid.

Lee et al. [64] studied V2G to determine the impact of peak load shaving when different levels of EV penetration. They concluded that V2G can significantly lower the peak load demand by returning the energy stored in the battery to the grid. Schmalfuß et al. [32] studied the impact of the implementation of EVs to balance the supply and demand of the grid. They found in their analysis that the integration of EVs into the electrical grid can potentially prevent or greatly reduce these peak demands. Bishop et al. [65] concluded that peak-shaving and regulation services are two of the most profitable ancillary services that can be provided by V2G. In these three studies, particularly, Bishop et al. [65], employed a notably realistic method, utilising UK data from the national travel survey (NTS) to in their model. However, irrespective of the varied methodologies, there is a unanimous agreement across these studies regarding the necessity of enhancing incentives to motivate EV owners' participation in V2G services, such as peak demand management. Additionally, despite these insights, significant limitations persist. The unpredictable availability of EVs for V2G services, owing to diverse driving habits, presents a substantial challenge. Fluctuations in power demand also pose difficulties in maintaining an optimal state of charge (SOC) to cover EV owners' needs, potentially degrading the performance of EVs when providing V2G services. Moreover, while aggregators play an integral role in monitoring SOC and managing charging and discharging behaviours, efficient peak shaving remains an issue, there is a need for more advanced strategies and technologies to reliably provide control demand-side responses.

Wang and Wang [66] proposed an objective function to control V2G systems for peak shaving and valley filling. They concluded that V2G can be helpful for the grid when the number of connected EVs is large enough and that it could even replace traditional systems that provide such services. Additionally, they mention that offering a variable price of charge and discharge throughout the day can be an effective measure to incentive EVs to participate in balancing power demand. However, in their study they only focus in two diffident 1-hour time windows of the day where it is assumed that the majority of EVs will be available. This means that while the strategy of variable charge and discharge pricing shows potential for demand management, their approach regarding the availability of EVs for V2G

integration shows that further research is necessary to fully better understand the of EVsposes a significant limitation.

Aluisio et al. [67] presented a day-ahead operation for integrating EVs and V2G to reduce the operational daily cost of a microgrid by controlling the load demand. They concluded that the existence of an EV aggregator coupled with the microgrid can result in a lower total operational cost for the microgrid and reduced costs for EV owners. However, the authors assume fixed periods for the availability of EVs, which may not fully reflect the complexities and dynamic nature of real-world EV usage. This fixed-time assumption may therefore limit the full cost-saving potential of the proposed day-ahead operation. Bhandari et al. [68] suggested offering incentives for providing peak-shaving via V2G can prevent wind or solar curtailment and minimise the impact of the intermittency nature of renewable sources. The authors determined EVs' participation in V2G activities using a randomised generation process. They flagged whether or not an EV was willing to participate in V2G during a certain period. By relying on a random flagging system for determining EVs' availability, the researchers may not fully capture the intricacies of the actual decision-making process of EV owners when participating in V2G services.

Ioakimidis et al. [69] proposed an optimisation scheduling model of EVs to minimise the power consumption of a non-residential building using V2G. They approached EV scheduling by combining a linear programming model with real-world data on power use and parking lot occupancy. They discovered that when a large number of EVs are available to supply V2G, the building can expect a power decrease of up to 20%. However, the availability time used was a traditional 9 to 5 office hours without considering uncertainty in the availability of EVs supply V2G. Sha'aban et al. [70] proposed an optimisation model to coordinate the charging schedule of EVs to take advantage of the lowest energy price during the day, resulting in savings of up to 63% when using V2G. However, they did not take into account driving habits and used fixed availability times.

Jian et al. [71] proposed a stochastic EV scheduling scheme for V2G operation to optimise charging scheduling, concluding that optimal scheduling can reduce the variance of the total peak demand for load, enhancing the efficiency of power grid operation. López et al. [72] analysed V2G as a solution to network congestion issues

in microgrids with a high penetration of EVs. They concluded that V2G can help alleviate microgrid congestion by stopping charging or supplying energy back to the microgrid. Furthermore, these two studies proposed different strategies to manage the uncertainty of EVs availability for V2G services. The first study proposed a strategy based on event-triggered scheduling, which reacts to the connection and disconnection events of EVs to the grid. This system relies on acquiring data such as the trigger point time, SOC, and the expected departure time of the newly connected EV. The second one, simplifies the availability problem by presuming EVs are available at fixed times based on a typical workday. Although this approach may not capture the full variability of real-world usage, it provides a straightforward model for potential V2G operations. These two different approaches may face challenges with data accuracy and unexpected user behaviour in the case of the study by Jian et al. [71], while López et al. [72]'s fixed availability assumption might overlook the variability in real-world EV usage and individual driving patterns. Both approaches, therefore, may result in inaccuracies in predicting the true potential and efficiency of V2G services.

2.4.2 Frequency response

As the National Grid [55] defines it, "System frequency is a continuously changing variable that is determined and controlled by the second-by-second (real-time) balance between system demand and total generation. If demand is greater than generation, the frequency falls, while if generation is greater than demand, the frequency rises". Different studies have explored the feasibility and benefits of providing this ancillary service by making use of EVs via V2G.

Peng et al. [73] reviewed previous research to establish the feasibility and effectiveness of EVs participating in frequency regulation services. Due to the fast response of batteries, the authors believe that participation in frequency regulation services is one of the V2G uses with the most potential. They found economic advantages for both the electrical grid and EV owners, such as reduced peak load, minimising the impact of renewable energy intermittency and lowering the total cost of an EVs. Despite the potential lower cost of owning an EV, they determined that the incentive should be more attractive for EV owners to participate in the frequency

service market and promote the adoption of this technology. The authors concluded that the price of charging and discharging and the availability of EVs to estimate the capacity available to provide frequency control services are critical aspects that require more investigation.

Martinenas et al. [74] examined the deployment of a system capable of providing frequency adjustment through V2G according to Danish technical conditions. After conducting their tests, they found that due to the quick response of EVs to any deviation in frequency observed, EVs are a strong fit to provide this ancillary service. In this study, the authors opted to bypass the availability factor of EVs altogether, concentrating instead on establishing their capability for frequency response through V2G. By conducting tests over different time windows, these studies aimed to determine the periods when EVs could optimally deliver this service, thereby contributing to the broader understanding of EVs' potential in grid stability and response.

Ota et al. [75] proposed a control scheme for V2G to provide frequency regulation services. Their control scheme managed to respond to the frequency deviations detected at the plug-in terminal. In this case, the total settling time of the system, including time lags caused by frequency detection, communication, and the response of the power conditioner, was within one second., demonstrating that V2G can provide frequency regulation and improve microgrid operation. However, the impact of availability was not taken into account in this study. Lund and Kempton [7] studied the integration of renewable energy and V2G to frequency regulation. Due to the fast response of the batteries inside EVs, V2G has the potential to replace traditional power plants that offer frequency control. They use predetermined fixed times of the day, divided into one-hour lots, to represent the available EVs.

Tomić and Kempton [76] analysed the economic potential of V2G. They concentrated on the frequency response market, as they believed to have the highest market value for V2G. They compared the net profits of four different energy regulating market locations across the United States to estimate the economic potential of V2G by analysing the net earnings of two separate utility fleets. They concluded that while V2G economic benefits are possible, the value of local ancillary services, infrastructure, and total EVs capacity are critical variables to make V2G more ap-

pealing. It is worth noting that the authors assumed that EVs are parked for the majority of the day, following a conservative daily pattern. This assumption could potentially oversimplify the dynamic nature of real-world EV usage, failing to account for the variability in individual driving and parking habits. Furthermore, the researchers highlighted a key barrier in their study, the absence of vehicle aggregators to manage multiple fleets and individual vehicles. This constraint could limit the practical implementation and scalability of their proposed models and strategies for integrating EVs into power grid management.

DeForest et al. [77] used a MILP model to optimise EV charging schedules and maximise profits from frequency regulation services via V2G. They used varying hourly energy rates and set a penalty for low SOC levels to encourage maintaining sufficient charge for frequency regulation. However, they found that this penalty had little effect on the results. They tested the model using different EV use patterns, generated randomly to reflect varied input parameters and based on observations from a specific site in Los Angeles, US. Their model was sensitive to changes in energy rates, which could be a problem given the unpredictable nature of energy prices. Also, using data from one location might not fully represent the varied usage patterns of EVs across different places and groups of people.

Lam et al. [78] introduced a V2G smart charging method that could offer regulatory services to the grid. They accounted for EVs's availability throughout the day, with the premise that EVs could engage in V2G based on the owner's travel requirements. They suggested that assessing the capacity of available EVs connected via V2G could support the design of business models to enhance V2G adoption. They modeled EV arrivals in the system as a random Poisson process, illustrated through a parking structure scenario where EVs arrived and departed independently. However, their research could only estimate the collective contribution from the EVs, which operated autonomously. This points towards a need for strategies that can efficiently manage EV integration into power systems considering this autonomy. Brandt et al. [79] explored the economic aspects of V2G integration by constructing a business model for EVs to aid in frequency regulation in parking garages in Germany. They factored in the availability of EVs, but utilized fixed times for all vehicles. Their analysis led them to conclude that due to the substantial investment

required for setting up the necessary infrastructure, the potential revenues and profits for the aggregator in the 2016 German market were limited. Similarly, profit expectations for EV owners were also modest. They argued that it would be more economical to charge EVs immediately upon entering the parking garage, rather than adjusting the charging profile to offer auxiliary services.

Uddin et al. [80] studied the possibility of prolonging the battery's life by offering V2G ancillary services such as frequency regulation and load balancing. They concluded that EVs that provide V2G auxiliary services have a longer battery life than EVs that do not participate in V2G. However, they considered that the availability was fixed to a traditional office time. Wang et al. [81] compared the battery degradation of an EV battery pack between driving only and driving and offering various V2G ancillary services, demonstrating that battery degradation is not significant if V2G ancillary services are offered intermittently, with periods of time that accumulate no more than 2 hours per day, which the authors considered a more realistic scenario for offering services such as peak load reduction and frequency control.

In their research, Liu et al. [82] stressed the importance of maintaining sufficient SOC in EVs for travel needs, particularly when these vehicles participate in grid frequency regulation services. They observed that the availability of EVs significantly influences the capacity that can be offered for such services. However, their assumption of EV users typically operating within a 8:00 to 17:00 timeframe could limit the practicality of their findings due to variability in users' schedules. Sarabi et al. [83], on the other hand, aimed to model the uncertainty of EV availability by considering daily driving behaviours. They identified frequency regulation as the most competitive ancillary service that V2G could provide in France and asserted that offering these services in workplaces is more reliable due to less variability in EV availability, as opposed to when EVs are connected at home. However, this approach also has limitations. Sarabi et al. [83] modelled EV availability using stochastic variables that reflect a Gaussian distribution relating to home and office scenarios. This may not fully capture real-world variations as it assumes consistent daily driving behaviour. Both studies underscore the need to consider the dynamic nature of EV usage and availability for an accurate assessment of V2G's potential.

Meng et al. [84] proposed a strategy to effectively use EVs for frequency response

and help integrate wind power into the electrical grid in Great Britain. They investigated the driving habits of EV drivers and their effect on the frequency response capacity, indicating that the frequency response capacity is affected by the availability of EVs. However, the EVs' availability times were assumed during fixed times of the day. They found that by providing frequency regulation, EVs can achieve a considerable reduction in frequency instability due to wind power generation intermittency and potentially reduce the operating expenses of traditional power plants. Finally, they added that the implementation of travelling behaviour and the availability of EVs need to be studied in more depth.

2.4.3 Reserve Services

The NGESO [56] defines reserve services as an extra power in the form of increased generation or demand reduction that enables the National Grid to compensate in the case of a mismatch in the forecasted electricity demand in the transmission system.

Previous studies have explored V2G that can support the delivery of this type of ancillary service, such as Donadee and Ilić [85] that studied the stochastic scheduling of EVs participating in the energy and reserve markets. They concluded that compared to fixed availability times, the unpredictability of EV availability reduces profits by up to 24%. Gough et al. [86] conducted an economic feasibility study of V2G as a EV-based energy storage system. They simulated three distinct V2G scenarios: direct power supply to a building, participation in the STOR ancillary service market, and trading in the wholesale energy market. The availability of EVs for these scenarios was assessed through a Monte Carlo approach, estimating the vehicles' arrival and departure times. The study also highlighted the substantial impact of battery degradation costs on V2G services. They concluded that engaging in these markets could potentially yield profits of approximately £8400 over a decade. However, the study's limitations emerge in the context of STOR services. The authors exclusively considered service provision when EVs are connected to a commercial building - in this case, a museum. This strategy, while simplifying the aggregation of power for STOR, is dependent on EVs being parked during the building's operating hours. This may not align with the with the different seasonal requirements of the NGESO, where participants must be ready to provide energy

during these specific committed windows. Furthermore, the study's consideration of only three different driving profiles regarding travel distance may not accurately represent a more diverse group of participants with differing travel needs and behaviours.

Bishop et al. [87] studied the effect of V2G on battery degradation when providing ancillary services to the grid. They found that providing energy services could lead to EV battery packs being replaced annually when supplying firm fast reserve, recommending limiting the amount of time that EVs participate to a couple of hours per week to minimise the depth of discharge when ancillary services are provided. Bishop et al. [65] conducted a study to determine the cost related to the degradation of the battery of EVs when providing V2G ancillary services. After studying a fleet of EVs providing fast reserves, they concluded that it would be quite difficult to deliver this service due to the number of EVs required and the number of EVs registered in the UK by 2015. Moreover, this suggests that energy operators would need to pay up to £105 to EV owners to compensate for battery degradation. However, both studies make assumptions about EVs availability and travel patterns that could potentially limit their conclusions' applicability. They split trips into morning and afternoon segments but assumed that trip duration and distance would be the same within these time frames. Although real-world data from the NTS informed these assumptions, this simplification could impact their results. They might not adequately account for variations in daily travel patterns, potentially affecting their estimates of battery degradation and the feasibility of providing ancillary services. More robust models might need to consider the heterogeneous nature of EVs usage and better assess the provision of V2G.

Morgan et al. [11] studied the various driving behaviours and their impact on the availability of vehicles to provide STOR services, particularly in the amount of energy required to provide this service. They highlighted the importance of acknowledging the main purpose of an EV and guaranteeing enough SOC that will be used for travel, as well as the importance of studying the effect of weekdays and weekends, holidays and seasonal differences on driving behaviour. They believed that V2G was best suited for STOR services due to the low frequency with which this service is required, typically around three times a week, potentially minimising

battery degradation by eliminating continuous cycling. In their study, the authors concluded that during winter in the UK, none of the three availability profiles studied by the authors matches the times of day when STOR services are required, such as the peak demand times in the morning and evening, emphasising the importance of understanding the availability of the EVs, which will play a crucial role given the annual increase in the number of EVs registered in the UK.

Predicting the availability of V2G for STOR with a large population of EVs is challenging. It depends on various factors including the number of EVs connected to the grid, their battery charge status, and the drivers' schedules and preferences. While some studies have created models to estimate this, exact predictions remain uncertain. More research is needed to improve our understanding and prediction of this availability and how could this impact the provision of STOR.

2.4.4 System Security Services

The NGESO employs a diverse range of strategies and services to ensure the security and quality of the power supply within the UK's transmission system [88]. A recent report highlights how NGESO is actively seeking ways to leverage renewable generation and distributed energy resources (DER) as potential facilitators of power system restoration. This comes in response to the decommissioning of traditional restoration service providers, predominantly large, synchronous power stations, due to significant changes in the energy landscape over the past decade [12]. This comprehensive report looks into the potential of several nontraditional technologies to provide this type of ancillary service, including EVs. Crucially, one of the most considerable challenges identified in qualifying EVs as viable candidates for participating in the provision of restoration services is their availability. The unpredictability surrounding the availability of SOC, along with knowing their SOC at any given time throughout the day, are some of the main challenges to overcome.

This report highlights that having enough available resources is critical for the successful use of EVs and other DERs for restoration or 'black start' services. As it is expected that by 2050, nearly 80% of UK households will smart charge their EVs, with almost 45% providing Vehicle-to-Grid (V2G) services [89], these technologies could greatly change the energy sector, but their real-world use greatly depends on

solving this big issue of availability.

Despite these challenges, there have been some explorations of using EVs in restoration services, as highlighted in the report. For instance, one study investigated the potential of a bi-directional EV charger for emergency power supply during restoration procedures [90]. Another proposed an intelligent integrated station for EVs that could provide higher start-up rates, better efficiency, and a more secure and economical restoration process [91]. However, neither of these studies specifically addressed the crucial aspect of EV availability and how it could impact the successful implementation of such systems. Apart from these studies, it's worth noting that there is a lack of extensive literature surrounding the use of V2G technology for providing restoration services.

As such, future research must give top priority to devising robust strategies and innovative solutions to overcome the availability challenge. For example, developing advanced forecasting models to predict EV availability with greater precision based on usage patterns could be a game-changing approach. Additionally, establishing incentive schemes that encourage EV owners to maintain a minimum SOC, thereby ensuring their availability for restoration services, is another promising avenue for exploration. While these technologies hold significant potential to transform the energy sector, their practical application is largely dependent on the resolution of key challenges, such as the aforementioned issue of availability and SOC for EVs.

Further, comprehensive studies on incorporating EVs and DERs within the current power system to provide restoration services are crucial. These studies should focus mainly on understanding the potential impacts of the availability of EVs on the power system. In this context, the importance of providing incentives to EV owners becomes evident, as it can significantly influence the availability of these vehicles for restoration services.

2.5 Peer-to-peer (P2P) energy trading

Peer-to-peer (P2P) energy trading describes flexible energy transactions in which any surplus energy from small-scale DER is traded between local customers [92]. In practice, P2P energy trading works by using advanced metering infrastructure

(smart meters), digital platforms, and automated systems to monitor energy generation and consumption in real time. Participants with excess energy (from a solar panel or battery storage, for example) can sell that energy directly to another participant who needs it. Pricing mechanisms can be designed to incentivize this kind of energy sharing, making it more economically attractive to trade energy locally rather than buying from or selling back to the grid. These systems (like solar panels or energy storage) can be used to supply power for P2P trading. Even with independent connections to the DNO, energy can be traded behind-the-meter within the microgrid, as long as the necessary metering and management systems are in place [93, 94]. In recent years, interest in participating P2P has increased as they represent an alternative way to use surplus energy and allow consumers to choose who they buy power from and to whom they sell it to and increase the use and implementation of distributed renewable energy. This energy trading can also help on the decarbonisation of the energy sector; however, the adoption of this type of energy trading business model, selling and buying energy must be attractive to both prosumers (who produce as well as consume) and consumers [20, 95].

Different works have explored the integration of P2P energy trading by studying pricing mechanisms that aim to encourage participants in a microgrid to share energy with their neighbours. Long et al. [96] proposed a game theory to simulate P2P energy exchange by using an energy exchange platform. They concluded that P2P energy trading has the potential to improve the local balance of energy generation and consumption within a microgrid. However, their simulation was limited to only one energy tariff to buy energy from the grid, which might not sufficiently capture the complexities of diverse electricity demand behaviours in larger populations with participants with a diverse type of energy tariffs. With energy prices calculated based on this single tariff's loads and solar generation, their model may overlook certain dynamics present in a more varied user base. Vangulick et al. [97] proposed a localised P2P electricity trading model for local buying and selling of electricity among plug-in hybrid electric vehicles (PHEVs) in microgrid. They explored the idea of using a blockchain approach set P2P prices. They concluded that their approach can achieve social welfare maximisation while protecting the privacy of the participants in the microgrid. However, they authors recognised that this approach

needs more testing and validation as some of the characteristics that they mentioned in their system are not compatible with the main existing blockchain technologies.

Morstyn and McCulloch [98] proposed a P2P energy market platform based on multiclass energy management that coordinates the trade between subscribed prosumers and the wholesale electricity market. They concluded that this strategy allows prosumers to change their scheduled power flows according to the wholesale energy price, reducing the expenses associated with network losses. However, their method differentiates trading prices across prosumer classes, which may not always be beneficial for all users. This can potentially discourage participation in P2P trading, indicating a need for a more balanced trading mechanism that is consistently profitable for all participants. The current approach may limit the broader adoption of P2P energy trading due to these profitability concerns.

Guo et al. [99] introduced an iterative settled market pricing mechanism in which the feedback of each round of bidding is used by the participants to update their new bids, and the market is settled if and when it converges, otherwise requiring an exit mechanism of some kind. However, the market pricing mechanism they introduced can potentially result in the market agent setting bids that may not be favourable to the participants. This could discourage their continued participation in P2P energy sharing.

Wang et al. [100] proposed a P2P multi-energy market mechanism. In this study, participants have the opportunity to join one of two coalitions based on their potential benefits. The energy markets are cleared separately per coalition and per energy provider and hence, multi-energy markets are modelled. They concluded that compared to scenarios where there is no P2P trading, the proposed mechanism benefits most peers, especially small ones. An et al. [101] proposed a pricing mechanism that calculates P2P prices based on the prosumers and consumer market participation. They concluded that this pricing mechanism can match the benefits for both prosumers and consumers and encourages trading energy with their peers within the microgrid.

Long et al. [92] proposed an auction-based pricing that aimed to emulate traditional energy markets to set P2P prices within a microgrid based on the total energy demand and generation. This resulted in reduced energy costs by increasing

self-consumption within the microgrid. Liu et al. [102] designed a dynamic internal pricing mode based on the supply and demand ratio (SDR) of the shared local PV generation. They considered the economic costs and willingness of users to participate in the trading of energy with their peers, as this would involve sharing data regarding their demand and generation. Their approach resulted in cost savings for prosumers and improved sharing of surplus PV energy within the microgrid.

Tushar et al. [103] proposed a game-theoretic approach in which P2P trading prices are set through the use of mid-market rate (MMR). This approach consists in offering prices depending on the supply and demand of the microgrid, where having oversupply resulted in prices close to the export price and having undersupply results in prices equal to the average of the buying from the grid and export prices to the grid. This is a similar approach to what Long et al. [96] did in their research, but with the introduction of stationary batteries among participants which provides a better perspective of how energy storage can be used to boos the potential of P2P. Englberger et al. [104] proposed a simple pricing mechanism based on offering fixed P2P prices based on the average of the buy price from the grid and the export to the grid. The authors suggested that implementing this simple pricing mechanism significantly reduces computational times and offers a fairer price for energy sellers and energy buyers. They also consider the use of stationary batteries and EVs as part of their model. However, it is worth noting that the authors' approach offered a simple P2P pricing mechanism centred on the German energy market. To ensure broader applicability, future research should aim to extend their model, offering the potential for its implementation in various energy markets without complications.

Hutty et al. [105] used a pricing calculation mechanism based on SDR which is an iterative bidding process offering buy and sell prices for each bidding round. They also considered different penetration rates of EV and PV to model the impact of having P2P to increase the adoption of these technologies. They concluded that the combination of V2H and P2P brings more benefits than having each technology individually, also savings in the electricity cost can exceed £200 in some situations. It is worth noting that the authors incorporated EV energy load optimisation in their pricing calculation for P2P, leading to variable prices depending on the optimised energy load. However, their approach rounds trip durations to 30-minute slots. This

may not adequately represent the granularity of diverse travel patterns with higher time resolution. This lack of granularity could affect the calculation of P2P prices, as microgrid management in real-world scenarios often requires consideration of shorter term fluctuations.

2.6 Machine learning approaches

Machine learning (ML) is a sub field of artificial intelligence (AI) and computer science that focuses on the use of data and algorithms to emulate how humans learn while gradually enhancing its accuracy [106]. It is worth noting that deep learning is actually a sub field of machine learning, and neural networks are a sub field of deep learning that differ from each other on how the algorithm learns from the data.

Reports suggests that utilising ML to understand driving patterns can be instrumental in optimising charging behaviours of electric vehicles. This predictive ability not only ensures that vehicles always have sufficient power for regular usage but also accommodate unforeseen travel needs. This optimisation not only supports the seamless integration of vehicles into the V2G system but also increases the system's reliability and consumer trust [107].

In general, different studies have explored the use of ML, EVs, V1G and V2G using different techniques and objectives. Shipman et al. [108] used a convolutional neural network - long short-term memory (CNN-LSTM) neural network and real-world data collected from a fleet of vehicles at the University of Nottingham to predict the aggregate available capacity for the next 24-hour period. They showed that their approach was capable of adapting to provide an accurate prediction of the amount of energy available for V2G service using historical data, highlighting the importance of availability of EVs in the delivery of V2G. Shipman et al. [109] studied machine learning algorithms to predict the potential times when an EV will connect and be ready for V2G by using travel data collected from a fleet of EVs. They found that, according to their data used for model training, using automated machine learning libraries achieved the best performance with an accuracy greater than 85%. While these studies provided valuable insight into how machine learning can aid in predicting near-term aggregate capacity forecasts for a fleet, its primary

focus was a commercial fleet of EVs used in a university setting. In both studies, their model may not directly apply to domestic usage due to differing driving patterns. Private owners may exhibit more unpredictable driving behaviours compared to a commercial fleet, potentially limiting the study's applicability in a domestic context. Furthermore, their use of 30-minute time steps might not capture detailed travel information as real-life management requires attention to shorter-term fluctuations.

Nogay [110] developed a long short term memory (LSTM) to predict the aggregated available capacity of a small fleet of 7 electric vehicles using historical data collected from 72 real drivers. They concluded that knowing the availability of EVs is critical when considering participation in ancillary service markets using V2G. While their model provides valuable insights for generating accurate near-term aggregated available capacity forecasts for small fleets, and provided valuable knowledge in market activity and V2G service export decisions, it is based only on a simulation of seven vehicles travelling for ten days. The real dataset used a one-second sampling time, whereas a 30-minute timestep was used in the simulation. This could result in potential downsides like the omission of driving variations throughout the year, and the loss of detailed travel data due to rounding drives into 30-minute timesteps.

Scott et al. [111] proposed a ML algorithm to predict the energy consumption and energy costs of a building and then reduce them using V2G to reduce carbon emissions from the building. They found that their approach results in energy savings between 35% and 65%. Although they successfully modelled a full year of usage, inconsistencies in the data led to substantial errors in some months. This situation emphasises the importance of data quality in modelling and when developing machine learning models. Frendo et al. [112] used historical data to train a regression model to address uncertain EV availability by predicting their departure times. They found that their proposed learning model resulted in accurate predictions of the availability of EVs. Jones et al. [113] developed a regression model aimed at reducing charging time and extending battery life by predicting charging behaviours affecting battery performance. However, their study mainly focused on predicting charge and discharge behaviour, without exploring applications of storage systems such as stationary batteries or EVs. This could be seen as a limitation, as it may miss potential optimisations and benefits from these systems.

Chung et al. [114] developed an ensemble predictive model using various machine learning algorithms to predict the charging behaviour of a fleet using historical data from real world EV travel information collected in the UK in combination with data from charging stations at UCLA University. The prediction results were then applied to an optimal EV charging scheduling algorithm to minimise the EV charging cost while providing energy to a building. They concluded that charging costs can reduce peak load by up to 27% and 4% costs compared to only using V1G. However, the limitation of this study is its lack of consideration for V2G technology, potentially missing out on the benefits and implications associated with bidirectional energy flow. Additionally, rounding travel data to 30-minute intervals may have its downsides. It could oversimplify the travel patterns, potentially missing out on crucial short-term fluctuations that might impact the predictive accuracy of the charging model. Shang et al. [115] developed a predictive model using k-nearest neighbors (k-NN) and LSTM to reduce the energy demand of a commercial building using V2G by scheduling the charge and discharge cycles of EVs, concluding that their proposed algorithm successfully reduces the energy load of the building with an accuracy of 94% compared to traditional optimisation algorithms. Like previous studies, they also rounded the travel information to 15-minute intervals, which may overlook the detailed demands of shorter-term fluctuations. Despite the smaller time step of 15 minutes, the model might still miss out on capturing some of the more granular information within these intervals.

2.7 Summary

V2G technology, which can supply energy back to the electrical grid when needed, can potentially bring higher economic value than V1G alone. However, the integration of EVs into the energy system as another type of storage must be approached differently. This is because EVs are mobile, not always grid-connected, and their available storage capacity is not fixed. Furthermore, EVs have the potential to provide similar value as stationary home batteries, both in terms of energy storage and grid support. Yet, they offer the added advantage of mobility, serving as a vehicle for travel in addition to their role in the energy system. This dual functionality

could enable EV owners to offset some costs of ownership and charging by participating in V2G schemes while enjoying the benefits of an electric vehicle for personal transportation.

A variety of factors can influence the economic value of V2G, including driving behaviour, the location of the V2G charger, and the plug-in rate, which has been shown to be about 30% of the time on average [8]. However, only a handful of studies have examined the availability of EVs, even though it is essential for V2G to rely on the capacity of EVs to be available and connected to a charger. In the studies that have considered EV availability, most have used fixed times, which do not reflect real-world scenarios, or sometimes, they use hourly or half-hourly resolution. This approach may overlook the importance of shorter-term fluctuations inherent in real-life management. This reveals the importance of studying the impact of EV availability on the value of V2G in the UK.

Most studies have shown that frequency response and demand side response are the most profitable ancillary services that V2G can provide. However, other potential ancillary services, like the delivery of reserve services or system security services, haven't been thoroughly considered. STOR, a reserve service, could potentially provide a revenue stream for EVs. Figure 2.3, shows some of the ancillary services that can be provided with V2G with potentially positive revenues. According to this figure, the income might seem modest initially, but financial incentives can offset some costs of EV ownership and charging. Plus, participating in STOR services contributes to the stability and reliability of the grid, as the energy sector transitions towards more renewable and distributed resources. As a result, demand for services like STOR is expected to grow, offering potentially greater returns for early EV adopters.

Despite the critical role STOR plays in grid stability, it has received limited attention, partly due to the unpredictability of EV availability. Given the significance of recent blackouts in the UK, discussion about leveraging new technologies, such as V2G, to support the grid and provide crucial ancillary services like STOR has increased. Studying the potential of EVs in delivering STOR services could be highly beneficial for grid stability and reliability in the future.

Even though STOR is essential to the electric grid, it has received limited at-

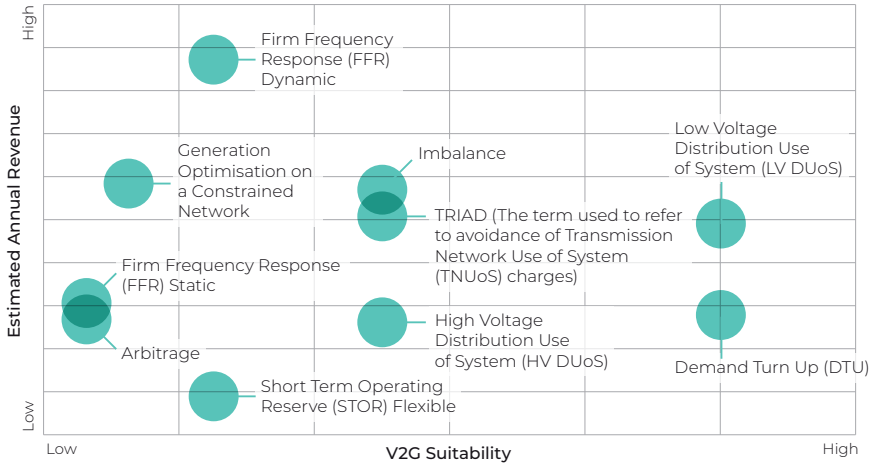

Figure 2.3: Comparison of the suitability of V2G revenue streams [8].

tention. Restoration services have also been understudied, as EVs cannot yet be considered a reliable provider due to the uncertainty of their availability. Given the current outlook for the energy sector in the UK, with different plans to ensuring security of electricity supplies for winter [116], discussion around harnessing new technologies like V2G to support the grid and offer vital ancillary services, such as STOR, has increased. As such, exploring the potential of EVs in delivering STOR services, and consequently generating profit for EV owners, could be incredibly beneficial for future grid stability and reliability.

The blackout event in early August 2019 [117, 118], which affected hundreds of thousands of UK users, coupled with the decommissioning of traditional black start providers, has increased discussions on the role of emerging technologies, like V2G, in grid support [12]. V2G, in particular, could help avert grid disruption by providing essential ancillary services, such as restoration services. These services demand the ability to supply power without external dependence, a requirement that V2G can partially fulfil, given that EVs only need to be connected when such an event occurs [119]. If some of the highlighted weaknesses like the uncertainty of EV availability and SOC during the day are addressed, V2G could meet some of the National Grid's criteria for this service [12].

The role of P2P transactions in the energy sector has also been studied, covering areas like pricing mechanisms, user willingness, integration of stationary storage, and

incorporation of renewable energy. Additionally, only a few studies have considered EVs and their availability, and these often opt to model EV behavior rather than use real-world EV travel data. Additionally, such work typically employs hourly or half-hourly resolution, potentially missing important details in the travel patterns.

Machine learning has significantly influenced various industries, including V2G technology, particularly in predicting EV availability [120]. However, most studies are based on data from commercial EV fleets in a workplace setting, which may not represent private vehicle use. Furthermore, these models often round travel data to 30-minute or hourly intervals, which could lose essential granular information, thereby affecting the accuracy of vehicle availability predictions and V2G efficacy. Despite this, few studies simulate the delivery of ancillary services beyond potential energy capacity or building energy demand reduction. Therefore, the importance of machine learning in predicting EV availability, the potential for EVs in providing STOR and restoration services, and the value of P2P transactions involving EVs all underscore the need for more comprehensive and real-world-focused studies. By exploring these areas, we can deepen our understanding of V2G's potential and address the current limitations more effectively.

In the literature we have reviewed, most studies examining V2G applications often focus on a limited time frame within a year and typically use a single energy tariff for energy drawn from the grid. This highlights the need to consider various factors that potentially impact V2G delivery, beyond EV availability. Therefore, studying a grid-connected microgrid inclusive of these considerations could provide comprehensive insights into diverse EV behaviours.

In summary, the role of EVs in energy systems is multifaceted. They not only serve as transport vehicles but also have the potential to provide significant ancillary services like STOR and restoration services. However, the real-world behaviour and availability of EVs need better consideration to harness their full potential. Machine learning has the potential to enhance our understanding of EV availability, thereby improving their utility in grid services. A comparison that needs to be explored is between EVs and stationary home batteries to understand their relative cost-effectiveness and efficiency. Moreover, the integration of EVs in P2P energy transactions within a microgrid environment can open new avenues for research.

A broader, more in-depth approach is needed to study V2G applications and the potential impact of the availability of EVs and different factors that could also impact their potential to provide V2G services should be explored.

Chapter 3

A Data-Driven Approach to Predict Electric Vehicle (EV) Availability for Vehicle-to-Grid (V2G) Services

In this chapter, we introduce a machine learning (ML) solution designed to predict the location and availability of electric vehicles (EVs) for vehicle-to-grid (V2G) services. Our predictive model consists of two separate classification models: one model predicts the start location and the other predicts the end location of EV trips. Each classification model was trained and validated using three different algorithms, all applied to historical travel data from the UK. This dataset includes start and end locations, start and end times, daily journey count, and trip distance. Based on their performance, one algorithm was selected for each model to best predict the start and end locations of EVs. These models offer precise insights into EV availability throughout the day, which results important for implementing V2G services. The selected models are then used to predict the start and end locations of real-world EV trip data from the UK. These predictions serve as the input for the optimisation model, which will be introduced in Chapter 4. This model will use the predicted data to optimise and schedule EV charging and discharging for different V2G services that will be introduced in Chapters 5–7.

In this project, we employ a two-dataset approach for the development and ap-

plication of our machine learning models. The historical travel data, according to the Department for Transport [121], predominantly composed of internal combustion engine vehicle (ICEV) travel data, serves as the foundation for training and validation of the two classification models. Despite the technological differences between ICEVs and EVs, many travel behaviours are universal, making ICEV data an invaluable resource for capturing general travel patterns. The validation of our models using the same ICEV data ensures they are robust and capable of generalisation, a crucial aspect of ML model development [122].

The second dataset, consisting of real-world EV travel data, becomes essential during the application phase of our models. In this phase, we are not just evaluating how well the models perform, but more importantly, we are testing their applicability to new situations. In other words, we are examining if the models can effectively use the patterns they learned from ICEV data to accurately predict the locations of EVs. While the EV dataset doesn't participate in the training and validation phase, its importance cannot be understated. It allows us to align our models with the primary objective of the study — optimising EV usage for V2G services. Therefore, our two-dataset strategy lays the foundation for the development of universally applicable models using ICEV data and validates their relevance to our V2G goals using real-world EV data.

Figure 3.1 provides an overview of the process we undertake in this chapter for each of the two classification models. It begins with the transformation of raw historical data through feature engineering, followed by splitting it into training and validation sets. These sets are used to develop predictive models using machine learning algorithms. The resulting predictive models are then applied to real-world EV data, referred as "new data", to predict their locations. These predictions, indicative of potential EV locations based on the patterns learned from historical data, become the input for our optimisation model which will be introduced in Chapter 4. Therefore, figure 3.1 effectively illustrates our methodology for developing and applying machine learning models to predict EV locations for optimising V2G services.

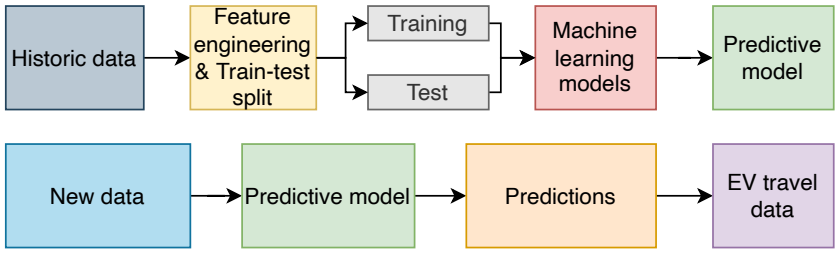

Figure 3.1: Overview of the process of training a predictive model, testing it, and then getting predictions from new data.

3.1 Historic Travel Data

This section is devoted to describing the data used to train the predictive classification model.

3.1.1 Data processing

For the purpose of training the predictive model, the national travel survey (NTS) data that contains information about personal travel patterns, such as how, why, when and where residents of England travel within the UK was used. The NTS is a household survey designed to track long-term travel trends and help in policy formulation [123]. These data include information based on hundreds of questions such as people's point of view on the quality of the road, whether they are satisfied with the public transport in their communities, household income, month that a trip took place, day of the week that a trip took place, etc.

As we further explore the historical data that will be used, it is important to acknowledge its strenghths and limitations based on information provided by the Department for Transport [124] in their website. The NTS, running annually since 1988, offers a wealth of detailed, long-term travel data, making it valuable for monitoring trends. Its large, representative sample allows for diverse demographic analyses. Despite fluctuating response rates, measures to boost inclusivity and accessibility have been implemented, including language accommodations and remote completion methods. An upcoming digital diary promises further advancements in data collection. The NTS enjoys a strong reputation as the gold standard of travel surveys in the UK, informing numerous transport policies and research studies. Its dataset is openly accessible, encouraging user engagement and self-directed explo-

ration. Regular consultations ensure the statistics continue to meet user needs and reflect current transport considerations.

However, while the NTS boasts comprehensive travel data, its reliance on self-reported data may not always accurately reflect actual travel behaviours due to inaccurate recall or estimation errors. Whilst there are extensive validation checks in place to minimise this type of errors, it is not possible to eliminate them entirely. Additionally, the survey's geographical coverage has been limited to England since 2013.

At the time of this work, the data, containing information from 2002 to 2019, are spread over 10 different files, each of which contains identification numbers that help identify the household or individual who answered the survey. For the data used to train the model, we had to combine two of the files, one called the main data (*filename = "trip_eul_2002-2019"*), which contains most of the data that will be used to train the predictive model, including data relevant to identifying the start and end locations of each trip, and another called the supplementary data (*filename = "household_eul_2002-2019"*), which contain information that includes the day of the week and the month of the year in which the trip took place.

In this work, we used data collected from 2002 to 2019 that contained 4,866,698 records of people who reported different travels, such as using their own car, public transport (bus, train, etc.), cycling or simply walking to their destination. As we seek to provide Vehicle-to-home (V2H) or V2G services, we are only interested in privately owned vehicles; therefore, we restrict the data to entries that were reported as the main driver of a privately owned car and that the car was the main mode of transport, leaving a total of 2,236,036 records. We then removed outliers based on the distance travelled, resulting in a final total of 2,120,058 records. It should be noted that to our knowledge, the survey did not report the type of vehicle (internal combustion engine (ICE) or electric) until the survey conducted in 2019, where according to an online report released in 2020 by the Department for Transport [121], in 2019, 63% of the cars owned by the people were petrol, 34% were diesel and 2% were other fuel types such as plug-in hybrid or electric. Therefore, we assume that a similar driving behaviour will apply to both EVs and ICE vehicle drivers. Table 3.1 shows the amount of data for each year that the survey was conducted.

All data was processed using the Python 3.8.13 [125] programming language and data manipulation and analysis libraries, such as Pandas 1.1.3 [126] and Numpy 1.18.5 [127].

Table 3.1: The number of records reported as the main driver of a privately owned vehicle per survey year.

Survey year	Number of records	Percentage (%)	Survey year	Number of records	Percentage (%)
2002	122,413	5.77	2011	119,068	5.62
2003	135,705	6.40	2012	128,375	6.06
2004	133,341	6.29	2013	102,302	4.83
2005	141,207	6.66	2014	105,329	4.97
2006	137,444	6.48	2015	98,220	4.63
2007	130,424	6.15	2016	102,807	4.85
2008	126,008	5.94	2017	92,857	4.38
2009	131,214	6.19	2018	94,477	4.46
2010	127,525	6.02	2019	91,342	4.31

As presented in table 3.1, the participation rates in the NTS from 2002 to 2019 show a diverse pattern. There was an initial rise in participation, peaking in 2005, followed by a period of fluctuation between 2005 and 2012. Post-2012, a more consistent decline is evident. The reasons behind these shifts could be multi-layered, potentially tied to societal trends such as survey fatigue, economic reasons or participants choosing alternative types of transports instead of using their private car, however, these are speculative hypotheses. Although the investigation of yearly fluctuations in participant numbers is indeed interesting, it falls outside the scope of this work.

The fluctuation in participation rates from 2002 to 2019 in the UK National Travel Survey, although intriguing, is beyond the primary focus of our current work. From an initial increase, peaking in 2005, to a subsequent gradual decrease, especially noticeable from 2012 onwards, the reasons behind these shifts could range from survey fatigue and societal trends towards digital communication to the impacts of the late-2000s economic recession. However, these hypotheses remain speculative and exploring them further would deviate from our central goal: the development of a predictive model and its application to optimise Vehicle-to-Grid services.

3.1.2 Feature engineering

The main objective is to predict the start and end locations of the vehicle during the day based on historical travel data reported in NTS. Moreover, the trained model will only be able to make predictions if and only if the same features are found in the new data from which we want to make predictions. This means that, for example, if we use data containing *"trip distance travelled in kilometres"* when training the model, the new data that will be fed into the model must have the same information *"trip distance travelled in kilometres"*. To this end, we only kept features that contain information about the start and end date and time of the trip, data that contain the number of journeys per day, and data that contain information about the distance travelled. For date and time data, this was collected from various separate columns containing the start and end information of the trip; in this case, the information used was hour, minute, days of the week, year, month and day of the month. This information was formatted as *YYYY-MM-DD hh:mm:ss*. Furthermore, data containing information on the start and end locations of the trip were preserved, as this will be used as labels or targets to predict. This information includes up to 23 different categories. To simplify the training of the model and obtain the best results, we reduced the 23 categories to only two categories, *Home* and *Other*. Here, the vehicle is at home if the reported location is "Home" and away if the reported location is otherwise. Table 3.2 shows the final distribution of the data on the start and end locations of the trips.

Table 3.2: Number of records for each of the two location categories used in this work.

Status	Location	Total values	Percentage (%)
Start	Home	905,528	42.71
	Other	1,214,530	57.29
End	Home	891,789	42.06
	Other	1,228,269	57.94

Table 3.3 shows an example of the main data information that was kept and later used to extract features to train the model, as well as the data columns for the starting and ending location that will be used as labels. Finally, table 3.4 and

table 3.5 show an example of the final data used to train the predictive model and a brief description of the data contained in each column, respectively. For simplicity, features are indicated as x and targets or labels as y.

Table 3.3: Example of the data extracted from the national travel survey records that will later be used to obtain features and labels to train the machine learning model.

start timestamp	end timestamp	daily journey number	trip distance in km	location	
				start	end
2002-01-28 12:18:00	2002-01-28 12:32:00	1	4.83	Home	Other
2002-01-28 12:35:00	2002-01-28 12:41:00	2	0.80	Other	Other
2002-01-28 17:30:00	2002-01-28 17:56:00	3	4.83	Other	Home
2002-01-28 20:20:00	2002-01-28 20:23:00	4	0.48	Home	Other
2002-01-28 21:10:00	2002-01-28 21:15:00	5	0.48	Other	Home

Table 3.4: Example of the data used in this work that was used to train the predictive model.

x_1	x_2	x_3	x_4	x_5	x_6	x_7	x_8	x_9	y_1	y_2
12	18	0	0	1	4.83	14	0	3	Home	Other
12	35	0	0	2	0.80	6	3	289	Other	Other
17	30	0	0	3	4.83	26	289	144	Other	Home
20	20	0	0	4	0.48	3	144	47	Home	Other
21	10	0	0	5	0.48	5	47	910	Other	Home

Table 3.5: Description of the parameters used to train the predictive model.

Parameters	Description
x_1	Start travel hour
x_2	Start travel minute
x_3	Start travel day of the week
x_4	Start travel weekend or not
x_5	Journey number on a given travel day
x_6	Trip distance in kilometres
x_7	Trip total time in minutes
x_8	Time since last trip in minutes
x_9	Time for next trip in minutes
y_1	Start location
y_2	End location

3.1.3 Data statistics

After processing the data, the remaining features contain information on the time and day of the week during which the trip took place. Figure 3.2 and figure 3.3 show the starting location and percentage of trips according to their departure time between Monday and Friday and between Saturday and Sunday, respectively. Here, both figures show that most trips start after 05:00 am during the week. For trips on weekdays, most trips between 07:00 and 10:00 start at *Home*, and trips between 15:00 and 18:00 start at the location *Other*. On weekends, most trips before 11:00 start at *Home*, after this time, most trips start at *Other*.

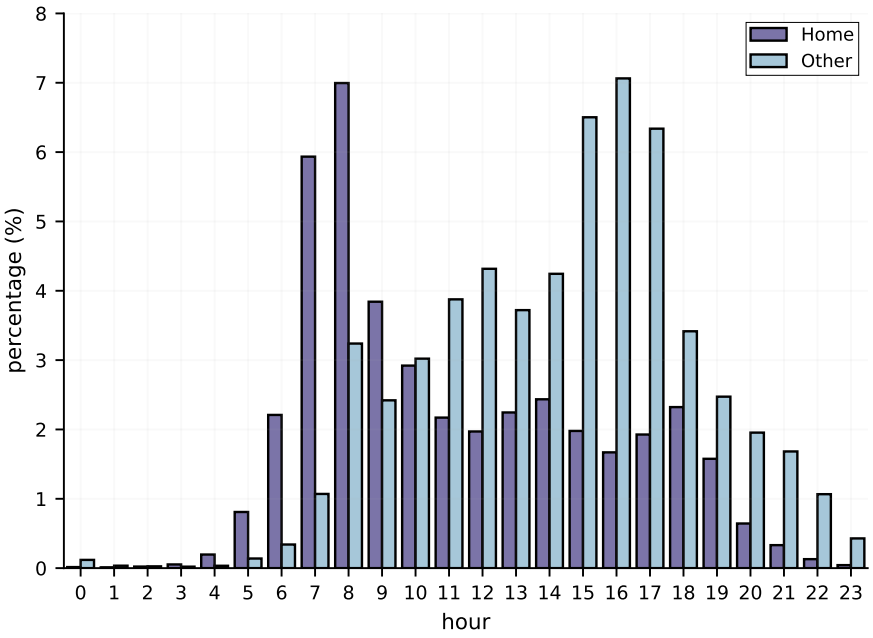

Figure 3.2: NTS data taken from surveys from 2002 to 2019 reported as private vehicles. Start location and percentage of travels made between Monday and Friday, according to the start time of the trip.

Similarly, figure 3.4 and figure 3.5 show the destination and percentage of trips according to their departure time between Monday and Friday and between Saturday and Sunday, respectively. For trips on weekdays, most trips that end at *Other* take place between 07:00 and 10:00, and most trips that end at *Home* take place between 15:00 and 17:00. On weekends, most trips before 15:00 head to *Other* and after this time most trips go to *Home*.

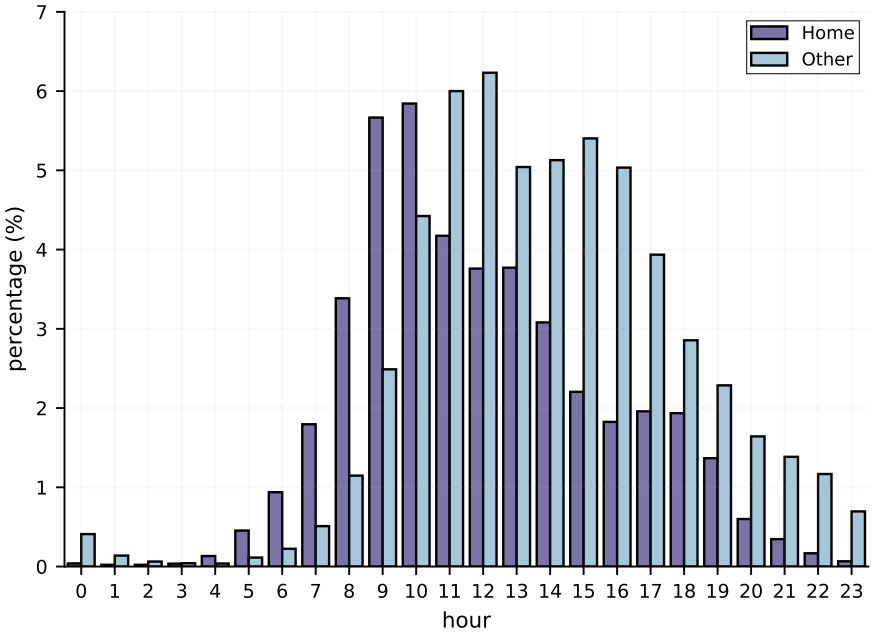

Figure 3.3: NTS data taken from surveys from 2002 to 2019 reported as private vehicles. Start location and percentage of travels made between Saturday and Sunday, according to the start time of the trip.

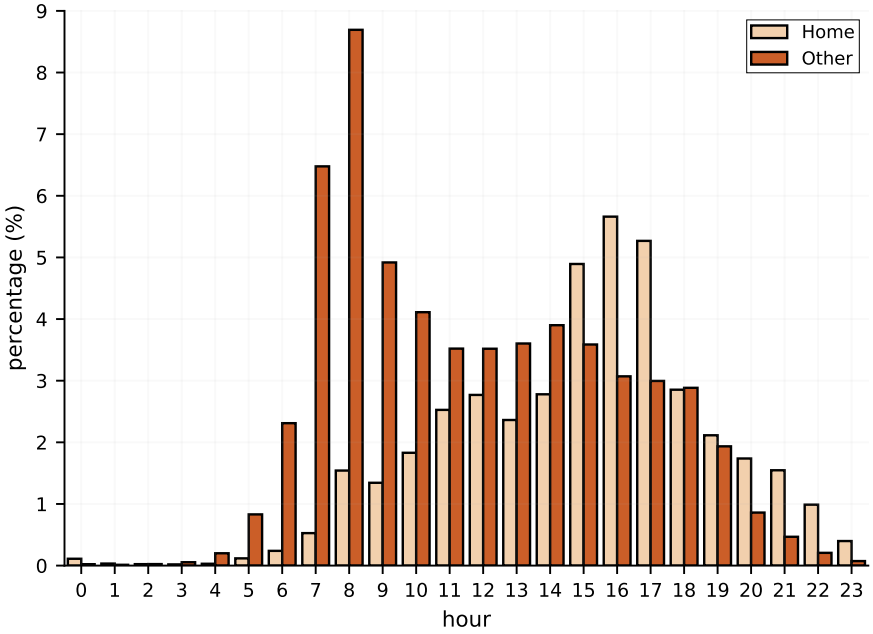

Figure 3.4: NTS data taken from surveys from 2002 to 2019 reported as private vehicles. End location and percentage of travels made between Monday and Friday, according to the start time of the trip.

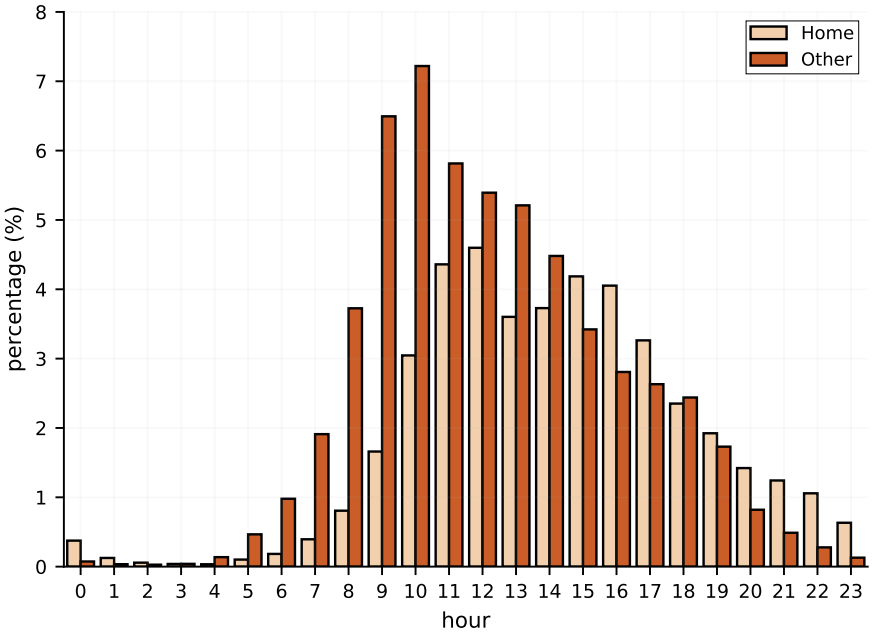

Figure 3.5: NTS data taken from surveys from 2002 to 2019 reported as private vehicles. End location and percentage of travels made between Saturday and Sunday, according to the start time of the trip.

According to the data, most drivers make between 1 and 5 trips per day and most of these trips are between 1 and 10 km long. Furthermore, most trips take less than 15 minutes to complete. This information is true regardless of the day of the week on which the trip takes place. Figure 3.6 gives a more detailed look at how the data is distributed with respect to the number of trips per day, the total distance travelled and the total time it takes to complete a trip.

3.1.4 Classification tasks

For the predictive model, three different classification algorithms were trained and compared: Logistic regression (LR), Random forest (RF) and Light gradient boosting machine (LightGBM). In the case of the first two techniques, the implementation by the Python library, Scikit-learn 0.24.1 [128], was used for this work. For LightGBM, the Python library, LightGBM 3.1.1 [129], which is the Python implementation of this technique, was used. These three algorithms were chosen due to their diverse approaches to classification problems. LR offers simplicity and interpretability, while RF provides robustness and handles complex feature interactions.

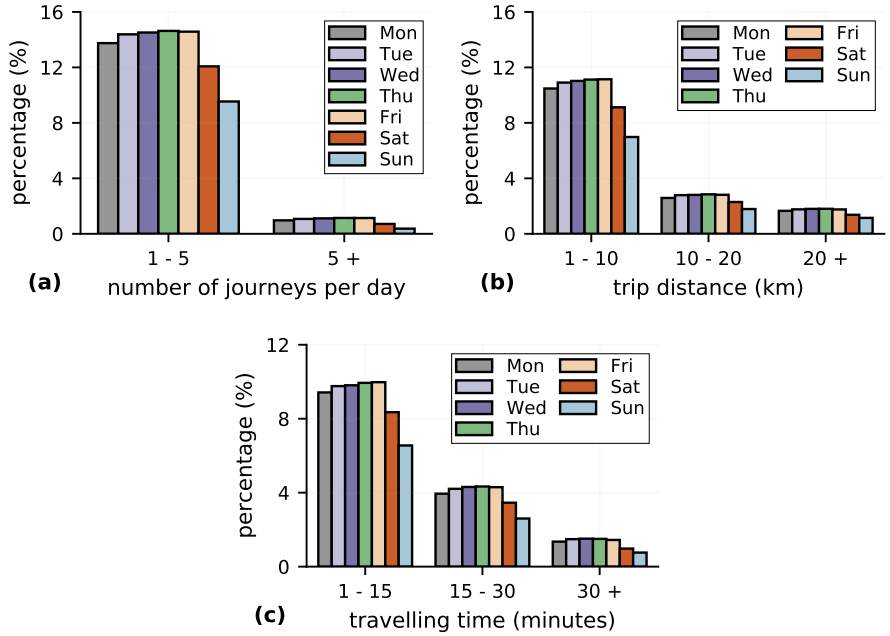

Figure 3.6: National travel survey data taken from surveys from 2002 to 2019 reported as private vehicles. **a.** Number of trips per day for each day of the week. **b.** Total distance travelled per trip for each day of the week. **c.** Total time per trip for each day of the week.

LightGBM is efficient and scalable, making it suitable for large datasets. These algorithms cover a range of complexities, from linear models to ensemble methods, allowing for a robust comparison to determine the best-suited algorithm for the given dataset and problem. This comparison also aids in understanding the predictive power of the selected features.

LR is a statistical model that calculates the probability that a label belongs to a specific class; it does so by computing a weighted sum of the input features and outputs a number between 0 and 1 using a sigmoid function [130]. RF is an ensemble learning method for classification that operates by building multiple decision trees when training a model. When using RF for classification, the random forest output is the class that receives the most votes [130]. LightGBM is a gradient boosting framework that uses tree-based learning algorithms. Similarly to RF, this algorithm is based on decision tree algorithms [129, 131]. What distinguishes LightGBM from other tree-based algorithms, is that LightGBM does not grow a tree level-wise – row by row – as most other implementations do; instead, it grows trees leaf-wise –

vertically – which makes the process dramatically faster and, in many cases, results in a more effective model while consuming less memory [132].

In this work, we establish two different classification tasks. These are explained below:

- A classification model was used to predict only the starting location of the trip.

  This model included all features $x_1 - x_9$ and was responsible for predicting y_1, the start location. This means that this model was not consider y_2, which is the end location of the trip. This model was called *task 1*.

- A second classification model was used to predict the end location of the trip.

  For this second model, similar to the previous one, all features were included $x_1 - x_9$ and, in this case, y_1 — start location — was also considered as a feature. Therefore, this model was responsible for predicting y_2, the end location. This model was called *task 2*.

To this end, the processed data was divided equally into two halves, resulting in two data sets containing 1,060,029 rows each. The split was performed using a stratified sample based on the parameter x_1 — start travel hour — this makes a split so that the proportion of values in the sample produced will be the same as the proportion of values provided to the parameter. Therefore, this will ensure that each data set gets 50% of each unique value within x_1. This was done using the Scikit-Learn function `train_test_split` as shown in listing 3.1 below:

```
# split in two datasets
from sklearn.model_selection import train_test_split

model_1, model_2 = train_test_split(
    nts_data, # data to split
    test_size=0.5, # divide equally, 50\% each data set
    stratify=nts_data['start_travel_hour'],
    random_state=42) # set random seed to get consistent results
```

Listing 3.1: Code used to split NTS into two data sets

The division of the historical data into two distinct subsets for the purpose of training two individual models follows key principles of model robustness and independence. As mentioned, this partition is stratified based on x_1 (start travel hour), which ensures that both subsets retain a similar distribution, thereby maintaining a balanced representation of the original data. This strategy enhances model reliability and mitigates the risk of overfitting, a phenomenon where models over-adjust to their training data, resulting in sub optimal performance on unseen data [133]. Moreover, employing separate datasets facilitates independent validation of each model, allowing for an accurate estimation of each model's predictive performance without the risk of data leakage [134]. This is particularly pertinent considering each model is designed to predict a different target variable.

As explained before, for the in the second model (*task 2*), y_1 (start location) is used as a feature. Importantly, this is not the y_1 predicted by the first model (*task 1*), but the actual y_1 values from the dataset used to train this second model. In other words, by not using the y_1 predicted by the first model as a feature for the second model, we avoid to potentially introduce bias or errors into the predictions produced by the second model, as any inaccuracies in the prediction of y_1 would directly affect the prediction of y_2 (end location). By training each model on a separate, stratified subset of the data, the independence of the second model's predictions from the first model is assured, improving the overall reliability of the models.

3.1.5 Data preparation for training

To obtain the best results and ensure that the final models generalise to new data, both data sets for each of the two models were split into a training set and a test set. The training set includes 70% of the data and the test set includes 30% of the data. This resulted in that each data set *task 1* and *task 2* had 742,020 records in the training set and 318,009 in the test set. For this, once again, the Scikit-Learn function `train_test_split` which is inside a custom function `preprocess_data_02_train_model` that processes all training data from start to finish and gets it ready for the predictive model, as shown in listing 3.2 below. Here, `X` on line 21 contains the features and `y` in line 22 contains the labels. Then, on line 28 the data is split into `X_train`, `X_test`, `y_train` and `y_test`.

```python
import pandas as pd

def preprocess_data_02_train_model(
            dataframe: pd.Dataframe = None, # data to process
            predict_from_or_to: str = "start", # select which "task" to process
            stratify_col: str = "start_travel_hour",
            test_size_number: float = 0.3): # test set size -> 30%

    # prepare data for "model_1"
    if predict_from_or_to == "start":
        # target column
        target = "start"
    # prepare data for "model_2"
    elif predict_from_or_to == "end":
        # target column
        target = "end"
    # assign features and labels accordingly
    X = dataframe.drop(target, axis=1).copy() # keep relevant features only
    y = dataframe[target].copy() # keep relevant target/label only

    # import relevant function
    from sklearn.model_selection import train_test_split

    # split train and test data
    X_train, X_test, y_train, y_test = train_test_split(
            X, # features
            y, # labels
            test_size=test_size_number, # test set size
            stratify=X[stratify_col],
            random_state=42 # random seed to obtain consistent results)
    ...
```

Listing 3.2: Custom function to pre-process the data before training models. Here, the training and test set are split inside the custom function.

The data in each training and test sets was prepared before passing them onto each of the three machine learning classification algorithms. This includes processing columns containing numeric values, features $x_1 - x_9$, and string or text values of the target or label, $y_1 - y_2$.

For the numeric values, the Scikit learn function `MinMaxScaler` was used. This function *"scales and translates each feature individually such that it is in the given range on the training set"* [135], in this case, each column was scaled between 0

and 1. This is shown in listing 3.3 which is part of the same custom function `preprocess_data_02_train_model`. In this case, `scaler` is fitted as shown in line 8 using the `X_train` data set, which contains the features that will be used to train the predictive model, and then transform the same data set as seen in line 9. Then we use the fitted `scaler` to simply transform the features in `X_test` as shown in line 19.

```
1   ...
2   from sklearn.preprocessing import MinMaxScaler
3
4   # Initiate scaler
5   scaler = MinMaxScaler()
6   # ---
7   # fit and transform features inside "X_train"
8   scaler.fit(X_train[cols_to_scale])
9   scaled_df = scaler.transform(X_train[cols_to_scale])
10  # Assign scaled data into a Dataframe
11  scaled_df = pd.DataFrame(scaled_df,
12                           columns=cols_to_scale,
13                           index=X_train.index)
14  # Replace original columns in "X_train" with the scaled ones
15  for col in scaled_df:
16      X_train[col] = scaled_df[col]
17  # ---
18  # transform data inside "X_test" using the scaler
19  scaled_df = scaler.transform(X_test[cols_to_scale])
20  # assign the same index as the dataframe in question
21  scaled_df = pd.DataFrame(
22      scaled_df, columns=cols_to_scale, index=X_test.index)
23  # Replace original columns with scaled ones
24  for col in scaled_df:
25      X_test[col] = scaled_df[col]
26  ...
```

Listing 3.3: Scaling each feature with numeric values to be in the range between 0 and 1.

For columns containing text or string values, in this case $y_1 - y_2$, the values were transformed into binary values where *Home = 0* and *Other = 1*. This was done using the Scikit-learn function `LabelEncoder`. This process is shown in listing 3.4 below, which is the final part of the custom function `preprocess_data_02_train_model`.

Here, the encoder is fitted to the data in `y_train`, which contain the labels that will be used to train the predictive models, and then transform the same data set as shown in lines 8 and 9, respectively. The encoder was then used to transform the labels in `y_test` as shown in line 11. Finally, the custom function returns the pre-processed training and test sets, as well as the scaler and encoder for later use.

```
1   ...
2   from sklearn.preprocessing import LabelEncoder
3
4   # initiate encoder
5   encoder = LabelEncoder()
6   # ---
7   # fit and transform "y_train"
8   encoder.fit(y_train)
9   y_train = encoder.transform(y_train)
10  # ---
11  # transform "y_test" dataset
12  y_test = encoder.transform(y_test)
13
14  # return data, scaler and encoder ready for training and testing
15  return X_train, X_test, y_train, y_test, scaler, encoder
```

Listing 3.4: Labels encoded with *Home = 0* and *Other = 1* before training the ML models.

Table 3.6 shows the data distribution for the training and test data sets for *task 1* which contains the label y_1 — start location. Here, both training and test sets have similar ratios of *Home = 0* and *Other = 1* similar to the ratio in table 3.2 that belongs to the *Start* data set.

Table 3.6: A summary of the label ratio of the training set and the test set for the *task 1* — start location. Here, the label *Home = 0* and the label *Other = 1*.

Data set	Label	Total values	Percentage (%)
Training	0	317,031	42.73
	1	424,989	57.27
Test	0	135,920	42.74
	1	182,089	57.26

Similarly to *task 1*, table 3.7 shows the data distribution for the training and

test data sets for *task 2* that contain the label y_2 — end location. Here, for both data sets, their ratios are similar to *Home = 0* and *Other = 1* to those that belong to *End* data set as shown in table 3.2.

Table 3.7: A summary of the label ratio of the training set and the test set for the *task 2* — end location. Here, the label *Home = 0* and the label *Other = 1*.

Data set	Label	Total values	Percentage (%)
Training	0	317,031	42.11
	1	424,989	57.89
Test	0	135,920	42.07
	1	184,223	57.93

Finally, figure 3.7 summarises the data process before training the predictive models as well as the label distribution in each training and test set for both tasks.

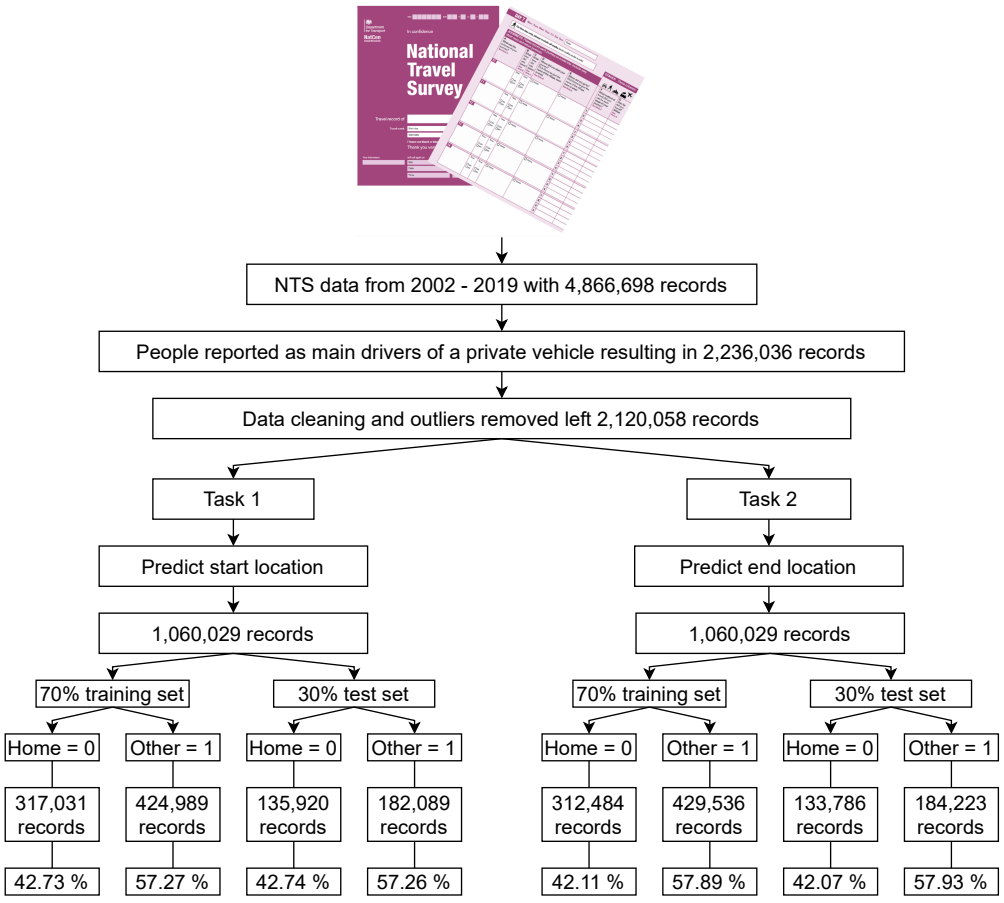

Figure 3.7: Diagram summarising the data pre-processing before training the ML models. It also shows the number of records in each data set for each task.

After pre-processing the data, both the training and the test sets are ready to pass them into the three ML algorithms, which will be discussed in the following section.

3.2 Results

3.2.1 Metrics

Three different ML classification algorithms were compared. The performance of these three models was evaluated using three different performance metrics widely used for classification tasks. The performance metrics considered in this work are Precision, Recall, and F1-Score. These performance metrics were chosen due to the imbalanced nature of the labels, as shown in tables 3.2, 3.6 and 3.7 where the *Home* label has around 42.00% and the *Other* has around 58.00% of the total data set for each task. These metrics provide a more comprehensive view of performance than just accuracy, which can be misleading in imbalanced scenarios.

Classifier performance metrics are defined using the confusion matrix that results from each predictive model, which has four fundamental quadrants shown in table 3.8. The main goal is to determine how frequently examples from class *Home = 0* are labelled as class *Other = 1* and the other way around.

Table 3.8: Confusion matrix layout.

		Predicted label	
		Home	Other
True label	Home	True Positive **(TP)**	False Negative **(FN)**
	Other	False Positive **(FP)**	True Negative **(TN)**

- True Positive **(TP)**: True Positive represents the number of values that were classified in the relevant class. For example, values that were predicted as *Home* that have been properly classified as *Home*.
- False Positive **(FP)**: False Positive represents the number of values that were classified in the relevant class but actually belong to the opposite class. For

example, values that were predicted as *Home* but their true label was *Other*, therefore, the values were incorrectly classified.

- False Negative **(FN)**: False Negative represents the number of values that were predicted in the opposite class that should be in the relevant class. For example, values that were predicted as *Other* but their true label belongs to *Home*, therefore, the values were incorrectly classified.

- True Negative **(TN)**: True Negative represents the number of values that were classified in the opposite class and actually belong to that class. For example, values that were predicted as *Other* that have been properly classified as *Other*.

As stated above, the performance metrics are calculated accordingly based on the confusion matrix. In addition, Scikit-learn offers multiple functions that can compute each of these metrics. Each of these metrics are defined below.

- **Precision** is the proportion of positive predictions that were correctly classified. This metric shows the classifier's exactness by measuring the ratio of true positives to predicted positives, helping minimise false positives [136]. This is defined by equation (3.1). To calculate this metric, the Scikit learn function `precision_score` is commonly used.

$$Precision = \frac{TP}{TP + FP} \tag{3.1}$$

- **Recall** is the proportion of actual positives that were correctly classified. This metric measures the classifier's ability to identify all positive instances, crucial in imbalanced datasets where missing a positive instance (false negative) can be costly [136]. This is defined by equation (3.2). To calculate this metric, the Scikit learn function `recall_score` was used.

$$Recall = \frac{TP}{TP + FN} \tag{3.2}$$

- **F1-Score** is the harmonic mean of precision and recall. This metric balances

Precision and Recall, providing a single metric that seeks to optimise both [130]. This is defined by equation (3.3). To calculate this metric, the Scikit learn function `f1_score` is commonly used.

$$F_1 = \frac{2}{\frac{1}{Precision} + \frac{1}{Recall}} = 2 * \frac{Precision * Recall}{Precision + Recall} = \frac{TP}{TP + \frac{FN+FP}{2}} \tag{3.3}$$

3.2.2 Model Training

In this work, each predictive model was trained using the training set and validated using the test set. To determine which model is most robust, we obtain the score for each model by using the Scikit-learn function `cross_validate` which evaluates a score by cross-validation, in this case Precision, Recall and F1-Score. This is done to avoid overfitting the training data and to improve the overall final performance of each model.

Cross-validation randomly divides the training set into K distinct *folds* — subsets, where K is the number of folds in which the data will be split, then trains and evaluates the predictive model K times [130]. Then 1 fold will be used for validation, while the remaining *K-1* will be used to train the data. This will be repeated until every fold has been used as a validation set. For this work, we used $K = 5$ as widely used. Listing 3.5 shows the process for the LR algorithm which is the same for the other two ML algorithms and also for both tasks. In this case, the performance metrics were calculated using the `scoring` parameter of the Scikit-learn *cross_validate* function. For this work, the training process was conducted using a Mac mini 2018 with a 3.2 GHz 6-Core Intel Core i7 processor and 32 GB of RAM.

Tables 3.9 and 3.10 shows the weighted averages that resulted from training task 1 and 2, respectively, using the three predictive models. The best results were obtained by LightGBM which is slightly better than the results from RF.

Here, using a single run for each of the three machine learning algorithm used with a set random seed (42), was a straightforward and effective approach for the initial model training, also, the use of a random seed ensured that the results were reproducible. Moreover, the application of a 5-fold cross-validation, as seen in listing 3.5 in line 17, significantly enhanced the reliability of the model evalua-

```python
from sklearn.linear_model import LogisticRegression
from sklearn.model_selection import cross_validate

# initiate 'Logistic Rregression'
lr = LogisticRegression(random_state=42)
# fit data
clf_lr = lr.fit(X_train, y_train)

# cross-validation
scores = cross_validate(
    clf_lr,
    X_train,
    y_train,
    scoring=['precision_weighted',
             'recall_weighted',
             'f1_weighted'],
    cv=5) # number of folds
```

Listing 3.5: Training process and cross-validation using $K=5$ for *task 1* using logistic regression.

Table 3.9: Resulting training data metrics for the task 1. Here, the weighted averages are reported.

	Task 1 — start location		
	Precision	Recall	F1-Score
Logistic Regression	0.759 ± 0.002	0.755 ± 0.002	0.748 ± 0.002
Random Forest	0.897 ± 0.001	0.897 ± 0.001	0.897 ± 0.001
LightGBM	0.899 ± 0.002	0.899 ± 0.002	0.899 ± 0.002

tion, giving us a more accurate and generalised measure of model performance than a simple train and test split would. Although the decision of training the models using a set random seed was successful, for an even more robust analysis, we can execute multiple runs of each algorithm multiple times with different random seeds. This would provide a more comprehensive view of the potential range of models performance and their ability to handle new data.

In this case, after training the data set, all three returned adequate results, but to choose one model, we still need to validate these results against the test set, which

Table 3.10: Resulting training data metrics for the task 2. Here, the weighted averages are reported.

	Task 2 — end location		
	Precision	Recall	F1-Score
Logistic Regression	0.866 ± 0.001	0.852 ± 0.002	0.853 ± 0.002
Random Forest	0.898 ± 0.001	0.898 ± 0.001	0.898 ± 0.001
LightGBM	0.901 ± 0.001	0.901 ± 0.001	0.901 ± 0.001

is the next step.

Each trained model was used to obtain predictions on the test set to compute the relevant metrics and to gauge their performance with data that the models had not seen. For this, the variable `y_pred` that contains the predictions and the variable `y_test` that contains the true labels are used in the Scikit-learn function `classification_report` that returns Precision, Recall and F1-Score at the same time for each model as seen in listing 3.6. Here in the example below, the LR model is used for *task 1*.

```
from sklearn.metrics import classification_report

# get predictions
y_pred = clf_lr.predict(X_test)

# get relevant metrics
classification_report(y_test, y_pred)
```

Listing 3.6: Get predictions and relevant metrics for the logistic regression model and *task 1*.

Table 3.11 shows the weighted averages that resulted from using the trained models to obtain predictions using the test set. Here, we can see that the results are quite similar to those obtained in tables 3.9 and 3.10, which means that the models are able to generalise well to new previously unseen data [137]. Furthermore, LightGBM produces slightly better results than RF and significantly better than LR in *task 1*. For *task 2*, the results of all three models are not too far from each other,

and then again LightGBM shows slightly better results for all three models.

Table 3.11: Resulting metrics from the predictions on the test set for both tasks. Here, the weighted averages are reported.

	Task 1 — start location			Task 2 — end location		
	Precision	Recall	F1-Score	Precision	Recall	F1-Score
Logistic Regression	0.759	0.755	0.748	0.866	0.851	0.852
Random Forest	0.898	0.898	0.898	0.898	0.898	0.898
LightGBM	0.899	0.899	0.899	0.900	0.900	0.900

When we consider LR, it can be observed that its performance, as indicated by precision, recall, and F1-Score values, is generally lower compared to the RF and LightGBM models. As a linear model, LR may not capture the complex relationships within the data as effectively as ensemble models, thus resulting in relatively lower performance scores. Nevertheless, its decent performance underscores the utility of simpler models, especially when computational resources are limited or when the relationships in the data are not overly complex. In some instances, such straightforward methods may offer an adequate balance between prediction accuracy and computational efficiency.

Additionally, it can be seen that the performance of RF and LightGBM algorithms are remarkably similar across both tasks, indicated by nearly identical precision, recall, and F1-Score values.

This similarity can be attributed to the fact that both RF and LightGBM are ensemble methods, meaning they combine multiple decision trees to generate their output. RF operates by creating numerous decision trees and aggregating their results, while LightGBM uses gradient boosting to construct a sequence of trees, each correcting the errors of its predecessor.

Despite their different approaches, both methods are known for their ability to model complex relationships and reduce the risk of overfitting, leading to reliable and robust predictions. This could explain the comparability of their performance in the tasks. However, slight variations in the scores, such as the marginally higher F1-Score of LightGBM in *task 2*, might be due to the differences in how these algorithms

handle certain aspects of the data, like outliers or missing values.

In summary, the close performance of the two models may speak to the strength of ensemble methods in handling this particular dataset and predictive tasks, yet further analysis would be necessary to understand the minute differences observed.

3.2.3 Fine-tuning

As LightGBM was the model that performed the best of the three compared, this model was used for each task to increase its performance by choosing the best hyperparameters for each model. For this, the Scikit-learn function `RandomizedSearchCV` performs a randomised search of a set of hyperparameters that are passed into the function, which means that it will explore random combinations of the range of hyperparameters values that are passed into the function — in this case, 10 different combinations, which is the default value — and will train each model 5 times using cross-validation [130, 138]. The training process is shown in listing 3.7, where the Scikit-learn function `KFold` is used to divide each fold that will be used in the cross-validation process.

Similarly to the process in listing 3.6, the test set is used to obtain predictions using the fine-tuned models for both tasks and to evaluate the performance of the model by obtaining the relevant metrics using the `classification_report` function. Table 3.12 shows the metrics resulting from both tasks. In this case, the results are slightly better than the original LightGBM models in table 3.11. Therefore, the fine-tuned models for both tasks will be used to predict the location of new data will be introduced in the next section.

As shown, the initial LightGBM model was already quite effective, which is evident from the modest improvement of 0.002 after applying `RandomizedSearchCV` for hyperparameter tuning. The decision to test 10 different hyperparameter combinations and employ a 5-fold cross-validation provides a smart balance between computational efficiency and exploration of the hyperparameters space. While exploring a larger set of hyperparameters or increasing the number of combinations tested could potentially improve the chosen LightGBM model, we must consider the computational cost related to his. Each additional combination tested adds to the computational workload, meaning that a broad hyperparameter search can

```
from sklearn.model_selection import KFold
from sklearn.model_selection import RandomizedSearchCV
from lightgbm import LGBMClassifier

# split in folds
kf = KFold(n_splits=5, # number of folds
           shuffle=True,
           random_state=42).split(X_train, y_train)

# initiate "LGBMCLassifier"
lgb_estimator = LGBMClassifier(boosting_type='gbdt',
                               objective="binary",
                               n_jobs=-1, # use all processors available
                               random_state=42)

# parameter grid with the hyper parameters to evaluate
param_grid = {'learning_rate': [0.05, 0.1],
              'max_depth': [7, 10, 13],
              'num_leaves': [31, 71, 81],
              'min_data_in_leaf': [100, 300, 400, 900, 1500]
              }

# initiate "RandomizedSearchCV"
r_search = RandomizedSearchCV(estimator=lgb_estimator,
                              param_distributions=param_grid,
                              cv=kf,
                              random_state=42)

# fit the model ---> "task 1" - start location
lgbm_model_1= r_search.fit(X_train, y_train)
# Choose the model with the combination of hyperparameters that performed the best
classifier_model_1 = lgbm_model_1.best_estimator_
```

Listing 3.7: Training of the model with `RandomizedSearchCV` using LightGBM for *task 1*.

become computationally expensive, requiring more time and resources. Balancing model performance improvement with computational efficiency is a crucial aspect of effective machine learning modelling [130].

Finally, for simplicity, for the remainder of this work, the fine-tuned LightGBM model for *task 1* – start location – will be referred as `classifier_model_1` and the fine-tuned LightGBM model for *task 2* – end location – will be called

Table 3.12: Resulting metrics from the predictions on the test set for both fine-tuned LightGBM models using `RandomizedSearchCV` for each task. Here, the weighted averages are reported.

	Task 1 — start location		
	Precision	Recall	F1-Score
Fine-tuned LightGBM	0.900	0.900	0.900
	Task 2 — end location		
	Precision	Recall	F1-Score
Fine-tuned LightGBM	0.902	0.902	0.902

`classifier_model_2`. In the next section, the process to get the predictions and the new travel data will be discussed.

3.3 New travel data

This section is devoted to describing the data used as new data that will be fed into the predictive model to obtain their starting and end locations.

3.3.1 Data processing

Data used to predict start and end locations contain real world EV travel data collected by EA technology (EA) [139] as part of a trial project called *"My Electric Avenue"* that was carried out for 18 months between 2014 and 2015 in England. This data will now be referred to as EA data.

The EA data contains 383,051 records from 215 unique users, which includes information on the start and end date and time of the trip, the distance travelled per trip, the power consumption of each trip, and the odometer information at the start of each trip. The EVs' telematics systems were used to record the driving behaviour of the trial participants. The telematics systems recorded the distance, times, power consumption, and odometer reading for each EV journey. As with all trial data, there are samples missing. Communication issues between the monitor controllers and the intelligent control box (ICB), as well as insufficient general packet radio service (GPRS) signal for the EVs to transmit data to the telematics system,

led to some missing samples in the data. In instances where there's an increase in the odometer reading without a corresponding recorded journey, this signifies a gap in the data [139]. Table 3.13 shows an overview of the data from the EA data set with the features the original features recorded during the trial.

Table 3.13: Example of the data included in the EA technology data set that was used to obtain predictions of start and end location for each trip.

start timestamp	end timestamp	journey number	trip distance in km	odometer at the start in km	power consumption in kWh
2014-08-02 16:45:00	2014-08-02 17:04:00	1	6.914	846	0.857
2014-08-02 18:11:00	2014-08-02 18:13:00	2	0.354	854	0.059
2014-08-02 18:18:00	2014-08-02 18:32:00	3	4.531	854	0.582
2014-08-03 06:14:00	2014-08-03 06:18:00	1	1.320	859	0.204
2014-08-03 06:20:00	2014-08-03 06:24:00	2	1.198	860	0.185

After cleaning the data and removing data from participants with fewer than 500 records in the entire data set as they only cover a few weeks of the year, 342,784 records were left from 205 unique users. For this work, only unique users with enough information to fill a year's worth of data were included, from 2014-August-01 00:00:00 to 2015-July-01 23:59:00, these dates returned the highest number of profiles that fulfil the requirement of having 365 days reported entries, which, in turn, left a diverse selection of 170 participants with different total number of trips ranging from participants with a total of 339 trips to participants with a total of 2,290 trips during those 365 days chosen. The selection criterion used in this work, which requires users to have 365 days of reported trips, is not necessarily indicative of selection bias. This criterion was chosen to ensure a consistent data quantity across all user profiles, thereby providing a more reliable base for analysis in our work. The intention here was to avoid incomplete data, which could potentially skew the results or make them less reliable.

Another critical aspect to consider is the temporal variation in the data. By

selecting profiles with a full year of data, this study ensures a balanced representation of the four different seasons of the year and their potential impact on driving behaviour. This is important because travel patterns can significantly vary depending on the season due to different factors such as weather condition, holidays and daylight hours. The requirement of 365 days of data allows to capture this seasonal variability across the participants. As a result, the selected profiles can be compared across different weeks of the year, maintaining consistency while accounting for potential seasonal fluctuations. Additionally, the final selection of participants showed a diverse range of total trips, as already mentioned, from 339 to 2,290 trips. This wide range of trip numbers indicates that both high and low usage participants were included in the dataset, which results in a comprehensive exploration of user behaviours avoiding a potential bias towards only high-frequency users. Therefore, the data provides the diversity necessary for a robust analysis, covering both frequent and less frequent users.

A final sample of 50 vehicles is then taken as a stratified sample by the total number of trips during the 365 days chosen as just explained; this is to help ensure that the optimisation models used in this work capture the diversity of having different vehicle schedules when providing V2H and V2G services.

The stratified sample was accomplished using Scikit-learns's `train_test_split` function, employing stratified sampling based on the total number of trips the participants made during the selected 365-day period. Stratified sampling is a statistical technique that involves splitting the population into homogeneous subgroups (also called strata) and drawing a random sample from each stratum. In this case, the total number of trips was used for that, ensuring the sample included vehicles across the diverse trip frequencies. Furthermore, each of these 50 vehicles was allocated to a single household, resulting in a total of 50 households with that own an EV in the sample. This method of allocating one vehicle per household will be explored further in Chapter 4 were the optimisation model will be introduced and how was designed to optimise each household inside of a microgrid.

Finally, the remaining 50 profiles of the EA data were processed to contain the same information as that used to train the predictive models, as otherwise it would be impossible to feed the data into the final predictive models and predict the start

and end locations. For this, data was processed and organised to include the same features $x_1 - x_9$ the same way as the data shown in table 3.4. The original EA data does not contain any information on its location, which means that labels $y_1 - y_2$ are not included, as this will be predicted using the final predictive model as will be explained in the following sections.

3.3.2 Data statistics

Similarly to the NTS data, the EA data contains trip information on the time and date when a trip took place. As discussed in the previous section, start and end locations are not included and will be predicted using the predictive model, hence the need of the predictive model which can predict the missing information; however, relevant statistics can still be extracted from date and time information. In this context, figure 3.8 shows information from the 50 profile samples about the total number of trips per day, the total distance travelled per trip and the total time to complete each trip.

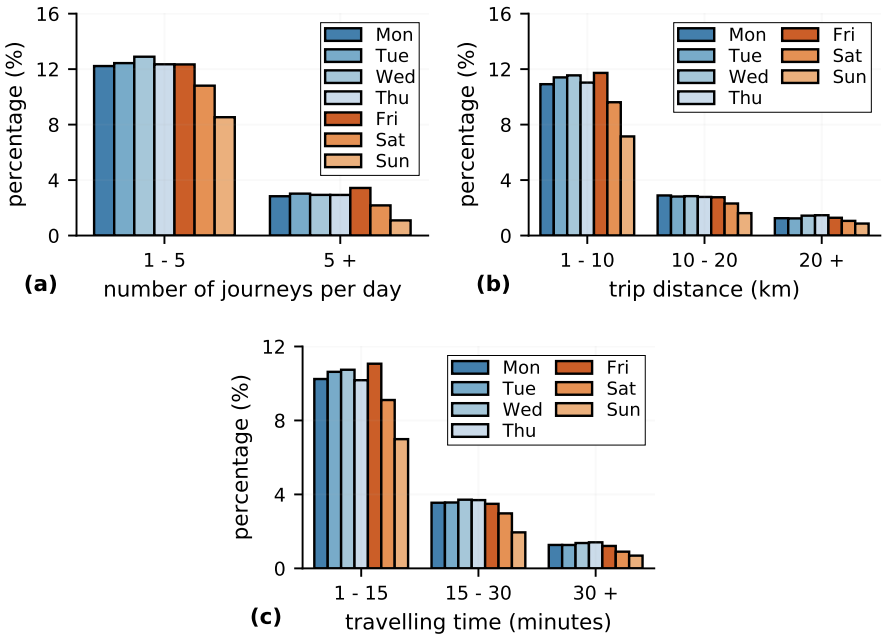

Figure 3.8: Electric vehicle trip information found inside the 50 profile sample extracted from the EA technology data. **a.** Number of trips per day for each day of the week. **b.** Total distance travelled per trip for each day of the week. **c.** Total time per trip for each day of the week.

According to this data, most users make between 1 and 5 trips per day. Most of these trips are between 1 and 10 km long and take between 1 and 15 minutes to complete. This information is true regardless of the day of the week on which the trip takes place, which is similar to the information found in the NTS data.

3.4 Predict start and end locations

As stated in this chapter, a predictive model was be used to predict the start and end location of a real world EV from EA to determine the availability to provide V2H or V2G services as this is only possible when EVs are connected at home. In this work, the prediction process was divided into two steps:

- **First step**: Data containing features $x_1 - x_9$ will be fed into the *task 1* final predictive model to predict the starting location, y_1.
- **Second step**: Data containing $x_1 - x_9$ and the newly predicted start location, y_1, which in this step will be treated as a feature, will be fed into the *task 2* final predictive model to predict the end location, y_2.

The first step can be seen in listing 3.8 which is part of a custom function that handles the predictions. As seen in this code snippet, the variable `ea_profile` in line 3 contains a copy of the preprocessed EV data of one profile of the stratified sample containing 50 profiles which was stored in the variable `profile_preprocessed`. Then, the variable `ea___start_data` only retains the relevant features to predict the start location, as seen in line 8. Furthermore, the features are scaled using the `scaler_model_1` produced during the training process as seen on line 11 and then reassigned to the variable `ea___start_data` before making predictions as seen on line 14. Then, the variable `predicted_start` contains the predicted labels, y_1, using `classifier_model_1`.

The second step can be seen in listing 3.9. Similarly to the process for the first step shown in listing 3.8, here the variable `ea___end_data` in line 6 contains a copy of the preprocessed EV data but this time it contains the relevant features to predict the end location, which means that the content of the variable `predicted_start` will be used as a feature. Moreover, the numeric data is scaled using `scaler_model_2`

```
...
    # pass preprocessed data of each EV profile
    ea_profile = profile_preprocessed

    # ---
    # 1st step
    # keep columns relevant to make predictions for "step 1"
    ea___start_data = ea_profile[features___step_1]

    # scale numeric columns
    data_scaled = scaler_model_1.transform(ea___start_data[cols_to_scale])

    # assign scaled data back to "ea___start_data"
    ea___start_data[cols_to_scale] = data_scaled

    # predict "Start" --> task 1
    predicted_start = classifier_model_1.predict(ea___start_data)
...
```

Listing 3.8: Process to predict start location using the `classifier_model_1` for one electric vehicle profile.

and reassigned to `ea___end_data`. Then, the variable `predicted_end` contains the predicted labels, y_2, using `classifier_model_2`.

After getting both labels $y_1 - y_2$ that contain the start and end locations for each EV profile of the 50 profile sample, the data is processed as a time series from 2014-08-01 00:00:00 to 2015-07-31 23:59:00 with 1 minute time steps to be fed into the optimisation model introduced in Chapter 4. The decision to keep the data with 1 minute time steps is due to the random nature of the trips, which according to the NTS and EA data sets, trips can start and end at any minute of the day.

3.4.1 Resulting profiles

Figure 3.9 shows the dates that will be used in each results chapter — chapters 5–7. Here, six different dates are reported that are representative of different seasons of the year.

Each plot consists of the total of EVs that are available at home throughout the day during the week, where, as seen, follows a trend of EVs mostly unavailable during typical working hours of the week from 9 am to 5 pm, showing that most EVs

```
...
    # ---
    # 2nd step
    # keep columns relevant to make predictions for "step 2"
    # which contains the "start" label as a feature
    ea___end_data = ea_profile[features___step_2]

    # scale numeric columns
    data_scaled = scaler_model_2.transform(ea___end_data[cols_to_scale])

    # assign scaled data back to "ea_profile"
    ea___end_data[cols_to_scale] = data_scaled

    # predict "End" --> task 2
    predicted_end = classifier_model_2.predict(ea___end_data)
...
```

Listing 3.9: Process to predict the end location using the `classifier_model_2` for one electric vehicle profile.

are at home after 7 pm. The plots also show that during Monday to Friday, it can be expected that fewer EVs are at home compared to the weekend. Furthermore, it should be noted that not all EVs are at home overnight during the week and depending on their electricity tariff, some participants may reduce the chances of saving money by not being able to charge their EV during the night, when electricity prices are usually cheap in some tariffs. All this holds true for the six different dates in the figure. As mentioned, only six weeks will be considered for the remainder of this work. These weeks are described below.

- **Week 1**: For spring, week *Spring - S1* from 2015-04-20 00:00:00 to 2015-04-26 23:59:00.
- **Week 2**: For summer, week *Summer - S2* from 2015-06-22 00:00:00 to 2015-06-28 23:59:00.
- **Week 3**: For summer, week *Summer - S3* from 2014-09-08 00:00:00 to 2014-09-14 23:59:00.
- **Week 4**: For autumn, week *Autumn - S4* from 2014-10-06 00:00:00 to 2014-10-12 23:59:00.

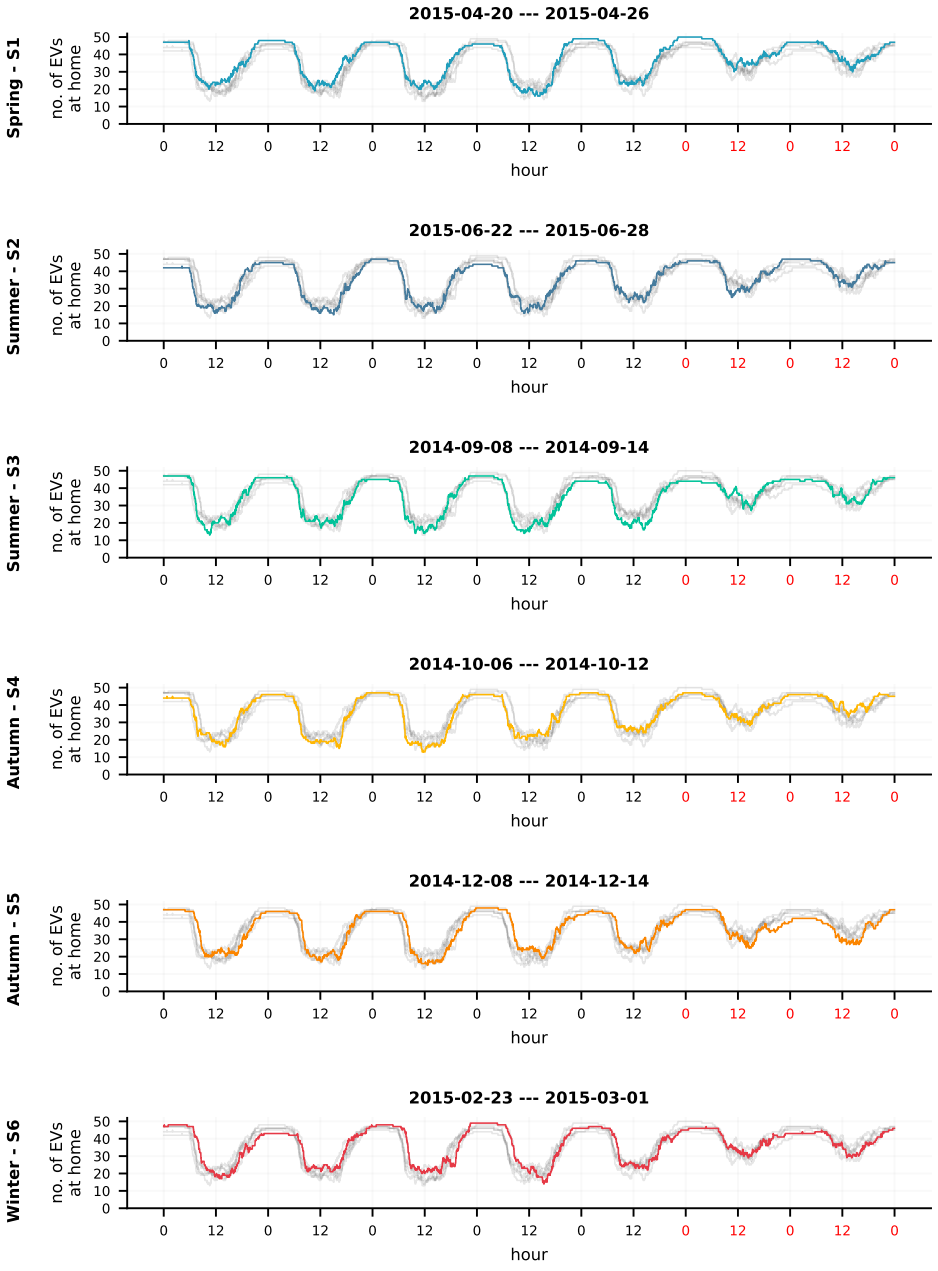

Figure 3.9: Predictions on the EA technology data set showing the number of electric vehicles that are available during a week for the six dates representative of the different seasons of the year that will be used in the following chapters. A comparison of the resulting profiles is made by highlighting the relevant data for each week with the other five weeks. Here, the black *X-axis* labels denote data from Monday to Friday and the red ones, data from Saturday to Sunday.

- **Week 5**: For autumn, week *Autumn - S5* from 2014-12-08 00:00:00 to 2014-12-14 23:59:00.
- **Week 6**: For winter, week *Winter - S6* from 2015-02-23 00:00:00 to 2015-03-01 23:59:00.

3.5 Conclusions

In this chapter, a predictive model was developed using historical data that contain travel information from the UK to predict the start and end location of new data that contain data from real EV residential users from the UK. The model was developed to study the impact of the availability of EVs when using real world EV travel data. Although the model was trained with historical data containing mainly information on ICEV vehicle trips, this approach can be beneficial when predicting travel behaviours irrespective of vehicle type. Despite the potential limitations in reflecting unique EV travel patterns, the predictive model in this chapter, this model, that was validated on mainly ICEV data, represents a crucial step in understanding and generalising travel behaviour. This provided a valuable starting point for studying the impact of EV availability. For this, the historical data was divided into two tasks, *tasks 1* which will predict the start location and *task 2* which will predict the end location.

Three ML algorithms are used and compared using a training and test set for each task. The results suggested that LightGBM outperforms the other two models with a weighted average f1 score of 0.899 and 0.900 for *tasks 1* and *task 2*, respectively. The predictive model was then fine-tuned to improve the chosen model, obtaining a weighted average f1 score of 0.900 and 0.902 for *tasks 1* and *task 2*, respectively.

After processing the new data, this was fed into the predictive model to obtain the start and end location of this new data, which will be used along with the data and the optimisation model which will be explained in the following section.

Chapter 4

Optimising Household Energy Management: A Mixed Integer Linear Programming Model (MILP) for Vehicle-to-grid (V2G) Technology with Peer-to-Peer (P2P) Trading in a Microgrid Context

This chapter introduces an optimisation model that will serve as a tool for studying various case studies involving vehicle-to-grid (V2G) technology. Initially adopted from previous work conducted by Barbour and González [140]. While it was first designed for stationary batteries, we made various modifications to better reflect the behaviour of electric vehicles (EVs), such as their availability during the day. Despite early computational inefficiencies, iterative modifications and testing led to significant improvement. The current model used in this work will be discussed in detail in section 4.2

The model uses mixed integer linear programming (MILP) to schedule EV battery usage at the household level, incorporating V2G technologies to leverage their potential for enhancing energy management and operates within the framework of a

microgrid, which is a localised energy network. The model additionally incorporates peer-to-peer (P2P) energy trading between households within the microgrid. This feature is introduced with the aim of enhancing the performance and value of V2G services. The direct energy exchanges enabled by P2P trading may not only enhance grid stability but also optimise the use of renewable energy. P2P energy transactions are facilitated through the power grid infrastructure within the microgrid, and costs are calculated based on two different price mechanisms, determined by the volume of energy traded.

The optimisation model functions to minimise the total cost of electricity for each household inside the microgrid. It does this by managing different energy sources and storage devices. Depending on the available resources for each case study, the model allocates energy usage efficiently, drawing from solar panels, battery storage, grid import, or P2P transactions. In addition, the model is designed to smartly utilise surplus solar energy, either by storing it in batteries for later use or selling it to the grid or to other households via P2P. The presence of a storage device enables the model to shift energy demand to off-peak hours, reducing the electricity bill further. The main objective of the system is to reduce grid dependency and optimise renewable energy use, all while aiming to minimise the household's total cost of electricity.

The real-world datasets utilised for our simulations, including household electricity demand, photovoltaic (PV) generation, and electricity tariff prices are also introduced in this chapter. Additionally, the different microgrid configurations, each representing a unique case study that will be explored in Chapters 5–7 will be discussed. Finally, we introduce a set of performance and solver metrics, essential for evaluating the microgrid and the optimisation model, respectively. This chapter sets the stage for a deeper investigation into the potential of V2G, P2P energy trading and more efficient energy usage within microgrids. Figure 4.1 shows an overview of the optimisation model used in this work.

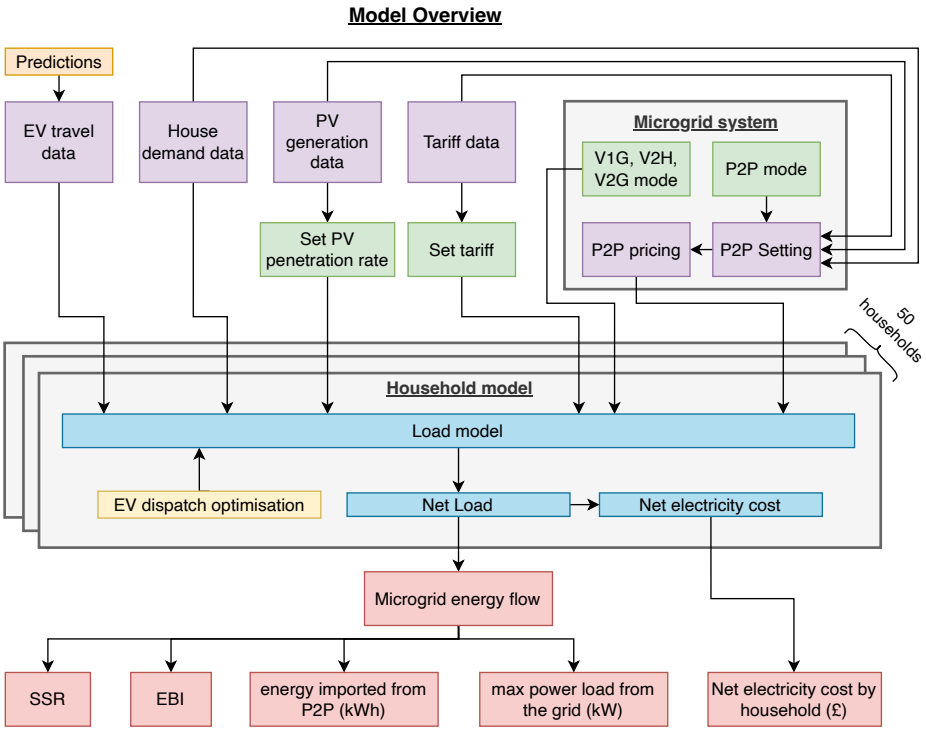

Figure 4.1: Overview of the model showing the flow of data through the optimisation model and the output of the relevant metrics.

4.1 Data processing

This section presents the source and processing of the data used in this research. The purpose of this section is to provide an overview of where the data came from and how it was prepared for use in this thesis. The data was used in Chapter 5, Chapter 6 and were also used to update previously published work described in this chapter.

4.1.1 Electricity house demand

Data collected between 2012 and 2014 by UK Power Networks [141] that contain readings of energy consumption were used for 5,567 London households. The data in question contained readings that were originally recorded at 30-minute intervals. In order to increase the time resolution of the data and make it more suitable for the analysis in this work, the data was processed using the 'interpolate' function from the Pandas library [126]. Specifically, the 'linear' method was applied. As a result, the

data was transformed to have a 1-minute interval resolution. For this work, we used a stratified sample of 50 households by their total annual electricity consumption only considering households with a total annual consumption between 3,000 and 5,000 kWh per year. This range is based on the average household electricity consumption in the UK of 3,731 kWh per year [142, 143]. Figure 4.2 shows an overview of the house demand data used in this work.

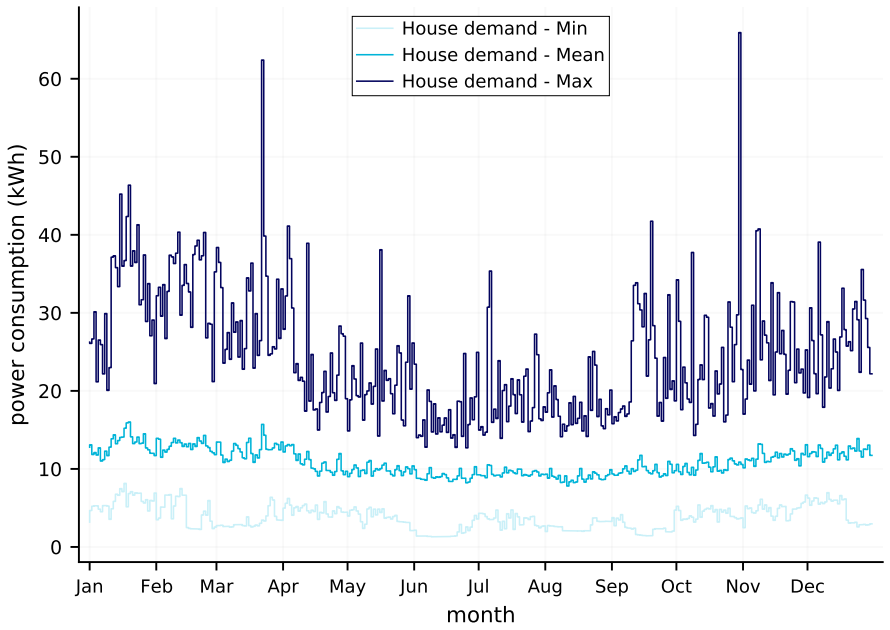

Figure 4.2: Household daily electricity consumption mean, minimum and maximum aggregated values in kWh/day for a year from Jan 01 00:00:00 2013 to Dec 31 23:59:00 2013.

4.1.2 Solar generation

Each modelled household had the same 3.5 kWp PV system. We use data collected by UK Power Networks [144] between 2013 and 2014 in London. These data contain readings that were taken at 1-hour resolution intervals and then interpolated into a 1-minute time resolution for this work. We only considered data collected from late August 2013 to late August 2014. We consider the same data for all households used in this work. Figure 4.3 shows an overview of the PV data used in this work.

The impact of using this uniform dataset, is considerable in this study. As every modelled household had the same 3.5 kWp PV system, this consistency in data

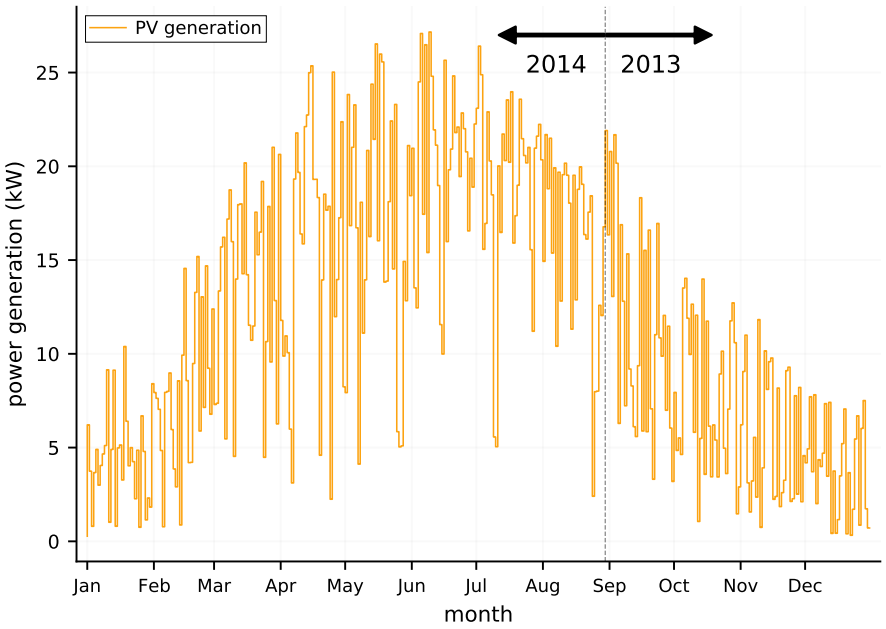

Figure 4.3: Averaged PV daily solar energy generation for a year from Jan 01 00:00 2014 to Aug 29 23:59 2014 and from Aug 30 00:00 to Dec 31 23:59 2013.

allows for a fair comparison of results across different households. This eliminates any potential variability that could arise due to differences in PV system capacity.

The 1-minute time resolution, obtained by interpolating from the original 1-hour interval readings, provides a detailed insight into the PV systems' performance. This granularity helps in understanding subtle fluctuations and trends in the energy output that might have been overlooked in a lower resolution dataset.

However, it is important to note that the data is specific to one geographical location and one-year period. Consequently, the findings might be less applicable to other locations or periods with different weather patterns, as solar power generation is highly dependent on such conditions. Furthermore, the universal use of the same data for all households may not account for unique household characteristics that could impact energy consumption and production patterns.

Overall, the high-resolution, consistent dataset allows for detailed and controlled analysis but may limit the study's wider applicability.

4.1.3 Electricity tariffs

The following section will describe various electricity tariffs and their prices used in this work. This information will be essential in assessing the impact of different energy tariffs in the following chapters.

4.1.3.1 Agile tariff

A dynamic tariff introduced by Octopus Energy in the UK was used, where the user has access to half-hourly energy prices tied to wholesale prices and updated daily [145]. Octopus Energy calls this tariff *Agile*. This energy price varies depending on the region in the UK. In this case, we used data for the London area. Figure 4.4 shows an overview of the prices of this tariff for 2019.

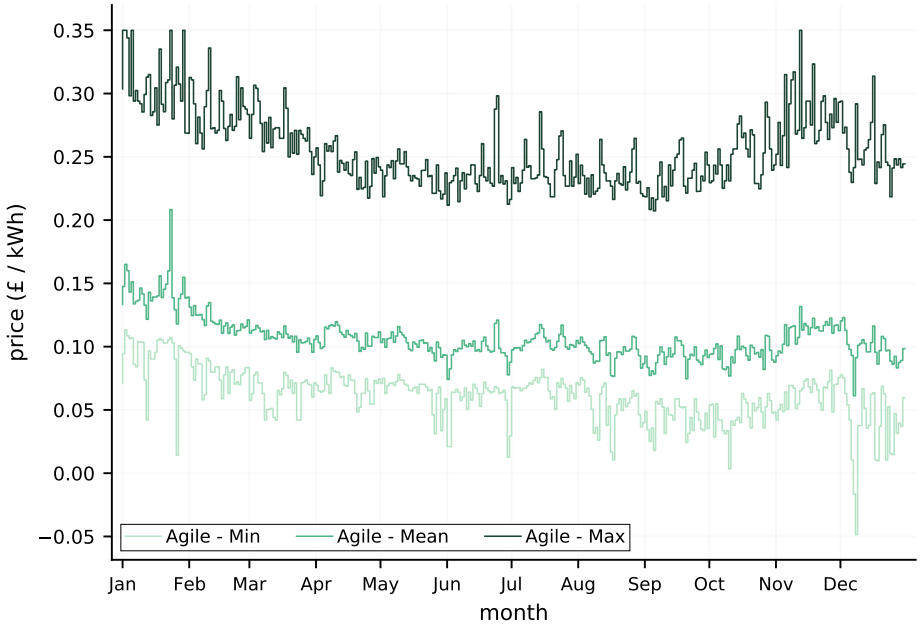

Figure 4.4: Agile energy tariff with mean, minimum and maximum values of daily prices for a year from Jan 01 00:00 2019 to Dec 31 23:59 2019.

4.1.3.2 Agile outgoing tariff

Figure 4.5 shows an overview of the prices that were used when selling surplus solar generation, taken from mid-May 2019 to mid-May 2020. These prices were introduced by Octopus Energy in the UK and they call this tariff *Agile Outgoing*

[146]. As in section 4.1.3.1, these sales prices vary depending on the region in the UK. Again, in this case, we used data for the London area.

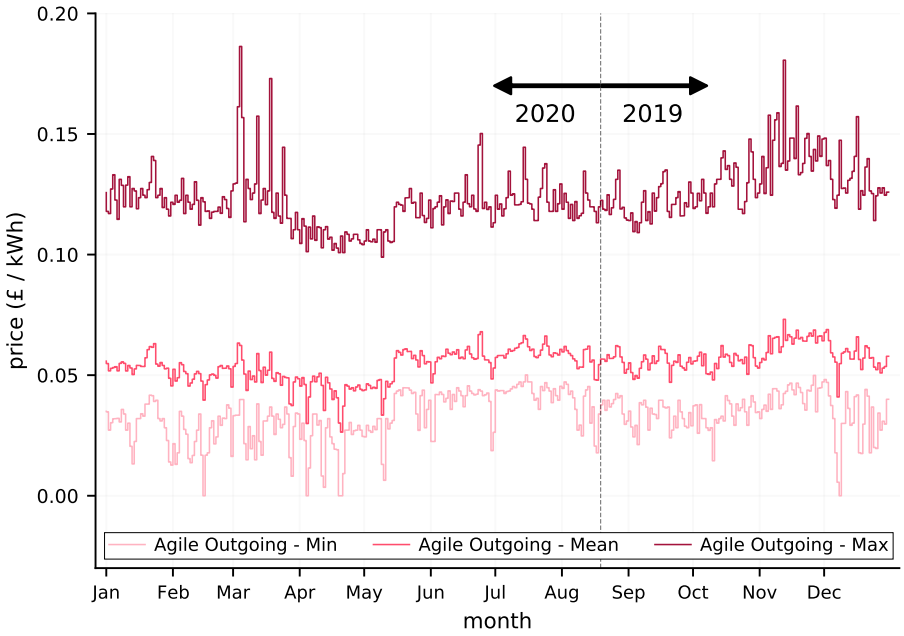

Figure 4.5: Agile outgoing energy tariff with mean, minimum and maximum values of daily prices for a year from Jan 01 00:00 2020 to May 15 23:59 2020 and from May 16 00:00 2019 to Dec 31 23:59 2019.

4.1.3.3 Fixed tariffs

For this work, we also used data that contain electricity tariffs for the price of electricity for a Flat tariff, which has the same price regardless of the time of the day [147]. A tariff called economy seven (E7) tariff that offers two different prices depending on the time of day with a lower price for seven hours at night [147]. A recently introduced tariff called *Agile Go* with a low rate for four hours every night and a competitive price rate for the rest of the day [148]. All these tariffs are offered by Octopus Energy for the London WC1E 6BT area. Finally, we also consider the price of changing an EV using rapid charging on the street [149, 150]. Table 4.1 shows a summary of the electricity price data for these tariffs.

Table 4.1: Summary of the fixed tariffs used in this work with prices for each time of day.

Tariff	time	price (£ / kWh)	time	price (£ / kWh)
Agile Go	00:30 - 04:29	0.05	04:30 - 00:29	0.2376
Economy 7	00:00 - 06:59	0.1766	07:00 - 23:59	0.2893
Flat	00:00 - 23:59	0.1835	-	-
Street Charging	00:00 - 23:59	0.30	-	-

4.2 Electric vehicle dispatch optimisation for a household

The optimisation model used in this research to schedule the battery charge and discharge cycles of EVs was initially adapted from previous work conducted by Barbour and González [140]. We then modified their model, which involved a stationary battery, to incorporate parameters indicating the availability and battery discharge in an EV during travel. This first model, despite effectively reflecting the behaviour of EVs, it was notably slow due to its design which consumed substantial computational resources when solving it. This adaptation, nonetheless, marked the beginning of a series of iterative developments, each aiming to improve efficiency and reduce resource use. The process culminated in the current study's model, which significantly improves its capabilities and efficacy.

Efficient model design is important in linear programming, as it directly influences the performance of the solver used. It is worth noting, however, that the model construction itself is also a time-consuming process, often taking up a significant portion of the overall solution process. Therefore, a thoughtful and efficient model design not only benefits the optimisation process but also reduces the time spent on constructing the model itself. The optimisation process heavily relies on the design of the model, which, if developed effectively, can significantly reduce computational load and improve solving times, as well as expedite the construction process [151, 152].

Furthermore, the first significant improvement to the model was described in Aguilar-Dominguez et al. [153]. The focus of this paper was on analysing EVs util-

ising Vehicle-to-home (V2H) technology versus traditional home batteries. Here, the model represented the behaviour of an EV, introducing constraints, parameters, and variables as necessary. The work published in Aguilar-Dominguez et al. [154] marked another substantial refinement, where we improved the model to address the availability of EVs more effectively. This led to further reduction in solving time, making the model a more efficient tool for analysis and optimisation. In Aguilar-Dominguez et al. [155], we made additional adjustments to the model to further improve solving times.

In between and alongside these published works, numerous smaller adjustments and refinements were made based on extensive testing. These continuous refinements have gradually improved the model's capabilities and efficacy, leading up to its current form in this study. Notably, the present model operates much more efficiently, taking approximately between 7 to 20 minutes per model - a significant reduction from the previous 6 hours, or in some rare cases more than that, it used to take to solve each microgrid scenario. This model can also handle multiple EVs simultaneously within a microgrid, a feature not available in the previous versions of the model. In addition, we have introduced P2P energy trading into the model in the current study, a new feature that allows us to explore the impact of implementing P2P within a microgrid.

Therefore, while the initial model was based on the previous work conducted by Barbour and González [140], the current model reflects a series of developments and refinements that we have made over the years. Through this iterative process, the model has evolved to be a more efficient and practical tool for assessing real-world scenarios.

The optimisation model described in this section uses a MILP approach and will be used in chapters 5–7. Any updates or modifications made to the model presented in this chapter will be discussed further in each respective chapter. Previous versions of this model can be found in publications [153, 154, 155].

The optimisation model will be solved using the Gurobi 9.5.2 [156] solver and was built using the Python 3.8.8 [125] programming language and the Pyomo 6.3.0 library [157]. This optimisation model is explained below.

4.2.1 Constraints on the electric vehicle battery

The model is constrained by the physical limits of EV's state of charge (SOC), given by equation (4.1). For this work, we consider $SOC^{min} = 0.05$ and $SOC^{max} = 0.95$. These values are used to mimic real-world conditions and preserve the longevity of the EV's battery [105].

Fully charging or discharging a battery, especially a lithium-ion battery commonly found in EVs, can be detrimental to its health over time, reducing its lifespan. Therefore, it's common to set a buffer on both ends to prevent these extremes.

The lower limit, $SOC^{min} = 0.05$, ensures that the battery never fully discharges, which can cause irreversible damage to the battery cells. On the other hand, the upper limit, $SOC^{max} = 0.95$ prevents the battery from being fully charged, which can also harm the battery due to excessive voltage.

$$SOC^{min} \leq E_{v,t}^{SOC} \leq SOC^{max}, \quad \forall v, t \tag{4.1}$$

Equations (4.2)–(4.4) describe the energy stored inside the battery for each vehicle, including initial and final values, where η refers to the efficiency of the charger. $E_{v,t}^{SOC}$ refers to the state of charge of the electric vehicle at time t. SOC^{init} and SOC^{final} are the initial and final SOC values for each electric vehicle, 50% of the original battery capacity in both cases. The SOC^{final} is the expected minimum SOC at the end of each week for each household, while the SOC^{init} is the initial SOC already in the battery system. This means that each household is expected to have at least 50% of its battery's original capacity at the end of each week, and that it will start each week with 50% of its battery's original capacity. $E_{v,t}^{charge}$ refers to the energy charged to the EV at time t when at *Home*. $E_{v,t}^{charge,street}$ refers to the energy charged to the EV from the use of street charging at time t when the EV is away from *Home* and is not used for travel purposes. $E_{v,t}^{discharge}$ refers to the energy discharged to the house at time t. $E_{v,t}^{discharge,v2g}$ refers to the energy discharged to the grid for V2G at time t. $E_{v,t}^{demand,vehicle}$ refers to the energy required for the EV's travel demand at time t. It is assumed that the same efficiency η applies for both charge and discharge cycles.

$$E_{v,init}^{SOC} = SOC^{init} * SOC, \quad \forall v \tag{4.2}$$

$$E_{v,final}^{SOC} \geq SOC^{final} * SOC, \quad \forall v \tag{4.3}$$

$$\begin{aligned} E_{v,t}^{SOC} = E_{v,t-1}^{SOC} &+ \left[\left(E_{v,t}^{charge} + E_{v,t}^{charge,street} \right) * \eta \right] \\ &- \left[\left(E_{v,t}^{discharge} + E_{v,t}^{discharge,v2g} \right) * \frac{1}{\eta} \right] \\ &- E_{v,t}^{demand,vehicle}, \qquad \forall v, t > 0 \end{aligned} \tag{4.4}$$

Equation (4.4) is the result of extensive testing aimed at improving the efficiency and accuracy of our EV energy model In this model, $E_{v,t-1}^{SOC}$ plays a crucial role as it represents the prior state of charge of the EV. It updates the SOC based on any relevant changes such as energy charged at home or on the street, discharged to the home or grid, or energy used for travel.

Equations (4.5) and (4.6) describe the maximum charge and discharge power of the bidirectional charger. In this case, $P^{max,ch}$ and $P^{max,dis}$ are 7.4 kW [158]. Equation (4.7) reflects the maximum charge power of the EV when using rapid charging on the street, where the maximum power in this case is 50 kW [149, 150]. dt refers to the time step, in this case $dt = 1\ min = \frac{1}{60}\ hr$.

$$E_{v,t}^{charge} \leq P^{max,ch} * dt, \quad \forall v, t \tag{4.5}$$

$$E_{v,t}^{discharge} + E_{v,t}^{discharge,v2g} \leq P^{max,dis} * dt, \quad \forall v, t \tag{4.6}$$

$$E_{v,t}^{charge,street} \leq P^{max,street} * dt, \quad \forall v, t \tag{4.7}$$

Equations (4.8) and (4.9) control the charge / discharge cycles of the EV. Here, $B_{v,t}^{charge}$ and $B_{v,t}^{discharge}$ are binary variables. Equation (4.10) manages street charging when the EV is not at *Home* and not driving. Equation (4.11) restricts charge and discharge at the same time when the EV is available at home. $\alpha_{v,t}^{avail,home}$ describes

the availability at home of each electric vehicle to charge or discharge at time t. $\alpha_{v,t}^{avail,street}$ describes the availability to charge with a street charger at time t. In both cases, 1 means that it is available and 0 means that it is not available. For $\alpha_{v,t}^{avail,street}$, the EV is available to be charged with a street charger, i.e. $\alpha_{v,t}^{avail,street} = 1$, when it is not at *Home* and also not in motion. This means that the EV is likely parked at a different location, which in this work is referred to as *Other*, and assumed to be parked with access to a public charging station available for street charging.

$$E_{v,t}^{charge} \leq B_{v,t}^{charge} * M, \quad \forall v, t \tag{4.8}$$

$$E_{v,t}^{discharge} + E_{v,t}^{discharge,v2g} \leq B_{v,t}^{discharge} * M, \quad \forall v, t \tag{4.9}$$

$$E_{v,t}^{charge,street} \leq \alpha_{v,t}^{avail,street} * M, \quad \forall v, t \tag{4.10}$$

$$B_{v,t}^{charge} + B_{v,t}^{discharge} \leq \alpha_{v,t}^{avail,home}, \quad \forall v, t \tag{4.11}$$

In our study, as mentioned, we effectively managed the charge and discharge cycles of EVs based on their availability using equation (4.11). Here, $\alpha_{v,t}^{avail,home}$ in this equation is sourced from a dataset we produced in Chapter 3. This dataset is in the form of a time series containing the availability information of the EVs. $\alpha_{v,t}^{avail,street}$ is also sourced from the same dataset. This specifically focuses on setting the availability of vehicles for street charging when they are away and not actively driving.

Despite some prior studies using availability data directly in the equations that describe the EV's SOC, as seen in references [105, 159], we took a different approach. Instead of directly using $\alpha_{v,t}^{avail,home}$ into our SOC in equation (4.4), we incorporated it into equation (4.11). During our testing, equation (4.11) has proven to be more efficient, improving the solution-finding of our model.

4.2.2 Solar generation

Equation (4.12) indicates the total power generated by the PV system of each household, where $E_{v,t}^{solar}$ is the solar generation at time t. $E_{v,t}^{solar,used}$ the solar power used by the home to its domestic loads, to charge the EV's battery or both. $E_{v,t}^{solar,export}$ is the surplus solar power sold to the grid. $E_{v,t}^{solar,p2p}$ is the solar power surplus sold towards P2P.

$$E_{v,t}^{solar} = E_{v,t}^{solar,used} + E_{v,t}^{solar,export} + E_{v,t}^{solar,p2p}, \quad \forall v, t \tag{4.12}$$

In equation (4.12), we propose to split the solar energy generated into three parts. This is different from our earlier work. With this equation, we can better keep track of solar energy use. It allows us to see how much of the solar energy goes directly to the house, how much is exported to the grid, and how much is used for P2P sharing. This P2P part is a new addition, and it helps us understand how much energy is shared with others within a microgrid, as it will be described in section 4.4.6.

4.2.3 Power Balance

Equations (4.13) and (4.14) describe the power balance and net power of each household, respectively, where $E_{v,t}^{import,total}$ and $E_{v,t}^{export,total}$ are the total energy imported and exported from and to the grid at time t. $E_{v,t}^{net}$ is the net power required for the house or exported from the household at time t. $E_{v,t}^{demand,house}$ is the energy required from the house at time t. Equation (4.15) describes that $E_{v,t}^{import,total}$ is the sum of $E_{v,t}^{import,grid}$ and $E_{v,t}^{import,p2p}$, which is the energy imported from the grid and from P2P at time t. Equation (4.16) describes that $E_{v,t}^{export,total}$ is the sum of all energy exported from the household to the grid or P2P.

$$E_{v,t}^{solar,used} + E_{v,t}^{import,total} + E_{v,t}^{discharge} = E_{v,t}^{demand,house} + E_{v,t}^{charge}, \quad \forall v, t \tag{4.13}$$

$$E_{v,t}^{net} = E_{v,t}^{import,total} - E_{v,t}^{export,total}, \quad \forall v, t \tag{4.14}$$

$$E_{v,t}^{import,total} = E_{v,t}^{import,grid} + E_{v,t}^{import,p2p}, \quad \forall v,t \tag{4.15}$$

$$E_{v,t}^{export,total} = E_{v,t}^{solar,export} + E_{v,t}^{solar,p2p} + E_{v,t}^{discharge,v2g}, \quad \forall v,t \tag{4.16}$$

Here, we also updated the equation (4.13) from our previous work. In this new version, we proposed to no longer include any reference to the energy exported, in this case, $E_{v,t}^{export,total}$. Instead, this equation consists of energy inputs to satisfy the demands on the right side of the equation.

It is important to note that now $E_{v,t}^{import,total}$ include two variables, one referring to the energy drawn from the grid and another include the energy that is imported from P2P energy sharing. Similarly, $E_{v,t}^{export,total}$ includes three variables, energy exported from the grid, energy exported to P2P within the microgrid, in this case both from solar surplus, and energy exported from the EV for V2G services.

We found that these changes improve the solution times, making the whole process more efficient.

Equations (4.17) and (4.18) prevent energy import when energy is exported from the household at time t. $B_{v,t}^{export}$ is a binary variable. M is a sufficiently large positive number.

$$E_{v,t}^{import,total} \leq \left(1 - B_{v,t}^{export}\right) * M, \quad \forall v,t \tag{4.17}$$

$$E_{v,t}^{export,total} \leq B_{v,t}^{export} * M, \quad \forall v,t \tag{4.18}$$

4.2.4 Peer-to-peer electricity exchange

Equation (4.19) shows that the power transferred into and out of the system by domestic users who participate in the P2P market should be equal over each period of time by domestic users who participate in P2P. For this work, only solar surplus generation will be used for P2P energy trading

$$\sum_{v} \left(E_{v,t}^{import,p2p}\right) = \sum_{v} \left(E_{v,t}^{solar,p2p}\right), \quad \forall t \tag{4.19}$$

Furthermore, while we were exploring the implementation of P2P dynamics within a microgrid,, we implemented equation (4.19). We found that the inclusion of this equation significantly reduced solving times, enhancing both computational speed and overall model efficiency.

This approach was taken to deepen our understanding of the impact of P2P energy sharing within a microgrid, particularly in terms of EVs and V2G systems such as the provision of short term operation reserve (STOR) services, which will be detailed in Chapter 6. Our tests consistently demonstrated that the addition of equation (4.19) led to faster solving times and improved result quality.

Interestingly, we found out near the end of our study that similar methodology had been implemented in earlier research, particularly by Yaldız et al. [160], with a primary focus on stationary batteries. While it was initially thought to be a novel contribution, our independent convergence on this method and effective application of equation (4.19) reaffirms the robustness of our methodology.

Even with prior applications, our study makes a significant contribution by successfully applying P2P in a microgrid context involving multiple EVs and V2G applications. It offers new insights and extends the current understanding of P2P interactions within microgrids.

4.2.5 Import and export costs

Equations (4.20)–(4.25) describe the different electricity costs involved in the exchange of energy in and out of the home. Here, $Pr_{v,t}^{buy,grid}$ is the price of the energy tariff for importing energy from the grid, and this price will vary depending on the energy tariff of each user. $Pr_{v,t}^{buy,street}$ is the price of charging with a street charger. For this work, this price is £0.30/kWh [149, 150]. $Pr_{v,t}^{buy,p2p}$ is defined as the price that will be charged for the import of energy from P2P. The price to sell surplus solar energy to the grid is $Pr_{t}^{sell,grid}$. In this case, it is assumed that all households are under the same selling tariff when selling energy to the grid. $Pr_{t}^{sell,p2p}$ is the price of selling energy to P2P. The calculation of P2P prices will be explained later. Finally, $Pr_{v,t}^{sell,v2g}$ is the price of selling energy to V2G. This price will be introduced in the relevant chapter.

$$C_v^{import} = \sum_t \left(Pr_{v,t}^{buy,grid} * E_{v,t}^{import} \right), \quad \forall v \tag{4.20}$$

$$C_v^{import,street} = \sum_t \left(Pr_t^{buy,street} * E_{v,t}^{charge,street} \right), \quad \forall v \tag{4.21}$$

$$C_v^{import,p2p} = \sum_t \left(Pr_{v,t}^{buy,p2p} * E_{v,t}^{import,p2p} \right), \quad \forall v \tag{4.22}$$

$$C_v^{export} = \sum_t \left(Pr_t^{sell,grid} * E_{v,t}^{solar,export} \right), \quad \forall v \tag{4.23}$$

$$C_v^{export,p2p} = \sum_t \left(Pr_{v,t}^{sell,p2p} * E_{v,t}^{solar,p2p} \right), \quad \forall v \tag{4.24}$$

$$C_v^{export,v2g} = \sum_t \left(Pr_t^{sell,v2g} * E_{v,t}^{discharge,v2g} \right), \quad \forall v \tag{4.25}$$

4.2.6 Objective function

From the end user's point of view, the cost of operation represents a fundamental target that needs to be minimised.

Here, the objective function represents the total cost of electricity for each household by choosing the most efficient way to meet its energy needs. This can include using solar panels, storing energy in a battery, importing electricity from the grid or from P2P, or selling solar surplus to the grid or for P2P. When solar generation is present, optimising the total cost of electricity can reduce the amount of energy that is imported from the grid, store it in the battery for later used, or also sell solar surplus energy to the grid. Additionally, if P2P energy trading is allowed, households can sell their excess electricity to other households, which can further reduce the amount of energy that is imported from the grid. This can benefit both buyers and sellers, as buyers can get cheaper electricity and sellers can make a profit. The presence of a battery can also help to shift the energy demand at certain times of

the day when prices tend to be high, which mostly happens during peak times. This can help to reduce the household's energy bill and its impact on the grid.

Therefore, a function that represents the total energy cost of a household is given by equation (4.26).

$$min \sum_{v} \Bigg(C_v^{import} + C_v^{import,street} + C_v^{import,p2p} - C_v^{export} - C_v^{export,p2p} - C_v^{export,v2g} \Bigg) \tag{4.26}$$

4.3 Peer-to-peer (P2P) price calculation

To calculate the prices for buying and selling energy from P2P, two different settings are explored. It is worth noting that in this work we considered that users may have different buying energy tariffs from each other, and, as was mentioned before, users have the same selling energy tariff. This means that participants will have buy and sell P2P prices according to the energy tariff they have. In addition, two different settings will be considered as seen Table 4.2.

Table 4.2: Overview of the different settings in which the microgrid can operate.

Name	Setting	Description
Setting one	$P2P\_Sett\_One$	Prices for buying and selling energy between peers will be calculated according to the local energy demand and the generation of the microgrid
Setting two	$P2P\_Sett\_Two$	Prices for buying and selling energy between peers will be calculated as the average price of the retail buying and selling prices of each participant

4.3.1 Setting one

In this setting, we use the mid-market rate (MMR) to set the trading price for both buying and selling energy through P2P [161, 103]. This setting applies only when $P2P\ setting\ =\ S1$. This trading setting consists of three different scenarios. MMR

price calculation requires to calculate $Pr_{v,t}^{mid,p2p}$ as in equation (4.27), which is the mean price of the purchase of the energy tariff for each user of the microgrid and the sale of the energy tariff to sell the surplus of their solar energy to the grid. Furthermore, we need to obtain $E_t^{delta,p2p}$, which is the energy imbalance between generation and demand of the entire community system, as given by equation (4.28).

$$Pr_{v,t}^{mid,p2p} = \frac{Pr_{v,t}^{buy,grid} + Pr_{v,t}^{sell,grid}}{2}, \quad \forall v, t \tag{4.27}$$

$$E_t^{delta,p2p} = \sum_v E_{v,t}^{solar} - \sum_v E_{v,t}^{demand,house}, \quad \forall t \tag{4.28}$$

- if $E_t^{delta,p2p} = 0, \quad \forall t$

  This scenario refers to the case where the total energy generation of the users is equal to their total energy demand. This means that users who participate in P2P energy trading will get the same P2P buying and selling prices as given by equation (4.29).

$$Pr_{v,t}^{buy,p2p} = Pr_{v,t}^{sell,p2p} = Pr_{v,t}^{mid,p2p}, \quad \forall v, t \tag{4.29}$$

- if $E_t^{delta,p2p} > 0, \quad \forall t$

  The total energy generation of users is greater than the total energy demand. This means that the P2P purchase price is equal to $Pr_{v,t}^{mid,p2p}$ and the P2P sale price may be lower than the agile outgoing price given by equation (4.30).

$$\begin{aligned} Pr_{v,t}^{buy,p2p} &= Pr_{v,t}^{mid,p2p}, \quad \forall v, t \\ Pr_{v,t}^{sell,p2p} &= \frac{Pr_{v,t}^{mid,p2p} * \sum_v E_{v,t}^{demand,house} + E_t^{delta,p2p} * Pr_{v,t}^{sell,grid}}{\sum_v E_{v,t}^{solar}}, \quad \forall v, t \end{aligned} \tag{4.30}$$

- if $E_t^{delta,p2p} < 0, \quad \forall t$

In this case, the total energy generation of the users is less than the total energy demand. This means that the P2P sale price is equal to $Pr_{v,t}^{mid,p2p}$ and the purchase price may be equal to the user's buying price tariff from the grid or close to $Pr_{v,t}^{mid,p2p}$ as in equation (4.31)

$$\begin{aligned} Pr_{v,t}^{buy,p2p} &= \frac{Pr_{v,t}^{mid,p2p} * \sum_{v} E_{v,t}^{solar} - E_{t}^{delta,p2p} * Pr_{v,t}^{buy}}{\sum_{v} E_{v,t}^{demand,house}}, \quad \forall v,t \\ Pr_{v,t}^{sell,p2p} &= Pr_{v,t}^{mid,p2p}, \quad \forall v,t \end{aligned} \tag{4.31}$$

4.3.2 Setting two

Similarly to section 4.3.1, MMR is used to calculate the trading price for both buying and selling energy through P2P. However, in this setting, the $Pr_{v,t}^{mid,p2p}$ described in equation (4.27) is used to set the buying and selling prices to trade energy between peers in the microgrid. This setting applies when $P2P\ setting = S2$. This approach has been used successfully by Englberger et al. [104] to assess the impact of P2P when using energy storage systems. With this approach, the incentive for participants to trade energy with their peers is the same for buying and selling for all participants in the microgrid. Therefore, for this setting, the prices are calculated as described in equation (4.32).

$$Pr_{v,t}^{buy,p2p} = Pr_{v,t}^{sell,p2p} = Pr_{v,t}^{mid,p2p} = \frac{Pr_{v,t}^{buy,grid} + Pr_{v,t}^{sell,grid}}{2}, \quad \forall v,t \tag{4.32}$$

4.4 Microgrid system configuration

In this work, we consider different configurations that affect the interaction of participants in a microgrid. These configurations affect the way households participate in smart charging (V1G), V2H, V2G and P2P trading. Table 4.3 shows an overview of the different modes that will change the way the microgrid will operate, three control how EVs will interact when connected to the home using a bidirectional charger, and two control whether or not to allow P2P energy trading. These modes

are discussed further in the following subsections.

Table 4.3: Overview of the different settings in which the microgrid can operate.

Name	Mode	P2P Status	Description
Smart charging	$V1G$	No $P2P$	EVs only allowed to use smart charging
Smart charging	$V1G$	$P2P$	EVs only allowed to use smart charging, P2P trading allowed
Vehicle-to-home	$V2H$	No $P2P$	EVs allowed to give energy to the house, includes the benefits of V1G mode
Vehicle-to-home	$V2H$	$P2P$	EVs allowed to give energy to the house, includes the benefits of V1G mode, P2P trading allowed
Vehicle-to-grid	$V2G$	No $P2P$	EVs allowed to give energy to the grid, includes the benefits of V1G and V2H mode
Vehicle-to-grid	$V2G$	$P2P$	EVs allowed to give energy to the grid, includes the benefits of V1G and V2H mode, P2P trading allowed

4.4.1 Smart charging (V1G) mode

V1G is a safe and practical method of charging an EV in periods when the demand for power is lower, including at night or when there is a surplus of renewable energy in the grid. Therefore, to achieve this mode and only allow EVs to participate in V1G, equation (4.33) applies only when $V2G\ mode\ =\ V1G$. This mode will be considered as the baseline setup, which means that households will take energy from the grid to cover their energy demand needs and EVs cannot participate in V2H. In this mode, households with solar energy generation will also be able to use it to charge the EV battery.

$$E_{v,t}^{discharge} + E_{v,t}^{discharge,v2g} \leq 0, \quad \forall v, t \tag{4.33}$$

Applying equation (4.33), the ability of EVs to discharge energy back to the home or to the grid is effectively deactivated and only allows the flow of energy from the home to the battery, which means that EVs will only be able to charge the necessary energy to provide transport.

4.4.2 Vehicle-to-home (V2H) mode

V2H and V2G are similar to each other, since both involve bidirectional power flows to and from the EVs' battery. What makes V2H different is that it uses the energy already stored in the EV' battery to power the participant's household.

In this mode, EVs are allowed to discharge energy back to the house whenever they are connected using the bidirectional charger at home. This will enable EVs to schedule the charging and discharge behaviour of the energy storage system when it is more convenient during the day, for example, when electricity prices are high or low, or if there is a surplus of solar energy and then used it later only to meet the energy needs of the household. This mode also enables the use of V1G and its benefits. Therefore, to achieve this mode, equation (4.34) applies only when $V2G\ mode\ =\ V2H$.

$$E_{v,t}^{discharge,v2g} \leq 0, \quad \forall v, t \tag{4.34}$$

With equation (4.34), the ability to provide energy for V2G is completely restricted.

4.4.3 Vehicle-to-grid (V2G) mode

V2G enables EVs to sell energy in the EV's battery back to the power grid. In this mode, EVs are allowed to discharge energy back to the grid whenever they are connected using the bidirectional charger at home. This will allow EVs to sell energy and will allow the owners to make a profit. This mode also enables the use of V1G and V2H and its benefits. Therefore, this mode does not apply any restrictions to the model and allows the energy discharge from the EVs' battery toward both the household and the grid. This mode occurs when $V2G\ mode\ =\ V2G$.

4.4.4 No Peer-to-peer (P2P) mode

For this work, we explore the impact of energy trading through P2P within a microgrid. This configuration controls the energy sources allowed to participate in P2P or not participate in P2P at all. This mode does not affect the self-consumption of solar generation and its use of EVs subject to $V2G\ mode$.

To assess this impact, we need to establish a baseline system in which households are not allowed to trade energy to P2P. Therefore, equation (4.35) only applies when $P2P\ mode\ =\ No\_P2P$.

$$E_{v,t}^{import,p2p} \leq 0, \quad \forall v, t \tag{4.35}$$

When this P2P mode is applied to the microgrid, households are not allowed to trade surplus solar generation between peers and are only allowed to use that surplus energy for self-consumption or sell it to the grid.

4.4.5 Peer-to-peer (P2P) mode

This mode will allow participants to trade energy with their peers in the microgrid. This mode is in place only if $P2P\ mode\ =\ P2P$. To properly operate this mode, one of the two settings described in section 4.3 must be selected.

4.4.6 Performance Metrics

To compare the performance of the different scenarios that will be explored in this work, different performance metrics are considered. These metrics are described in the following.

- **Self-suffiency ratio (SSR):** This metric is responsible for measuring the independence of the microgrid and is defined as the percentage of the demand of the microgrid that is directly met by solar generation or battery discharge on site, rather than being met by the electrical grid [162, 163]. This is calculated by equation (4.36).

$$SSR = \sum_{v} \sum_{t} \left[\frac{\left(E_{v,t}^{demand,house} + E_{v,t}^{charge} \right) - E_{v,t}^{import,grid}}{\left(E_{v,t}^{demand,house} + E_{v,t}^{charge} \right)} \right] * 100 \quad (4.36)$$

- **Energy balance index (EBI):** This metric is a grid independence metric similar to SSR, but penalises both imports and exports from and to the grid [105, 164]. The EBI is a measure of the net power exchange between microgrid and the electrical grid, specifically the imports and exports between the two. This can be used to identify areas where there may be a need for network reinforcement as large power flows in either direction may require costly network reinforcement. It can also be helpful in identifying microgrids that are exporting a lot of energy or that are importing a lot of energy. This metric is defined by equation (4.37).

$$EBI = \left\{ 1 - \sum_{v} \sum_{t} \left[\frac{E_{v,t}^{import,grid} + E_{v,t}^{solar,export}}{\left(E_{v,t}^{demand,house} + E_{v,t}^{charge} \right) + E_{v,t}^{solar}} \right] \right\} * 100 \quad (4.37)$$

- **Total energy imported between peers:** This is the total energy imported from the energy shared between peers when P2P is allowed in the microgrid. This is described in equation (4.38).

$$\text{Total energy imported P2P} = \sum_{v} \sum_{t} \left(E_{v,t}^{import,p2p} \right) \quad (4.38)$$

- **Maximum power load:** This is the maximum power load of the microgrid registered when energy is imported from the grid.

- **Weekly mean electricity cost:** This is the mean electricity cost per week of the profiles in the microgrid.

- **Annual electricity cost:** This is an estimate of the annual electricity cost of the profiles in the microgrid. This estimation of annual electricity costs is done assuming 52 weeks to a year. Each chapter will include details of how

the dates used will contribute towards the annual electricity cost. Here, the mean annual electricity costs will be considered.

4.4.7 Solver Metrics

In this work, Gurobi 9.5.2 [156] is used as a solver for the models presented in the following chapters. Gurobi is a mathematical optimisation solver that can solve a wide variety of optimisation problems, including linear programming (LP), MILP, quadratic programming (QP), and mixed integer quadratic programming (MIQP).

In the case of solving MILP problems using Gurobi, these are generally solved using a LP based branch-and-bound algorithm. This algorithm is based on recursively dividing the problem into smaller subproblems and solving them to find an optimal solution. The branch-and-bound algorithm relies on the concepts of upper and lower bounds to find the optimal solution. The upper bound represents the best known solution, while the lower bound is the minimum possible value that can be obtained. The difference between these bounds, called the gap, indicates the optimality of the solution. When the gap reaches zero, the optimal solution has been found [165].

For a MILP minimisation problem, to determine the lower bound, a relaxation of the subproblem is solved at each surviving node of the search tree and subsequently selecting the minimal objective value among these nodes. As a result, during the solving process, at any given point the upper bound is known to be feasible since it comes from the incumbent solution — the best integer solution identified thus far during the algorithm's search process. While it is unclear if further improvements can be achieved, it is assumed that the optimal objective value cannot exceed the lower bound. Moreover, the upper bound is improved as new incumbents are found, and the lower bound is refined as nodes are removed from the search tree [166].

To improve the efficiency of the branch-and-bound algorithm on getting an optimal solution as fast as possible, Gurobi implements various techniques, such as presolve, cutting planes, heuristics, and parallelism. Presolve is a technique that can be used to reduce the size of the problem before the branch-and-bound algorithm is applied, making it easier to solve. Cutting Planes are mathematical constraints that can be used to eliminate parts of the search space, further simplifying the search pro-

cess. Heuristics generate good starting points for the branch-and-bound algorithm, which can lead to faster convergence. Parallelism is a technique that can be used to speed up the solution of the problem by dividing it into multiple subproblems that can be solved concurrently [165].

In order to evaluate the quality of the solutions produced by Gurobi, and by extension, the results presented through this work, the optimality gap will be used as a metric. This metric is described below.

- **Optimality gap:** As already introduced, the optimality gap, which is the difference between the upper and lower bounds, shows how good the solution is. In other words, it provides a clear indication of how far we are from the optimal solution and how effective the solver is in locating it [167]. This value was obtained from the log file that Gurobi provides after solving each model.

Moreover, the computer specifications that were used to solve each model will be described in each chapter. This will include the computer memory size and the processor used to solve the models.

4.4.8 Assumptions Guiding the Energy Management Model in a Microgrid Context

In this research, we use a MILP model to schedule household-level EV battery usage, integrated with V2G technologies, to optimise energy management. This model is deployed within a microgrid, a localised energy network. The model's assumptions are as follows:

- All households own either an EV (same model for all participants), or a stationary battery, as discussed in Chapter 5.
- Households with solar PV systems all possess 3.5 kWp systems, each household owns their own system.
- All participants can sell surplus solar energy to the grid at a uniform rate.
- All households are located within close proximity, sharing the same distribution transformer, thereby forming a suburban neighbourhood-like grid-connected microgrid.

- When P2P energy sharing is enabled, any participant producing surplus solar energy can sell it to peers within the microgrid.
- Participants have a single energy tariff price for energy drawn from the grid.
- Each household has distinct electricity demand and driving patterns.
- The optimisation model applies to all 50 households within the microgrid.

These assumptions underpin the proposed model, guiding the scheduling of energy resources and transactions within the microgrid for enhanced energy management.

4.5 Conclusions

In this section, we provided an in-depth overview of the data and methodologies used in this study. The electricity household demand, solar generation, and different electricity tariffs data that we used our research.

We also introduced the optimisation model, a tool crucial for scheduling the charge and discharge cycles of the EV batteries. We the how this model works including including the P2P aspect and its objective function. Then, a detailed explanation of the P2P price mechanisms used, in this case two different price mechanism, was also provided.

Further, we explored the microgrid's functionality and explained the different configurations on how the microgrid will behave. Notably, whether V1G, V2H or V2G was allowed, and the different ways that P2P will work inside the miocrogrid.

The section further introduced the performance metrics, explaining how they help evaluate the microgrid's performance and its different aspects. Additionally, the metric that will help to evaluate the quality of the solutions produced by the solver. The final part of this section outlined the assumptions that framed the research, enabling us to study and analyse various aspects effectively.

Overall, this section has provided a comprehensive insight into the work's framework, bringing together the various elements that contribute to our understanding of the availability of EVs within a grid-connected microgrid. This underpinning frame-

work sets the stage for the subsequent in-depth exploration of EVs in the following chapters.

Chapter 5

Comparison of Smart Charging (V1G) and Vehicle-to-Home (V2H) Systems against Stationary Batteries for Minimising Consumer Electricity Costs

In the following chapter, the effectiveness of using a microgrid connected to the grid to reduce the electric bill of households that own a stationary battery or an electric vehicle (EV) with a bidirectional charger. We will describe the data used to simulate the microgrid, an overview of the different scenarios that will be explored, and gauge the performance of stationary home batteries and EVs using the data and the model described in previous chapters in different scenarios that will be introduced later in the chapter.

5.1 Model overview

The optimisation model introduced in chapter 4 is used to simulate the EVs and data is taken from the resulting profiles in chapter 3. For stationary home batteries, an adjusted version of the optimisation model from chapter 4 is used to simulate

their behaviour. The objective of the optimisation model is to minimise household electricity costs. This is achieved through several strategies. If a house has a photovoltaic (PV) system installed, the model aims to maximise the self-consumption of solar energy produced. The model also considers the possibility of peer-to-peer (P2P) energy trading among households. Additionally, it manages the scheduling of energy storage systems' charge and discharge cycles to provide Vehicle-to-home (V2H) and further minimise the electricity bill. This scheduling considers various factors, such as times of high or low electricity prices, as well as periods with a surplus of solar energy, to determine the most cost-effective operation. For EVs, a bidirectional charger is used to allow EVs to discharge energy already stored in the battery toward the house. The impact of different electricity tariffs is compared, as well as different PV penetration rates and possible advantages of P2P energy trading between households within the microgrid is compared. Furthermore, in the case of EVs, a comparison of smart charging (V1G) and V2H is also explored. The full list of scenarios explored in this chapter will be described in greater detail in section 5.1.4.

5.1.1 Data

A grid-connected microgrid consisting of a sample of 50 households located in London, previously described in section 4.1.1 is used. All households have a stationary home battery or an EV. Table 5.1 shows the specifications of the two batteries, EV and the bidirectional charger that are considered in this work. Here, a Nissan/Eaton [168] and a Tesla Powerwall [169] are used, as well as a Nissan Leaf 2018 [170]. In addition, a 7.4 kW bidirectional charger – V1G and V2H enabled – was considered for the EV simulations [158]. For EVs, a comparison of V1G and V2H is also explored. Data that resulted from chapter 3 is used to simulate the travel behaviour of the EVs.

Four different electricity tariffs are used as described in section 4.1.3.1 and table 4.1. These four electricity tariffs are the Agile tariff, the Agile Go tariff, the economy seven (E7) tariff and the Flat tariff.

To assess the impact of local solar generation, different PV penetration rates are used; in this case, 0%, 10%, 25%, 50%. 75%, 90% and 100%. These PV penetration

Table 5.1: Overview of stationary home batteries, electric vehicle and the bidirectional charger considered in this work.

Name	Type	Capacity (kWh)	Power (kW)	Efficiency (%)
Nissan/Eaton	Stationary battery	6	3.6	90
Tesla Powerwall	Stationary battery	13.5	5	90
Nissan Leaf 2018	Electric Vehicle	37	-	-
Wallbox Quasar	Bidirectional charger (charge / discharge)	-	7.4	93

rates mean the percentage of the 50 houses with solar panels installed, for instance, a PV penetration rate of 10% will only have 5 houses with solar panels. To simulate solar generation, the data introduced in section 4.1.2 and the sell tariff, the Agile Outgoing tariff, from section 4.1.3.2 is used.

In this work, three different P2P scenarios are explored, one without P2P energy trading, one with P2P energy trading using the setting introduced in section 4.3.1 and one with P2P energy trading using the setting introduced in section 4.3.2.

5.1.2 Representative weeks of the year

The simulations were conducted using four different weeks that are representative of the four seasons of the year to study any seasonal variation. This information has already been introduced in figure 3.9 where it is provided for six different weeks of the year. In this chapter, only four dates are considered, as explained below.

- **Week 1**: For spring, week *Spring - S1* from 2015-04-20 00:00:00 to 2015-04-26 23:59:00.
- **Week 2**: For summer, week *Summer - S2* from 2015-06-22 00:00:00 to 2015-06-28 23:59:00.
- **Week 3**: For autumn, week *Autumn - S4* from 2014-10-06 00:00:00 to 2014-10-12 23:59:00.
- **Week 4**: For winter, week *Winter - S6* from 2015-02-23 00:00:00 to 2015-03-01 23:59:00.

A total of 28 days are simulated overall, these weeks will contribute equally to the calculation of the estimate annual electricity cost, which will be discussed later in the chapter. This means that each week's weighting is 0.25.

5.1.3 Energy storage system dispatch optimisation for a household

The optimisation model used to schedule the charging and discharge behaviour of EVs was introduced in section 4.2.

In the case of the stationary home battery, the model in section 4.2 was appropriately modified to reflect availability throughout the day and that there is no energy discharge for travel purposes. These changes are described in equations (5.1)–(5.3), where $\alpha_{v,t}^{avail,home}$, $\alpha_{v,t}^{avail,street}$ and $E_{v,t}^{demand,vehicle}$ are modified to reflect the behaviour of a stationary home battery that is available at all times and does not need to consume energy for travel purposes.

$$\alpha_{v,t}^{avail,street} = 0, \quad \forall v, t \tag{5.1}$$

$$\alpha_{v,t}^{avail,home} = 1, \quad \forall v, t \tag{5.2}$$

$$E_{v,t}^{demand,vehicle} = 0, \quad \forall v, t \tag{5.3}$$

5.1.4 Microgrid system configuration overview

A comparison of different microgrid configurations or microgrid scenarios of the system is considered. These scenarios are summarised in table 5.2. Since the main purpose of having a stationary home battery is to store energy that can be used later at home, as opposed to EVs which can be operated in three different modes according to section 4.4, for stationary home batteries, there is only one configuration, which will be called *Batt*. Each battery used here will be called *Eaton* for the Nissan/Eaton battery and *Tesla* for the Tesla Powerwall battery. When EVs are used, the case studies will be identified using *EV* and only two modes will be considered, the V1G mode and the V2H mode.

The different microgrid scenarios described in table 5.2 will be simulated using

Table 5.2: Overview of the different microgrid configurations explored in this chapter with a description of the microgrid configuration.

Microgrid configuration or scenario	Description
Nissan/Eaton battery	
$Batt\_\_\_Eaton\_\_\_No\_P2P$	Case Study one; No P2P.
$Batt\_\_\_Eaton\_\_\_P2P\_S1$	Case Study one; P2P Setting one.
$Batt\_\_\_Eaton\_\_\_P2P\_S2$	Case Study one; P2P Setting two.
Tesla battery	
$Batt\_\_\_Tesla\_\_\_No\_P2P$	Case Study two; No P2P.
$Batt\_\_\_Tesla\_\_\_P2P\_S1$	Case Study two; P2P Setting one.
$Batt\_\_\_Tesla\_\_\_P2P\_S2$	Case Study two; P2P Setting two.
EVs	
$EV\_\_\_V1G\_\_\_No\_P2P$	Case Study three; V1G; No P2P.
$EV\_\_\_V1G\_\_\_P2P\_S1$	Case Study three; V1G; P2P Setting one.
$EV\_\_\_V1G\_\_\_P2P\_S2$	Case Study three; V1G; P2P Setting two.
$EV\_\_\_V2H\_\_\_No\_P2P$	Case Study four; V2H; No P2P.
$EV\_\_\_V2H\_\_\_P2P\_S1$	Case Study four; V2H; P2P Setting one.
$EV\_\_\_V2H\_\_\_P2P\_S2$	Case Study four; V2H; P2P Setting two.

the four weeks described in section 5.1.2 and the different PV rates and energy tariffs, both described in section 5.1.1. However, for energy tariffs, five different energy tariff configurations or tariff scenarios will be explored. These five scenarios are described in table 5.3 where it shows the number of profiles that each energy tariff will use for each tariff scenario.

Table 5.3: Overview of the different energy tariff configurations explored.

Tariff configuration	Description
Agile	100% of profiles using the Agile tariff
Agile Go	100% of profiles using the Agile Go tariff
E7	100% of profiles using the Economy seven tariff
Flat	100% of profiles using the Flat tariff
All tariffs	25% of profiles using each of the four energy tariffs

Finally, the number of simulations considered for each microgrid configuration – described in table 5.2 – is 140 in total, which considers seven different PV penetration rates – described in section 5.1.1 – and five different tariff configurations – described in table 5.3. Therefore, in this chapter, a grand total of 1,680 simulations are explored.

5.1.5 Metrics

The performance metrics already introduced in section 4.4.6 will be used to evaluate the performance of each scenario described in this chapter. Furthermore, to assess the quality of the results presented, the optimality gap metric described in section 4.4.7 will be used.

5.2 Results

In this section, we present our findings from a week-long summer microgrid study – referred to as 'Summer - S2'. Specifically, we focus on the results when using the Agile Go tariff. We compare the usage and performance of stationary home batteries and EVs based on the metrics introduced in section 4.4.6. Then, we assess the impact of various representative weeks on the microgrid's performance under each tariff. We also analyse the estimated annual total electricity cost for each scenario and tariff combination. Finally, we briefly discuss the validity and quality of the results obtained from our study based on the metrics introduced in section 4.4.7.

For this chapter, as stated in section 4.2, each simulation was built using the Python 3.8.8 [125] programming language and the Pyomo 6.3.0 library [157] and then solved using Gurobi 9.5.2 [156].

5.2.1 Results comparison between stationary home batteries and electric vehicles for a week in summer using the agile go tariff

The simulation results presented in figures 5.1 and 5.2 outline the dynamic behaviour of EVs (in this case, $EV\_\_\_V2H\_\_\_P2P\_S1$) and stationary home batteries (in this case, $Batt\_\_\_Tesla\_\_\_P2P\_S1$) in a microgrid environment with a PV penetration rate of 90% and using the Agile Go tariff during a summer week - in this case the Summer - S2 week. As observed in both figures, these energy resources

exhibit a clear preference for charging during periods when the price of electricity is at its lowest, particularly when solar generation is high. This behaviour significantly reduce the energy drawn from the grid. The energy draw from the grid peaks at night, with EVs reaching up to 205 kW and home batteries up to 180 kW. In contrast, charging during the day takes advantage of local solar generation, which significantly reduces the energy drawn from the grid.

EVs and home batteries also display a tendency to discharge during the evening hours. This coincides with a period of lower solar generation. In the context of these two scenarios, surplus solar generation is predominantly sold to the grid as it provides a more beneficial financial return than self-consumption or P2P trading, as seen in **(b)** of figures 5.1 and 5.2. The comparatively lower P2P selling prices, a consequence of solar generation saturation, make selling to the grid a more profitable option under *Setting one* ($S1$), as explained in section 4.3.1.

Over the course of the week, the total energy shared via P2P when using EVs was observed to be 222 kWh, while home batteries were noted to share 128 kWh of energy. Interestingly, despite the differing amounts of energy shared, the self-suffiency ratio (SSR) of both setups was closely matched, with EVs achieving 83.33% and home batteries 83.26%. This underlines the effective utilisation of predicted availability and location data, suggesting that both stationary batteries and EVs can be efficiently integrated into the energy management strategies of a microgrid.

5.2.2 Performance of Microgrid Configurations for a week in summer using the agile go tariff

Figures 5.3a and 5.3b summarise the performance metrics for scenarios using EVs and stationary home batteries in different microgrid configurations during the summer week with the Agile Go tariff. In both figures, each row contains five different metrics, which are described below.

- **Row A:** Contains results for SSR.
- **Row B:** Contains results for energy balance index (EBI).
- **Row C:** Contains results for the energy imported from the exchange via P2P in kWh.

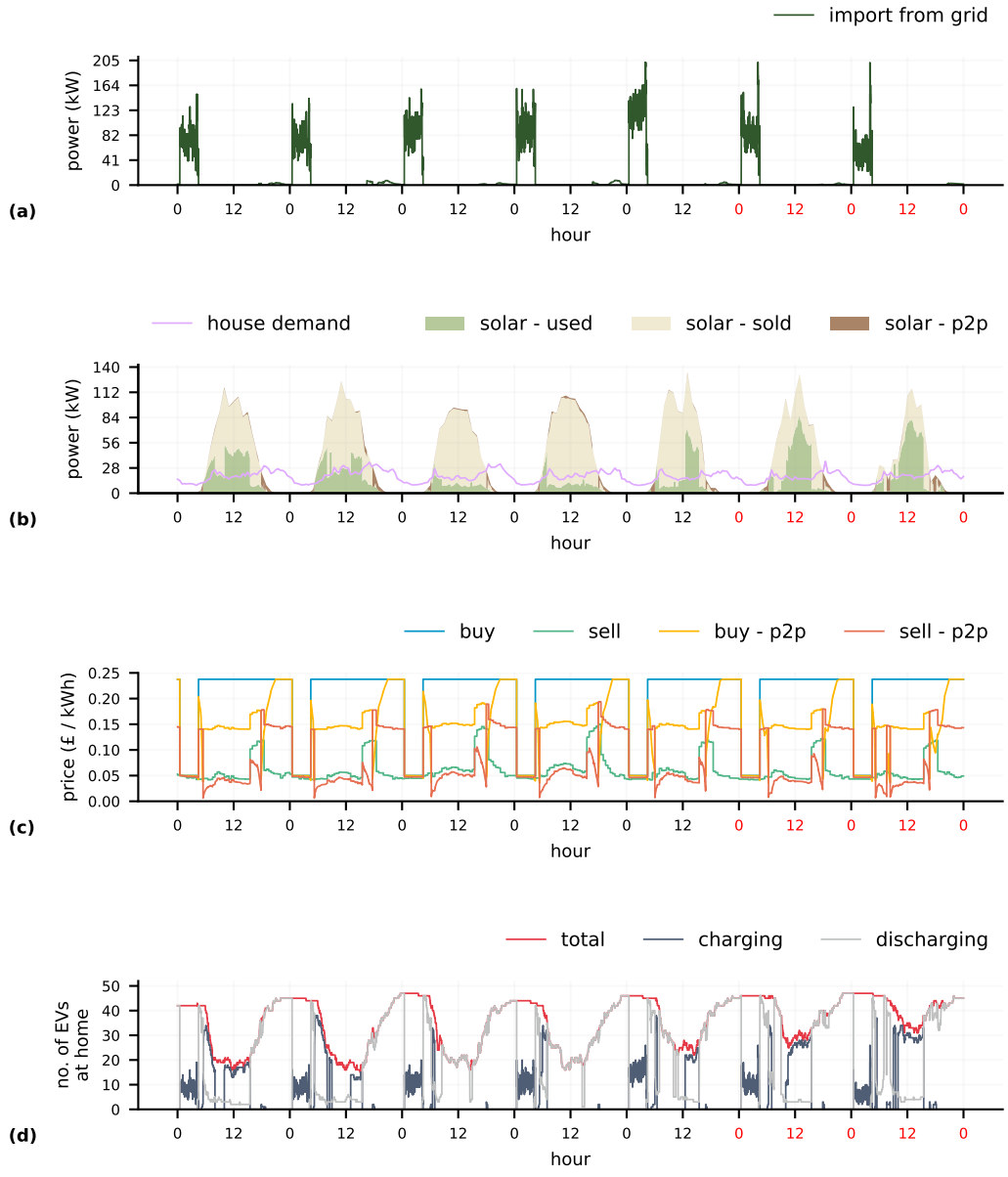

Figure 5.1: Simulation results for the Summer - S2 week showing the microgrid operation using EVs with a PV penetration rate of 90% and using the Agile Go tariff. In this case, this date belongs to the microgrid configuration $EV\_\_V2H\_\_P2P\_S1$. The tick labels on *X-axis* in black denote data from Monday to Friday, and the red labels, data from Saturday and Sunday. **a.** Power import from the grid. **b.** Household demand and energy consumed, shared and sold from solar generation within the microgrid. **c.** Buy and sell prices from the grid and from P2P energy trading. **d.** Number of EVs available at home charging and discharging and the total number of numbers available at home.

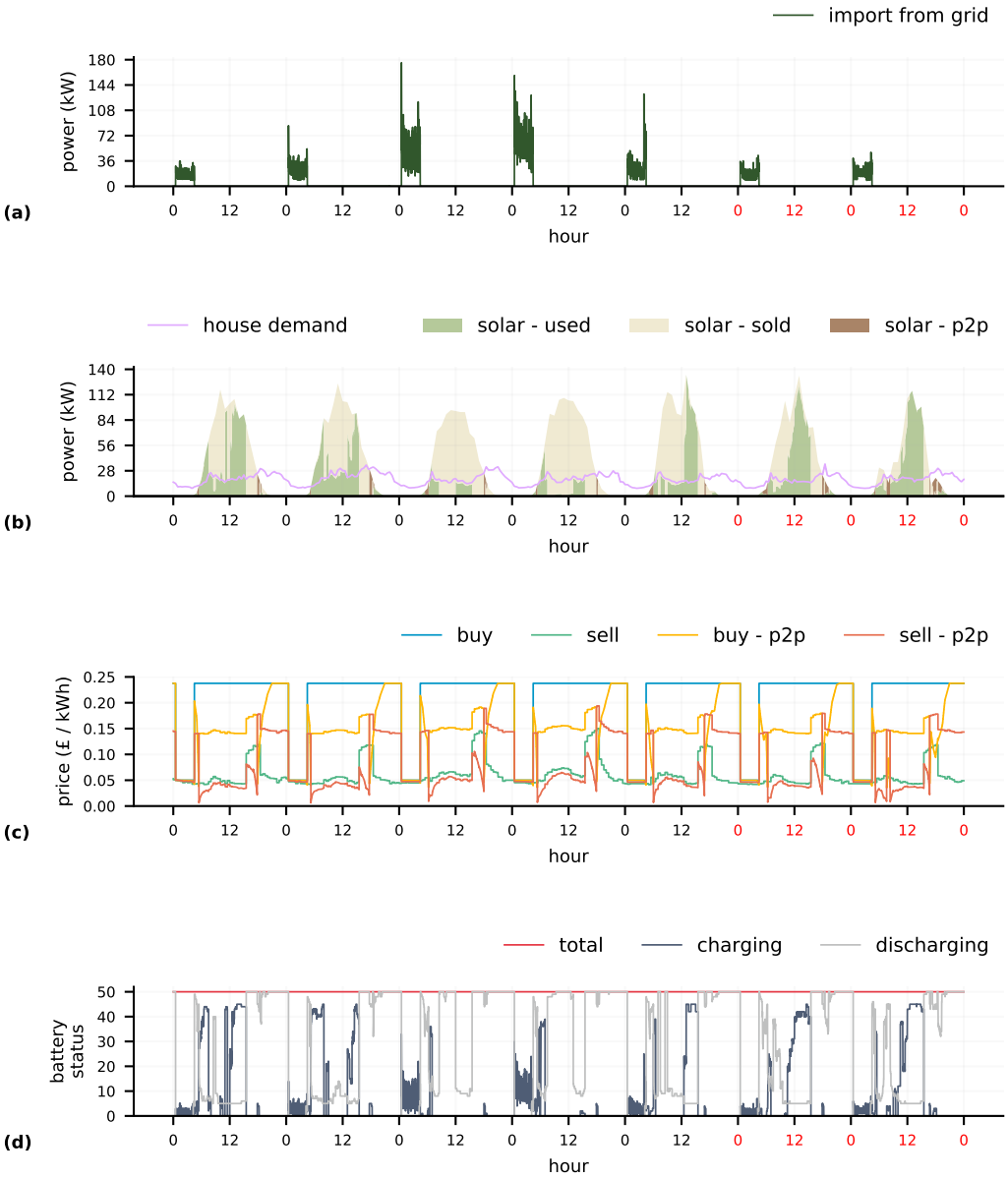

Figure 5.2: Simulation results for the Summer - S2 week showing the operation of the microgrid operation using EVs with a PV penetration rate of 90% and using the Agile Go tariff. In this case, this date belongs to the microgrid configuration $Batt\_\_Tesla\_\_P2P\_S1$. The tick labels on *X-axis* in black denote data from Monday to Friday, and the red labels, data from Saturday and Sunday. **a.** Power import from the grid. **b.** Household demand and energy consumed, shared and sold from solar generation within the microgrid. **c.** Buy and sell prices from the grid and from P2P energy trading. **d.** Number of home batteries that are charged and discharged.

- **Row D:** Contains results for the maximum power load from the energy imported from the grid in kW.

- **Row E:** Contains results for the mean electricity cost per week in British pounds (£).

These results generally show a strong correlation between PV penetration rates, P2P settings, and SSR. For home batteries, SSR with a PV penetration rate of 100% increases from 30.71% to 84.16% for Eaton batteries and 41.13% to 88.37% for Tesla batteries. For EVs with the same PV penetration rate, SSR increases from 0.00% to 71.81% when only V1G is allowed and 27.70% to 79.85% with V2H. However, different metrics peak under varying PV penetration rates, such as EBI, maximum power load, and energy imported from P2P.

In scenarios where P2P is not allowed, SSR results for both Eaton and Tesla batteries fluctuate according to PV penetration rates, with ranges between 30.71% to 56.39% and 41.14% to 61.14% respectively at rates of 0% to 50%. These values increase to between 70.05% to 82.65% for Eaton and 73.87% to 86.54% for Tesla batteries at rates from 75% to 100%.

In scenarios where only V1G is enabled, SSR ranges from 0% to 28.60% with PV penetration rates of 0% to 50%. The scenario which allows EVs to discharge energy via V2H increases SSR from 27.70% to 43.33% with PV penetration rates of 0% to 50%, still lower than the batteries. The import of power from the grid ranges from 91 to 120 kW with V1G and 253 to 299 kW with V2H. Electricity costs are nearly halved across all PV penetration rates when V2H is enabled compared to V1G.

Allowing P2P trades in *Setting two* yields optimal results for both technologies, owing to its more attractive prices for both buying and selling energy. This is particularly useful for home batteries, whose primary role is storing energy for later use, and for EVs using V2H, which essentially function as intermittent household batteries.

Setting two also significantly increases the energy exchanged, with the largest difference being over 1 MWh in the $Batt\_\_\_Tesla\_\_\_P2P\_S2$ microgrid configuration. In general, the implementation of P2P under this price setting results in reduced grid energy imports, particularly at higher PV penetration rates, due to the ability

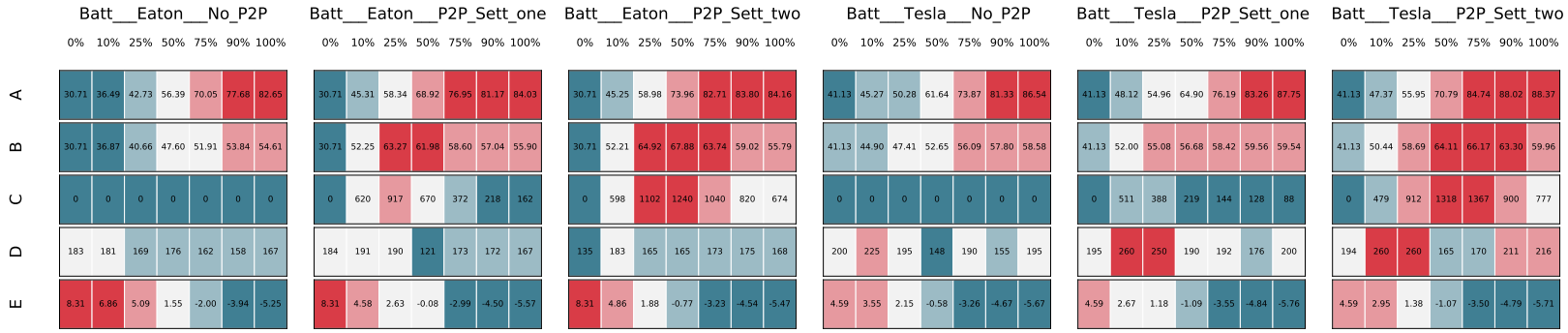

(a) Home batteries

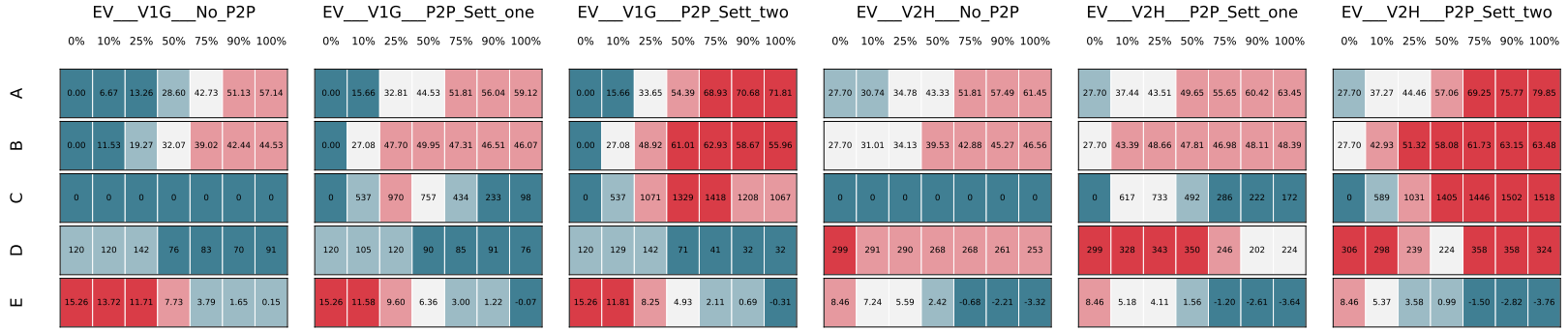

(b) EVs

Figure 5.3: Performance metrics for the microgrid for the Summer - S2 week using the Agile Go tariff. Each block belongs to one microgrid configuration or scenario, where columns are each specific scenario, and rows each performance metric. *X-axis* denotes the increase of PV penetration rates from 0% to 100%. Dark red represents the highest values for each row, and dark blue represents the lowest. **a.** Self-suffiency ratio. **b.** Energy balance index. **c.** Energy imported from P2P (kWh). **d.** max power load from the grid (kW). **e.** Mean electricity cost per week (£).

to sell surplus local solar generation to peers at a mid-market rate price.

Specifically, for home batteries, grid energy imports are significantly reduced across all PV penetration rates, with the greatest reductions seen at 100% PV penetration: Eaton battery imports decrease from 3,466 kWh to 851 kWh, and Tesla from 3,714 kWh to 701 kWh. With P2P allowed in both settings, there is a small further reduction in grid imports at high PV penetration rates.

Similarly, for EVs, grid energy imports decrease proportionally with increasing PV penetration rates. Without P2P, imports drop from 4,645 kWh at 0% PV penetration to 1,991 kWh at 100% penetration for V1G, and from 4,940 kWh to 2,389 kWh for V2H. These higher import levels for V2H may be attributed to EVs charging during periods of low energy prices. With P2P enabled, *Setting one* yields minor reductions in grid imports at 100% PV penetration, while *Setting two* results in substantial reductions, from 1,991 kWh to 1,309 kWh for V1G, and from 2,389 kWh to 1,246 kWh for V2H. These reductions occur at all PV penetration rates, with *Setting two* consistently resulting in less grid energy importation.

Compared to home batteries, EVs yield a less significant reduction in grid energy imports due to the need to charge extra energy for users' driving needs. The highest max power loads are found with EVs using V2H (201-358 kW), possibly as most EVs charge simultaneously at times of low electricity prices to meet future travel energy requirements, as well as for later use in the house. Tesla batteries show the second highest values, followed by Eaton batteries at a lower range (121-260 kW) due to their smaller charge/discharge power. The lowest maximum power loads occur with EVs using V1G, suggesting households only charge their EVs to meet any energy required for trips during the day.

Given all microgrid configurations can sell surplus solar generation to the grid, in some cases this may be more profitable, reducing SSR, EBI, energy shared to P2P, and the max power load from the grid, thereby increasing grid energy dependency. However, it may also reduce weekly electricity bills by earning profits from energy sold to the grid. A possible solution to balance these factors with financial benefits for EV owners could be to incorporate incentives into the objective function to promote self-sufficiency, energy balance, and P2P sharing, while still profiting from selling surplus energy.

The lowest mean electricity prices per week are found when using the Tesla battery in all microgrid configurations or scenarios. Eaton batteries and EVs with V2H yield similar results for most PV penetration rates, whether P2P is enabled or not. The highest prices occur when EVs are used with V1G, and in all cases, the highest PV penetration rates return the lowest mean weekly electricity prices.

The following summary provides a review of this section's findings, comparing the impacts of home batteries (Eaton and Tesla) and EVs with V1G and V2H capabilities under different PV penetration rates and P2P energy sharing.

- SSR increases with higher PV penetration rates across all technologies. Home batteries (Eaton and Tesla) show an SSR range from 30.71% to 88.37% at 100% PV penetration, while EVs with V1G and V2H functionalities demonstrate SSR between 0.00% to 71.81% and 27.70% to 79.85% respectively. The V2H scenario displays a significant improvement over V1G.

- P2P energy sharing settings (*Setting one* and *Setting two*) greatly influence SSR and grid energy imports. *Setting two*, providing more advantageous P2P energy prices, consistently delivers higher SSR and larger reductions in grid imports across all PV penetration rates compared to *Setting one*. This leads to *Setting two*generally resulting in lower weekly electricity costs.

- The import of grid energy decreases across all PV penetration rates with the most substantial reductions observed at 100% PV penetration for both home batteries and EVs, and further reductions when P2P is enabled. However, EVs result in less reduction in grid energy imports due to additional charging needs for driving.

- The highest maximum power loads, indicating peak energy demands, are observed with EVs with V2H due to combined home and vehicle charging needs. Tesla batteries show the second-highest values, while Eaton batteries show lower values due to their smaller charge/discharge power.

- All microgrid configurations tend to sell surplus solar generation to the grid rather than using it for self-consumption or sell it via P2P, potentially reducing SSR, increasing grid dependency, but also lowering electricity bills.

- In terms of mean weekly electricity costs, Tesla batteries consistently result in the lowest prices across all scenarios, while the highest prices are associated with EVs with V1G. The lowest prices are achieved at the highest PV penetration rates.

5.2.3 Results of all microgrid configurations and tariffs over the different representative weeks in a year

The figures presented in this section include values in all microgrid configurations or scenarios. The values are divided into two sections, the column on the left – column 1 – contains the average values from 0% to 50% PV penetration rates and the right column – column 2 – contains the average values from 51% to 100% PV penetration rates. Moreover, each row includes each of the five tariff scenarios – rows 1 to 5 – that were explored, different colours are used to differentiate between the four representative weeks of the year and different marker shapes are used to help distinguish them between each microgrid configuration. *X-axis* tick labels also include information about each microgrid configuration.

In this section, our focus will primarily be on a select set of performance metrics: SSR, energy shared from P2P, and the average weekly electricity cost. Additional metrics, such as EBI, the maximum power load from the grid, and total energy imported from the grid, are detailed in Appendix B, specifically under appendix B.1.1.

Figure 5.4 shows a comparison of the SSR, the different weeks of the year have a noticeable difference between each other for all scenarios and tariffs. It can be seen that the Summer - S2 week returns the highest SSR value in most columns and rows followed by the Spring - S1 week, with the exception of 51-100% PV penetration rate and the Agile Go tariff during the Spring - S1 week (column 2, row 2) using the Tesla battery and EVs with V2H. The Winter - S6 week tends to return the lowest SSR values in most cases in column 1 when using EVs with V1G. Column 1 returns results close to each other regardless of tariff; there is no major gap between values in the different weeks. Column 2 shows a larger gap between the different weeks, depending on the tariff scenario used. In this case, the P2P scenarios return the highest SSR values for both settings; however, *Setting two* seems to perform better than *Setting one*.

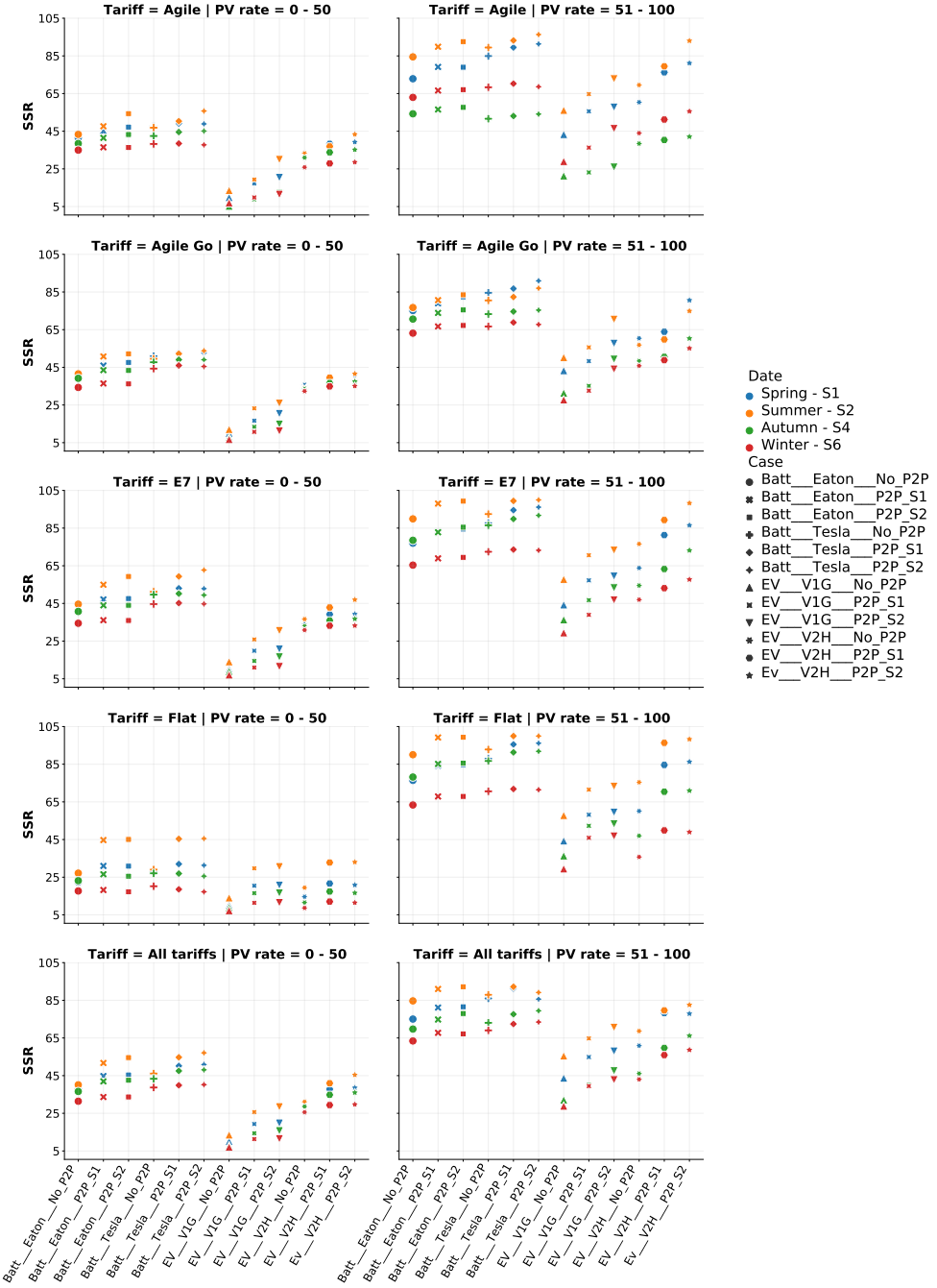

Figure 5.4: Self-suffiency ratio values for the four representative weeks of the year, the five tariff scenarios and all microgrid configurations explored in this chapter. The left column contains the average values from 0% to 50% PV penetration rates and the right column contains the average values from 51% to 100% PV penetration rates.

Figure 5.5 shows a comparison of the total energy imported from P2P. In this case, only relevant scenarios with P2P and PV penetration rates are considered from 10% to 100%. Here, a higher PV penetration rates result in more energy being imported from P2P. With lower PV penetration rates , shown in column 1, Summer - S2 has the highest energy values for all microgrid configurations and tariffs. In column 2 different weeks return the highest energy imported from P2P, for example, depending on the microgrid configuration and tariff, Winter - S6 is the one that returns more energy being imported from P2P with *Setting one*. This could be because the way the prices of each of the settings P2P prices are calculated as explained in section 4.3.1, where having more solar generation could result in lower P2P sell prices, which will result in less motivation to trade energy within the microgrid and instead sell it to the grid or use it locally as self-consumption. In the case of *Setting two*, scenarios in this setting import more energy from P2P during Summer - S2 week, since the way prices are calculated can influence users to trade instead of selling to the grid or use it locally, since both buy and sell prices are an average of the buy and sell prices from the grid, as explained in section 4.3.2.

Figure 5.6 shows a comparison of the mean electricity price per week. Here, the lowest prices can be met during the Summer - S2 week in all scenarios and tariffs, opposite to the Winter - S6 week, which results in the highest prices of all weeks. Overall, mean prices per week are between 30.0 and -7.0 British pounds (£) for all scenarios, weeks and tariffs, with negative prices found where PV penetration rates are high, that is, households get paid instead of paying for their bill. Home batteries returned low electricity costs when using P2P and *Setting two*, and the Tesla battery had slightly lower energy costs per week than the Eaton battery. For EVs, having V1G and no P2P had the highest electricity price with the E7 tariff and with V2H with P2P and *Setting two* electricity prices are close to those when using home batteries.

5.2.4 Annual electricity costs

In this section, the estimated annual electricity costs will be presented. The results were calculated as explained in section 5.1.2. The figures contain the average estimated annual electricity cost for the four main tariffs, Agile tariff, Agile Go tariff,

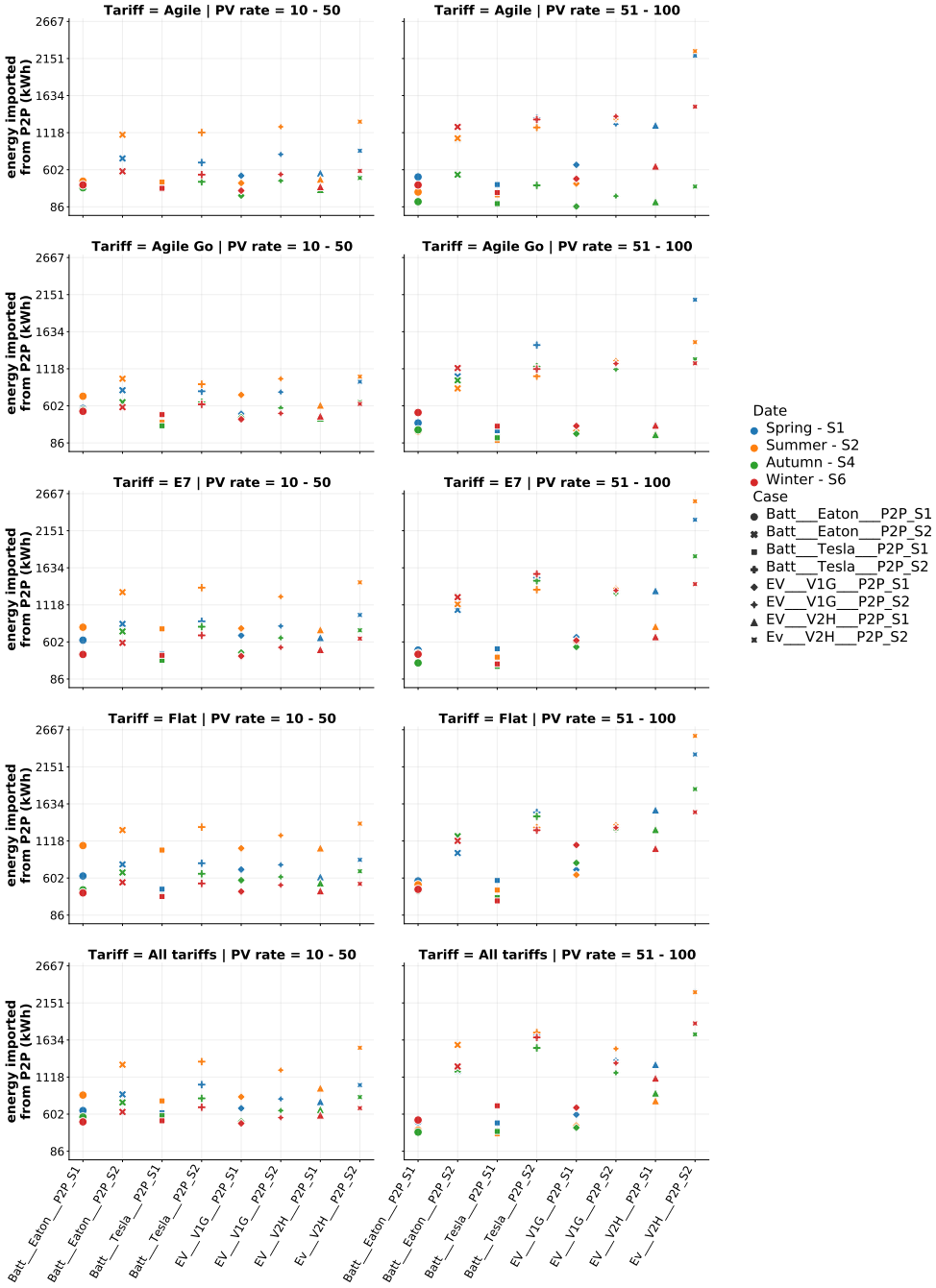

Figure 5.5: Energy shared from P2P for the four representative weeks of the year, the five tariff scenarios and all microgrid configurations explored in this chapter. The left column contains the average values from 0% to 50% PV penetration rates and the right column contains the average values from 51% to 100% PV penetration rates.

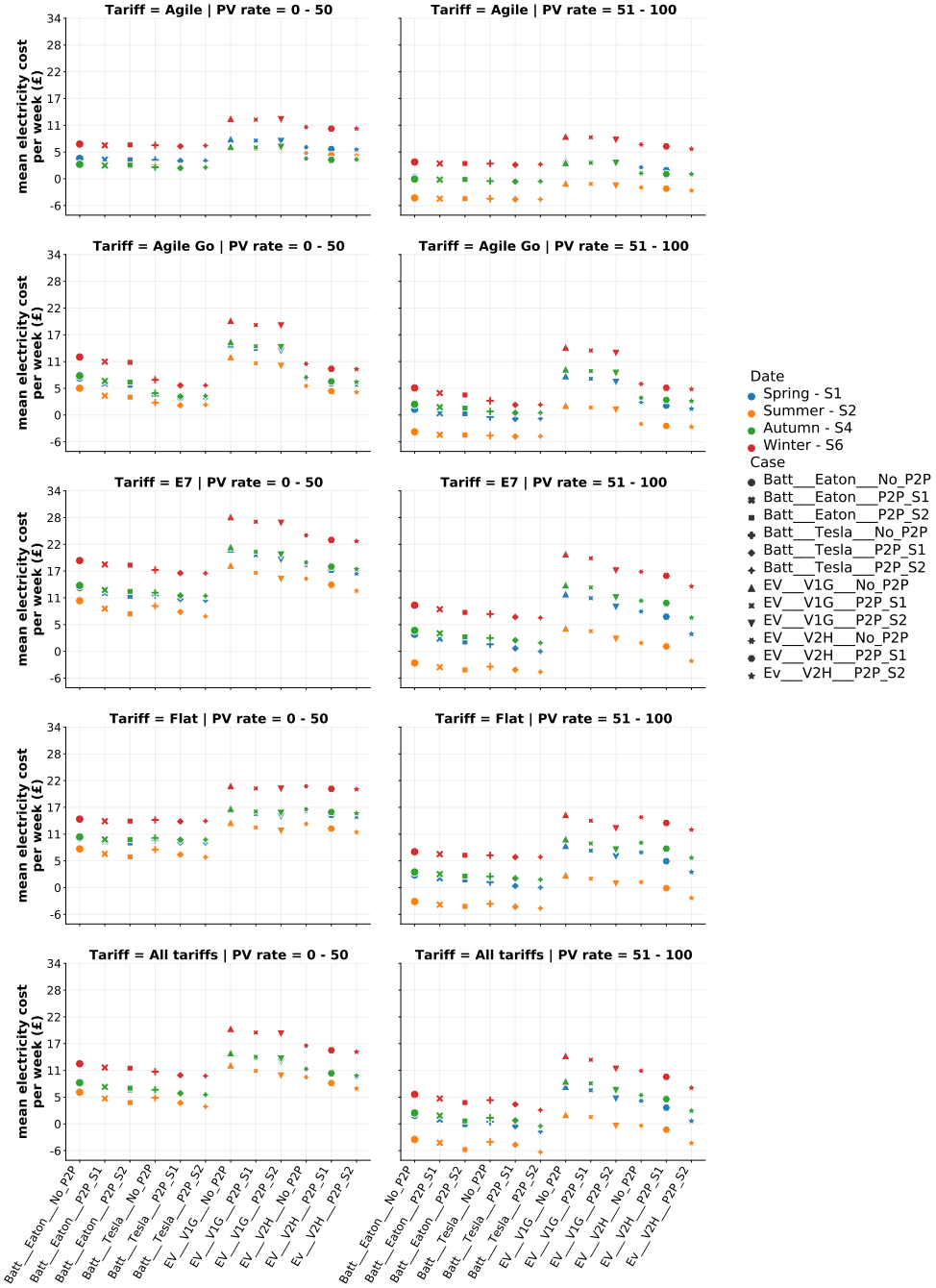

Figure 5.6: Mean electricity cost per week for the four representative weeks of the year, the five tariff scenarios and all microgrid configurations explored in this chapter. The left column contains the average values from 0% to 50% PV penetration rates and the right column contains the average values from 51% to 100% PV penetration rates.

E7 tariff and Flat tariff in figures 5.7a and 5.7b for home batteries and EVs, respectively. Similarly, in the case of the All tariffs scenario, where 25% of profiles use each of the four energy tariffs, as described in table 5.3, these results are the average estimated annual electricity costs according to the number of households that are under each different tariff, as described in table 5.4. Figures 5.7c and 5.7d show the results for the All tariffs scenario for home batteries and EVs, respectively.

Table 5.4: Number of users under each different tariff for the All tariffs scenario.

Tariff name	Number of households
Agile	13
Agile Go	13
E7	12
Flat	12

In the data represented in figures 5.7a–5.7d, it's evident that higher PV penetration rates lead to reduced average annual prices across all microgrid configurations and tariffs. For both home batteries and EVs, lowest prices are achievable with 100% PV penetration rate in particular settings, such as Agile and Agile Go tariffs and P2P settings.

Home batteries, particularly the Tesla battery, generate negative prices, implying users can earn rather than pay for their electricity usage. The Agile tariff consistently returns the lowest electricity cost, for both home batteries and EVs.

For EVs, the lowest price can be achieved with Agile tariff and 100% PV penetration rate in the $EV\_\_\_V2H\_\_\_P2P\_S2$ scenario, yet no negative prices are recorded here. Importantly, EVs with V2H services show significantly lower prices (£28) compared to those with only V1G services (£121), demonstrating the economic benefit of V2H.

In all configurations, the E7 tariff results in the highest average annual costs. EVs with V1G services also generate the highest annual electricity costs, but these costs are substantially reduced when V2H services are implemented. Similarly, allowing P2P further reduces costs.

Under the All tariffs scenario, the Agile Go tariff beneficiaries are primarily home battery users and EVs with V2H. Negative prices are observed with the Eaton and

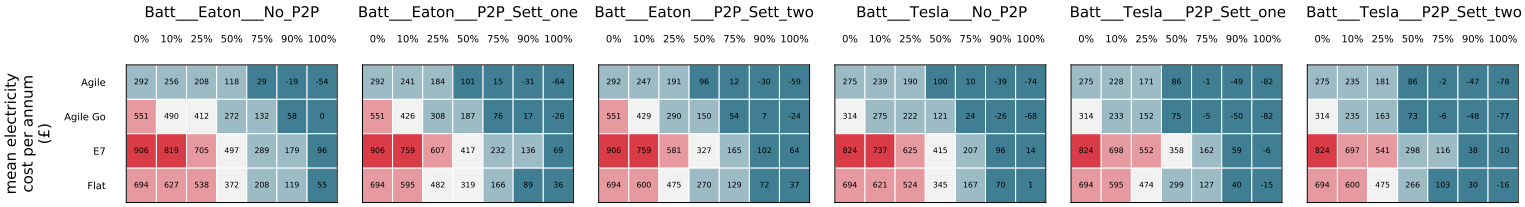

(a) Home batteries

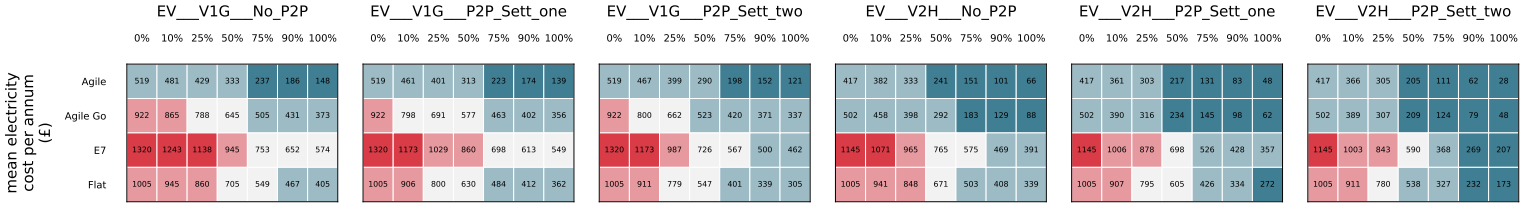

(b) EVs

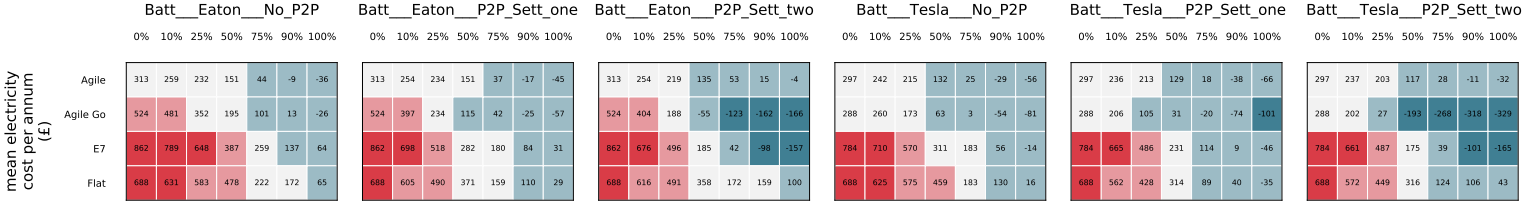

(c) Home batteries

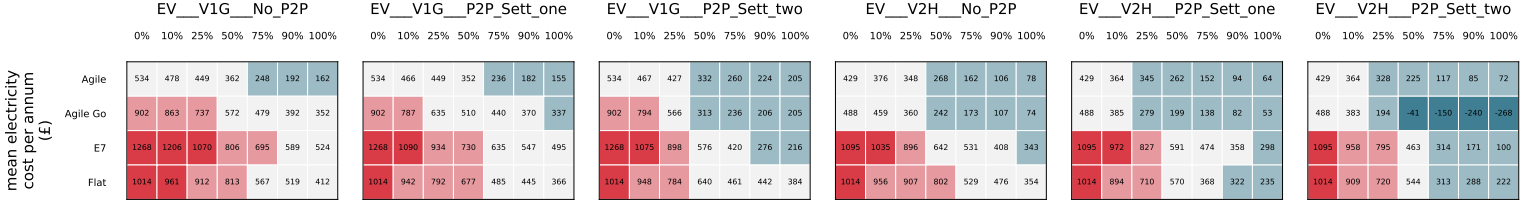

(d) EVs

Figure 5.7: **(a) - (b)**. Estimated annual electricity cost for Agile tariff, Agile Go tariff, E7 tariff and Flat tariff when using home batteries showing the mean prices within the microgrid. **(c) - (d)**. Estimated annual electricity cost for each tariff inside the All tariffs scenario when using home batteries showing the mean prices within the microgrid.

Tesla batteries, -£45 and -£66 respectively, under specific tariffs and settings. For EVs, the lowest average annual costs are reported when V2H is allowed and Setting two is used, resulting in an average annual cost of -£268. Higher PV penetration rates, appropriate tariff selection, and P2P settings all contribute to reducing electricity costs, with V2H services offering particular cost advantages over V1G services.

5.2.5 Solution quality

In this section, the optimality gap explained in section 4.4.7 will be shown. This metric will measure the quality of the results presented so far in this chapter, which means that it will give a clearer picture of how far the results are from the optimal solution according to the solver, in this case Gurobi 9.5.2 [166]. Additionally, the computer specifications that were used to solve each microgrid configuration or scenario.

Table 5.5 shows the optimality gap value ratio of the 1,680 models in his chapter obtained after solving each model. Here, the majority of models are under a gap of 0.50% and only a handful are above this threshold. To put things into context, a model with a 0.50% gap implies that the feasible solution identified by Gurobi is quite close to the optimal solution. This small gap is considered satisfactory in many cases, as it demonstrates its effectiveness in solving the optimisation problem with reasonable accuracy. The closer the gap to 0.00%, the higher the confidence in the quality of the solution, which makes it suitable for decision-making or further analysis [166].

Table 5.5: Optimality gap value ratio of the resulting models.

Gap	Number of models
≤ 0.50	1,668
$0.50 <$	12

Table 5.6 shows the total number of models that were solved on each PC. According to the Gurobi documentation, the results can vary when solved on different hardware, which means that although optimal results are found, the path to them might be different, which may yield different data [171].

Table 5.6: Number of models solved using each computer and their specifications.

Number of models	Processor name	Processor speed (GHz)	Cores	RAM (GB)
631	12th Gen Intel (R) Core (TM) i9-12900K	3.20	16	128
769	11th Gen Intel (R) Core (TM) i5-1135G7	2.30	4	64
280	Intel (R) Xeon (R) E5-2620 v4	2.10	16	128

5.3 Discussion

This work has used an optimisation model to investigate the performance of stationary batteries and EVs using V1G and V2H through four different weeks representative of the seasons of the year, different PV penetration rates, in combination with four different tariffs and two different mechanisms of P2P price calculation based on mid-market rate (MMR). This was achieved through the use of real-world data from home energy demand, local solar generation, and EV travel that included predicted data on their ability to be connected at home. The simulation results show that when P2P trading is allowed, the use of home batteries and EVs can produce significant technical and economic benefits with different energy tariffs. In some cases, the use of V2H, which allows EVs to provide energy to the household when connected at home, can provide further benefits for EVs than V1G. For home batteries, the Agile tariff and the Agile Go tariff can achieve average electricity costs per week of around £2.00 with 0-50% PV penetration rates during the summer with P2P, especially the Tesla battery, which has more capacity and power than the Eaton battery, and with 51-100% PV penetration rates the average electricity cost can be around -£5.00 for all tariff scenarios explored with P2P allowed, which means that the household will be paid instead of paying for their electricity bill. EVs with V2H, P2P with 0-50% PV penetration rates can match the mean electricity cost per week during the summer that resulted from the same week for home batteries when there is no P2P. In all scenarios, tariffs and PV penetration rates, the introduction of V2H and P2P further reduces the weekly cost of electricity compared to the use of V1G

alone with electricity costs ranging from -£5.00 to £15.00.

PV penetration rates of 51-100% can also increase SSR in all microgrid configurations during summer with most tariffs, reducing the need for energy from the grid, with SSR values from 55% to close to 100% in the case of home batteries with P2P, for EVs with P2P from 25% to close to 75% for EVs with V1G and from 40% to close to 100% with V2H. In most cases, *Setting two* is the one that leads to the best results with high PV penetration rates. With lower PV penetration rates, *Setting one* tends to improve the results due to the way the P2P prices are calculated, where having less solar generation within the grid may result in the best P2P prices. Furthermore, P2P can benefit PV owners by sharing surplus energy within the microgrid for users to charge their EVs at a lower cost than buying energy from the grid regardless of whether they have PV installed at home. This is because unlike home batteries, EVs are not available at different times of the day because they are used for travel.

Estimated annual electricity costs show that users with home batteries benefit more with the Agile tariff and have P2P using *Setting one* and 100% PV penetration rate with costs as low as -£64 for the Eaton battery and -£82 for the Tesla battery. EVs also benefit the most when using the Agile tariff with P2P and having 100% PV penetration rate, but in this case using *Setting two* results in a cost of £121 with V1G and £28 with V2H.

In addition, P2P energy trading, when allowed, notably impacts the cost dynamics within the microgrid system. P2P energy sharing allows more flexibility and potential for cost reduction across all options - V1G, V2H and stationary batteries. Additionally, the lowest annual costs are observed when P2P is allowed. This highlights the importance of incorporating P2P mechanisms into the energy management strategies of microgrid systems, along with the appropriate selection of EV services and stationary batteries.

As pointed out in different previous work [105, 172, 173], energy buyers benefit more from P2P price mechanisms than sellers. In this study, we compared two different price mechanisms, both based on MMR, based on simulation results, the first price mechanism, *Setting one*, tends to favour buyers more than sellers, as the way this price is calculated penalises the selling prices the higher the solar generation

is within the microgrid and with selling prices often below the price that the grid would pay for any surplus energy.

The way in which the optimisation model was designed guarantees that all energy traded via P2P is used among other participants inside the microgrid, which in some cases leads some users to be "forced" to sell energy to their peers even if it is not profitable for the seller as long as the total cost, the objective function, is minimised. This results in some microgrid configurations where having a lower PV penetration rates increases the performance metrics of the model, as selling prices via P2P results in more profit for the PV owners. To reduce this effect, a second pricing mechanism *Setting two*, was introduced in which buyers and sellers buy and sell at the same price, in this case the price is the average of their energy tariff and the export tariff. This resulted in a more fair mechanism for participants in the microgrid, which in most cases resulted in higher performance metrics such as SSR and the amount of energy shared within the grid.

Finally, when evaluating the economic viability of EVs versus stationary batteries, several factors come into play. The capital expenditure (CapEx) of a Nissan Leaf 2018 (£26,995) and bidirectional charger (Wallbox Quasar - £5,999) stands at £32,994. The operating expenditure (OpEx), based on the Agile tariff with P2P energy sharing using *Setting two* and assuming a 100% PV penetration rate, as mentioned, vary between £121 and £28 annually for V1G and V2H, respectively. These values result in total costs over a five-year period of £33,599 for V1G and £33,134 for V2H.

Stationary batteries present lower CapEx at £3,500 for the Nissan/Eaton and £5,700 for the Tesla Powerwall 2. The OpEx, based on using the Agile tariff with P2P energy sharing using *Setting one* and assuming a 100% PV penetration rate, these batteries generate annual income rather than cost, leading to costs as low as -£64 for the Nissan/Eaton battery and -£82 for the Tesla battery. Over five years, this translates to total costs of £3,180 for Nissan/Eaton and £5,290 for Tesla Powerwall.

When comparing these two technologies, the consideration is whether to opt for the added transportation utility of EVs, despite their higher initial investment, or to choose the income-generating stationary batteries, which, although lower in cost,

lack transport utility.

5.4 Conclusions

In this chapter, the potential technical and economic benefits of using home batteries and EVs with different PV penetration rates, P2P using different price calculation systems, and five different tariff scenarios were investigated in four different weeks representing the seasons of the year.

In general, having an energy storage system and PV at home can lower electricity costs by charging during periods of low energy prices or by charging when during the day when solar power is readily available and then supplying power to the household when prices increase. This not only reduces reliance on the grid but also leads to savings on household electricity bills. In this case, the availability of EVs throughout the day reduces some of the benefits, and more so when PV generation exists, as this happens during the time of day when EVs are most likely away. The introduction of P2P mitigates this by allowing participants with PV to sell energy to their peers on the microgrid while their vehicle is away and still make a profit. Depending on the P2P price mechanism, having a higher or lower PV penetration rates within the microgrid can increase the technical and economic benefits of the microgrid. Moreover, dynamic tariffs, such as Agile tariff, that follows the wholesale electricity price, or Agile Go tariff, designed specially for owners with EVs further increases these benefits, compared to more traditional tariffs such as E7 and Flat Tariff. For EVs, combining P2P and V2H shows that, in some cases, the performance of EVs can match the performance of a stationary battery with the added value of providing travel, which could be of interest for potential EV owners.

Our analysis has shown a marked difference between the costs of EVs and stationary batteries over a five-year period when using the Agile tariff with P2P energy sharing and assuming a 100% PV penetration rate. The combined CapEx and OpEx for the EV options, specifically the Nissan Leaf 2018 with a bidirectional charger, amounted to £33,599 for V1G and £33,134 for V2H. In comparison, stationary batteries such as the Nissan/Eaton and Tesla Powerwall presented lower overall costs, £3,180 and £5,290 respectively, over the same period thanks to their ability to gen-

erate income rather than costs and low initial investment.

While EVs require a larger initial investment, they offer the additional benefit of personal transportation. On the other hand, stationary batteries, though lacking in mobility, provide a financially attractive option due to their income generation capability. Future considerations and policy decisions should carefully evaluate these trade-offs.

Chapter 6

Provision of short term operating reserve (STOR) via vehicle-to-grid (V2G)

This chapter investigates the potential effectiveness of reducing electric bills for households with electric vehicles (EVs) connected to a microgrid that also provides vehicle-to-grid (V2G) services for short term operation reserve (STOR). The analysis involves simulating the microgrid, exploring various scenarios, and evaluating the performance of EVs when delivering STOR services in different microgrid configurations. Furthermore, the chapter provides an overview of the model and the data used to simulate the microgrid, and outlines the different scenarios that will be investigated.

6.1 Model overview

Similarly to chapter 5, the optimisation model introduced in chapter 4 is used to simulate EVs and travel data is taken from the resulting profiles in chapter 3. The optimisation model aims to minimise the electrical bill of homes by maximising self-consumption if a photovoltaic (PV) system is installed in the house, a bidirectional charger is used to allow EVs to schedule charging and discharging behaviour when it is more convenient during the day when connected at home, exploring the possibility of energy trading through P2P, and simultaneously maximising energy supplied for STOR via V2G. Here, the provision of STOR by the EVs inside the microgrid is

done my considering the aggregated power of the EVs available at home at the time when energy is required for STOR. The impact of different electricity tariffs is compared, as well as different PV penetration rates and the possible advantages of peer-to-peer (P2P) energy trading between households within the microgrid using two different price calculation settings.

6.1.1 Data

As previously described in section 4.1.1, a grid-connected microgrid is used comprising a sample of 50 London-based households. Every household has an electric vehicle. The Nissan Leaf 2018 [170] specifications are shown in table 6.1. Furthermore, a 7.4 kW bidirectional V2G and Vehicle-to-home (V2H) charger was considered for EV simulations [158]. The data from chapter 3 is used to simulate the travel behaviour of EVs.

Table 6.1: Overview of stationary home batteries, electric vehicle and the bidirectional charger considered in this work.

Name	Type	Capacity (kWh)	Power (kW)	Efficiency (%)
Nissan Leaf 2018	Electric Vehicle	37	-	-
Wallbox Quasar	Bidirectional charger	-	7.4	93

As described in section 4.1.3.1 and table 4.1, four different electricity tariffs are used. The Agile tariff, the Agile Go tariff, the economy seven (E7) tariff, and the Flat tariff are the four electricity tariffs.

Different penetration rates are used to assess the impact of local solar generation; in this case, 0%, 10%, 25%, 50%, 75%, 90% and 100%. Similar to section 5.1.1, these PV penetration rates mean the percentage of the 50 houses with solar panels installed, for instance, a PV penetration rate of 10% will only have 5 houses with solar panels. The data described in section 4.1.2 used to simulate solar generation and the Agile Outgoing tariff data, introduced in section 4.1.3.2, is used as a feed-in tariff.

Finally, three different P2P scenarios are explored: one without P2P energy trading, one with P2P energy trading using the *Setting one* described in section 4.3.1, and one with P2P energy trading using the *Setting two* described in section 4.3.2.

6.1.2 STOR seasons and committed windows

According to the National Grid [174], STOR runs from April to April and is divided by seasons, these seasons define the committed windows for each STOR service day where STOR is required. The need for STOR varies depending on the season, weekday and time of day, as dictated by the system demand profile at that time; which is why the National Grid Electricity System Operator splits each running year into six different seasons accounting for working days, Monday to Saturday, and non-working days, Sundays and bank holidays, and sets the periods of time for each STOR service day when STOR might be required. These times are considered from 05:00 to 05:00 the next day. These service days are called committed windows.

To model these committed windows, in this work the year referred to by the National Grid as *"Year 15 STOR Seasons – 1 April 2021 to 1 April 2022"* was used [174]. These seasons and committed windows are described in table 6.2 where two different start and end times can be seen, which belong to the morning and evening of each day. Here, *Mr* denotes the morning and and *Ee* the evening.

Table 6.2: Description of the STOR seasons and committed windows used in this work. *Mr* denotes the morning and *Ee* the evening.

Seasons	Dates	Time	Working days		Non-working days	
	(MM-DD)		start time	end time	start time	end time
1	April 01 to	*Mr*	06:00	13:00	10:00	14:00
	May 03	*Ee*	19:00	22:00	17:30	22:00
2	May 03 to	*Mr*	06:30	14:00	10:30	13:30
	August 23	*Ee*	16:00	22:00	17:30	22:00
3	August 23 to	*Mr*	06:30	13:00	10:30	12:30
	September 27	*Ee*	16:00	22:00	17:30	22:00
4	September 27 to	*Mr*	06:00	13:00	10:30	13:00
	October 25	*Ee*	17:00	22:00	17:30	22:00
5	October 25 to	*Mr*	06:00	13:00	10:30	13:30
	January 24	*Ee*	16:00	20:30	16:00	19:30
6	January 24 to	*Mr*	06:00	13:00	10:30	13:00
	April 01	*Ee*	16:30	20:30	16:30	20:00

6.1.3 STOR technical requirements and case studies

The National Grid requires participants to meet certain technical requirements before providing STOR services. These technical requirements are described below as stated by the National Grid [174].

- Participants must provide a minimum of 3 MW of generation or consistent demand reduction. This can be compiled from multiple sites.
- Respond to an instruction in no more than 20 minutes.
- Sustain the response for a minimum of two hours.
- Respond again after a recuperation period of not more than 1,200 minutes.

Although the microgrid explored in this work may not meet some of the technical requirements, especially the one that sets the minimum power supply of 3 MW, we are interested in exploring the impact of the availability of EVs when providing this service.

It is worth noting that the National Grid states that *"It is not possible to provide other services at the same time as providing STOR"*, this unless the provision of other balance services is outside the contracted availability windows, i.e. committed windows. Given that V2H is sometimes regarded as offering balancing services [39, 175], providing STOR at the same time could represent an issue. With respect to this, we assume that EVs can participate in V2H and V2G as this can open new markets for EV owners.

Moreover, since participants are paid in two ways, one for being available during committed windows and two, for the energy provided for STOR, mostly known as utilisation payments, a report from National Grid ESO [176] shows that there is an increase in users willing to participate in a flexible STOR service, that is, they have the ability to withdraw from STOR and participate in other markets in real time. In other words, participants are only paid for the energy provided for STOR and have more flexibility, which could be of interest for EVs owners. Therefore, in this work, only the utilisation payment is considered. Table 6.3 shows the utilisation payments for providing energy for STOR taken from Gough et al. [86].

Table 6.3: STOR utilisation payments for each of the six seasons.

Season	Payment (£ / kW h^{-1})
1	0.1710748
2	0.1704394
3	0.1673483
4	0.1672806
5	0.1711733
6	0.1713413

Furthermore, four different case studies were explored. These case studies were designed to explore the impact of the availability of EV has when providing STOR of the EVs predicted in chapter 3. It should be noted that according to Gough et al. [86], National Grid ESO [176] there are only three STOR events per week during the year or 155 days per year. Here, random simulated STOR events were generated for each of the four case studies covering the six STOR seasons and are within each committed window. These STOR events are unique to each STOR season for the first two case studies, and for the other two, fixed times and days of the week were passed into the model. The four case studies are introduced in table 6.4.

Table 6.4: Summary of the representative dates used in this work, the STOR seasons that each of these weeks will cover, and the weighting considered to estimate the annual electricity cost.

Case study	Description
ST_1	Three events per week per STOR season. The events were distributed across the 7 days of the week.
ST_2	Six events per week per STOR season. The events were distributed across the 7 days of the week.
ST_3	Three events per week during weekdays per STOR season. Two events in the same day, one in the morning, one in the evening. Followed by one event the next morning.
ST_4	Three events per week during weekends per STOR season. Two events in the same day, one in the morning, one in the evening. Followed by one event the next morning.

Case study ST_1 is meant to explore the amount of energy of all EVs within the microgrid that can be used for STOR when three events occur during the week -

as mentioned above, the expected amount of events to occur per week during the year. For this case study, each event will be assigned at random through the week and time of the day. The latter means that the event can take place either in the morning or evening. The purpose of this case study is to see the performance of the microgrid and the amount of energy that can be provided for STOR. Case study ST_2, explores the amount of energy of all EVs within the microgrid that can be used for STOR when six events occur during the week. Similar to the case study ST_1, each STOR event is assigned at random during the week and time of the day. The purpose of this case study is to test the performance of the EVs when providing STOR, it would be interesting to observe how they perform under an increased frequency of STOR events per week, and determine whether this results in any changes to the efficiency or effectiveness of the EVs. To this end, six events per week were explored.

Case study ST_3 is meant to explore the possibility of providing energy for STOR in less than 1,200 minutes during the weekdays. This can be accomplished by selecting specific days of the week and times of day that remain constant, regardless of the STOR season. In this way, there will be one event in the morning and another in the evening on the same day - both on Wednesday, followed by an additional event the following morning - Thursday. The purpose of this case study was to see the impact on the performance on the delivery of energy for STOR and if the EVs are capable to respond to STOR events in less than the required time of 1,200 minutes during weekdays. Case study ST_4, similarly to case study ST_3, is meant to explore the possibility of providing energy for STOR in less than 1,200 minutes, but in this case during the weekends. Here, specific days of the week and times of day that remain constant, regardless of the STOR season, were selected. This way, there will be one event in the morning and one event in the evening on the same day - both on Saturday, followed by another event the next morning - Sunday. The purpose of this case study was to see the impact on the performance on the delivery of energy for STOR and if the EVs are capable to respond to STOR events in less than the required time of 1,200 minutes during weekends.

It is worth noting that all STOR events across the four case studies were generated by simulating an instruction to provide STOR 20 minutes prior to actually

providing energy. For case study ST_1 and ST_2, the events were generated randomly, and as already mentioned for case study ST_3, the STOR events take place at fixed times of the day regardless of the STOR season. For all four cases, the STOR events were generated taking into account the start and end times of each committed window for every STOR season, which are listed in table 6.2.

6.1.4 Representative weeks of the year

To comprehensively represent the six STOR seasons of the year, as introduced in table 6.2, six distinct weeks were selected. Coincidentally, each of these weeks also corresponds to one of the four seasons of the year, with one week for spring, two different weeks for summer, two different weeks for autumn, and one week for winter. Furthermore, each of these weeks represents the six seasons in which the provision of STOR is divided, as explained in section 6.1.2 as well as being used to study any seasonal variation. A total of 42 days are simulated overall. These weeks are described in the following.

- **Week 1**: For spring, week *Spring - S1* from 2015-04-20 00:00:00 to 2015-04-26 23:59:00.
- **Week 2**: For summer, week *Summer - S2* from 2015-06-22 00:00:00 to 2015-06-28 23:59:00.
- **Week 3**: For summer, week *Summer - S3* from 2014-09-08 00:00:00 to 2014-09-14 23:59:00.
- **Week 4**: For autumn, week *Autumn - S4* from 2014-10-06 00:00:00 to 2014-10-12 23:59:00.
- **Week 5**: For autumn, week *Autumn - S5* from 2014-12-08 00:00:00 to 2014-12-14 23:59:00.
- **Week 6**: For winter, week *Winter - S6* from 2015-02-23 00:00:00 to 2015-03-01 23:59:00.

Table 6.5 shows a summary of these dates and how each will contribute to the estimated annual electricity cost metric. These weights are based on the number of days that each STOR season lasts, as described in table 6.2.

Table 6.5: Summary of the representative dates used in this work, the STOR seasons that each of these weeks will cover, and the weighting considered to estimate the annual electricity cost based on the number of days in each STOR season.

Week - STOR season	From	To	Weighting
Spring - S1	2015-04-20 00:00:00	2015-04-26 23:59:00	32 / 365
Summer - S2	2015-06-22 00:00:00	2015-06-28 23:59:00	112 / 365
Summer - S3	2014-09-08 00:00:00	2014-09-14 23:59:00	35 / 365
Autumn - S4	2014-10-06 00:00:00	2014-10-12 23:59:00	28 / 365
Autumn - S5	2014-12-08 00:00:00	2014-12-14 23:59:00	91 / 365
Winter - S6	2015-02-23 00:00:00	2015-03-01 23:59:00	67 / 365

6.1.5 Electric vehicle dispatch optimisation for a household

As previously stated in this chapter, the optimisation model presented in chapter 4 was employed for the analysis. However, in order to adequately account for the provision of STOR, additional variables were were taken into consideration. These additional variables are explained below

Equation (6.1) guarantees that the EVs will only provide energy for STOR when there is a STOR event in progress. ST_t^{event} is defined as a situation where energy is required for STOR and is represented by $ST_t^{event} = 1$, otherwise $ST_t^{event} = 0$. As already mentioned, each STOR event has a duration of 120 minutes. Therefore, if the EVs are requested to respond to an instruction at 09:20, the value of ST_t^{event} will remain 0 until 09:40, after which it will be set to 1 for the next 120 minutes.

$$E_{v,t}^{discharge,v2g} \leq ST_t^{event} * M, \quad \forall v, t \tag{6.1}$$

Equation (6.2) describes the theoretical maximum energy expected if all EVs inside the microgrid were connected and provide energy for STOR. Here, the variable $ST^{threshold,theory}$, as mentioned, is the theoretical maximum energy from the EVs for STOR. $P^{max,dis}$ is the discharge power of the bidirectional charger. dt refers to the time step in this case $dt = 1\ min = \frac{1}{60}\ hr$. $Profiles$ is the number of profiles inside the microgrid, in this case $Profiles = 50$.

$$ST^{threshold,theory} = \Big(P^{max,dis} * dt\Big) * Profiles \tag{6.2}$$

Equation (6.3) determines the actual maximum energy threshold that EVs can provide throughout the week for 120 minutes. $ST_t^{threshold,max}$ refers to the maximum amount of energy that can be sustained for 120 min for all STOR events. $ST^{percentage}$ is the value that will determine the actual maximum energy provided throughout the week considering the availability of EVs.

$$ST_t^{threshold,max} = ST^{threshold,theory} * \Big(\frac{ST^{percentage}}{100}\Big), \quad \forall t \tag{6.3}$$

Equation (6.4) describes the aggregated energy of EVs that is provided for STOR.

$$ST_t^{demand,aggregated} = \sum_v E_{v,t}^{discharge,v2g}, \quad \forall t \tag{6.4}$$

Equation (6.5) makes sure that the aggregated demand is not higher than the actual maximum energy that EVs can provide for STOR.

$$ST_t^{demand,aggregated} \leq ST_t^{threshold,max}, \quad \forall t \tag{6.5}$$

Equation (6.6) outlines a Min-Max approach that guarantees that the model yields the highest amount of energy for STOR in each simulation.

$$\sum_t \left[\Big(ST_t^{threshold,max} * ST_t^{event}\Big) - ST_t^{demand,aggregated}\right] \leq 0, \quad \forall t \tag{6.6}$$

In this chapter, the objective function in equation (4.26) is modified to accommodate the newly introduced variables. The objective is to minimise the total cost of operating the microgrid and, at the same time, maximise the energy that can be provided for STOR. We found that adding $ST^{percentage}$ helps the solver find an optimal solution faster.

$$min \left[\sum_{v} \left(C_v^{import} + C_v^{import,street} + C_v^{import,p2p} - C_v^{export} - C_v^{export,p2p} - C_v^{export,v2g} \right) - \sum_{t} \left(ST_t^{demand,aggregated} \right) - ST^{percentage} \right] \tag{6.7}$$

In the case of the percentage of energy sustained when providing STOR for all events of the week, these values are a percentage of the theoretical maximum energy expected if all EVs within the microgrid were connected and provide energy for STOR, as described in equation (6.2), this is $ST^{threshold,theory} = 6.1667\ kWh = 370\ kW$, as calculated in equation (6.8).

$$ST^{threshold,theory} = \left(7.4\ \ kW * \frac{1}{60}\ \ hr\right) * 50 = 6.1667\ \ kWh \tag{6.8}$$

For example, in the case where the solver returns a $ST^{percentage} = 40$, the maximum amount of energy that can be provided during the week for each STOR event, $ST^{threshold,max}$, and that can be sustained for 120 minutes – the minimum technical requirement, as explained in section 6.1.3 – is calculated as shown in equation (6.9) below, as introduced in equation (6.4).

$$ST_t^{threshold,max} = 6.1667\ \ kWh * \left(\frac{40}{100}\right) = 2.4667\ \ kWh, \quad \forall t \tag{6.9}$$

In this example, the resultant $ST^{threshold,max} = 2.4667\ kWh = 148\ kW$ is the maximum amount of energy that can be provided and sustained in all STOR events of the week.

6.1.6 Microgrid system configuration overview

A comparison of different microgrid configurations or microgrid scenarios of the system is considered. EVs can be operated in three different modes according to section 4.4, however, in this case only the V2G mode is considered, which also includes the benefits of using smart charging (V1G) and V2H. Here, each case study

will be identified in the same way as described in table 6.4. Similarly, to chapter 5, microgrid configurations will be referred to as the combination of the different modes in which the microgrid operates and the type of P2P pricing calculation to be used, if applicable. These microgrid configurations are explained in table 6.6.

Table 6.6: Overview of the different microgrid configurations explored in this chapter with a description of the microgrid configuration.

Microgrid configuration or scenario	Description
$ST\_1\_\_\_V2G\_\_\_No\_P2P$	Case Study one; V2G; No P2P.
$ST\_1\_\_\_V2G\_\_\_P2P\_S1$	Case Study one; V2G; P2P Setting one.
$ST\_1\_\_\_V2G\_\_\_P2P\_S2$	Case Study one; V2G; P2P Setting two.
$ST\_2\_\_\_V2G\_\_\_No\_P2P$	Case Study two; V2G; No P2P.
$ST\_2\_\_\_V2G\_\_\_P2P\_S1$	Case Study two; V2G; P2P Setting one.
$ST\_2\_\_\_V2G\_\_\_P2P\_S2$	Case Study two; V2G; P2P Setting two.
$ST\_3\_\_\_V2G\_\_\_No\_P2P$	Case Study three; V2G; No P2P.
$ST\_3\_\_\_V2G\_\_\_P2P\_S1$	Case Study three; V2G; P2P Setting one.
$ST\_3\_\_\_V2G\_\_\_P2P\_S2$	Case Study three; V2G; P2P Setting two.
$ST\_4\_\_\_V2G\_\_\_No\_P2P$	Case Study four; V2G; No P2P.
$ST\_4\_\_\_V2G\_\_\_P2P\_S1$	Case Study four; V2G; P2P Setting one.
$ST\_4\_\_\_V2G\_\_\_P2P\_S2$	Case Study four; V2G; P2P Setting two.

The various microgrid scenarios stated in table 6.6 will be simulated using the six weeks described in section 6.1.4, as well as the various PV penetration rates and energy tariffs described in section 6.1.1. However, for energy tariffs, five potential energy tariff configurations or tariff scenarios will be investigated. These five scenarios are the same as in chapter 5 as summarised in table 5.3, which also provides the percentage of profiles that use each energy tariff in each tariff scenario.

For this chapter, the number of simulations considered for each microgrid configuration – described in table 6.6 – is 210 in total each, which considers the seven different PV penetration rates and the five tariff scenarios – described in table 5.3 and the six different weeks described in section 6.1.4. Therefore, for this chapter, a grand total of 2,520 simulations will be explored.

6.1.7 Metrics

The performance metrics already introduced in section 4.4.6 will be used to evaluate the performance of each microgrid configuration or scenario described in this chapter. To assess the quality of the results presented, the metric described in section 4.4.7 will be used.

Furthermore, two new metrics are introduced to measure the impact of the availability of the EVs has when providing energy for STOR. These are described below.

- **Highest number of EVs providing energy for STOR:** This is the highest number of EVs registered that discharged energy for STOR of all the STOR events of the week.
- **Percentage of energy sustained when providing STOR:** This is the percentage of energy provided for all STOR events of the week. This is the variable $ST^{percentage}$ introduced in equation (6.3).

6.2 Results

In this section, we introduce the results of the microgrid for the case studies during the summer, specifically Summer - S2, using the Agile Go tariff. A description of its performance according to the established metrics explained in section 6.1.7. The impact of the different representative weeks, the performance of the microgrid for each tariff and the provision of STOR is then evaluated before calculating the estimated annual total electricity cost for each scenario and tariff. Finally, a brief evaluation of the quality of the results is provided.

For this chapter, as stated in section 4.2, each simulation was built using the Python 3.8.8 [125] programming language and the Pyomo 6.3.0 library [157] and then solved using Gurobi 9.5.2 [156].

6.2.1 Results comparison between two case studies for a week in summer using the agile go tariff

In this section, the plots for $ST\_1\_\_\_V2G\_\_\_P2P\_S2$ and $ST\_2\_\_\_V2G\_\_\_P2P\_S2$ will be presented first to give a general idea of how the microgrid operates. These two

scenarios were selected randomly using a simple Python script to choose two out of the 2,520 resulting simulations.

Figure 6.1 shows the simulation results of the scenario $ST\_1\_\_\_V2G\_\_\_P2P\_S2$ with 90% PV penetration rate PV and using the Agile Go tariff during a week in summer – Summer - S2. This figure shows the energy imported from the grid, the house demand and solar generation showing the energy that is locally used, the energy that is sold to the grid and the energy shared to other members of the microgrid, the internal microgrid buy and sell prices for importing energy and selling energy from the grid and from the energy shared via P2P with *Setting two* and the total number of EVs available during the day and how many are charging and discharging. It also shows STOR events for the same case study with a total of EVs available at home and a total of EVs providing energy for STOR highlighting the highest number of EVs providing energy of all STOR events and the lowest number of EVs available at home during the week.

Similarly to figure 6.1, figure 6.2 shows the simulation results of the scenarios $ST\_2\_\_\_V2G\_\_\_P2P\_S2$, with PV penetration rate of 90% and using the Agile Go tariff during the summer week – Summer - S2 and the simulated STOR events for this case study.

In both figures 6.1 and 6.2, row **(a)** and **(b)** show an increase in the demand for energy from the grid during periods when the price of electricity is low, mainly due to the EVs charging at night. This results in a maximum energy drawn from the grid of up to 165 kW for $ST_1___V2G___P2P_S2$and up to 235 kW for $ST\_2\_\_\_V2G\_\_\_P2P\_S2$. Here, the increase in peak demand can be attributed to EVs charging energy in advance for later use to provide energy for STOR, as in $ST_2___V2G___P2P_S2$has six STOR events during the week. Moreover, EVs also tend to charge when local solar generation is available, particularly around 12:00 with a few exceptions where it might make more financial sense to sell surplus energy to the grid. It could also be the case that EVs are required to provide energy for STOR when charging is not possible, as EVs can charge or discharge at each time step.

In these two scenarios, row **(b)** shows that solar energy is sold to both the grid and P2P on most days, as in some cases, selling to one or the other will be more

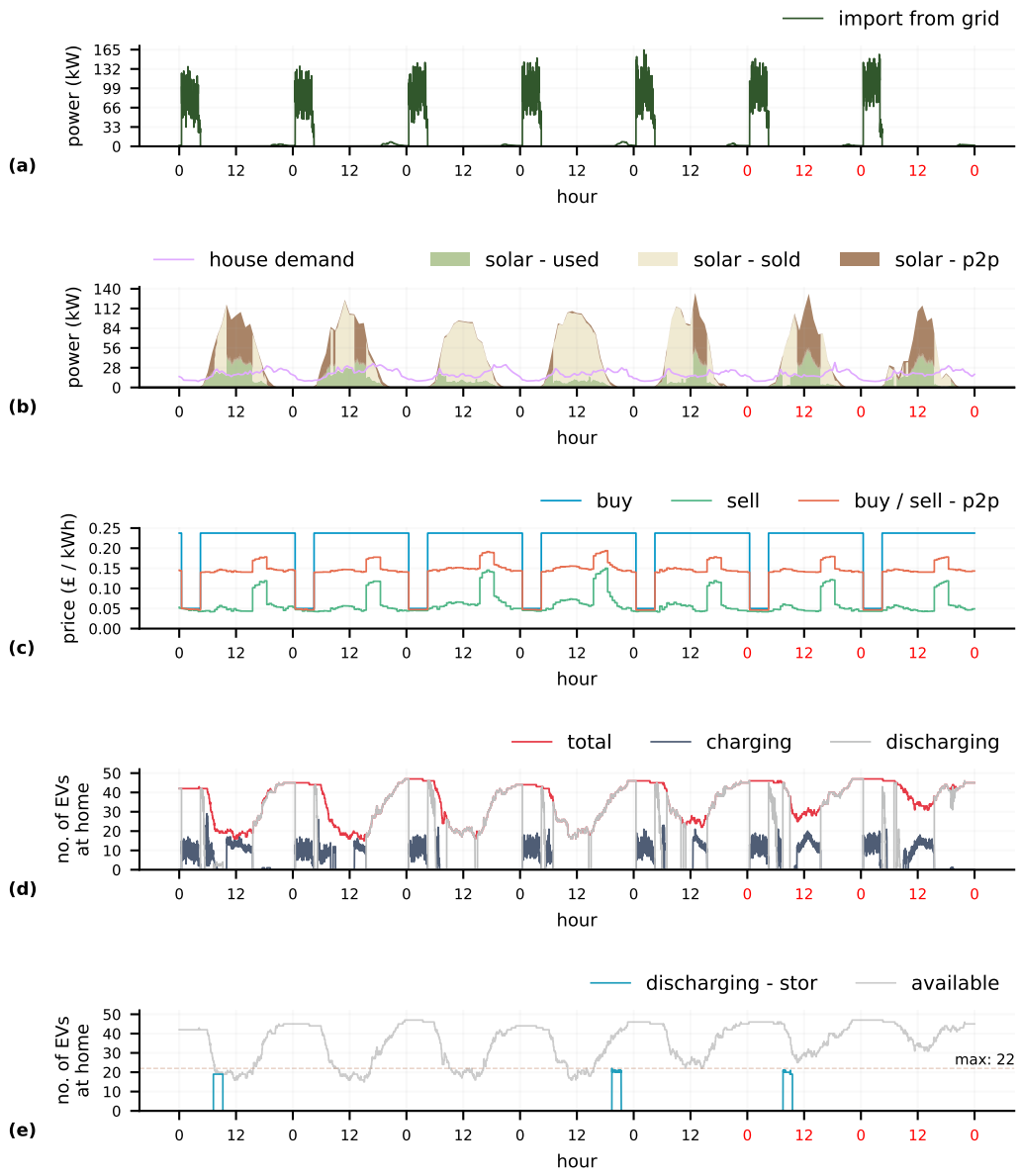

Figure 6.1: Simulation results for the Summer - S2 week showing microgrid operation with a PV penetration rate of 90% and using the Agile Go tariff. This date belongs to the *ST_1___V2G___P2P_S2* microgrid configuration. The tick labels on *X-axis* in black denote data from Monday to Friday, and the red labels, data from Saturday and Sunday. **a.** Power import from the grid. **b.** Household demand and energy consumed, shared and sold from solar generation within the microgrid. **c.** Buy and sell prices from the grid and from P2P energy trading. **d.** Number of EVs available at home charging and discharging and the total number of EVs available at home. **e.** Simulated STOR events showing the total number of EVs available at home and the number of EVs providing energy for STOR. The brown dashed line is the highest number of EVs that provide energy at the same time of all STOR events of the week.

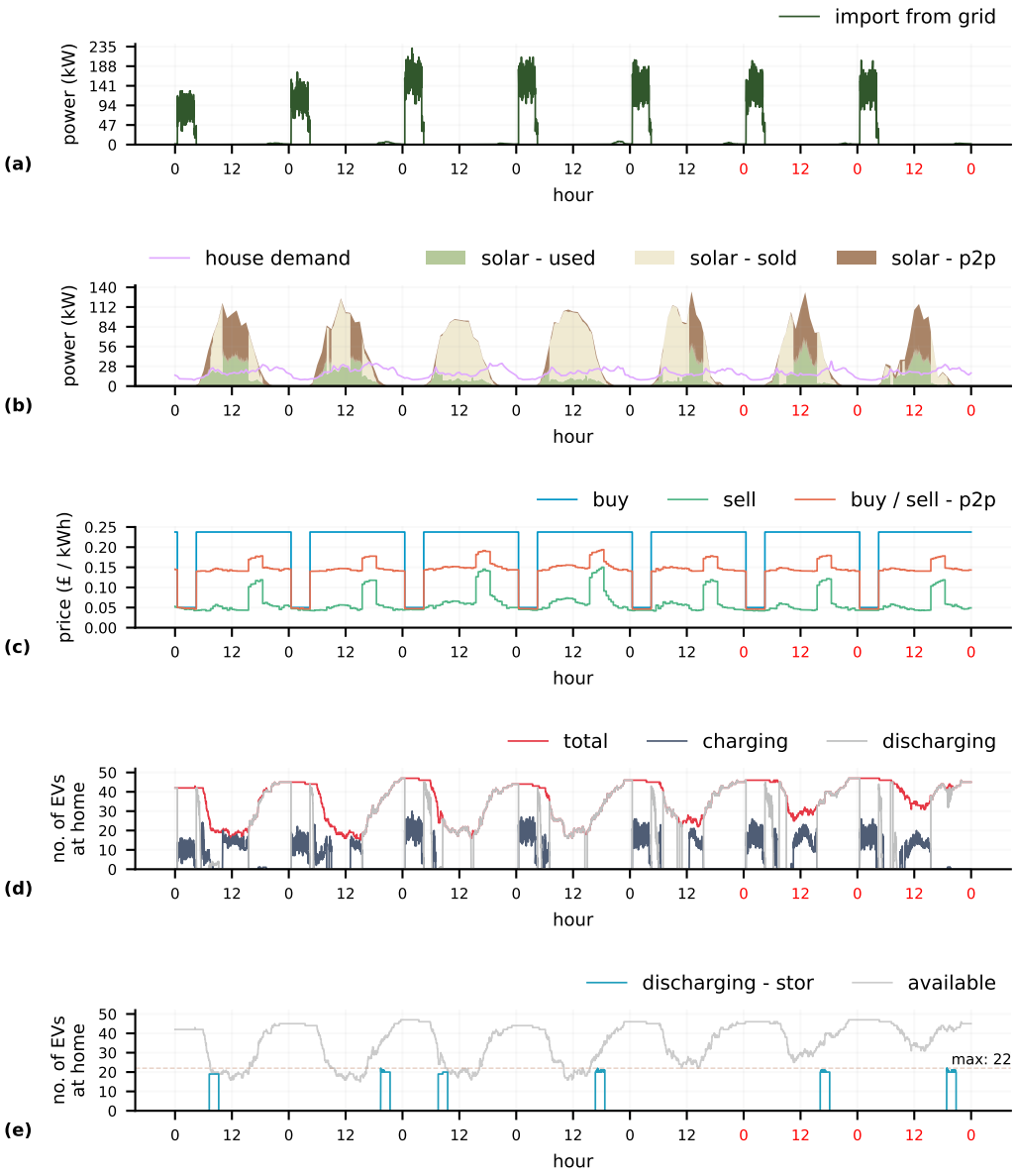

Figure 6.2: Simulation results for the Summer - S2 week showing microgrid operation with a PV penetration rate of 90% and using the Agile Go tariff. This date belongs to the $ST\_2\_\_\_V2G\_\_\_P2P\_S2$ microgrid configuration. The tick labels on *X-axis* in black denote data from Monday to Friday, and the red labels, data from Saturday and Sunday. **a.** Power import from the grid. **b.** Household demand and energy consumed, shared and sold from solar generation within the microgrid. **c.** Buy and sell prices from the grid and from P2P energy trading. **d.** Number of EVs available at home charging and discharging and the total number of EVs available at home. **e.** Simulated STOR events showing the total number of EVs available at home and the number of EVs providing energy for STOR. The brown dashed line is the highest number of EVs that provide energy at the same time of all STOR events of the week.

profitable for households with PV generation. It is worth noting that when EVs discharge energy for STOR, the home is not allowed to import energy from the grid and if there is a solar surplus, this surplus energy has to be sold to either the grid or P2P as prices on *Setting two* can offer better value for PV owners. This is because the model functions in a way that allows households to either draw energy from the grid or export energy to it, but not both simultaneously, as explained in equations (4.17) and (4.18). In essence, the model only allows a one-way flow of energy between the house and the grid. This could be seen as a limitation, as it restricts the flexibility of energy exchange between the household and the grid. This can be seen in both figures 6.1 and 6.2 on some days of the week EVs that the energy is discharged for STOR when they are connected at home and the solar energy is exported instead of being used locally. This results in a total energy shared for $ST_1___V2G___P2P_S2$of 1,678 kWh and self-suffiency ratio (SSR) results of 64.98%, for the case study $ST_2___V2G___P2P_S2$a total energy shared of 1,610 kWh and SSR results of 57.26%.

6.2.2 Performance of Microgrid Configurations for a week in summer using the agile go tariff

In this section, we will present and compare the four case studies, focusing on their performance metrics. Here, only the metrics outlined in the section 4.4.6 will be discussed. The two new metrics introduced to evaluate the effect of EV availability on the provision of energy for STOR, as mentioned in the section 6.1.7, will be explored in the following section.

Figures 6.3a and 6.3b displays a summary of the resulting performance metrics of the case studies ST_1, ST_2 and ST_3, ST_4, respectively, for all microgrid configurations or scenarios for the Summer - S2 week using the Agile Go tariff. Each row in both figures comprises five separate metrics as described in section 6.1.7, which are detailed in the following.

- **Row A:** Contains results for SSR.
- **Row B:** Contains results for energy balance index (EBI).
- **Row C:** Contains results for the energy imported from the exchange via P2P

in kWh.

- **Row D:** Contains results for the maximum power load of the energy imported from the grid in kW.

- **Row E:** Contains results for the mean electricity cost per week in British pounds (£).

Similarly to the results in chapter 5, in general, these findings indicate a considerable link between PV penetration rates and whether P2P is allowed and which of the two P2P settings is used. As expected, SSR tends to increase at the same time as the PV penetration rates increase for all microgrid configurations or scenarios. This metric reaches its highest value in both cases when PV penetration rate is 100%, P2P is allowed and *Setting two* is used.

Here, the SSR in ST_1 is between 24.44% and 68.75%, for ST_2, it is between 21.87% and 60.91%, for ST_3, it's between 24.85% and 70.25% and for ST_4, it falls between 21.30% and 63.63%. Across the different case studies, ST_1 to ST_4, the introduction of P2P under *Setting one* results in only a marginal increase in SSR, but this growth is significant when PV penetration rates are over 50% under *Setting two*. EBI follows the same trend, where higher PV penetration rates increase this metric value in all case studies and microgrid configurations and *Setting two* shows the highest values when compared to not using P2P or using P2P and *Setting one*.

Concerning energy sharing through P2P, there's a noticeable difference between *Setting one* and *Setting two*. The shared energy under *Setting one* is considerably less due to less advantageous pricing in high PV penetration rates, making self-consumption of local solar generation or selling to the grid more sensible. However, *Setting two* benefits from more beneficial prices for both buyers and sellers, which in turn increases energy sharing among peers.

For instance, with a 25% PV penetration rate under *Setting one*, energy sharing within the microgrid varies from 728 kWh (ST_1) to 782 kWh (ST_4). Under *Setting two*, the shared energy peaks at a 100% PV penetration rate for ST_1 and ST_3 (1,681 kWh and 1,673 kWh respectively), and at a 75% PV penetration rate for ST_2 and ST_4 (1,629 kWh and 1,652 kWh respectively).

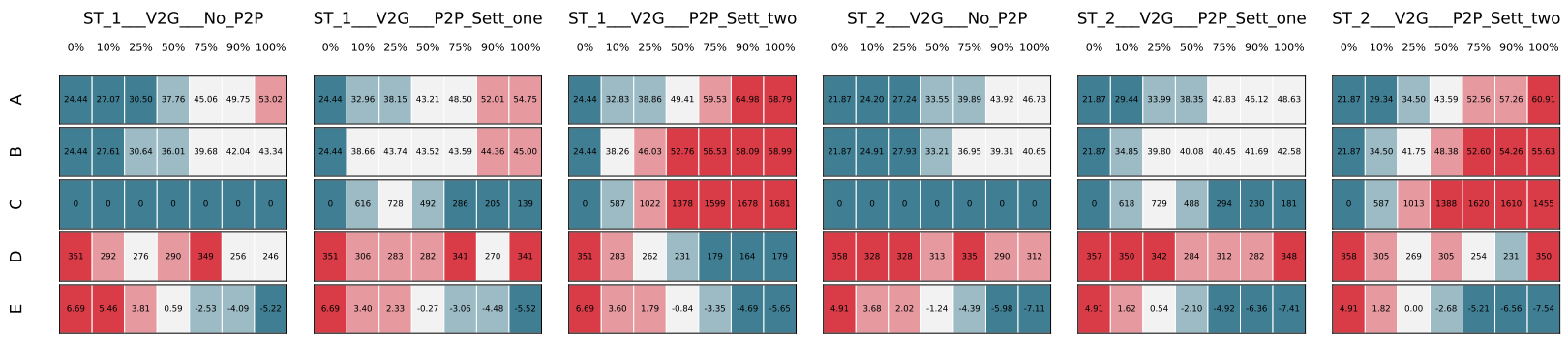

(a) *ST_1* and *ST_2*

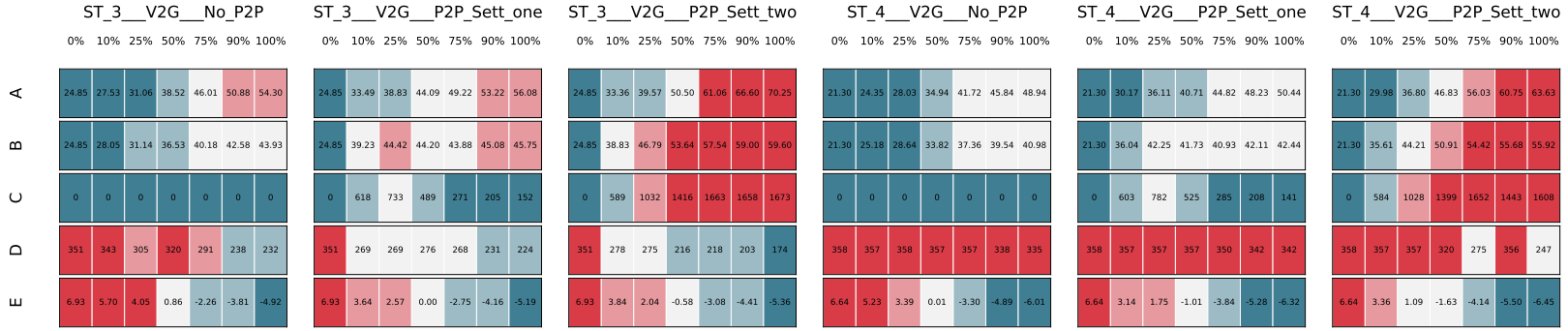

(b) *ST_3* and *ST_4*

Figure 6.3: Performance metrics for the microgrid for the Summer - S2 week using the Agile Go tariff. Each block belongs to one microgrid configuration or scenario, where columns are each specific scenario and rows each performance metric. *X-axis* denotes the increase of PV penetration rates from 0% to 100%. Dark red represents the highest values for each row, and dark blue represents the lowest. **a.** Self-suffiency ratio. **b.** Energy balance index. **c.** Energy imported from P2P (kWh). **d.** max power load from the grid (kW). **e.** Mean electricity cost per week (£).

However, it's important to note that these results across the four studies are quite similar. This is because the only variable that changes between each case study is the number and timing of the STOR events, which can influence the EV charging and discharging behaviours, as they can't occur at the same time. This is evident, for example, in the four cases with a 25% PV penetration rate and P2P allowed under *Setting two*, where the energy shared between peers ranges from 1,022 to 1,032 kWh.

The maximum power load from the grid varies with the PV penetration rates across all four studies, generally decreasing as the PV penetration rates increase. For instance, $ST\_1\_\_\_V2G\_\_\_No\_P2P$ ranges from 246 kW (100% PV penetration rate) to 351 kW (0% PV penetration rate). For $ST\_1\_\_\_V2G\_\_\_P2P\_S1$, the range is between 351 kW (0% PV penetration) and 270 kW (90% PV penetration). For $ST\_1\_\_\_V2G\_\_\_P2P\_S2$, the range is from 179 kW (75% and 100% PV penetration rates) to 351 kW (0% PV penetration rate). In ST_2, the lowest maximum power from the grid is observed with a 90% PV penetration rate, with respective values of 290 kW (No P2P), 282 kW (P2P and *Setting one*), and 231 kW (*Setting two*). In ST_3 and ST_4, both with 100% PV penetration and P2P trading under *Setting two*, the values are 174 kW and 247 kW respectively.

Across all case studies, energy import from the grid decreases significantly as PV penetration rates increase. For $ST\_1\_\_\_V2G\_\_\_No\_P2P$, import decreases from 5,850 kWh to 3,386 kWh; for $ST\_2\_\_\_V2G\_\_\_No\_P2P$, from 6,759 kWh to 4,334 kWh; for $ST\_3\_\_\_V2G\_\_\_No\_P2P$, from 5,724 kWh to 3,206 kWh; and finally, for $ST\_4\_\_\_V2G\_\_\_No\_P2P$, from 6,224 kWh to 3,854 kWh. The introduction of P2P reduces energy import further. Under *Setting one*, the decrease is slight, as observed in $ST\_2\_\_\_V2G\_\_\_P2P\_S1$ with a reduction to 3,758 kWh. However, under *Setting two*, the reduction is significant, nearly 900 kWh less compared to not using P2P or using P2P with *Setting one*.

High import energy values could be due to EVs charging more energy when electricity prices are low to participate in STOR provision. The number of STOR events also impacts energy import. ST_2, with six STOR events during the week, displays some of the highest values in all its microgrid configurations compared to other studies.

Mean electricity costs per week generally decrease with higher PV penetration rates, ranging from £6.93 to -£7.54, with negative costs implying earnings instead of payments. Not using P2P tends to return the highest costs, while usingP2P, particularly with *Setting two*, results in the lowest costs across all case studies. Furthermore, the number of STOR events in a week influences the mean electricity cost, with more events offering more opportunities to supply STOR energy and increase profits. For instance, ST_2 exhibits the lowest weekly mean electricity costs compared to the other three studies, which have similar costs to each other.

As in Chapter 5, all microgrid configurations enable participants to sell solar energy to the grid. However, opting to do so decreases SSR, EBI, and microgrid P2P energy sharing, while increasing the maximum power load from the grid, thus making the microgrid more grid-dependent. Nevertheless, selling energy to the grid can reduce weekly mean electricity costs, depending on whether P2P is allowed and the selected setting. Overall, allowing P2P under *Setting two* delivers the best outcomes for the five performance metrics compared to other scenarios.

The following summary provides a review of this section's findings when using the Agile Go tariff during a week in summer:

- In all four case studies (ST_1 to ST_4), both the SSR and the EBI saw increases with higher PV penetration rates and the inclusion of P2P energy sharing. The SSR ranged between 21.30% and 70.25%. Both metrics experienced a minor increase when comparing scenarios where P2P is allowed against the ones where P2P is allowed under *Setting one*, while a considerable rise was seen with *Setting two* for PV penetration rates over 50%.

- The amount of energy shared via P2P in the case studies differed notably between *Setting one* and *Setting two*. Under *Setting one*, energy shared within the microgrid at a 25% PV penetration rate ranged from 728 kWh (ST_1) to 782 kWh (ST_4). In contrast, *Setting two*, recorded peaks in energy shared at the highest PV penetration rates (75%-100%), with values between 1,629 and 1,681 kWh.

- The maximum power load drawn from the grid and energy imported from the grid were inversely related to PV penetration rates across all studies. Higher

PV penetration rates resulted in lower maximum power load, with the lowest values seen between 174 kW ($ST\_3\_\_\_V2G\_\_\_P2P\_S2$, 100% PV penetration rate) and 351 kW ($ST\_1\_\_\_V2G\_\_\_No\_P2P$, 0% PV penetration rate). Additionally, energy import saw a significant decrease with increasing PV penetration rates and further reduction with P2P trading, especially under *Setting two*.

- Mean weekly electricity costs also tended to decrease with higher PV penetration rates, with the lowest costs (even reaching negative values, implying earnings for the households rather than costs) associated with P2P under *Setting two*. ST_2, the case study with the most number of STOR events (6 events during the week), consistently exhibited the lowest mean costs.

- The option to sell solar energy to the grid across all case studies resulted in decreased SSR, EBI, and energy shared within the microgrid, and an increased maximum power load from the grid. However, it also had the potential to reduce the mean weekly electricity cost, depending on whether or not P2P energy sharing was allowed and which price mechanism was used.

- While all studies followed similar trends in terms of PV penetration rates, P2P settings, and STOR events' impacts on SSR, EBI, energy sharing, power load, energy import, and electricity costs, specific values varied. This variance was primarily due to differences in the number and timing of the STOR events in each case study, influencing EV charging and discharging behaviours and overall energy dynamics.

6.2.3 Results of all microgrid configurations and tariffs over the different representative weeks in a year

This section presents an analysis of the metrics introduced in Section 4.4.6 and Section 6.1.7. The first part will focus on three performance metrics: SSR, P2P energy sharing, and the mean weekly electricity cost. These three performance metrics help assess the practicality and economic viability of the microgrid configurations and case studies in this work. In the second part, the specific metrics to measure the role of EVs in providing energy for STOR are analysed. This section covers the

four different case studies across the different microgrid configurations.

The division of these topics into two distinct subsections was deemed necessary to ensure clarity. It allows for an in-depth, separate analysis of each aspect of the research, resulting in a more precise understanding of the outcomes and implications of each set of metrics in our study.

6.2.3.1 Performance metrics

Similarly to section 5.2.3, the figures presented include values in all microgrid configurations or scenarios. The values are divided into two sections; the column on the left, column 1 contains the average values from 0% to 50% PV penetration rates and the right column, column 2 contains the average values from 51% to 100% PV penetration rates. Moreover, each row includes each of the five tariff scenarios, rows 1 to 5, that were explored, different colours are used to differentiate between the six representative weeks of the year, and different marker shapes are used to help distinguish them between each microgrid configuration. *X-axis* tick labels also include information about each microgrid configuration.

In this section, as in section 5.2.3, the focus will primarily be on a select set of performance metrics: SSR, energy shared from P2P, and the average weekly electricity cost. Additional metrics, such as EBI, the maximum power load from the grid, and total energy imported from the grid, can all be found in Appendix B, specifically in appendix B.1.2.

Figure 6.4 presents a detailed comparison of the SSR, across different tariff scenarios and different weeks of the year.

The first column shows slight differences between each week for the first three tariffs and the All Tariffs scenario, ranging from 20% to about 40%. The Flat tariff, in contrast, shows more noticeable differences, with values ranging from 0% to approximately 30%. In certain situations, the Summer - S2 tariff outperforms other weeks in the first column, yet there are instances where the Agile Go, E7 tariffs, or All Tariffs scenario perform comparably.

In the second column, the Summer - S2 tariff again generally performs the best, except for with the Agile Go tariff, where the Spring - S1 tariff demonstrates superior performance. This column shows performance values ranging from 15% to nearly

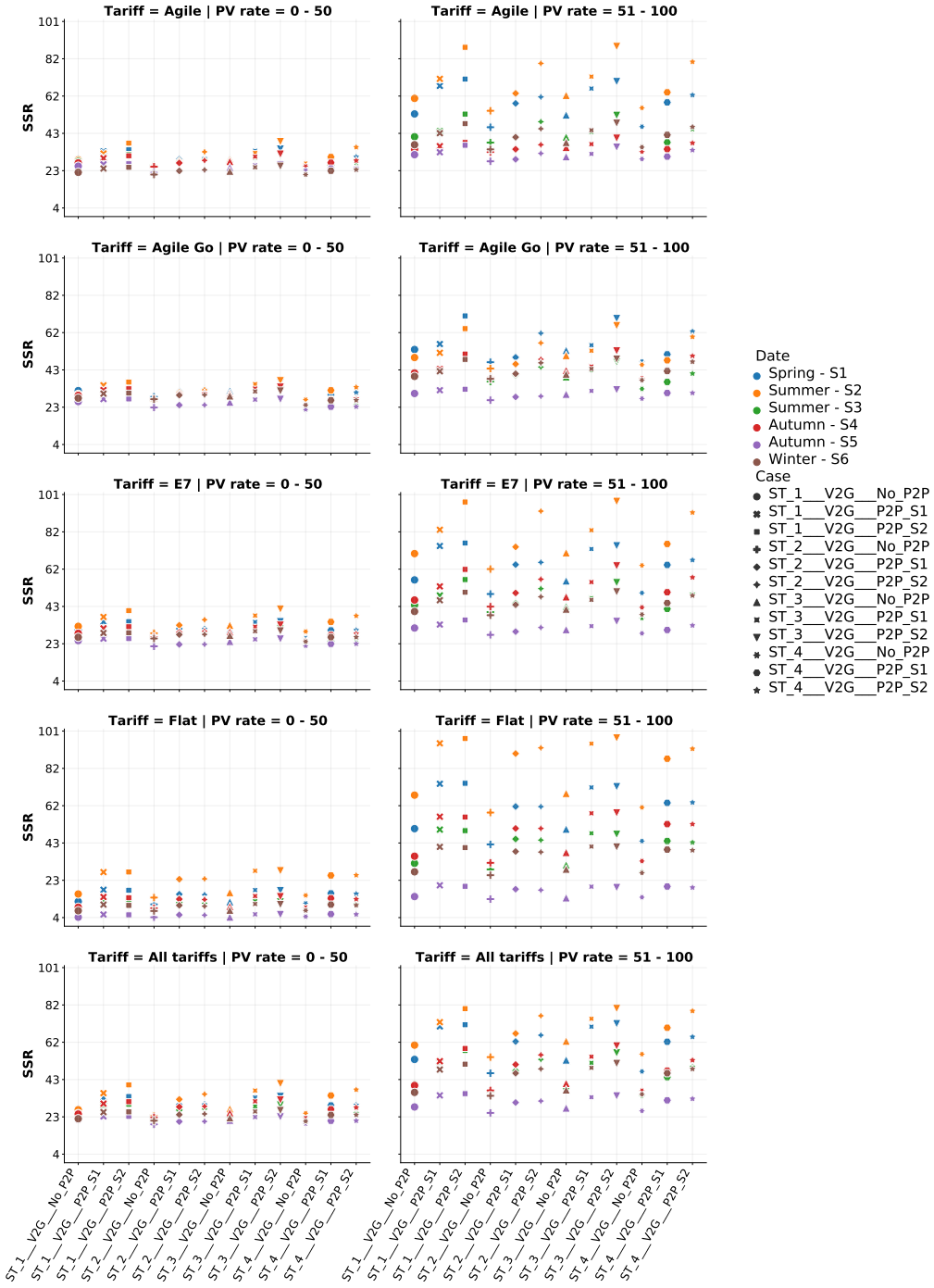

Figure 6.4: Self-suffiency ratio values for the six representative weeks of the year, the five tariff scenarios and all microgrid configurations explored in this chapter. The left column contains the average values from 0% to 50% PV penetration rates and the right column contains the average values from 51% to 100% PV penetration rates.

100% for the E7 and Flat tariff. A significant difference in performance across the weeks of the year is observed, likely due to the variations in solar generation throughout the year. Autumn - S5 often has the lowest performance values, which corresponds with the decrease in sunlight during this season.

An important observation is that microgrid configurations that allow P2P energy sharing, especially under the *Setting two*, consistently have the highest performance values compared to those microgrid configurations where P2P is allowed under *Setting one* or those microgrid configurations without P2P allowed. This finding suggests that enabling P2P energy sharing w could significantly enhance the effectiveness of microgrid configurations under a price mechanism that benefits both sellers and buyers such as *Setting two*.

Figure 6.5 provides a comparison of the total energy imported via P2P energy sharing within a microgrid. For this analysis, only scenarios with P2P, both *Setting one* and *Setting two*, and PV penetration rates ranging from 10% to 100% are considered, focusing on how these two systems affect the performance of the microgrid. These elements are significant within the context of energy import and trade within a microgrid, and both directly influencing the performance of the microgrid.

In figure 6.5, microgrid configurations in column 1 operating under *Setting one*, are observed to trade less energy in comparison to those under *Setting two*. This behaviour is primarily attributed to the differences in P2P prices that are offered to energy buyers and sellers within the microgrid, as explained in section 4.3. Here, the overall energy shared within the microgrid under *Setting one* , particularly during Spring - S1 and Summer - S2, can be around half of the amount of energy traded under *Setting two*.

Column 2, compared to column 1, contains the results of higher PV penetration rates, which in this case shows a substantial increase in the amount of energy traded within the microgrid, reaching up to 3,700 kWh. This pattern suggests that a higher degree of solar energy availability potentially facilitates more energy transactions. Consistent with our previous observation, configurations operating under *Setting two* continue to show higher results. Overall, as shown in both columns 1 and 2, the total energy traded under *Setting one* shows small increments from week to week. In contrast, *Setting two* presents a more dynamic scenario, showing considerable

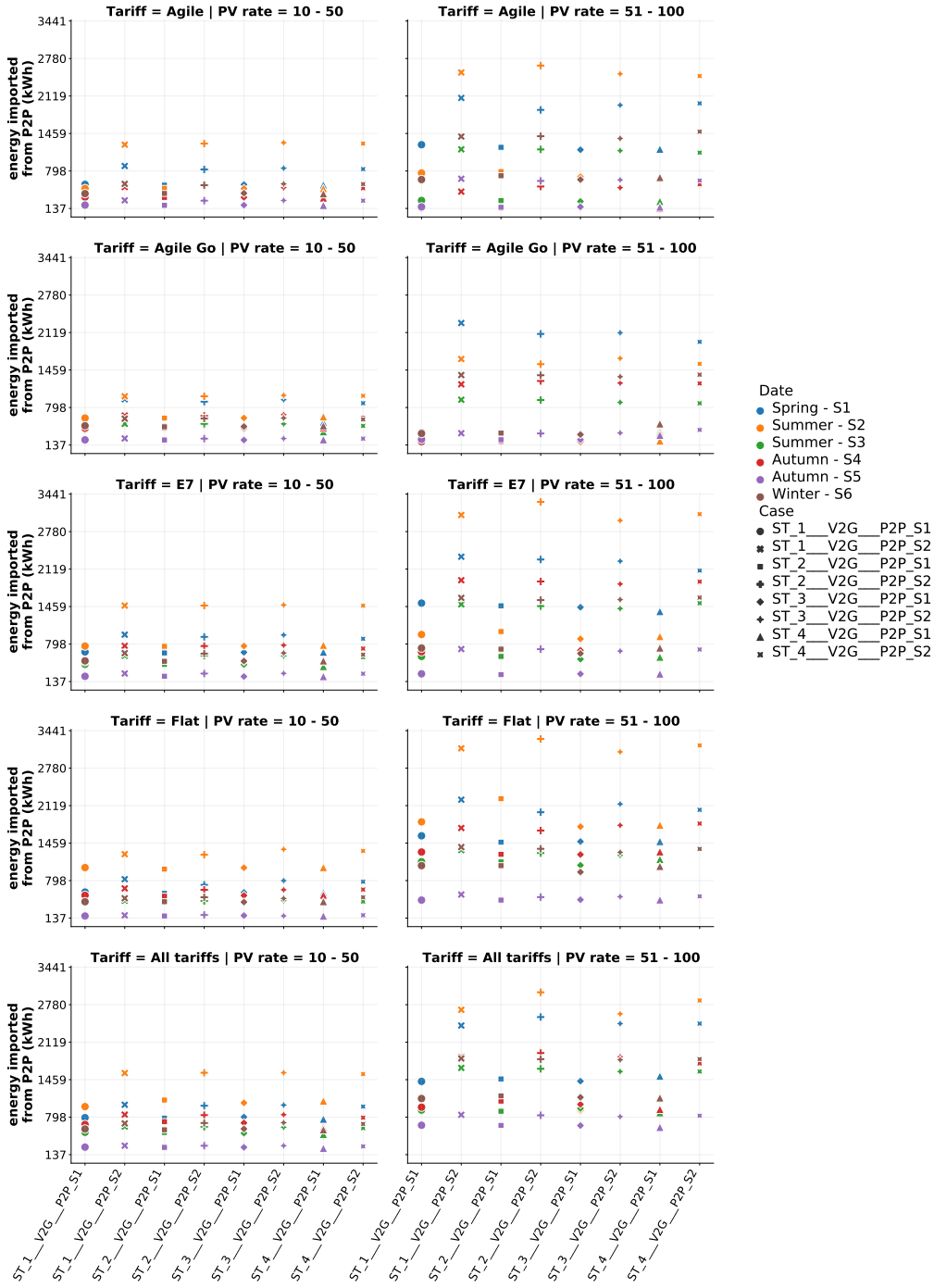

Figure 6.5: Energy shared from P2P for the six representative weeks of the year, the five tariff scenarios and all microgrid configurations explored in this chapter. The left column contains the average values from 0% to 50% PV penetration rates and the right column contains the average values from 51% to 100% PV penetration rates.

fluctuations in the weekly energy exchanges.

It is important to note that the amount of energy exchanged within the microgrid is not solely influenced by settings or PV penetration rates. Seasonal variations in sunlight also play a crucial role. For instance, during Summer - S2, more energy is traded, mainly due to the greater availability of solar surplus. In contrast, during Autumn - S5, energy trading reduces due to lesser sunlight during this time of the year.

Additionally, the impact of different tariff scenarios on energy trading becomes apparent. As tariff data is quite important to calculating P2P prices, the choice of tariff can have significant implications. For instance, when the Agile Go tariff is used exclusively within the microgrid alongside high PV penetration rates, the total energy exchanged within the microgrid is less than in the other four tariff scenarios. In this case, the average energy traded is less than 2,500 kWh, with the highest results observed during Spring - S1 rather than the sunnier Summer - S2 week.

Figure 6.6 presents a comparative analysis of the mean weekly electricity prices within different microgrid configurations. One observable trend is that configurations with P2P under *Setting two* consistently show lower prices compared to other configurations. The prices span from -£9 to £27 across all the weeks of the year, both columns (lower and higher PV penetration rates) and all rows (different energy tariff scenarios).

A closer look shows that the Summer - S2 week typically corresponds to the lowest costs. There's an exception when the Agile tariff with PV penetration rates of 0-50% is employed; here, the lowest costs are observed during the Autumn - S4 week. Moreover, the highest prices generally occur during Autumn - S5 or Winter - S6, depending on the tariff and PV penetration rates. Additionally, as PV penetration rates increase, the difference in weekly results also increases. As expected, during periods of the year with abundant sunlight, there are some instances where electricity cost are of negative, meaning that the user gets paid instead of paying their electricity bill.

It is worth noting that these prices are influenced by the frequency of STOR events each week. Participation in STOR provision can generate profit for households. However, the timing of these events is crucial. Which means that, during a

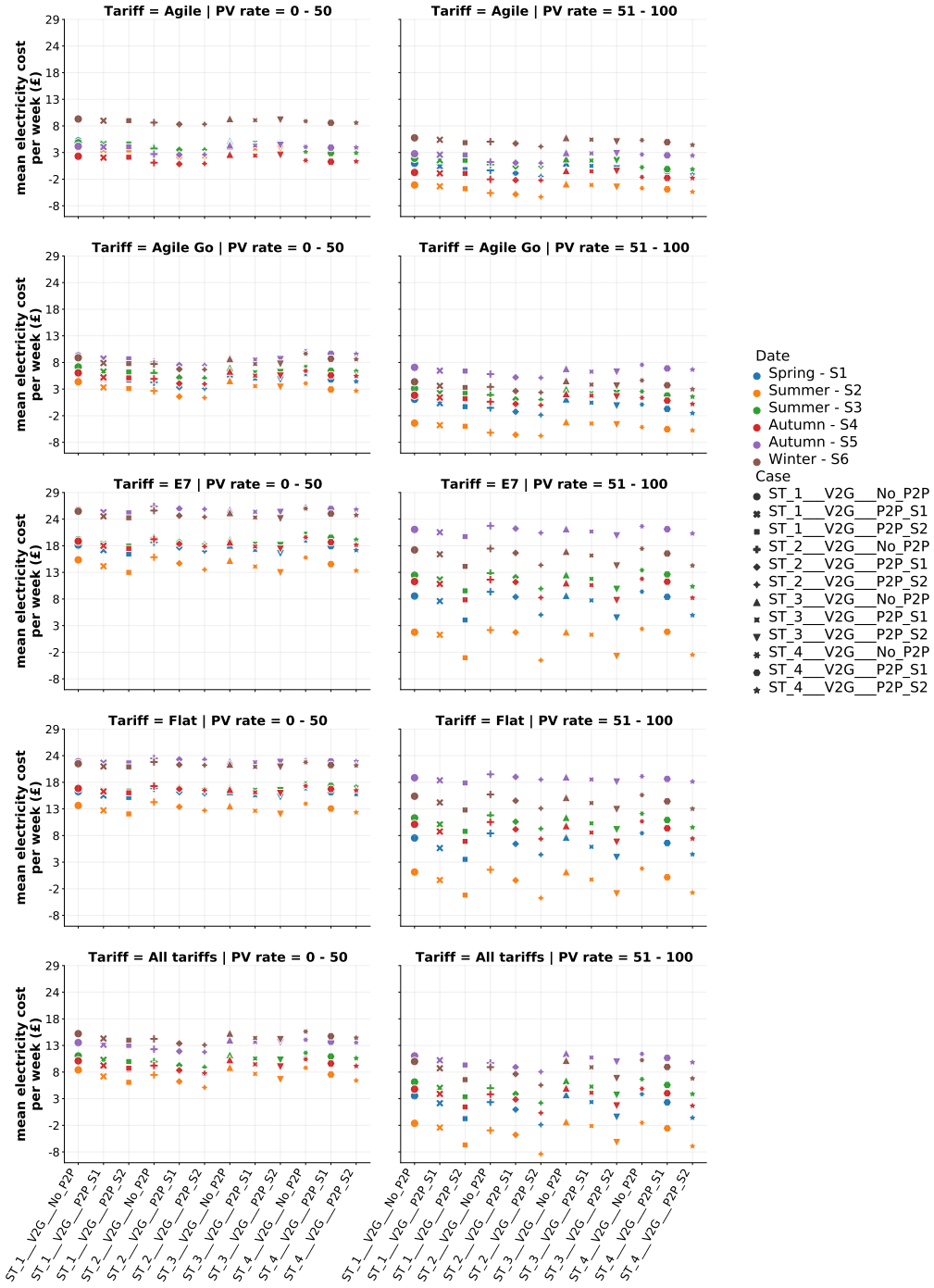

Figure 6.6: Mean electricity cost per week for the six representative weeks of the year, the five tariff scenarios and all microgrid configurations explored in this chapter. The left column contains the average values from 0% to 50% PV penetration rates and the right column contains the average values from 51% to 100% PV penetration rates.

STOR event, any EVs discharging will not be able to take advantage of charging using solar generation. Instead, any surplus energy from the household must either be exported to the grid or shared with peers within the microgrid. The results indicated the importance of STOR events and their influence on a household's energy generation and consumption. Particularly, how households responded to these events by altering how they handle their energy resources, which had potential implications for cost minimisation and profit generation.

6.2.3.2 Short Term Operating Reserve (STOR) Performance

Up to this point, the performance metrics from section 4.4.6 have been explored. Moving forward, we will focus on the metrics from section 6.1.7. As mentioned before, these metrics specifically measure the impact of EV when providing energy for STOR across the four different case studies.

Figures 6.7 and 6.8 shows a comparison percentage of energy sustained when providing STOR for all events of the week and the highest number of EVs that provide energy for STOR. It can be seen that there is a correlation between the number of EVs and the amount of energy discharged for STOR. Here, the highest number of EVs provides more energy in all the weeks studied. The difference between weeks is highly dependent on the amount of EVs available, the number of events per week, and when these events take place, as this will change the amount of energy that can be provided for STOR. In general, the different tariffs and the different PV penetration rates have little impact on the amount of energy that can be provided for STOR.

As mentioned, these values are highly dependent on the time of day when the event STOR takes place, as can be seen in figures 6.9 and 6.10, where the different case studies and their STOR events are shown for the six different weeks of the year using the Agile Go tariff with 90% PV penetration rate, P2P and *Setting two*. Each of these figures shows the total number of EVs available throughout the week and the number of EVs that provide energy for STOR. In addition, each graph includes the highest number of EVs that provides energy for STOR identified by a horizontal brown dashed line, as well as the lowest number of EVs identified by the horizontal magenta dashed line.

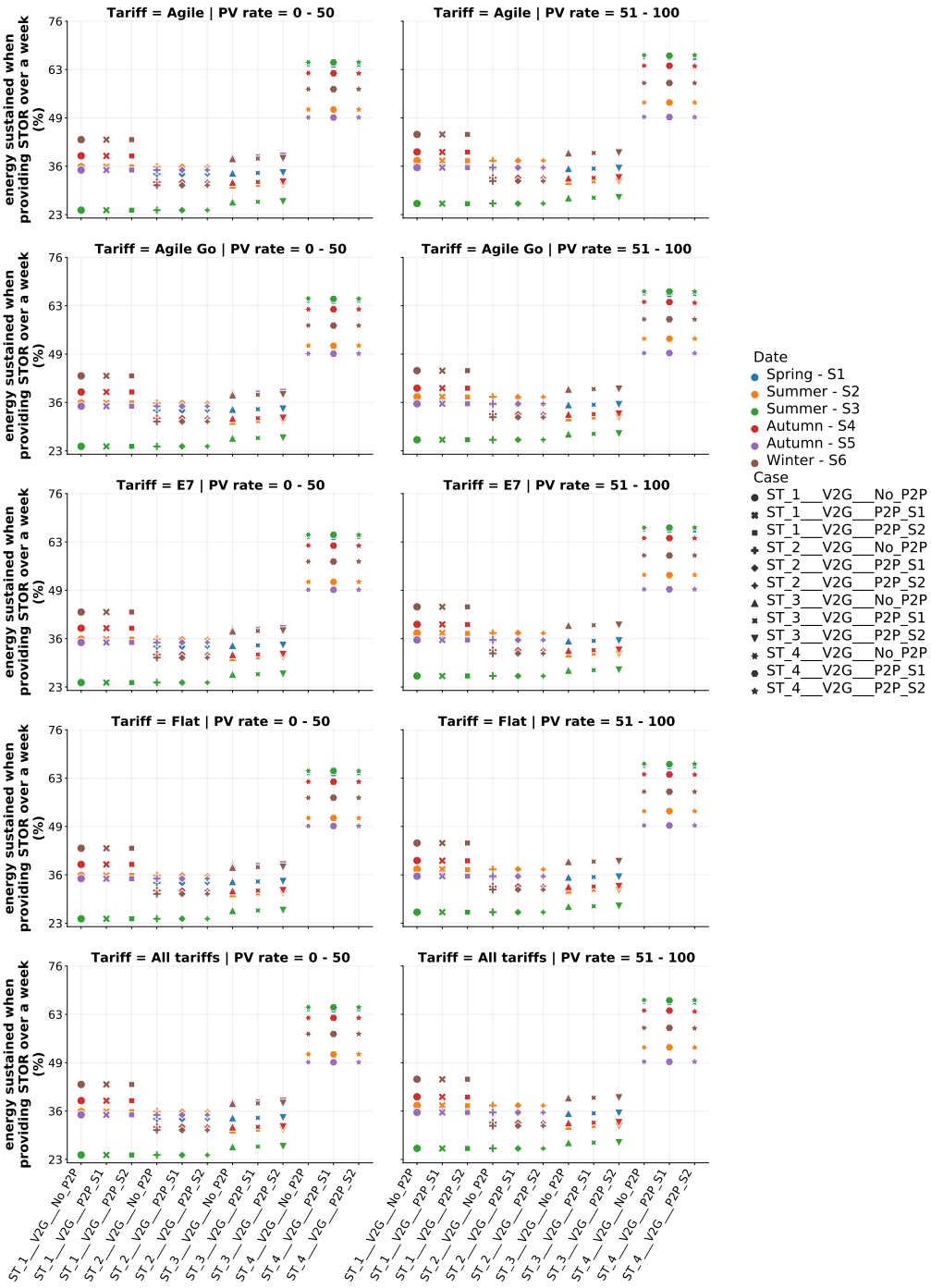

Figure 6.7: Percentage of energy that can be provided for STOR for all STOR events of the week for the six representative weeks of the year, the five tariff scenarios and all microgrid configurations explored in this chapter. This is the resulting value of $ST_t^{threshold,max}$, which means the percentage of 50 EVs $*$ 7.4 kW. The left column contains the average values from 0% to 50% PV penetration rates and the right column contains the average values from 51% to 100% PV penetration rates.

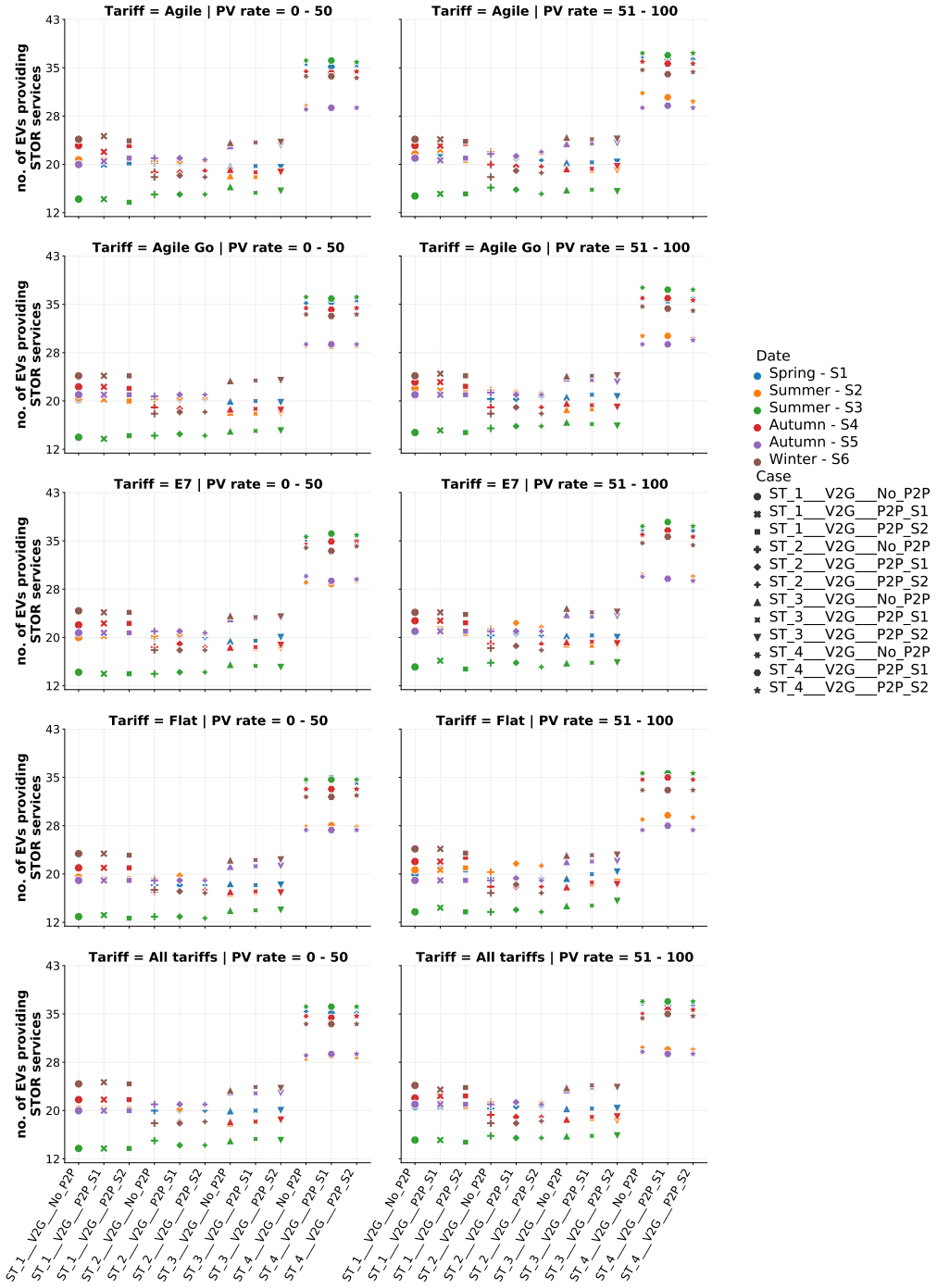

Figure 6.8: The highest number of EVs providing STOR for the six representative weeks of the year, the five tariff scenarios and all microgrid configurations explored in this chapter. The left column contains the average values from 0% to 50% PV penetration rates and the right column contains the average values from 51% to 100% PV penetration rates.

For example, the case study ST_4 shows that the percentage of energy is higher, as is the number of EVs that provide energy for STOR, which happens for this case study, that the STOR events occur during the weekend when there is a higher number of EVs available at home, compared to other days of the week. Moreover, in the same case study, figure 6.10, it can be seen that during Winter - S6 the second STOR event has the highest number of EVs compared to the other two events, with 30 being the lowest number of EVs instead of 34, and these two events can still provide the same amount of energy for STOR. In this case, the participant EVs may be discharging more energy to provide energy for STOR. Similarly, the case ST_3, figure 6.9, during the Autumn - S5 week where the highest number is 23 during the second event and starts with the same number, 23 and reduces the number of EVs according to their availability at home. However, this gap between the highest number of EVs and the lowest number is not too large; in this case the largest gap is 4 between the highest and lowest number of EVs , as otherwise it can affect the amount of energy that can be provided for STOR. Of course, depending on the number of events and the time they occur, affect the different metrics already explored, as in some cases, like ST_2 (see figure B.7) more energy will be required to charge the EVs to be able to provide energy for the six STOR events.

All four cases explored can respond to a request to provide STOR within a 20-minute window. This was possible by simulating STOR instructions during committed windows and then responding to them. This is evident in all four case studies, where they were all able to provide energy without any issues. The amount of energy provided can change based on how many EVs are available. Simply put, more EVs mean more energy for STOR.

In addition, EVs are capable of maintaining a constant energy supply for 120 minutes and respond again after less than 1,200 minutes. Again, this can be seen in some weeks of the case studies ST_1 and ST_2 (see figures B.7 and B.8), and more precisely ST_3 and ST_4 where the delivery of three consecutive STOR events as explained in section 6.1.3, i.e., one in the morning, one in the evening and one in the following morning, during weekdays and weekends, respectively. Here we can see that EVs are capable of providing energy for STOR in the three consecutive events, however, once again depending on the number in which the time of the day

the event takes place and the number of EVs available at that time is the amount of energy that will be provided for STOR.

It is worth noting that in all four case studies and microgrid configurations, the energy from the number of EVs used does not meet the 3 MW requirement, which is the necessary energy to provide STOR services. Nonetheless, the study of 50 EVs within a microgrid yields valuable insights, offering a better understanding of the potential energy contribution they can make for STOR services.

6.2.4 Annual electricity costs

In this section, the estimated annual electricity costs will be presented. The results were calculated as explained in table 6.5. Here, the results are presented in a way similar to that of section 5.2.4. Figure 6.11a contains the case studies ST_1 and ST_2 resulting average estimated annual electricity costs for the four main tariffs, the Agile tariff, the Agile Go tariff, the E7 tariff, and the flat tariff. The results of the case studies ST_3 and ST_4 are in figure 6.11b. Similarly to chapter 5, in the case of the All tariffs scenario, these results are the average estimated annual electricity costs according to the number of households that are under each different tariff, as described in table 5.4. 6.11c and 6.11d show the results for the All tariffs scenario for the case studies ST_1 and ST_2 and for the case studies ST_3 and ST_4, respectively.

Consistently with Chapter 5, the highest costs appear in the lower left corner, and the lowest in the upper right of each microgrid configuration. Notably, higher PV penetration rates and allowing P2P lead to considerable cost reduction. In this chapter, the average yearly electricity costs are less than those in Chapter 5's EVs scenarios when using V2H. This is related to the fact that the participants in the grid have the choice to sell energy via V2G to provide STOR services and be paid for it according to the amount of energy provided for this service. Certain tariffs can decrease costs by approximately £140, as seen when using the Agile tariff. Particularly, case study ST_2 exhibits the lowest costs due to the provision of energy for six STOR events weekly, increasing selling opportunities and further reducing average electricity costs compared to other case studies.

As expected, higher PV penetration rates cut annual electricity costs by utilising

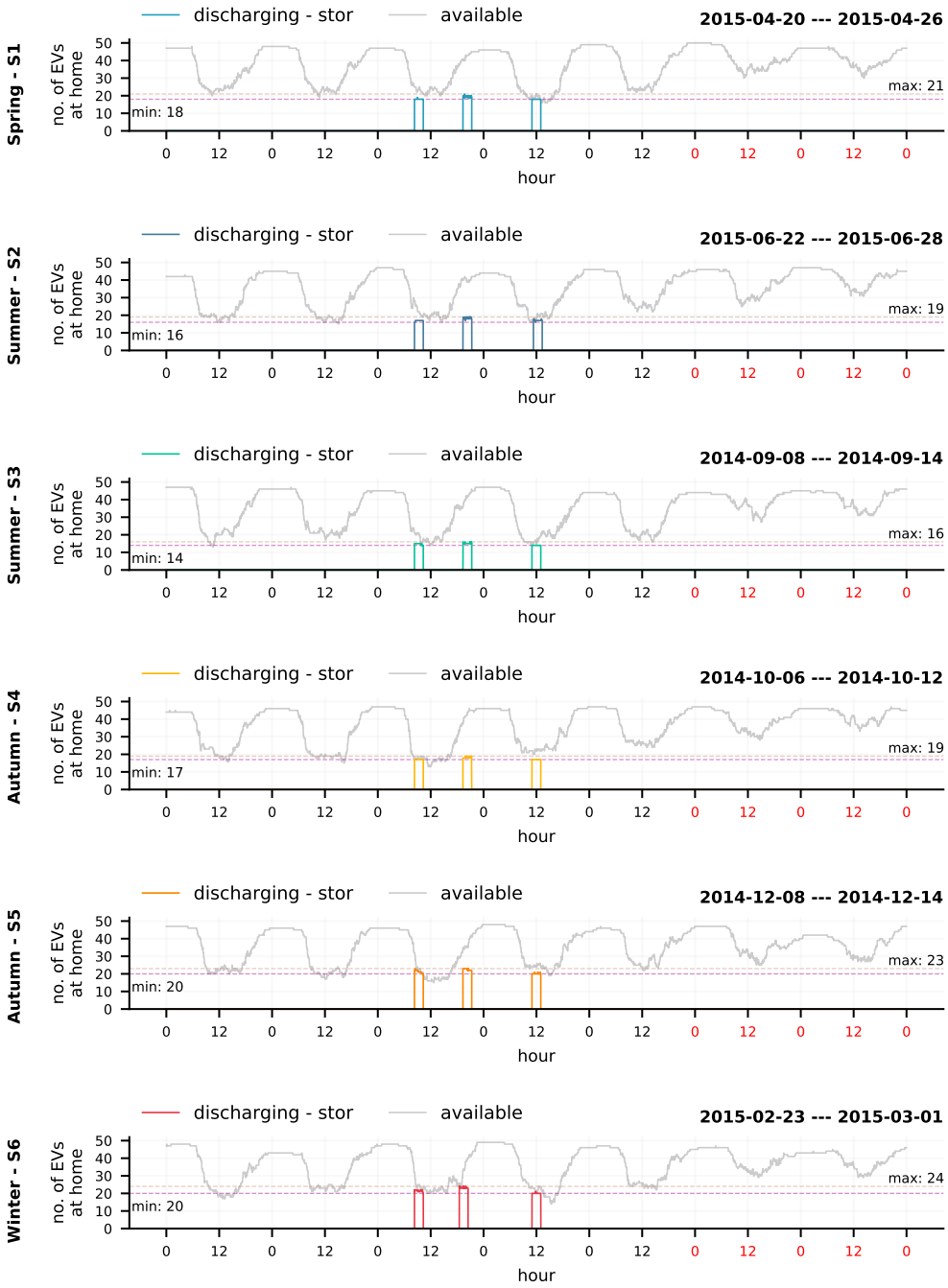

Figure 6.9: STOR events in the case study *ST_3* for the six representative weeks of the year using the Agile Go tariff with 90% PV penetration rate, P2P and *Setting two*. Here, the number of EVs available at home during each week and the number of EVs that are discharging energy to provide STOR. Here, the black *X-axis* labels denote data from Monday to Friday, and the red labels, data from Saturday to Sunday.

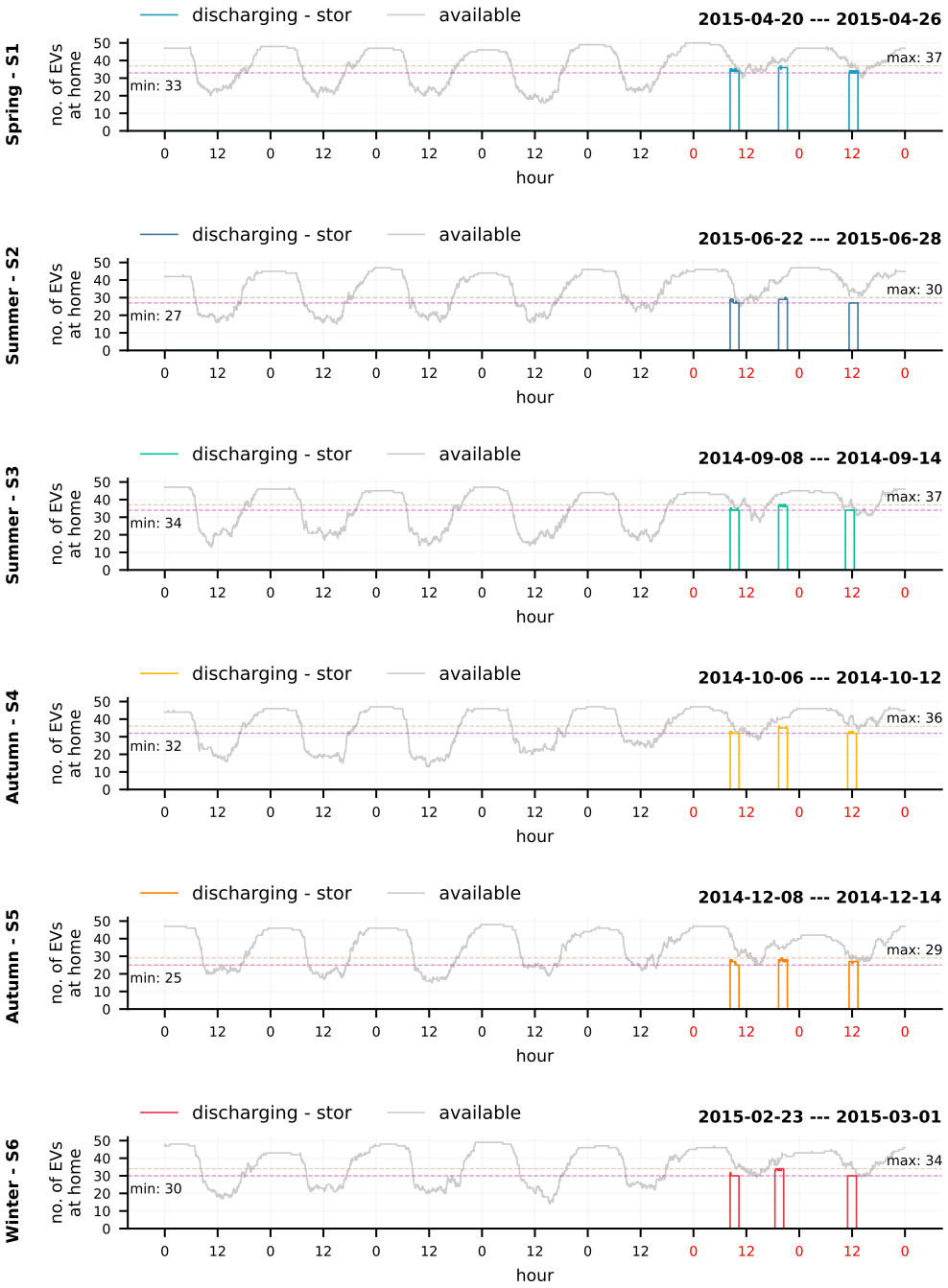

Figure 6.10: STOR events in the case study *ST_4* for the six representative weeks of the year using the Agile Go tariff with 90% PV penetration rate, P2P and *Setting two*. Here, the number of EVs available at home during each week and the number of EVs that are discharging energy to provide STOR. Here, the black *X-axis* labels denote data from Monday to Friday, and the red labels data from Saturday to Sunday.

excess solar energy either for self-consumption or grid sales. Further cost reduction is observed when P2P is allowed, independent of the price mechanism, with *Setting two* yielding lower costs than *Setting one*. In scenarios featuring single tariff use within the microgrid, the Agile tariff reduces cost across all four case studies. Without P2P, prices range from £330 (0% PV penetration) to -£76 (100% PV penetration). With P2P under Settings one and two, the range varies from £330 to -£89 and -£108, respectively. This is followed by the Agile Go tariff, hitting a low of -£63 with P2P and *Setting two* for the ST_2 case study. The other two tariffs, E7 and Flat, result in higher costs, with E7 registering the highest in all case studies and microgrid configurations.

The All tariffs scenario, as seen in figures 6.11c and 6.11d, shows a comparable decrease in mean annual electricity costs to the chapter 5 results. Around £170 reduction is noted in relation to the equivalent tariff scenario from chapter 5 for EVs with V2H. Overall, the Agile Go tariff returns the lowest yearly electricity costs compared to the rest, hitting lows of -£411, -£625, -£373, and -£347 for ST_1 to ST_4 respectively, when P2P is allowed under *Setting two*. These costs are followed closely by the Agile tariff in similar microgrid configurations.

Under the same All tariffs scenario, users operating under the E7 tariff, annual electricity costs are the highest. This scenario yields elevated costs for users across tariffs with lower PV penetration rates as opposed to when only one tariff is allowed within the microgrid. On the other hand, higher PV penetration rates lower costs relative to identical results when a single tariff is applied within the microgrid. It should be noted that in this tariff scenario, P2P prices are calculated based on the tariff being used, leading to varying buy and sell P2P prices for each participant in the microgrid.

6.2.5 Solution quality

The resulting optimality gap described in section 4.4.7 will be presented in this section. This metric will assess the quality of the results reported thus far in this chapter, providing a clearer picture of how much the results deviate from the ideal solution determined by the solver, in this case Gurobi 9.5.2 [166]. Also, the computer specifications used to solve each microgrid configuration.

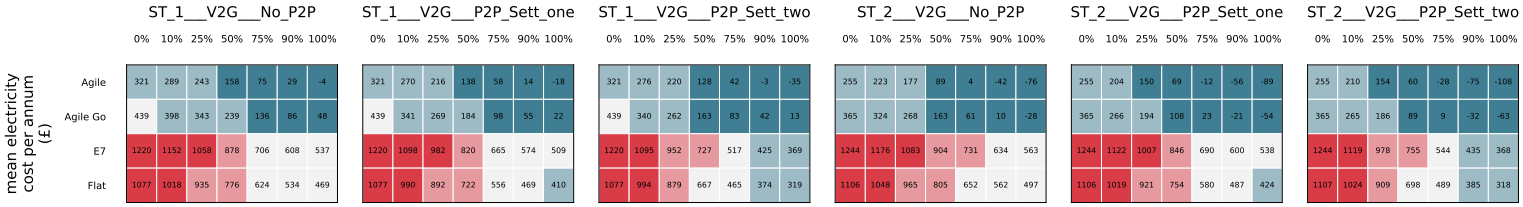

(a) ST_1 and ST_2

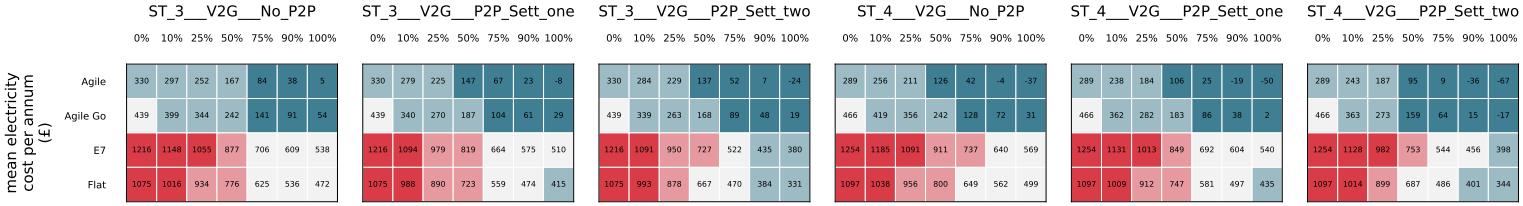

(b) ST_3 and ST_4

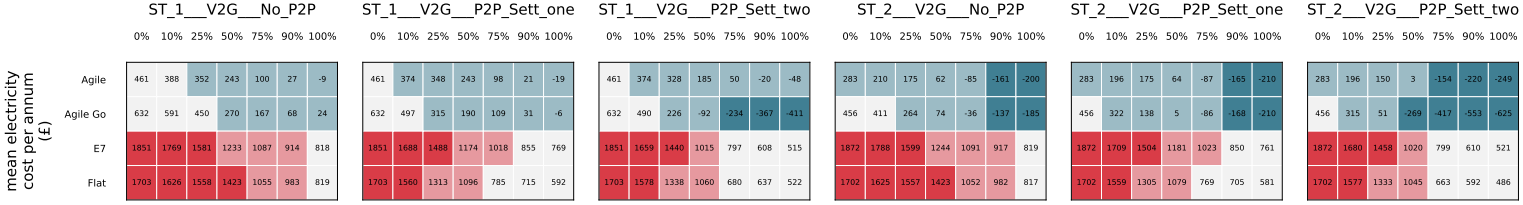

(c) ST_1 and ST_2

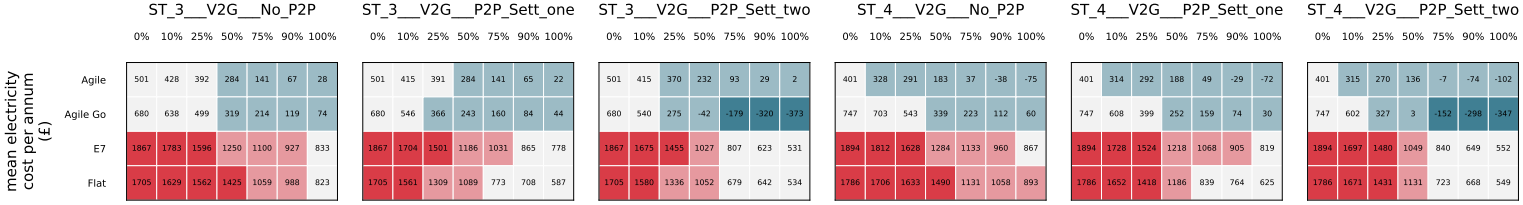

(d) ST_3 and ST_4

Figure 6.11: **(a) - (b)**. Estimated annual electricity cost for Agile tariff, Agile Go tariff, E7 tariff and Flat tariff showing the mean prices within the microgrid. **(c) - (d)**. Estimated annual electricity cost for each tariff inside the All tariffs scenario when using home batteries showing the mean prices within the microgrid.

After solving each model in his chapter, table 6.7 shows the number of solutions that are under 0.50% optimality gap threshold for each of the 2,520 models in this chapter. As explained in Section 5.2.5, a model with a 0.50% gap implies that the feasible solution identified by Gurobi is quite close to the optimal solution. This small gap is considered satisfactory in many cases, as it demonstrates its effectiveness in solving the optimisation problem with reasonable accuracy. The closer the gap to 0.00%, the higher the confidence in the quality of the solution, which makes it suitable for decision-making or further analysis [166]. Here, only 1 solution is over 0.50%, meaning that the results are good enough.

Table 6.7: Optimality gap value ratio of the resulting models.

Gap	Number of models
≤ 0.50	2,519
$0.50 <$	1

Table 6.8 shows the total number of models in this chapter that were solved on each PC. According to the Gurobi documentation, the results can vary when solved on different hardware, which means that although the optimal results are found, the path to them might be different, which may yield different data [171].

Table 6.8: Number of models solved using each computer and their specifications.

Number of models	Processor name	Processor speed (GHz)	Cores	RAM (GB)
1,540	12th Gen Intel (R) Core (TM) i9-12900K	3.20	16	128
592	11th Gen Intel (R) Core (TM) i5-1135G7	2.30	4	64
388	Intel (R) Xeon (R) E5-2620 v4	2.10	16	128

6.3 Discussion

Using an optimisation model, a microgrid was examined to assess the impact of the availability of EVs when providing energy for the provision of STOR in four case

studies covering six weeks representative of the seasons of the year that also cover the six STOR seasons and committed windows when STOR is required, different PV penetration rates, in conjunction with four different tariffs and two different P2P price calculations based on mid-market rate (MMR). This was achieved using real-world data from residential energy use, local solar power and EV travel, including predicted data on their ability to be connected at home. The simulation results indicate that the availability of EVs has a substantial effect on the amount of energy that can be offered for STOR regardless of the energy tariff and whether P2P is allowed that can produce different technical and economic benefits for EV owners, these benefits are in addition to the benefits of providing V2H. When providing STOR services via V2G there is a negligible impact when different energy tariffs are used, different PV penetration rate or whether P2P is allowed, as this does not reduce or increase the amount of energy provided for STOR, on the other hand, the availability of the EVs during the day has a significant impact on the provision of STOR, more precisely, when an STOR event occurs as depending on the time of the day, the number of EVs available at home will increase or reduce the amount of energy that can be provided for STOR. However, this does not mean that the different energy tariffs, PV penetration rates and P2P have no impact on the overall performance within the microgrid. In general, participants can achieve average electricity costs per week ranging from £25 to -£9 depending on the energy tariff and PV penetration rates. With 0-50% the Agile tariff, users can get average electricity costs between £0 and £10 per week, and with 51-100% PV penetration rates the lowest costs can be achieved with more traditional tariffs such as the E7 and the Flat tariff with costs ranging from £23 to -£9. These lowest costs are possible when P2P is used with the *Setting two*. SSR in all microgrid configurations shows an increase during weeks with more hours of sunlight during the year when PV penetration rates are high, with in some cases values close to 100% under traditional tariffs like E7 and Flat tariff. Moreover, the energy imported from P2P increases when PV penetration rates are 51-100%, specially in scenarios where *Setting two* is used.

When providing energy for STOR, the max power load from the grid increases with peaks between 150 and 400 kW with 0-50% PV penetration rates due to users charging energy at the same time during low electricity prices during the day to be

able to participate in the provision of STOR that can return extra profits at the end of the week. This behaviour also increases the amount of energy that is drawn from the grid in different microgrid configurations without P2P. Higher PV penetration rates can reduce these parameters in certain weeks of the year, but this depends on the energy tariff used; for example, the Agile Tariff with 51-100% PV penetration rates results in similar peak demands compared to having lower PV penetration rates for the six weeks of the year. Estimated annual electricity costs show reduced costs compared to those in chapter 5, this is due to the additional profit available from providing energy for STOR, with further reductions between £140 and £170 depending on the tariff and P2P setting.

In terms of the availability of the EVs at home, the simulations show that the amount of energy for STOR varies depending on the number of EVs available at the time when a STOR occurs. Showing that in all four case studies EVs are capable of sustaining the discharge of energy for 120 minutes, respond to an instruction to provide STOR in no more than 20 minutes and respond again in less than 1,200 minutes after the last STOR event, as required by the National Grid. According to the results from figures 6.9 and 6.10, which all use the Agile Go tariff, it was also shown that EVs can sustain the same provision of the same amount of energy even within a tolerance of 4 EVs between the minimum and the maximum of EVs providing energy, or in this case 8% percent of the total of participants in the microgrid. This means that if a STOR event starts, EVs can go and come as long as the number of participants does not drop more than 4 participants from the maximum number of EVs when providing energy for STOR.

This tolerance was calculated based on the equation equation (6.3) where is explained that $ST^{percentage}$ is the value that will determine the actual maximum energy provided throughout the week considering the availability of EVs, and as mentioned, the tolerance is then obtaied by the minimum and maximum number of EVs providing energy for STOR.

Furthermore, according to the results from all microgrid scenarios and tariffs, 15% extra vehicles are required from the total of participants in the microgrid in order to sustain the response. For example, under ideal conditions, around 410 EVs with a 7.4 kW bidirectional charger are required to provide 3 MW; however, to

maintain the provision of this amount of energy for the 120 minutes required, the number of EVs should be around 485. For instance, under ideal conditions, approximately 410 EVs plugged to a 7.4 kW bidirectional charger are needed to supply 3 MW of power. However, to consistently deliver this energy level for the necessary 120-minute duration, the total number of electric vehicles should be increased to about 485 in order to guarantee a smooth STOR provision of at least 3 MW.

In this study, participants inside the microgrid know in advance when the STOR events will occur and can prepare accordingly by charging the EV in advance to provide energy for STOR when required. This is not the case in the real world, where STOR events can occur at any time inside the committed windows, therefore, EVs may not be able to plan ahead and charge enough energy for STOR. Although the optimisation model used in this chapter does not account for this, one potential solution to address this challenge is to study the implementation of a payment scheme based on the state of charge (SOC) of EVs throughout the day. Under this system, participants would be required to maintain a minimum SOC level to qualify for STOR participation. Furthermore, as shown in this chapter, the availability of the EVs generally does not affect the provision of STOR, but it will impact the amount of energy that can be provided for STOR services, which is something that needs to be taken into account when considering the option of asking EVs owners to maintain a minimum SOC level. However, when a minimum SOC level is required for EVs to participate in STOR, the number of available EVs meeting this criterion might be low and could directly influence the capacity and responsiveness of the microgrid during these events. If the availability of EVs with the necessary SOC is limited, the number of EVs might need to be higher than the around 485 EVs mentioned above - considering a 7.4 kW bidirectional charger -, ultimately impacting the performance and reliability of using EVs to provide energy for STOR.

Additionally, the study could impose different rules in the system to further promote charging during off-peak hours or apply strict rules to discourage charging during peak demand periods. By doing so, the microgrid can increase the number of EVs available with sufficient SOC, ensuring a more robust and reliable response to the unexpected nature of STOR events, and could also improve the overall performance of the microgrid. Further exploration of this payment scheme or charge and

discharge strategies could involve modelling various SOC thresholds and analysing their impact on the overall reliability and efficiency of the microgrid. As mentioned, it is important to develop strategies that encourage EV owners to maintain their vehicles' SOC above the required threshold, which in consequence, could potentially increase the pool of available EVs that can provide energy for STOR. Although not explored in this work, such options could be of interest to both EV owners and system operators.

6.4 Conclusions

In this chapter, the impact of the availability of EVs has when providing STOR in four case studies, with different PV penetration rates, P2P using different price calculation systems, and five different tariff scenarios in six weeks representative of the seasons of the year which also cover the six STOR seasons and committed windows when STOR is required, was explored. Concluding that EVs can meet most of the technical requirement to provide STOR considering that they can respond to an instruction in less than 20 minutes, sustain the response for 120 minutes and respond again in less than 1,200 minutes.

In general, the availability of EVs does impact the provision of STOR which depends on the time of the day when the STOR event occurs, the number of EVs available will increase or reduce the amount of energy that can be provided for STOR. In this case, the different energy tariffs, PV penetration rates and having P2P or not, have a negligible impact on the amount of energy that can be provided for STOR. These different parameters do impact the performance of the microgrid, increasing SSR when high PV penetration rates and P2P is using *Setting two* over 50% during the Summer - S2 week, the Agile tariff produces the lowest estimated annual electricity cost compared to the results in chapter 5 when using EVs with V2H. However, this comes with a higher dependence on importing energy from the grid and a higher maximum power load from the grid due to EVs charging in advance for the provision of STOR.

Chapter 7

Exploring the possibility to provide restoration services by using vehicle-to-grid (V2G)

In the following chapter, a microgrid connected to the grid is considered to study the effectiveness of reducing the electric bill of households that own an electric vehicle (EV) with a bidirectional charger while maximising the amount of state of charge (SOC) that can be held in all EVs during a week for the possibility of providing restoration services (formerly known as black start services). Furthermore, an overview of the model and the data used to simulate the microgrid will be introduced, as well as a description of the different scenarios that will be investigated. Finally, an analysis of the findings will be provided.

7.1 Model overview

Similarly to chapters 5 and 6, the optimisation model introduced in chapter 4 is used to simulate EVs and travel data is taken from the resulting profiles in chapter 3. The optimisation model aims to minimise the electrical bill of homes by maximising self-consumption if a photovoltaic (PV) system is installed in the house. It achieves this by scheduling charging and discharging behaviours for EVs with bidirectional chargers during optimal times when connected at home. The model also considers the potential for peer-to-peer (P2P) energy trading. In this chapter, one of the main goals is focus to maximise the amount of SOC that can be held in all EVs during a

week for the possibility of providing restoration services. This is done by introducing a payment mechanism that aims to encourage EVs to increase the amount of SOC throughout the week. The impact of different electricity tariffs is compared, as well as different PV penetration rates and the possible advantages of P2P energy trading between households within the microgrid using two different price calculation settings. Finally, the impact of different payment rates to encourage participants to increase their SOC during the week are explored.

7.1.1 Data

As previously described in section 4.1.1, a grid-connected microgrid is used, comprising a sample of 50 London-based households. Every household has an electric vehicle. The Nissan Leaf 2018 [170] specifications are shown in table 6.1. Furthermore, a 7.4 kW bidirectional vehicle-to-grid (V2G) and Vehicle-to-home (V2H) charger was considered for EV simulations [158]. The data from chapter 3 is used to simulate the travel behaviour of EVs.

As described in section 4.1.3.1 and table 4.1, four different electricity tariffs are used. The Agile tariff, the Agile Go tariff, the economy seven (E7) tariff, and the Flat tariff are the four electricity tariffs.

Different penetration rates are used to assess the impact of local solar generation; in this case, 0%, 10%, 25%, 50%, 75%, 90% and 100%. Similar to sections 5.1.1 and 6.1.1, these PV penetration rates mean the percentage of the 50 houses with solar panels installed, for instance, a PV penetration rate of 10% will only have 5 houses with solar panels. The data described in section 4.1.2 used to simulate solar generation and the Agile Outgoing tariff data, introduced in section 4.1.3.2, is exclusively used as a feed-in tariff.

Finally, three different P2P scenarios are explored: one without P2P energy trading, one with P2P energy trading using the *Setting one* described in section 4.3.1, and one with P2P energy trading using the *Setting two* described in section 4.3.2.

7.1.2 Restoration services case studies

The National Grid must have resources available to restore power in the event of a total or partial shutdown of the national electricity transmission system [119].

Considering that the National Grid is increasingly interested in using distributed energy resources (DER) such as solar energy as a cleaner and greener alternative to large fossil fuel generators. Although the size of production for DER is typically smaller, their rapid rise on distribution networks gives the potential to coordinate a restoration services based on renewable energy. As the number of EVs in the UK continues to increase, there is growing potential for these vehicles to contribute to the energy landscape in a manner similar to that of renewable energy sources. Just like DER with smaller production sizes, the rapid rise of EVs across the country presents an opportunity to coordinate restoration services by harnessing the energy stored in their batteries. This approach could effectively complement renewable energy sources and further enhance the resilience and sustainability of the power grid. Additionally, the provision of this service using EVs has been explored before, where it was found that due to the uncertainty surrounding the availability of EVs and their SOC in the event of shutdown, EVs need to be further studied before being considered for the provision of this service [12]. In this work, we will focus on looking at the minimum SOC available from EVs within a microgrid that can be of interest for future projects.

For this, a payment for the final energy stored in each EV is introduced to encourage participants to increase their available SOC during the week and increase the minimum amount of SOC that can be held through the week of the microgrid. This financial model could not only enhance the microgrid's stability and reliability but also potentially boosts the energy available for restoration services. By incentivising EVs owners to maintain a higher SOC throughout the week, the model promotes sustainable practices, more efficient energy management, and overall improved microgrid performance. Furthermore, three case studies are explored with a starting payment of 0.055 £/kWh for the first case study, then 0.110 £/kWh for the second and 0.165 £/kWh for the third case study. The starting price was calculated by getting the mean value of the Agile Outgoing tariff data introduced in section 4.1.3.2, which is a little less than what has been considered as a payment for the final energy stored in previous work [105]. These case studies are summarised in table 7.1.

Table 7.1: Case study payment amount for the final energy stored.

Case study	Payment (£ / kWh)
BS_1	0.055
BS_2	0.110
BS_3	0.165

7.1.3 Representative weeks of the year

Similarly to chapter 5, the simulations were carried out using four different weeks that are representative of the four seasons of the year to study any seasonal variation. This information has already been introduced in figure 3.9 where it is provided for six different weeks of the year. In this chapter, only four dates are considered, as explained below.

- **Week 1**: For spring, week *Spring - S1* from 2015-04-20 00:00:00 to 2015-04-26 23:59:00.
- **Week 2**: For summer, week *Summer - S2* from 2015-06-22 00:00:00 to 2015-06-28 23:59:00.
- **Week 3**: For autumn, week *Autumn - S4* from 2014-10-06 00:00:00 to 2014-10-12 23:59:00.
- **Week 4**: For winter, week *Winter - S6* from 2015-02-23 00:00:00 to 2015-03-01 23:59:00.

A total of 28 days are simulated overall; these weeks will contribute equally to the calculation of the estimate annual electricity cost, which will be discussed later in the chapter. This means that each week's weighting is 0.25.

7.1.4 Electric vehicle dispatch optimisation for a household

As stated above, for this chapter, the optimisation model introduced in chapter 4, however, additional variables were considered to reflect the minimum SOC that can be held for all EVs during a week. This is done by introducing a payment for the amount of SOC that each EV has at the end of the week. Without this payment

mechanism, EVs might prioritise charging to their maximum SOC (SOC^{max}) immediately after using energy for driving, since it could be more profitable depending on the incentives discussed in table 7.1, rather than giving energy back to the house. However, this is not the scope of this work. By incorporating a payment mechanism for maintaining a minimum SOC throughout the week and being at the end of the week, we ensure that EVs can both maximise the minimum SOC that can be held for all EVs during a week and provide energy back to the house when needed, in line with the objectives of our study.

In this case, the $E^{SOC}_{v,final}$ introduced in equation (4.3), is set to 0% to avoid forcing EVs to get a certain SOC at the end of the week. These new variables are explained below. The variable $BS^{percentage}$ shown in equation (7.1) describes the minimum SOC percentage that can be held during a week for all EVs. This constraint is applied on an individual EV basis, and each vehicle should maintain at least this minimum SOC percentage throughout the week. It is worth noting that this constraint is not an average across all vehicles, as it applies to each EV individually.

$$E^{SOC}_{v,t} \geq \Big(SOC * \frac{BS^{percentage}}{100}\Big), \quad \forall v, t \tag{7.1}$$

Equation (7.2) describes the payment for the final energy stored in each EV. $C^{SOC,final}_{v}$ describes the total cost to be paid for each EV depending on their final SOC, $E^{SOC}_{v,final}$, according to the prices set for each case in table 7.1, where $Pr^{SOC,final}$ will vary depending on the case study.

$$C^{SOC,final}_{v} = Pr^{SOC,final} * E^{SOC}_{v,final}, \quad \forall v \tag{7.2}$$

In this chapter, the objective function in equation (4.26) is modified to accommodate the newly introduced variables. The objective is to minimise the total cost of operating the microgrid and, at the same time, maximise the minimum SOC percentage that can be held for a week for all EVs. Here, we found that adding $BS^{percentage}$ helps the solver find an optimal solution faster. We also discovered

that excluding $C_v^{SOC,final}$ from the objective function causes the EVs to fully deplete their batteries daily, only charge enough energy to cover their driving needs and maintain a low minimum SOC throughout the week. The vehicles also tend to charge only on the week's final day to obtain a high SOC and receive the corresponding payment. This exclusion also results in the solver taking longer to find an optimal solution.

$$\begin{aligned} min \Bigg[\sum_v \Bigg(& C_v^{import} + C_v^{import,street} + C_v^{import,p2p} \\ & - C_v^{export} - C_v^{export,p2p} - C_v^{export,v2g} \\ & - C_v^{SOC,final} \Bigg) - BS^{percentage} \Bigg] \end{aligned} \tag{7.3}$$

7.1.5 Microgrid system configuration overview

A comparison of different microgrid configurations or microgrid scenarios of the system is considered. EVs can be operated in three different modes according to section 4.4, however, in this case only the smart charging (V1G) and V2H modes are considered. Similarly, to chapter 5, microgrid configurations will be referred to as the combination of the different modes in which the microgrid operates and the type of P2P pricing calculation to be used, if applicable. These microgrid configurations are explained in table 7.2.

In this chapter, the number of simulations considered for each microgrid configuration – described in table 7.2 – is 140 in total each, which considers the seven different PV penetration rates and the five tariff scenarios – described in table 5.3 and the four different weeks described in section 7.1.3. Therefore, for this chapter, a grand total of 2,520 simulations will be explored.

7.1.6 Metrics

The performance metrics already introduced in section 4.4.6 will be used to evaluate the performance of each microgrid configuration or scenario described in this chapter. To assess the quality of the results presented, the metric described in section 4.4.7 will be used.

Table 7.2: Overview of the different microgrid configurations explored in this chapter with a description of the microgrid configuration.

Microgrid configuration or scenario	Description
Case Study one	
$BS\_1\_\_\_V1G\_\_\_No\_P2P$	V1G; No P2P.
$BS\_1\_\_\_V1G\_\_\_P2P\_S1$	V1G; P2P Setting one.
$BS\_1\_\_\_V1G\_\_\_P2P\_S2$	V1G; P2P Setting two.
$BS\_1\_\_\_V2H\_\_\_No\_P2P$	V2H; No P2P.
$BS\_1\_\_\_V2H\_\_\_P2P\_S1$	V2H; P2P Setting one.
$BS\_1\_\_\_V2H\_\_\_P2P\_S2$	V2H; P2P Setting two.
Case Study two	
$BS\_2\_\_\_V1G\_\_\_No\_P2P$	V1G; No P2P.
$BS\_2\_\_\_V1G\_\_\_P2P\_S1$	V1G; P2P Setting one.
$BS\_2\_\_\_V1G\_\_\_P2P\_S2$	V1G; P2P Setting two.
$BS\_2\_\_\_V2H\_\_\_No\_P2P$	V2H; No P2P.
$BS\_2\_\_\_V2H\_\_\_P2P\_S1$	V2H; P2P Setting one.
$BS\_2\_\_\_V2H\_\_\_P2P\_S2$	V2H; P2P Setting two.
Case Study three	
$BS\_3\_\_\_V1G\_\_\_No\_P2P$	V1G; No P2P.
$BS\_3\_\_\_V1G\_\_\_P2P\_S1$	V1G; P2P Setting one.
$BS\_3\_\_\_V1G\_\_\_P2P\_S2$	V1G; P2P Setting two.
$BS\_3\_\_\_V2H\_\_\_No\_P2P$	V2H; No P2P.
$BS\_3\_\_\_V2H\_\_\_P2P\_S1$	V2H; P2P Setting one.
$BS\_3\_\_\_V2H\_\_\_P2P\_S2$	V2H; P2P Setting two.

Furthermore, one new metric is introduced to measure the minimum amount of SOC during a week within the microgrid. This is described below.

- **Minimum amount of SOC:** This is the percentage of SOC that all EVs within the microgrid can hold for the entire week. This is measured by the variable $BS^{percentage}$ introduced in equation (7.1).

7.2 Results

In this section, we introduce the results of the microgrid for a case study case during the summer, specifically Summer - S2, using the Agile Go tariff. A description

of its performance according to the established metrics explained in section 7.1.6. The impact of the different representative weeks, the performance of the microgrid for each tariff and the comparison of the minimum amount of SOC that was also introduced in section 7.1.6. Finally, a brief evaluation of the quality of the results is provided.

In this chapter, as stated in section 4.2, each simulation was built using the Python 3.8.8 [125] programming language and the Pyomo 6.3.0 library [157] and then solved using Gurobi 9.5.2 [156].

7.2.1 Results comparison between two case studies for a week in summer using the agile go tariff

In this section, the plots for $BS\_2\_\_\_V2H\_\_\_P2P\_S1$ and $BS\_3\_\_\_V2H\_\_\_P2P\_S1$ will first be presented to give a general idea of how the microgrid operates, both using V2H and P2P with *Setting one*. The three case studies and their resulting performance metrics will be introduced and compared during the same week. Here, the new metric introduced to measure the minimum SOC held during a week for EVs within the microgrid in section 7.1.6 will not be introduced here; instead, it will be introduced in the next section.

Figure 7.1 shows the simulation results of the scenario $BS\_2\_\_\_V2H\_\_\_P2P\_S1$ with a PV penetration rate 90% PV and using the Agile Go tariff during a week in summer – Summer - S2. This figure shows the energy imported from the grid, the house demand and solar generation showing the energy that is locally used, the energy that is sold to the grid, and the energy shared with other members of the microgrid, the internal microgrid buy for importing and from the grid and via P2P, and selling energy to the grid and through P2P with *Setting one* and the total number of EVs available during the day and how many are charging and discharging.

Similarly to figure 7.1, figure 7.2 shows the simulation results of the scenario $BS\_3\_\_\_V2H\_\_\_P2P\_S1$, with PV penetration rate of 90% and using the Agile Go tariff during the summer week – Summer - S2.

In both figures 7.1 and 7.2, row **(a)** and **(b)** show an increase in the demand for energy from the grid during periods when the price of electricity is low, mainly due to the EVs charging at night. Peak demand can be seen at the beginning

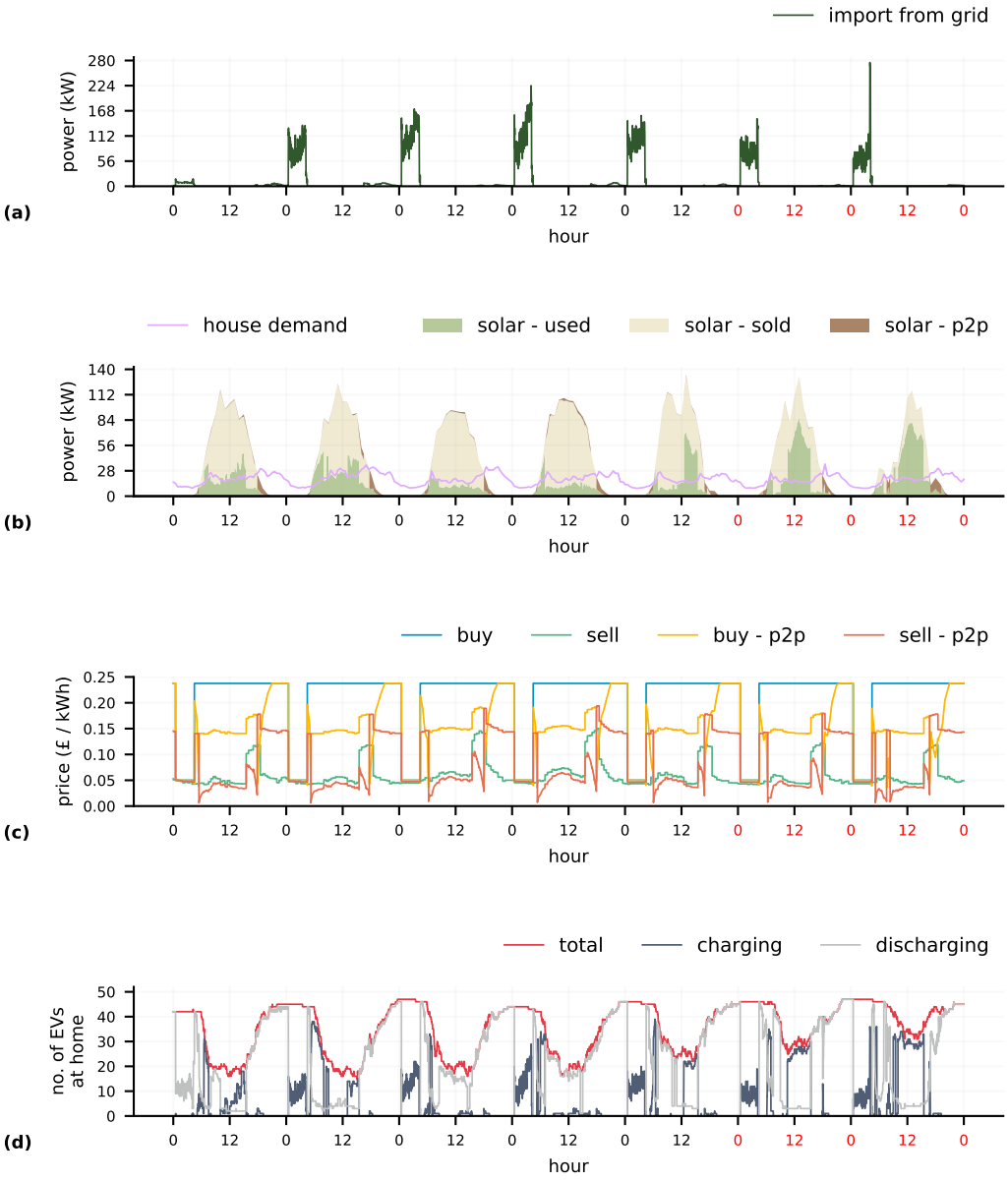

Figure 7.1: Simulation results for the Summer - S2 week showing microgrid operation with a PV penetration rate of 90% and using the Agile Go tariff. This date belongs to the $BS\_2\_\_\_V2H\_\_\_P2P\_S1$ microgrid configuration. The tick labels on *X-axis* in black denote data from Monday to Friday, and the red labels, data from Saturday and Sunday. **a.** Power import from the grid. **b.** Household demand and energy consumed, shared and sold from solar generation within the microgrid. **c.** Buy and sell prices from the grid and from P2P energy trading. **d.** Number of EVs available at home charging and discharging and the total number of EVs available at home.

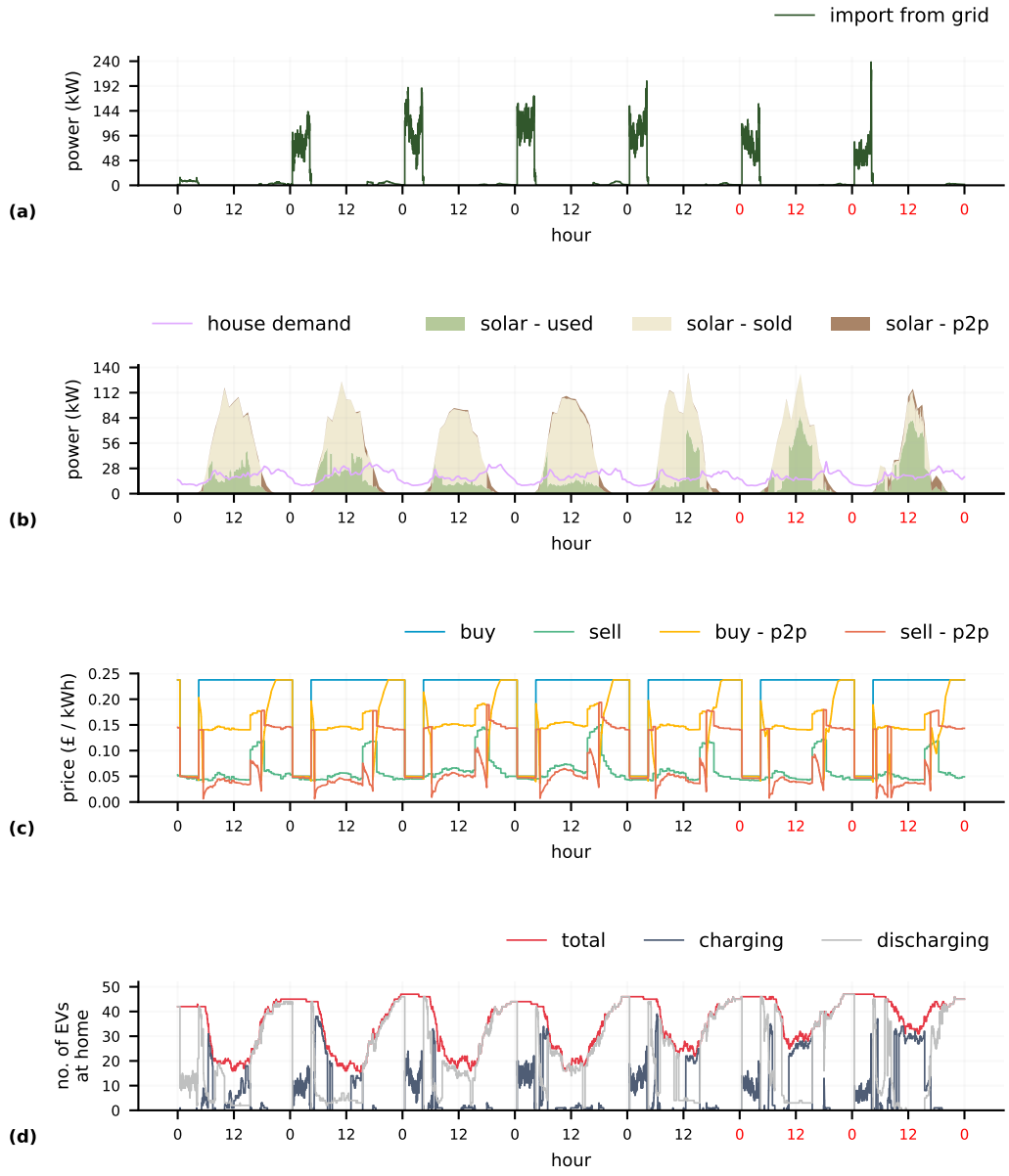

Figure 7.2: Simulation results for the Summer - S2 week showing microgrid operation with a PV penetration rate of 90% and using the Agile Go tariff. This date belongs to the $BS\_3\_\_\_V2H\_\_\_P2P\_S1$ microgrid configuration. The tick labels on *X-axis* in black denote data from Monday to Friday, and the red labels, data from Saturday and Sunday. **a.** Power import from the grid. **b.** Household demand and energy consumed, shared and sold from solar generation within the microgrid. **c.** Buy and sell prices from the grid and from P2P energy trading. **d.** Number of EVs available at home charging and discharging and the total number of EVs available at home.

and end of the low electricity prices, 00:30 and 04:30 hrs, where most of the time the peak demand is below 150 kW in both scenarios. The highest peak demand during the week can be observed at the end of the week, Sunday, close to the end of the low electricity prices under this tariff, this results in a maximum energy drawn from the grid of up to 280 kW for $BS_2___V2H___P2P_S1$and up to 240 kW for $BS\_3\_\_\_V2H\_\_\_P2P\_S1$. This increase in peak demand can be attributed to EVs charging in advance to store more energy before the end of the week, since they will be paid for the amount of SOC that is registered by the end of the week, that is, $E^{SOC}_{v,final}$. During the day, the EVs that are charged tend to track the rise and fall of solar generation, then discharge during the evening. In addition, an increase in solar energy is used towards the end of the week, particularly on Saturday and Sunday, to charge the EVs and increase the amount of SOC at the end of the week. This behaviour can be seen in both scenarios.

In these two scenarios, row **(b)** shows that solar energy is sold to both the grid and P2P on most days, as in some cases, selling to one or the other will be more profitable for households with PV generation. Here, most surplus generation is sold to the grid because it may be more profitable than selling it to its peers due to the way P2P prices are calculated with *Setting one*, where having more solar generation within the microgrid tends to reduce the selling price, which reduces the chances for generators of selling surplus energy in this way. This results in a total energy imported from the grid of 2,250 kWh for $BS_2___V2H___P2P_S1$a self-suffiency ratio (SSR) of 62.07%, for $BS_3___V2H___P2P_S1$a total of 2,252 kWh and a SSR of 62.07%.

7.2.2 Performance of Microgrid Configurations for a week in summer using the agile go tariff

In this section, we will present and compare the four case studies, focusing on their performance metrics. Here, only the metrics outlined in the section 4.4.6 will be discussed. Similarly to Chapter 6, The new metric introduced to evaluate the effect of EV availability on the minimum amount of SOC of all EVs within the microgrid during a week, as mentioned in the section 7.1.6, will be explored in the following section.

Figures 7.3a–7.3c displays a summary of the resulting performance metrics of the case studies BS_1, BS_2 and BS_3, respectively, for all microgrid configurations or scenarios for the Summer - S2 week using the Agile Go tariff. Each row in both figures comprises five separate metrics as described in section 7.1.6, which are detailed in the following.

- **Row A:** Contains results for SSR.
- **Row B:** Contains results for energy balance index (EBI).
- **Row C:** Contains results for the energy imported from the exchange via P2P in kWh.
- **Row D:** Contains results for the maximum power load of the energy imported from the grid in kW.
- **Row E:** Contains results for the mean electricity cost per week in British pounds (£).

Similarly to the results in Chapters 5 and 6, in general, these findings indicate a considerable relationship between PV penetration rates and whether P2P is allowed and which of the two P2P settings is used. As expected, SSR tends to increase at the same time as the PV penetration rates increase for all microgrid configurations or scenarios. This metric reaches its highest value in both cases when PV penetration rate is 100%, V2H is used, P2P is allowed, and *Setting two* is used.

In the case study BS_1 using V1G, SSR increases substantially with PV penetration rates exceeding 50%, peaking at 100% rate. When P2P is allowed t allowance brings a moderate SSR rise in *Setting one*, peaking at 57.81% at 100% PV penetration. *Setting two* shows a more notable SSR growth, reaching 65.52% at 100% PV penetration. V2H usage in BS_1, compared to V1G, results in a 7-10% SSR surge for PV penetration rates above 50%, and an even larger increase as PV penetration rate increases up to 50%. As mentioned in Chapter 5, this is attributed to EVs' capability of charging at times with low electricity costs or during solar surplus, then supplying household energy needs. BS_2 and BS_3 demonstrate similar trends, with slight SSR increments of 0.05% and 0.10% respectively, in all microgrid configurations compared to BS_1.

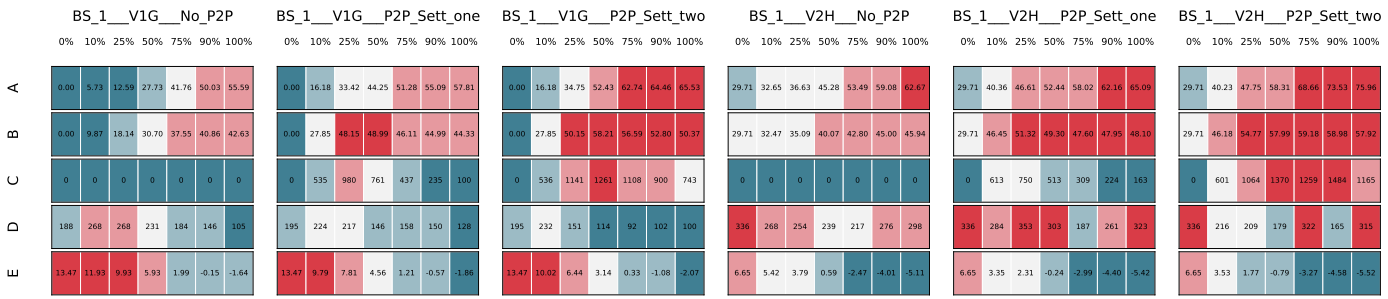

(a) *BS_1*

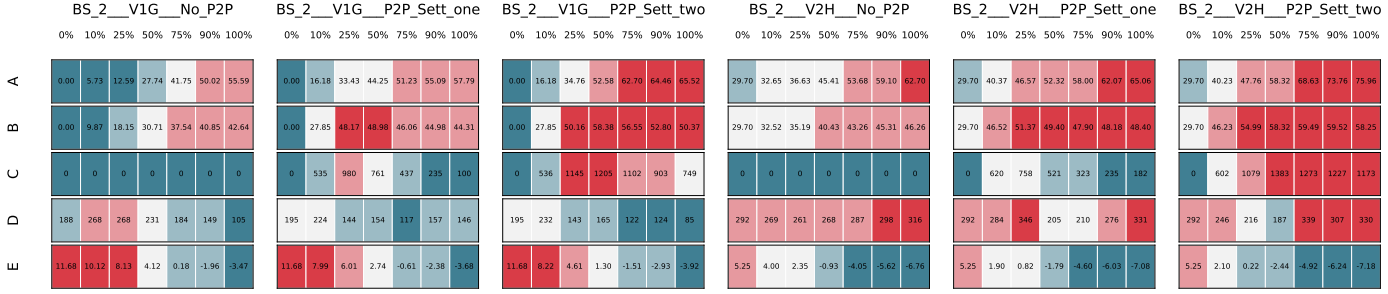

(b) *BS_2*

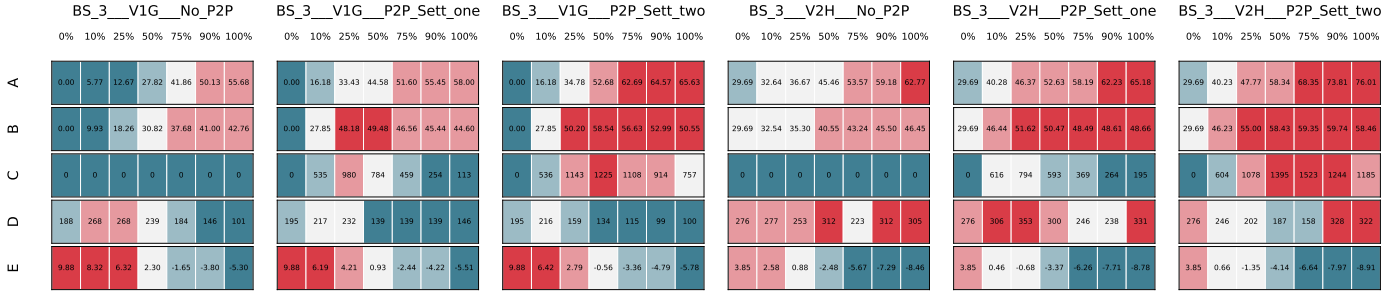

(c) *BS_3*

Figure 7.3: Performance metrics for the microgrid for the Summer - S2 week using the Agile Go tariff. Each block belongs to one microgrid configuration or scenario, where the columns are each specific scenario, and rows each performance metric. *X-axis* denotes the increase in PV penetration rates from 0% to 100%. Dark red represents the highest values for each row, and dark blue represents the lowest. **a.** Self-suffiency ratio. **b.** Energy balance index. **c.** Energy imported from P2P (kWh). **d.** max power load from the grid (kW). **e.** Mean electricity cost per week (£).

As for energy shared via P2P, both settings peak at lower PV rates in all three case studies, specifically, at 50% PV penetration rate. *Setting one* shares less energy than *Setting two* due to the pricing calculation of P2P being less profitable in the former setting, whereas the latter provides more equitable prices. Energy shared in each case study is relatively identical, differing by around 40 kWh. Shared energy varies from 100 to 1,523 kWh across all microgrid configurations. The highest value occurs in $BS\_3\_\_\_V2H\_\_\_P2P\_S2$ at 75% PV penetration. The amount of shared energy increases in V2H with *Setting two* compared to V1G, while an increase is noted with *Setting one* and V1G.

In general, higher PV penetration rates generally decrease the grid's maximum power load in all three case studies, with similar outcomes differing by approximately 30 kW. The highest peak demands, varying from 155 to 353 kW, occur with V2H usage. Allowing P2P energy sharing consistently reduces the peak power load, with *Setting two* achieving further reduction. The peaks decline as PV penetration rates increases when using V1G, unlike with V2H, peak loads fluctuate significantly across all PV penetration rates. In some instances, the highest peak loads occur at 0% PV penetration rate, closely followed by the maximum peak load at 100% PV penetration rate. These increases are mainly due to the likelihood of EVs taking advantage of low electricity prices at night. Also, this is more likely to occur towards to the end of the week, when EVs charge energy for compensation based on their end-week SOC, as seen in figures 7.1 and 7.2.

Energy consumption from the grid decreases as the PV penetration rates increase, with all three cases presenting roughly similar results. Energy consumption varies between 4,496 kWh at 0% PV penetration rate to 1,421 kWh at 100% PV penetration rate. Allowing P2P energy sharing further reduces grid energy consumption, often by hundreds of kWh under *Setting two*. Using V2H leads to more energy drawn from the grid than V1G, as EVs charge at night when electricity costs are low to supply the house during the day, particularly in the evening when energy prices tend to be high. The grid's increased energy consumption can also be attributed to EVs charging enough energy before the end of the week for compensation based on their SOC, a potentially more profitable strategy than not charging at all.

The mean electricity cost per week shows reduced costs with higher PV penetra-

tion rates. In this case, the prices vary between case studies, ranging from £13.47 to -£8.91, where negative costs mean that the participant does not pay the electricity bill but instead gets paid. Using P2P with *Setting two* returns the lowest cost for $BS\_3\_\_\_V2H\_\_\_P2P\_S2$ which uses V2H. On the other hand, V1G returns the highest cost. Here, in the three case studies, costs are around £2.00 away from each other; this can be caused by the different payments for the amount of energy stored in the EVs' battery at the end of the week.

All microgrid configurations, like those described in Chapters 5 and 6, allow participants to sell solar energy to the grid. Choosing to sell energy to the grid reduces SSR, EBI, energy shared within the microgrid, and increases the maximum power load from the grid, making the microgrid more dependent on the use of the grid. However, depending on whether P2P is allowed and the setting chosen, selling energy to the grid can reduce the average electricity cost per week.

The following summary provides a review of this section's findings when using the Agile Go tariff during a week in summer:

- There's a strong correlation between PV penetration rates and P2P settings, with SSR generally increasing as PV penetration rates rise in all microgrid configurations and all three case studies, BS_1, BS_2, and BS_3. The highest SSR is observed with 100% PV penetration, V2H usage, and P2P allowed with *Setting two*.

- Case study BS_1 using V1G sees a notable SSR surge above 50% PV penetration, peaking at 100% without P2P. Allowing P2P under *Setting one* leads to a modest SSR rise, reaching 57.81% at 100% PV penetration rate. P2P under *Setting two* at 100% PV penetration achieves a higher SSR of 65.52%. V2H usage in BS_1 increases SSR by 7%-10% for PV rates over 50%, a significant increase over V1G. BS_2 and BS_3 yield similar results to BS_1 across all microgrid configurations, with slight SSR increases.

- The EBI is impacted by various factors in the study. Notably, the decision to sell solar energy to the grid results in a decrease in EBI, as it reduces the energy shared within the microgrid, making it more reliant on the grid. However, this

effect can vary based on whether P2P energy sharing is permitted and the price mechanism used.

- Energy sharing via P2P, in most cases, reaches its peak at lower PV penetration rates, specifically, around 50% PV penetration rate. More energy is shared under P2P with *Setting two* compared to *Setting one* due to a more favourable pricing model for both buyers and sellers. The energy shared across all three case studies and microgrid configurations ranges from 100 to 1,523 kWh.

- As PV penetration rises, both maximum power and energy drawn from the grid decrease across all case studies. P2P use, especially with *Setting two*, further reduces these values. Peak demand increases are likely when EVs exploit low electricity costs during the night. Utilising V2H over V1G can lead to more energy drawn from the grid, as EVs often charge at night with lower prices, and then discharging to the house during the day.

- The mean electricity cost per week decreases with higher PV penetration rates. Implementing P2P with *Setting two* results in the lowest cost, whereas V1G leads to the highest cost. There is a variance of approximately £2.00 in costs across the three case studies, which is attributed to different payments received for the amount of energy stored in the EVs' batteries. Overall, electricity costs range from £13.47 to -8.91 across all three case studies and microgrid configurations

7.2.3 Results through the different representative weeks of the year

This section presents an analysis of the metrics introduced in Section 4.4.6 and Section 7.1.6. The first part will focus on three performance metrics: SSR, P2P energy sharing, and the mean weekly electricity cost. These three performance metrics help assess the practicality and economic viability of the microgrid configurations and case studies in this work. In the second part, the specific metrics to minimum amount of SOC that can be held for all EVs within the microgrid. This section covers the three different case studies across the different microgrid configurations.

Similarly to Chapter 6, the division of these topics into two distinct subsections was deemed necessary to ensure clarity. It allows for an in-depth, separate analysis of each aspect of the research, resulting in a more precise understanding of the outcomes and implications of each set of metrics in our study.

7.2.3.1 Performance metrics

Similarly to sections 5.2.3 and 6.2.3, the figures presented include values in all microgrid configurations or scenarios. The values are divided into two sections; the column on the left, column 1 contains the average values from 0% to 50% PV penetration rates and the right column, column 2 contains the average values from 51% to 100% PV penetration rates. Furthermore, each row includes each of the five tariff scenarios that were explored, rows 1 to 5, different colours are used to differentiate between the four representative weeks of the year, and different marker shapes are used to help distinguish them between each microgrid configuration. *X-axis* tick labels also include information about each microgrid configuration.

Figure 7.4 shows a comparison of the SSR values over different weeks and microgrid configurations. The three case studies perform similarly with minor variations based on the tariff in use. Differences are small in 0-50% PV penetration rates across all tariffs, except for a minor decrease in the Flat tariff for BS_3's microgrid configurations. Higher PV penetration rates of 51-100% show similar patterns with all tariffs performing uniformly across weeks, displaying a consistent increase in this metric as microgrid configurations transition from V1G to V2H and from non-P2P to P2P usage. Notably, P2P usage enhances this metric's performance, especially with V2H and P2P in *Setting two*. SSR scores highest during weeks with more sunlight, Spring - S1 and Summer - S2, based on tariff types, with traditional tariffs yielding the highest values near 100% at higher PV penetration rates.

Figure 7.5 highlights the total energy imported from P2P within the microgrid. Only relevant scenarios with P2P and PV penetration rates of 10% to 100% are considered. Similar to Chapter 6, *Setting one* microgrid configurations tend to trade less energy due to differing pricing mechanisms for buyers and sellers. Lower PV penetration rates generally share less energy, between 150 and 1,500 kWh during the Summer - S2 week, depending on the tariff and price machanism used. Higher

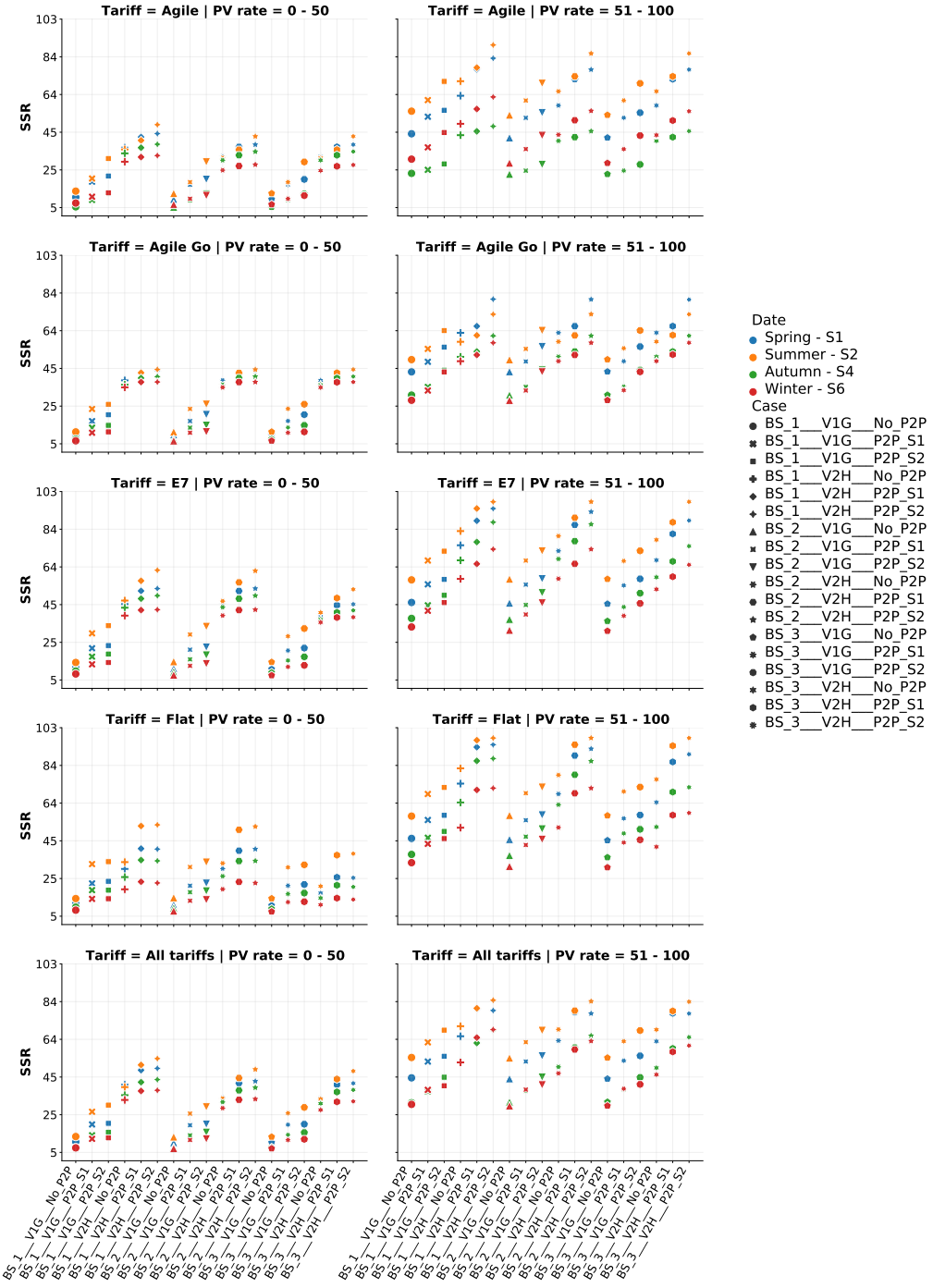

Figure 7.4: Self-suffiency ratio values for the four representative weeks of the year, the five tariff scenarios and all microgrid configurations explored in this chapter. The left column contains the average values from 0% to 50% PV penetration rates and the right column contains the average values from 51% to 100% PV penetration rates.

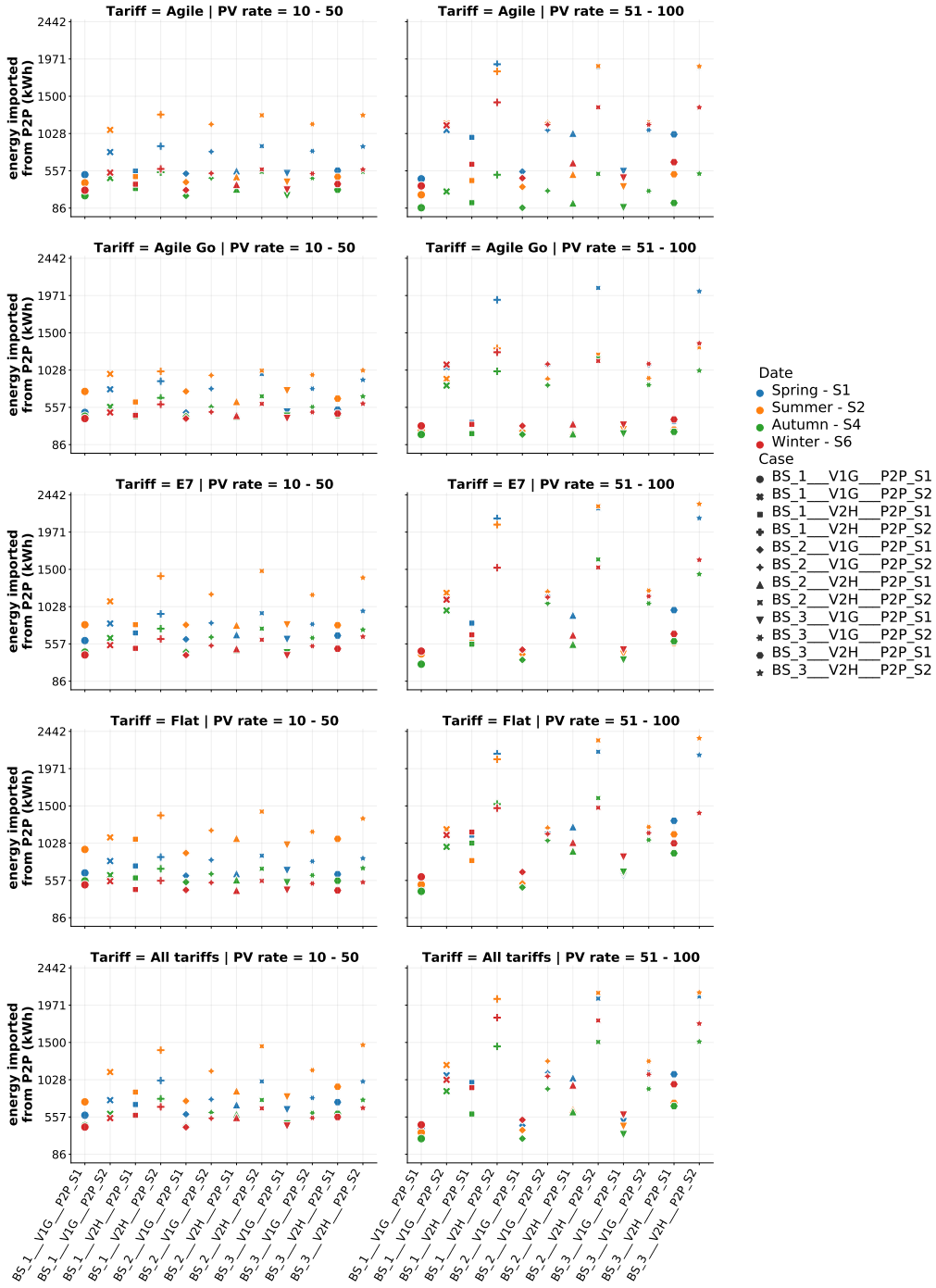

Figure 7.5: Energy shared from P2P for the four representative weeks of the year, the five tariff scenarios and all microgrid configurations explored in this chapter. The left column contains the average values from 0% to 50% PV penetration rates and the right column contains the average values from 51% to 100% PV penetration rates.

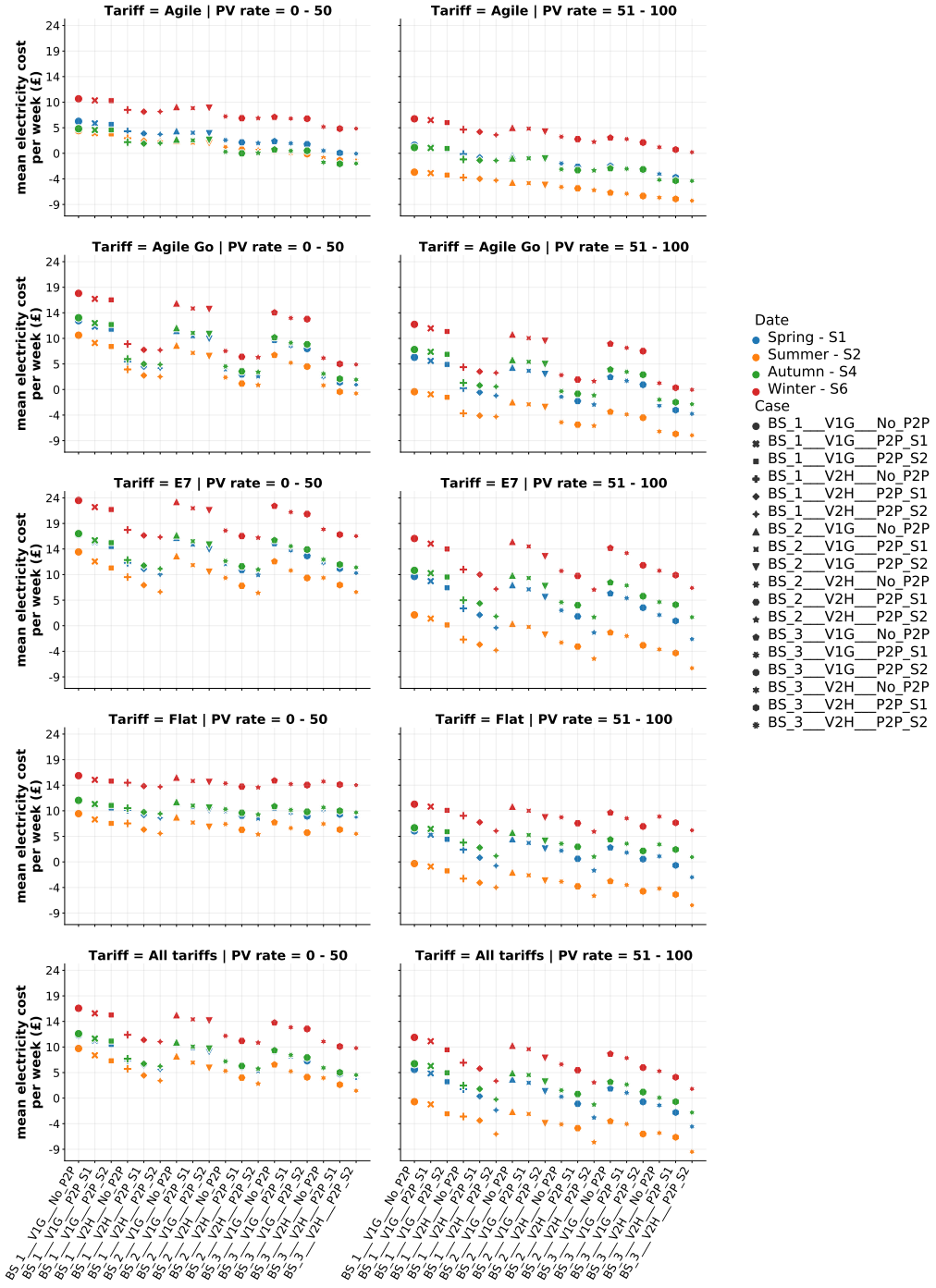

Figure 7.6: Mean electricity cost per week for the four representative weeks of the year, the five tariff scenarios and all microgrid configurations explored in this chapter. The left column contains the average values from 0% to 50% PV penetration rates and the right column contains the average values from 51% to 100% PV penetration rates.

PV penetration rates see shared energy ranging from 86 to 1,100 kWh with *Setting one*, and 86 to around 2,450 kWh with *Setting two*. V1G usage results in less shared energy than V2H, with $BS\_3\_\_\_V2H\_\_\_P2P\_S2$ sharing more energy than other microgrid configurations. Weeks with less sunlight, notably during Autumn - S4 and Winter - S6, typically share less energy. Furthermore, households can import more energy from P2P with surplus generation to charge their EVs and increase the SOC by the end of the week, especially with *Setting two*, as it may be cheaper than grid importation.

Figure 7.6 shows a comparison of the average weekly electricity price. Similarly to Chapter 6, a trend can be seen where microgrid configurations with P2P and *Setting two* exhibit marginally lower prices than other configurations.

The cost fluctuates between -£9 and £24 across both columns and all rows, with Summer - S2 and Autumn - S4 (under the Agile tariff) recording the lowest costs. Higher PV penetration rates considerably cut electricity costs when using V2H and P2P with *Setting two* as opposed to similar configuration but using V1G. The E7 tariff with 0-50% PV penetration rates returns the steepest electricity costs. Winter - S6 shows the highest costs across all case studies and configurations. Moreover, case study BS_3 typically yields the lowest electricity costs due to a higher end-of-week SOC payment.

7.2.3.2 Minimum State of Charge (SOC) Performance

So far, the performance metrics described in section 4.4.6 have been presented. The remainder of this section will present the metrics described in section 7.1.6 which aim to assess the impact of the availability of EVs on the minimum SOC they can hold during the week.

Figure 7.7 shows a comparison of the minimum SOC maintained over a week as a percentage for all EVs within the microgrid. The Agile tariff exhibits some of the highest values, ranging between 44% and 65% irrespective of the PV penetration rates and across all three case studies. The availability of low-cost energy throughout the day may encourage EVs to charge and sustain a high SOC over the week, though values slightly diminish when using V2H compared to using V1G exclusively. P2P does not significantly affect these results, with Winter - S6 week presenting the

lowest values.

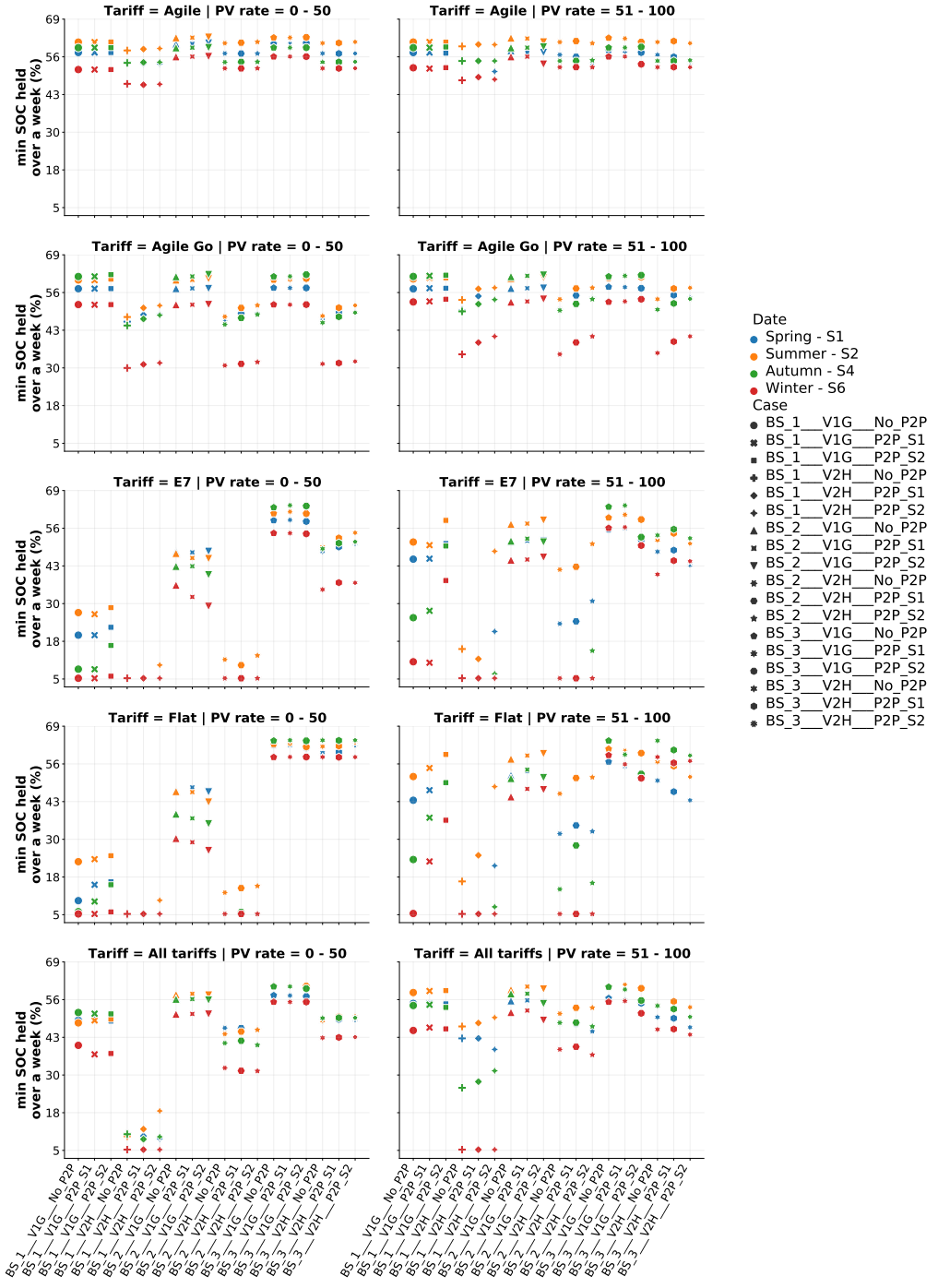

Figure 7.7: Percentage of energy that can be held during the week for all EVs for the four representative weeks of the year, the five tariff scenarios and all microgrid configurations explored in this chapter. The left column contains the average values from 0% to 50% PV penetration rates and the right column contains the average values from 51% to 100% PV penetration rates.

The Agile Go tariff results in high values when using V1G across all three case studies. The results across the four weeks are consistent in all case studies, showing a minor increase when utilising P2P with *Setting two*. Higher PV penetration rates show a notable improvement when using V2H versus exclusively using V1G, with values fluctuating from 34% to 58% at 51-100% PV penetration rates.

The E7 tariff shows a broad range of values from 5% to 65%. With 0-50% PV penetration rates, BS_1 using V1G yields values near 30% in Summer - S2 week, while using V2H results in less than 10% in all weeks. BS_2 shows over 30% using V1G compared to V2H with the same penetration rates. BS 3 significantly outperforms both with values between 35% and 65%. Lower PV penetration rates with P2P and Setting two slightly increase, and values surge significantly at 51-100% penetration using V1G for BS 1 and BS_2. In contrast, BS_3 results for both V1G and V2H are close to each other with of 0-50% PV penetration rates, and in some cases allowing P2P occasionally reducing these values.

The Flat tariff behaves similarly to the E7 tariff, with low values when using V2H at lower PV penetration rates for BS_1 and BS_2. However, BS_3 significantly exceeds the E7 tariff's values when using V2H. 51-100% PV penetration rates follow a similar trend to the E7 tariff across most weeks. P2P increases results with V1G, but for V2H, P2P with *Setting two* further reduces values for BS_3.

In the All tariffs scenario, 0-50% PV penetration yields higher values with V1G compared to using V2H for all weeks studied. These values can be improved using V2H for BS_2 and BS_3, with results ranging from 30% to 50%. Lower PV penetration rates show similar results regardless of whether P2P is used or not. For both V1G and V2H, 51-100% PV penetration rates mirror lower penetration results for BS_1 and BS 2, but improve when using V2H. For BS_3, P2P tends to slightly lower the results.

7.2.4 Annual electricity costs

In this section, the estimated annual electricity costs will be presented. The results were calculated as explained in section 7.1.3. Here, the results are presented in a way similar to that of section 5.2.4. The results of the estimated average annual electricity costs for the four main tariffs, the Agile tariff, the Agile Go tariff, the E7

tariff and the Flat tariff are shown in figures 7.8a–7.8c for BS_1, BS_2 and BS_3. Similarly to chapter 5, in the case of the All tariffs scenario, these results are the average estimated annual electricity costs according to the number of households that are under each different tariff, as described in table 5.4. The results of this scenario are shown in figures 7.9a–7.9c for BS_1, BS_2 and BS_3.

Similar to Chapter 5, the highest costs typically fall in the bottom left corner, while the lowest costs are in the top right corner of each microgrid configuration. Higher PV penetration rates significantly reduce these costs, with further reductions introduced when allowing P2P energy sharing. Compared to Chapter 5, this chapter's average annual electricity costs are lower for EV scenarios using V1G and V2H due to the weekly SOC-based payment to EVs. Here, savings of approximately £340 are achieved with some tariffs versus Chapter 5's results for both V1G and V2H. Among the three case studies, the Agile tariff produces the lowest electricity costs, ranging from £231 to -£252 across all microgrid configurations, while the E7 tariff results in the highest costs, from £1,060 to -£62. BS_3 records the lowest cost with the Agile tariff when using V2H and P2P with *Setting two*.

Higher PV penetration rates are expected to decrease annual electricity cost by utilising excess solar energy for self-consumption or grid sales. Generally, allowing P2P energy sharing can reduce costs by roughly £100 with V1G and about £50 with V2H versus not allowing P2P. Cost reduction is further improved with *Setting two*due to its more attractive price calculation compared to *Setting one*.

In the All tariffs scenario figure 7.8c, the mean annual electricity costs display a similar reduction to Chapter 5, with savings around £200 compared to the same tariff scenario for EVs with V2H in Chapter 5. BS_3 saves up to £300 with V1G, depending on the tariff. Agile tariff exhibits the lowest costs for the three case studies when using V1G, ranging from £424 (0% PV penetration rate) to -£127 (100% PV penetration rate) without P2P, -£134 with P2P and *Setting one*, and -£124 with P2P under *Setting two*. For V2H, costs span from £306 (0% PV penetration) to -£209 (100% PV penetration rate) without P2P, -£224 with P2P and *Setting one*, and -£219 with P2P under *Setting two*. The E7 tariff has the highest costs, followed by Agile Go and Flat tariffs. Overall, P2P results in the lowest cost, with *Setting one* outperforming *Setting two* in some cases. Higher PV penetration rates significantly

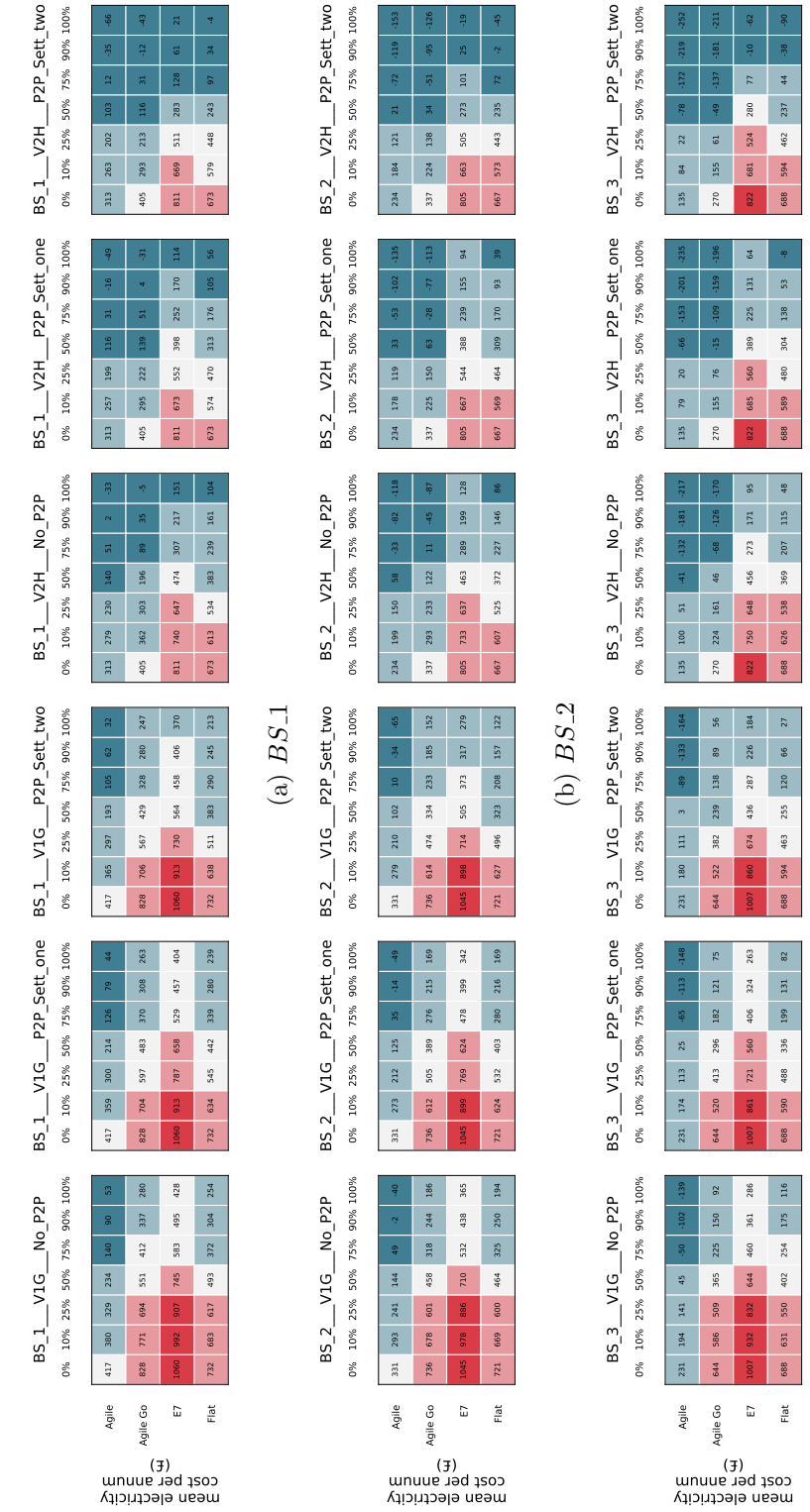

(a) BS_1

(b) BS_2

(c) BS_3

Figure 7.8: Estimated annual electricity cost for Agile tariff, Agile Go tariff, E7 tariff and Flat tariff showing the mean prices within the microgrid.

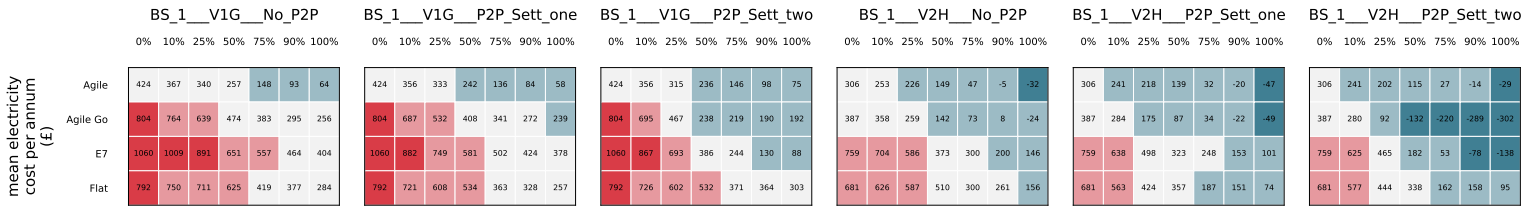

(a) *BS_1*

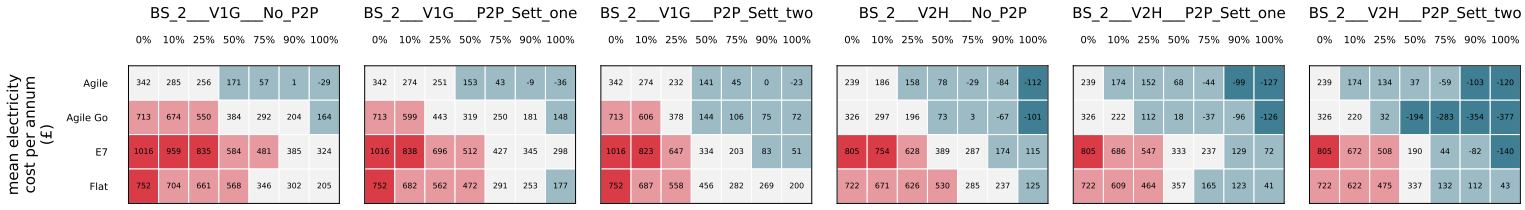

(b) *BS_2*

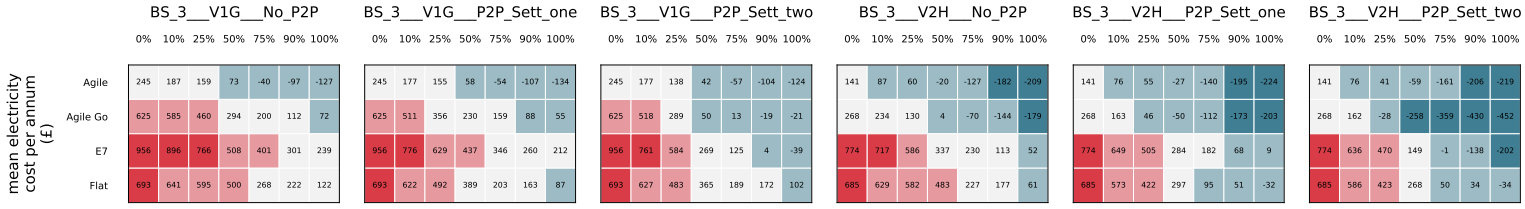

(c) *BS_3*

Figure 7.9: Estimated annual electricity cost for each tariff inside the All tariffs scenario when using home batteries showing the mean prices within the microgrid.

cut costs compared to Chapter 5's results.

7.2.5 Solution quality

This section will present the resulting optimality gap described in section 4.4.7. This metric will evaluate the quality of the findings provided thus far in this chapter, offering a clearer view of how far the results are from the solver's optimal solution, in this case the solver uses is Gurobi 9.5.2 [166]. Additionally, the specifications of the computers used to solve each microgrid configuration.

After solving each model in his chapter, table 7.3 shows the number of solutions that are below the 0.50% optimality gap threshold for each of the 2,520 models in this chapter. As explained in Sections 5.2.5 and 6.2.5, a model with a 0.50% gap implies that the feasible solution identified by Gurobi is quite close to the optimal solution. This small gap is considered satisfactory in many cases, as it demonstrates its effectiveness in solving the optimisation problem with reasonable accuracy. The closer the gap to 0.00%, the higher the confidence in the quality of the solution, which makes it suitable for decision-making or further analysis [166]. Here, only 4 solutions are over 0.50%, which means that the results are good enough.

Table 7.3: Optimality gap value of the resulting models.

Gap	Number of models
≤ 0.50	2,516
$0.50 <$	4

Table 7.4 shows the total number of models in this chapter that were solved on each PC. According to the Gurobi documentation, the results can vary when solved on different hardware, which means that although the optimal results are found, the path to them might be different, which may yield different data [171].

7.3 Discussion

Using an optimisation model, a microgrid was examined to assess the impact of the availability of EVs within a microgrid on the minimum amount of SOC that can be held during a week in three case studies covering four weeks representative of

Table 7.4: Number of models solved using each computer and their specifications.

Number of models	Processor name	Processor speed (GHz)	Cores	RAM (GB)
1,969	11th Gen Intel (R) Core (TM) i5-1135G7	2.30	4	64
551	Intel (R) Xeon (R) E5-2620 v4	2.10	16	128

the seasons of the year, different PV penetration rates, in conjunction with four different tariffs and two different P2P price calculations based on mid-market rate (MMR). This was achieved using real-world data from residential energy use, local solar power and EV travel, including predicted data on their ability to be connected at home. The simulations indicate that the availability of the EVs have an impact between the weeks explored on how much SOC can be held during the week, but this mostly depends on the energy tariff used, the PV penetration rates, and if V1G or V2H is used. The use of P2P tends to reduce the minimum SOC that can be held during the week when V2H is used, whereas for V1G there is a slight increase in the results. These results also vary in the three case studies, where the case study BS_3, the one with the highest payment rate at the end of the week, shows a higher minimum SOC that can be held during a week.

Using V1G tends to higher minimum SOC values, which is because the EVs only charge to meet any travel needs during the week, whereas using V2H allows EVs to discharge energy to the household during the day, resulting in a lower minimum SOC per week. Although V1G only means that EVs will not be able to discharge to the grid, the use of a bidirectional charger that only allows discharge to the grid when an instruction from the grid to provide restoration services –i.e. otherwise restricted to V1G – can increase the amount of energy that can be provided to the grid and still make a profit as restoration services are paid according to their availability [119], though this type of payment was not explored in this work, it can be of interest for system operators to explore this further.

In general, participants can achieve average electricity costs per week ranging from £25 to -£9 depending on the energy tariff, PV penetration rates and whether P2P is allowed or not depending on *Setting two* . These average electricity costs

per week are similar to those of chapter 6. These costs depend on the energy tariff used, in this case using the Agile tariff as the only tariff in the microgrid is the one that results in the lowest electricity costs. Furthermore, having PV penetration rates 51-100% can reduce these costs even further. SSR also increases with higher PV penetration rates reaching their highest values, close to 100% when using more traditional tariffs, such as E7 and Flat tariffs, during the Spring - S1 and Summer - S2 weeks. The SSR significantly increases when using V2H combined with P2P with *Setting two*with 51-100% PV penetration rates.

As participants are paid according to the amount of SOC at the end of the week, this leads to higher demand peaks close to the end of the week, where participants tend to take advantage of low prices, for certain energy tariffs, and charge their EVs before the end of the week. This results in peaks close to 400 kW for the Agile tariff regardless of using P2P or PV penetration rates . The estimated annual electricity costs in the case studies BS_1 and BS_2 are approximately £ 200 and up to £ 300 less in the case study BS_3 compared to the equivalent microgrid configuration results in chapter 5. This is due to participants being paid at the end of the week depending on the amount of SOC when the simulation ends, and showing that, as expected, getting paid more will result in a higher amount of SOC that can be held during the week.

It is worth noting that the introduction of a daily payment during our early tests only lead EVs to exclusively using energy for travel and nothing else, even under V2H. Perhaps improving the objective function could help when daily payments are introduced in order to avoid increasing the energy demand during the weekend.

7.4 Conclusions

In this chapter, the impact of the availability of EVs has on the minimum amount of SOC that can be held during the week for EVs within a microgrid was explored in three case studies, with different PV penetration rates, P2P using different price calculation systems and five different tariff scenarios in four weeks representative of the seasons of the year.

In general, the availability of EVs influences this value throughout the explored

weeks, but the greatest impact comes from the energy tariff that is used. Depending on P2P, PV penetration rates and if V1G or V2H is used, this value can increase. However, these parameters do impact SSR, the maximum power load and the average electricity cost per week.

We found that using dynamic energy tariffs, like the Agile tariff, in combination with V1G typically results in higher minimum SOC values throughout the week. The exceptions are when using V2H with Agile tariff or a Flat tariff, where the values are nearly as high as with V1G. System operators may be interested in limiting users to V1G, essentially restricting giving energy back to the house i.e. restricting V2H, while connected to a V2G bidirectional charger, only allowing energy usage for restoring services and compensating for availability.

The introduction of incentives for EVs to pay them according to the amount of SOC at the end of the week tends to increase this minimum SOC value where higher payment rates yield the highest minimum SOC than can be held for the week in all EVs. Also, thanks to this payment, average electricity costs tend to be lower than the previous results in chapter 5 when using EVs with V2H.

Chapter 8

Conclusion

8.1 Electric Vehicles availability prediction

The work presented in Chapter 3 aimed to address the research question:

- Can machine learning models be trained to predict the start and end locations of electric vehicles (EVs) trips for the purpose of optimising vehicle-to-grid (V2G) services, including smart charging (V1G) and Vehicle-to-home (V2H)? Can the travel patterns learned from mostly internal combustion engine vehicles (ICEVs) data be effectively used to predict the locations of EVs?

This study utilised a dual-dataset approach to develop a predictive model for understanding the availability of EVs during the day. For this, the national travel survey (NTS) dataset, comprising over 2 million entries of private vehicle travel information within the UK was used.

Utilising this dataset, the model was trained and validated to predict the start and end locations of each trip. For this analysis, two key categories of locations were examined: *Home* and *Other*. The *Home* category represented instances where the EV was parked at home and available for charging or discharging. In contrast, the *Other* category denoted instances where the EV was away from home, potentially in motion and unable to charge or discharge at home, but capable of charging using a street charger if the EV was not in motion i.e. not travelling. For this, three machine learning algorithms were compared and a 5-fold cross-validation strategy was used. The data was split into two subsets, each tasked with a specific purpose - one to

predict the start location of a vehicle, and the other to predict the end location. The model achieved F1-scores of 0.900 and 0.902 for tasks 1 and 2, respectively.

Subsequently, the predictive model was applied to a second dataset, consisting of real-world UK EV travel data. This data included the time of the trip, the distance travelled, and the energy consumed during the trip. Though not employed in the training and validation phase, this EV dataset was fundamental in aligning our models with the study's primary objective — optimising EV usage for V2G services, including V1G and V2H. The resultant predicted locations were then utilised for further analysis in chapters 5–7.

The predictive model was able to reflect the driving behaviour of EVs during the day and properly classify their location, showing that the majority of EVs are not at *Home* between 9 and 5 pm from Monday to Friday, which matches typical office hours, with the number of EVs available slowly increasing throughout the evening, showing that the majority of EVs are at home during the night. During the weekends, the number of EVs is higher during the same hours from 9 to 5 pm.

In general, of the 50 EVs considered, approximately 15 EVs are available at *home* at all times during the six weeks studied, with the lowest number of EVs during the week around 12 pm. The highest number of EVs at *Home* can be seen in the evenings and early hours of the morning during the week. In the six weeks studied covering the four seasons of the year, there is no noticeable difference in the number of EVs available during the day.

Importantly, the NTS dataset is predominantly composed of ICEV travel data. Despite the apparent technological differences between ICEV and EVs, many travel behaviours are universal, which made the ICEV data an invaluable resource for capturing general travel patterns. Validating our models with the same ICEV data was a crucial step to ensure their robustness and capacity for generalisation, an essential aspect of machine learning model development.

However, certain limitations are worth mentioning. The primary concern relates to the dependence on the NTS data. Although, it is a comprehensive dataset, it relies on self-reported data, possibly leading to inaccuracies. Additionally, the single-set random seed approach, while efficient, may not entirely reflect the variability of model performance.

While the technological differences between ICEVs and EVs could influence the accuracy of EV location predictions, this work argues that many travel behaviours are indeed universal, thus affirming the relevance of ICEV data. However, understanding the full extent of these technological differences on location prediction remains an area for future research and model refinement, which is beyond the scope of this study.

Despite these limitations, this study lays a solid foundation for optimising V2G services using machine learning models trained on ICEV data. Future work should explore the training of models on real-world EV data to possibly enhance their accuracy and applicability.

8.2 Performance of electric vehicles and home batteries

The work presented in chapter 5 aimed to address the research question:

- What impact does the availability of EVs have on the effective implementation of V1G and V2H services services within a microgrid? How does the application of the predictive model to real-world EV data inform and optimise V1G and V2H services, and how does this technology compare to stationary batteries in terms of leveraging the predicted EV availability and location data?

This study explored the potential technical and economic benefits of using stationary home batteries and EVs, the role of EV availability in the implementation of V1G and V2H services, under different conditions, such as varying photovoltaic (PV) penetration rates, peer-to-peer (P2P) using different price mechanisms, and five different tariff scenarios, throughout the four seasons of the year. This was done using the optimisation model introduced in Chapter 4 with a slight modification to the model to reflect the particularities of a stationary home battery.

It was found that having a stationary home battery or an EV, coupled with a PV system, can help households lower their electricity costs. These systems can be charged when energy prices are low or during the day when there is solar surplus generation, and then supply power to the household when prices are high or nduirng the evening. This reduces the household's reliance on the grid and leads to savings on electricity bills. However, EV availability throughout the day can reduce some of

these benefits, particularly when PV generation is high as this is usually when most EVs are away.

The introduction of P2P can mitigate this potential disadvantage, as it allows participants with a PV system to sell the solar excess to their peers on the microgrid while their EVs are away, which in most situations it more profitable than selling it to the grid. Moreover, the benefits of having an EV can be increased depending on the P2P price mechanism used and PV penetration rates within the microgrid. Dynamic tariffs like the Agile tariff, which follows the wholesale electricity price, or the Agile Go tariff, designed specifically for EV owners, can boost these benefits, outperforming more traditional tariffs such as E7 and Flat Tariff. Combining P2P with V2H for EVs shows that, in some cases, the performance of EVs can almost match that of a stationary battery. However, EVs provide an added benefit - transportation - making them an attractive choice for potential owners.

In this work, the predictive model produced in Chapter 3 contributed to understanding the effects of EV availability on V1G and V2H services. Despite not providing absolute accuracy, by capturing common travel patterns from the NTS data, the model was able to provide a reasonable estimation of the start and end locations of EVs during the day. This offered valuable insights into how the availability of EVs could impact the provision of V1G and V2H services.

Besides understanding EV availability, we also considered the economic viability of EVs versus stationary batteries. The upfront cost, capital expenditure (CapEx), of a Nissan Leaf 2018 and a bidirectional charger (Wallbox Quasar) totals £32,994. The running costs, operating expenditure (OpEx), assuming a 100% PV penetration rate, range from £121 to £28 per year for V1G and V2H, respectively. Over five years, these costs add up to £33,599 for V1G and £33,134 for V2H.

In contrast, stationary batteries like the Nissan/Eaton and Tesla Powerwall have lower upfront costs at £3,500 and £5,700 respectively. They also have the potential to generate income rather than costs, leading to costs as low as -£64 per year for the Nissan/Eaton battery and -£82 for the Tesla battery. Over five years, this totals £3,180 for Nissan/Eaton and £5,290 for Tesla Powerwall.

When comparing these two technologies, potential owners need to consider the added transport utility of EVs, despite their higher initial investment, versus the

potential to generate income rather than cost of stationary batteries. The latter, while lower in cost, do not provide any transport utility.

However, this study has a few limitations that may influence the results obtained. As mentioned before, the model, trained on predominantly ICEV data, could face accuracy issues in predicting EV locations due to technological differences between ICEVs and EVs may exhibit varied driving patterns, which could influence the predictive model's predictive accuracy. Also, the use of self-reported NTS data might introduce potential inaccuracies.

Despite these limitations, this study has made an important contribution towards understanding the impact of EV availability on V1G and V2H service implementation and the broader implications for microgrid performance. Future work should be on refining these models and their application in various EV scenarios, with an emphasis on exploring training the model using real-world EV data for improved performance and accuracy.

8.3 Using vehicle-to-grid technology for short term operating reserve provision

The work presented in Chapter 6 aimed to address the research question:

- Are EVs capable of providing short term operation reserve (STOR) services within a microgrid when connected at home? How does the availability of EVs impact the provision of these services and their ability to fulfil technical requirements as outlined by the National Grid in the UK?

The potential of EVs to provide STOR services within a microgrid was explored. This was achieved by utilising the resulting data from Chapter 3 and slightly modifying the optimisation model introduced in Chapter 4 to accommodate the provision of STOR. The results suggest that EVs successfully meet most of the technical requirements stipulated by the UK's National Grid, including an ability to respond to an instruction in under 20 minutes, sustain that response for 120 minutes, and be ready to respond again within 1,200 minutes.

In this study, some important considerations and potential areas for further development have been identified within this context. Firstly, a crucial aspect identified

is the impact of EV availability on the provision of STOR services. The amount of energy that can be supplied for STOR is largely dependant on the number of available EVs during a STOR event. This suggests the necessity for an additional margin of EVs beyond the total needed, to ensure a consistent energy supply even during potential fluctuations in EV availability.

In this context, the data suggests a surplus of about 15% EVs over the total participants in the microgrid can help ensure resilience. As such, to provide 3 MW of energy under optimal conditions, the number of necessary EVs increases from the initial 410 EVs, with a 7.4 kW bidirectional charger, to about 480 EVs, factoring in the 120-minute response requirement.

The study indicates that the effective provision of STOR services within a microgrid is influenced by the number of available EVs. However, the concept of aggregator's role in managing these vehicles and their charging infrastructure is pivotal to this process. Aggregators could serve as an intermediary between the EV owners and the grid, ensuring the optimal utilisation of available resources while maintaining grid stability.

Moreover, the context of the microgrid as a component within a larger power system is also a significant aspect to consider. The capacity of a microgrid to provide STOR services exists within a larger network dynamic, where it contributes to, and is influenced by, the wider grid's operational mechanics. An expanded analysis is necessary, one that includes factors such as load balancing, peak demand management, and the role of energy storage in maintaining grid stability. A comprehensive approach like this is essential to fully understand the potential and constraints of a microgrid in contributing to overall grid resilience and efficiency.

Secondly, the way that the model used was in this study assumes that EVs know when STOR events will occur and can charge in advance to provide energy for STOR. While in reality, STOR events can occur at any time during the committed windows. Therefore, it would be worthwhile to further study this aspect to account for this randomness and perhaps suggest participants to maintain a certain level of state of charge (SOC) if contracted or willing to participate in the provision of STOR services.

Another limitation is related to the way the model work when EVs discharge

energy for STOR services. The model used permits only a one-way energy flow, allowing households to either import or export energy at a given time, but not both simultaneously. Moreover, if there is a solar surplus during a STOR event and a household's EV is participating, this excess energy must be sold to the grid, as sharing energy P2P would involve other participants importing energy this way, which is not allowed under current rules as they will also be in "export" mode. The model's one-way flow of energy potentially results in the suboptimal use of surplus solar energy, particularly when EVs are exporting energy for STOR. A potential mitigation could involve refining the model to allow flexibility of energy exchange and allowing for more efficient use of solar surplus.

Despite certain limitations in the model used and the challenges posed by the availability and charging behaviour of EVs, overall, this study highlight potential factors that could influence the scalability and reliability of EVs in providing STOR services in real-world scenarios. For the study's results and conclusions to be applicable on a larger scale, effective management of, and where possible, prediction of EV availability is crucial.

In future studies, it is recommended to further develop strategies for managing EV availability, which has been shown to be a critical factor in providing a steady energy provision for STOR. Finally, it would be valuable to explore how advancements in EV and charger technology could improve the capacity of EVs to provide STOR services.

8.4 Minimum amount of state of charge that can be held for a week

The work presented in chapter 7 aimed to address the research question:

- What strategies or mechanisms can be implemented to encourage EVs to consistently increase their SOC throughout the week? What are the impacts of V1G and V2H strategies on the minimum SOC maintained in EVs for potential restoration services? How does the availability of EVs influence the capacity the minimum SOC that can be maintained over the course of a week?

In this study, the impact of the availability of EVs on the minimum amount of

SOC that can be held during the week for all EVs within a microgrid was explored. The optimisation model from Chapter 4 was used with a slight modification to the model to properly study the minimum SOC during the week.

We found that several mechanisms and strategies were particularly effective in encouraging EVs to keep a higher EV throughout the week. Most notable among these was a higher payment rate system where compensation to EV owners was determined by the SOC level at the end of the week. This approach successfully increased the minimum EV values while simultaneously reducing average weekly electricity costs.

The interaction between V1G and V2H strategies and the minimum SOC kept in all EVs for potential restoration services presents an interesting perspective. Our findings suggest that the implementation of V1G along with dynamic energy tariffs such as the Agile tariff typically leads to higher minimum SOC values throughout the week. Conversely, V2H used in conjunction with Agile or Flat tariffs produces nearly similar SOC values. Despite this, our study recommends that system operators limit users to V1G, thereby restricting energy supply back to the home and encouraging energy usage predominantly for restoration services. Essentially, this would mean that V2G would be active but without the benefits of V2H, allowing EVs to provide energy for restoration services if required.

Although the availability of EVs clearly impacts the minimum SOC that can be held over a week, our findings demonstrate that this impact is not more significant than other factors such as PV penetration rates, energy tariffs and the different P2P price mechanisms. Therefore, efforts to increase EV availability should be part of a larger strategy that includes efficient energy tariffs, power management, and incentive schemes to improve SOC management.

Nevertheless, the main focus of this study was to evaluate the potential of EVs by exploring the minimum SOC to estimate the amount of energy that could be available for restoration services. It is important to consider the study's limitations when interpreting the results. Firstly, the study did not include a simulation of a restoration service, leaving a significant gap in our understanding of how the stored SOC could be utilised for such services. This area requires further research.

Secondly, this study is inherently limited by the data produced in Chapter 3.

Any inaccuracies or limitations inherent to this data set could potentially impact the findings in this study, thereby affecting the reliability and effectiveness of our results.

Thirdly, the weekly payment scheme, while successful in encouraging a higher SOC, has unintended consequences. It leads to increased demand on the electrical grid, especially towards the end of the week as EV owners charge their vehicles to maximise their SOC and get compensation accordingly. This strategy, while effective in the short term, could potentially strain the electrical grid, rendering it unsustainable in the long term.

Finally, it is worth noting that a related concern arose during the early tests of the study when we were introducing a daily payment scheme. This led to all EVs maintaining maximum SOC at all times and only consuming energy for travel, even under the V2H scenario. This behaviour, although ensuring a consistently high SOC, unexpectedly limited the versatility of energy use by EVs. Future research could focus on improving the model to address this, creating a more balanced scenario that can adapt to these behaviours.

In conclusion, this study has provided valuable insights despite its limitations. It shed light on the role of EV availability, energy tariffs, V1G and V2H strategies, and different P2P energy price mechanisms in managing minimum SOC over the week within a microgrid. Particularly noteworthy is the introduction of a payment mechanism that has shown to effectively incentivise EV owners to maintain a higher SOC, paving the way for potential improvements in energy management. Future studies should include simulations of restoration services to better understand the potential contribution of stored SOC and explore more balanced payment schemes that encourage high SOC without overloading the grid or limiting the versatility of energy use.

8.5 PV penetration rates, energy tariffs and P2P impact within a microgrid

The work presented in chapters 5–7 aimed to address the research question:

- How do varying conditions, such as different PV penetration rates and energy

tariffs, impact the implementation of V1G, V2H and V2G services within a microgrid throughout different weeks of the year? How does the P2P energy trading, and specifically the variation in P2P prices, impact the provision of V2G services within a microgrid?

In the analysis of the microgrid system, the combination between PV penetration rates and energy tariffs emerges as a vital factor in implementing V2G services effectively. With higher PV penetration rates, households experience improved performance, while different metrics such as self-suffiency ratio (SSR) increases and electricity costs decrease. This surplus energy can be stored in the battery for later use or sold as surplus solar energy back to the grid. Moreover, if P2P energy trading is allowed, households can sell their excess electricity to others within the microgrid, thereby reducing grid reliance. This P2P trading system can mutually benefit both buyers, who acquire cheaper electricity, and sellers, who profit from their surplus. Importantly, P2P energy sharing was found to offer significant benefits to EV owners. For instance, when owners are away and unable to charge their EVs, they have the opportunity to sell the surplus energy to their peers, often at prices more competitive than buying from or selling to the grid.

Certainly, the integration of different systems such as PV, P2P energy trading, and different energy tariffs, particularly dynamic tariffs, have demonstrated substantial potential in enhancing the performance of EVs within a microgrid. Notably, the results showed that with the correct combination of these elements, there was an improve in performance from EVs with V1G, and when V2H is used, the performance of the EVs could rival that of stationary batteries, illustrating the potential benefits of this integrated system approach.

As for EVs providing STOR, the impact of PV penetration rates, P2P, and energy tariffs was less pronounced. While P2P and higher PV penetration rates brought benefits in terms of overall system performance and cost efficiency, their effect on the provision of STOR was minimal. This highlights the need for further research to explore how these technologies could be better integrated to enhance the capability of EV to provide STOR.

Regarding the effect of these system combinations on the minimum SOC that EVs can hold during the week that could potentially be used for restoration services.

The different PV penetration rates, energy tariffs and the choice of using P2P do not have a significant impact on this. Interestingly, the use of dynamic tariffs, like the Agile tariff, in combination with V1G typically often resulted in higher minimum SOC values throughout the week. It was also found that when using Agile tariff or a Flat tariff in combination with V2H, the SOC values during the week are nearly as high as with V1G. This suggests a promising potential to increase the energy available for restoration services when using EVs, highlighting the benefits of this integrated system for improving microgrid resilience.

Throughout the various studies conducted in this research, dynamic tariffs, such as the Agile tariff and the Agile Go tariff, this last one specifically designed for EVs, consistently returned the best results across most weeks of the year. This tariff performance, combined with higher PV penetration rates, significantly increased the performance of the microgrid. Interestingly, during weeks with more sunlight, especially in the summer, these tariffs consistently yielded better results compared to other periods of the year, like winter. This pattern underscores the potential of leveraging seasonal variations in sunlight for more efficient energy use within the microgrid. In particular, the consistent use of P2P under *Setting two*, which calculates the price for buying and selling energy within the microrgrid based on the mid-market rate (MMR) prices, yielded further enhancements in performance. This finding points to the value of maintaining higher PV penetration rates and the use of P2P trading for maximum microgrid efficiency.

However, one limitation of these results lies in the objective of the optimisation model from Chapter 4, which was primarily focused on minimising electricity costs for participants within the microgrid. In some instances, this led to demand peaks that could potentially affect the stability of the electrical grid. To address this, future studies could consider incorporating the energy demand from the grid into the objective function of the optimisation model. This approach could help strike a balance between reducing electricity costs and maintaining grid stability, thereby contributing to the overall sustainability of the microgrid system.

Another potential limitation of this study is that the simulations only represented six distinct weeks of the year, corresponding to the four seasons. A more thorough exploration spanning a full year could provide deeper insight into seasonal impacts

on the results. Future studies might also consider including more energy tariffs available to the public to better understand each tariff's unique effects. This expanded approach would provide a more comprehensive understanding of how tariffs and seasonality influence the performance of microgrids, especially when providing V2G services.

Additionally, this study's findings are inherently tied to the data from Chapter 3. Any inaccuracies or limitations within this data could potentially influence our conclusions, impacting their reliability and effectiveness.

Despite these limitations, the research has provided valuable insights into the impact of PV penetration rates, energy tariffs, P2P energy trading on V2G services within a microgrid. Future work should focus on addressing the limitations highlighted in this work to improve energy management and the performance of EVs within a microgrid.

8.6 Future work

Through the course of developing this research, several opportunities for additional research were identified that were beyond the scope of the original work. Nevertheless, it would be interesting to investigate them more in the future, and they are described below.

- Although the predictive model proved useful in this work, travel data only includes information on the UK. It would be useful to adapt the proposed methodology and to use travel information from other countries to make a comparison of potential markets where V2G can be useful.

- The simulations in this work were restricted to only 7 days a week due to time constraints and computation time to solve each model. Increasing the number of days studied may be interesting to consider, as it could capture in more depth the impact of the availability of EVs and V2G.

- An analysis of environmental impacts when providing ancillary services with V2G could be beneficial for policy makers and system operators.

- Including other technologies in the optimisation model such as combined heat and power (CHP) and other renewable energies may be interesting to look at.
- Combining the use of a home battery and an EV using V2G can be interesting to investigate.
- Adapting the optimisation model to use EVs as community storage is something that has been examined in the literature, but it may be interesting to use the proposed predictive model to assess the impact of the availability of EVs.
- Studying battery degradation when providing V2G is something that has been done before; however, in most cases, the availability of EVs is not considered or is considered during fixed times of the day.

Appendix A

List of publications

The work carried out during the course of this PhD has led to the following publications.

- Donovan Aguilar-Dominguez, Alan Dunbar, and Solomon Brown. *"The electricity demand of an EV providing power via vehicle-to-home and its potential impact on the grid with different electricity price tariffs"*. In Energy Reports, volume 6, pages 132–141. Elsevier Ltd, 5 2020.

- Donovan Aguilar-Dominguez, Jude Ejeh, Alan D.F. Dunbar, and Solomon F.Brown. *"Machine learning approach for electric vehicle availability forecast to provide vehicle-to-home services"*. Energy Reports, 7:71–80, 2021. ISSN 23524847.

- Donovan Aguilar-Dominguez, Jude Ejeh, Solomon Brown, and Alan Dunbar. *"Exploring the possibility to provide black start services by using vehicle-to-grid."* Energy Reports, 8:74–82, 11 2022.

Appendix B

Supplementary results

B.1 Expanded results through the different representative weeks of the year

In this section, we present extended data sets and analyses of the different microgrid configurations across a variety of representative weeks throughout the year. Each figure in this section contains data collected from the metrics that were not covered in their relevant results section of each chapter, specifically in sections 5.2.3, 6.2.3 and 7.2.3. Therefore, energy balance index (EBI), maximum power load from the grid and energy imported from the grid are included.

The figures presented in this section include values in all microgrid configurations or scenarios. The values are divided into two sections, the column on the left – column 1 – contains the average values from 0% to 50% photovoltaic (PV) penetration rates and the right column – column 2 – contains the average values from 51% to 100% PV penetration rates. Moreover, each row includes each of the five tariff scenarios – rows 1 to 5 – that were explored, different colours are used to differentiate between the four representative weeks of the year and different marker shapes are used to help distinguish them between each microgrid configuration. *X-axis* tick labels also include information about each microgrid configuration.

B.1.1 Chapter 5 - Performance metrics supplementary results

In Chapter 5, the effectiveness of using a microgrid connected to the grid to reduce the electric bill of households that own a stationary battery or an electric vehicle

(EV) with a bidirectional charger was analysed.

Figure B.1 shows a comparison of the results of EBI where it can be seen that the scenarios with peer-to-peer (P2P) perform better than those without P2P. As this metric penalises both imports and exports from and to the grid, the results differ between columns, rows, and weeks; however, it can be seen that this metric increases when there is a higher PV penetration rate present.

Figure B.2 shows a comparison of the maximum power load from the grid. Here, in most rows in columns 1 and 2, the Winter - S6 week has the highest maximum power load, and Summer - S2 the lowest compared to the other weeks. Furthermore, scenarios with P2P tend to draw more power from the grid at the same time compared to those without it. In column 1, home batteries seem to have lowest values across all scenarios and weeks, which is mostly true as well for column 2, however, all this depends on the tariff that is used. Column 2 shows more diversity across all scenarios and tariffs with dynamic pricing during the day, such as Agile tariff, Agile Go tariff and economy seven (E7) tariff, compared to Flat tariff and the All tariffs scenario. EVs with Vehicle-to-home (V2H) tend to draw more energy than the rest of the scenarios; again, this could be due to charging when prices are low to meet travel needs and give energy back to the house during the day.

Figure B.3 shows a comparison of the energy imported from the grid. Columns 1 and 2 show that Winter - S6 import the most energy for scenarios and tariffs, with the exception of the Agile tariff with 51-100% PV penetration rates where home batteries and EVs with V2H are used, and the lowest energy imported from the grid occurs during the Summer - S2 week in most cases. Furthermore, the most energy imported from the grid occurs when using EVs where it can reach more than 6,000 kWh with 0-50% PV penetration rates and up to 5,000 kWh with 51-100% PV penetration rates.

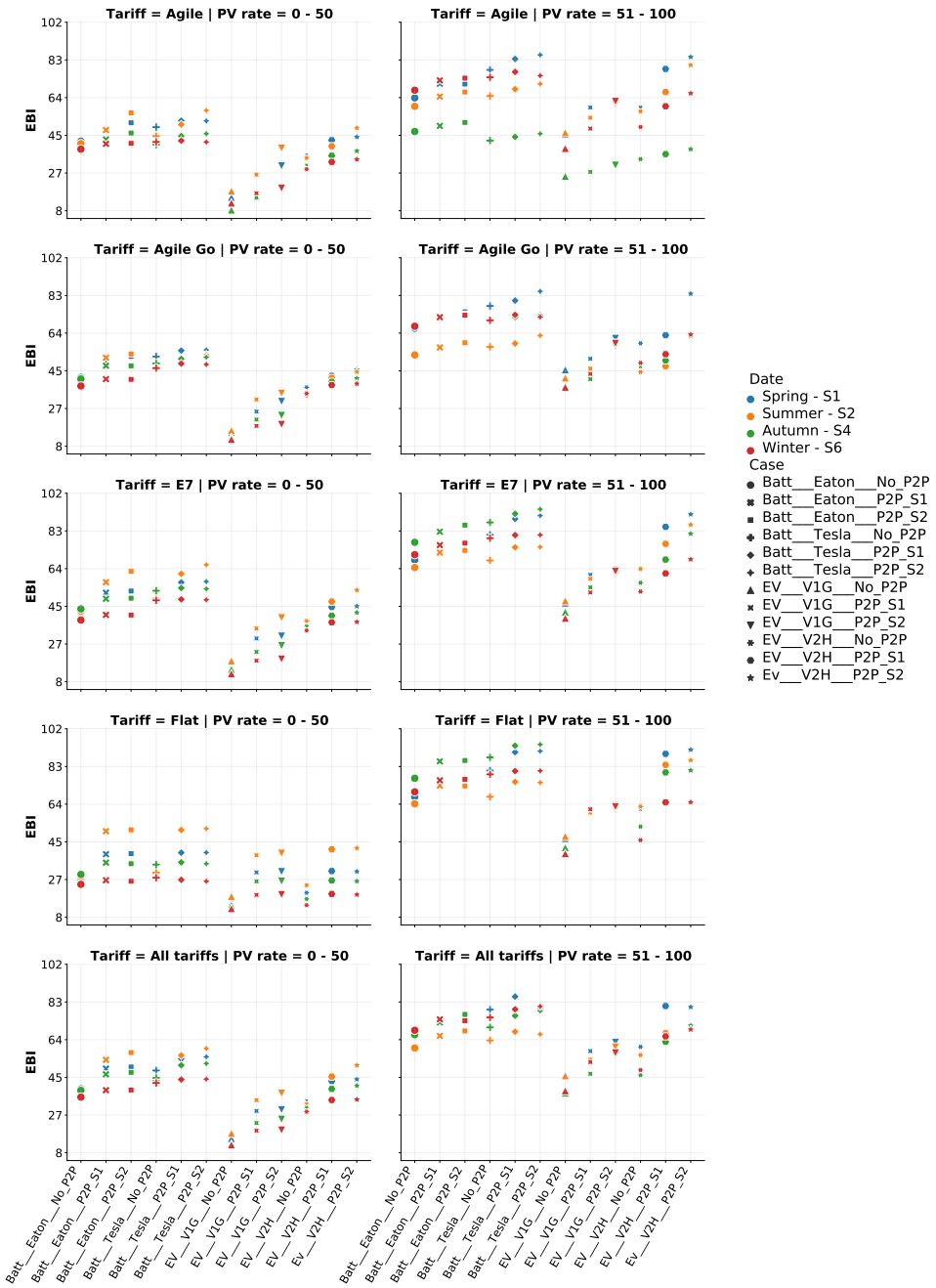

Figure B.1: Comparison of stationary batteries and EVs energy balance index values for the four representative weeks of the year, the five tariff scenarios and all microgrid configurations explored in this chapter. The left column contains the average values from 0% to 50% PV penetration rates and the right column contains the average values from 51% to 100% PV penetration rates.

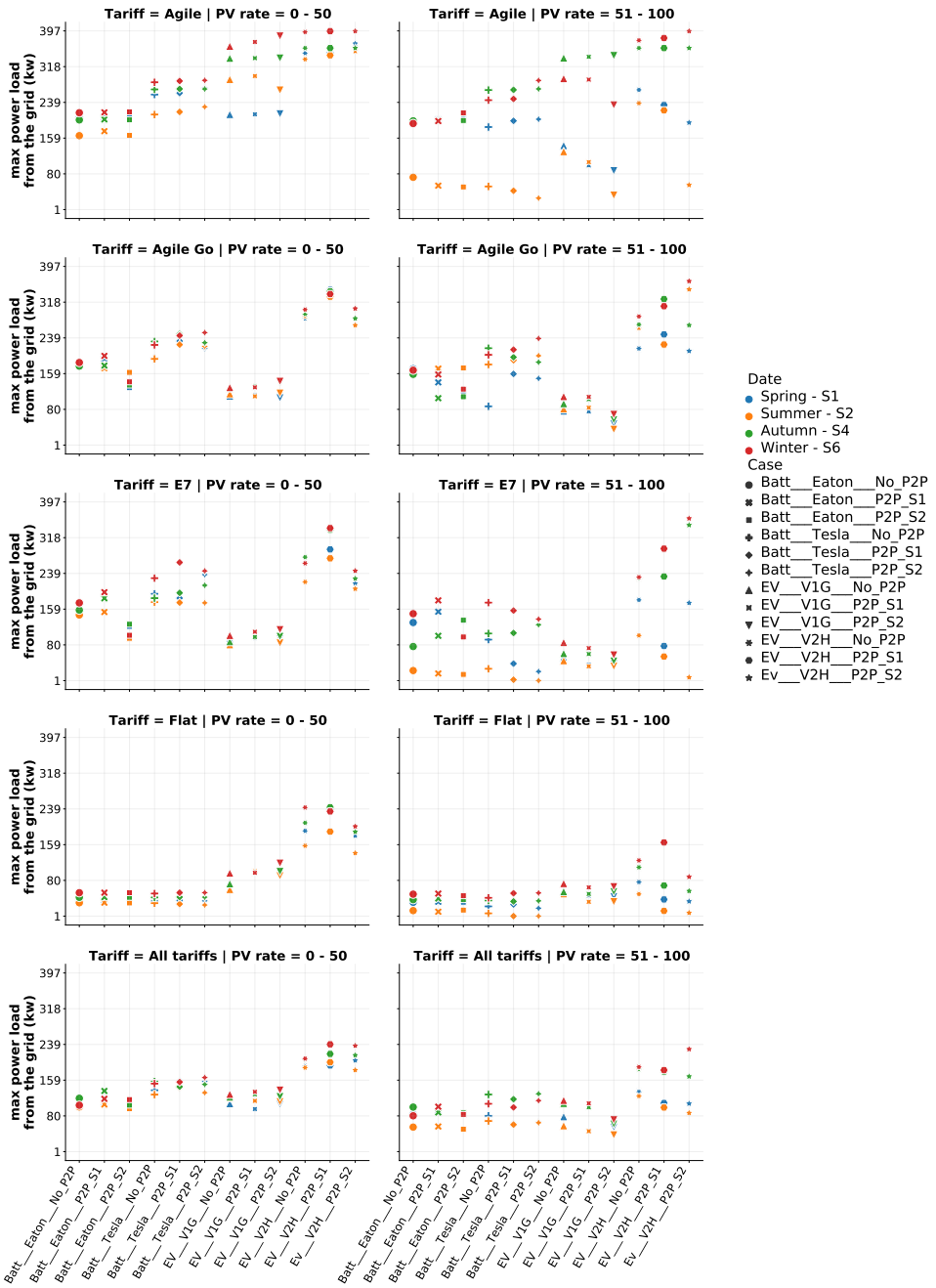

Figure B.2: Comparison of stationary batteries and EVs max power load from the grid for the four representative weeks of the year, the five tariff scenarios and all microgrid configurations explored in this chapter. The left column contains the average values from 0% to 50% PV penetration rates and the right column contains the average values from 51% to 100% PV penetration rates.

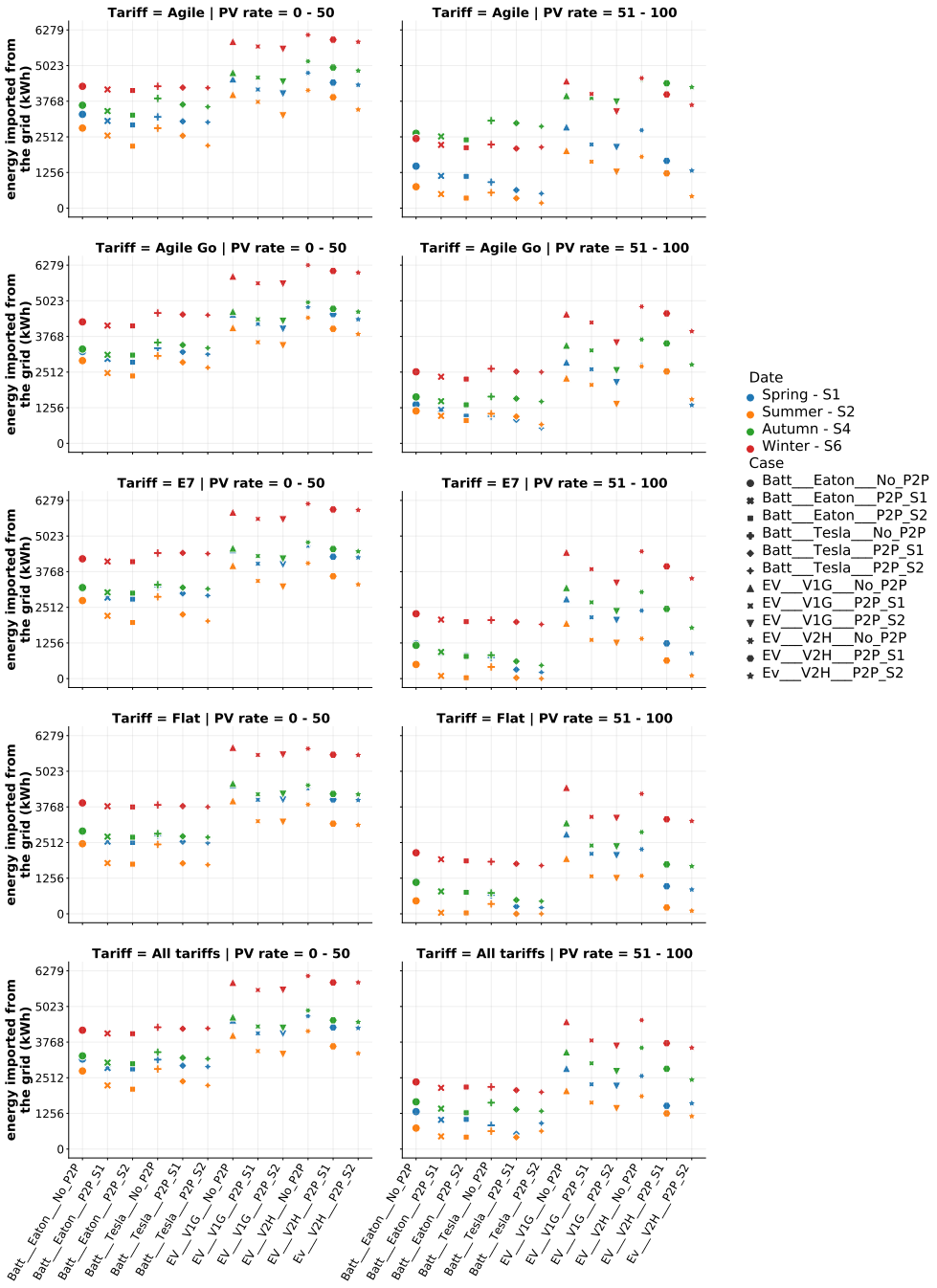

Figure B.3: Comparison of stationary batteries and EVs energy imported from the grid for the four representative weeks of the year, the five tariff scenarios and all microgrid configurations explored in this chapter. The left column contains the average values from 0% to 50% PV penetration rates and the right column contains the average values from 51% to 100% PV penetration rates.

B.1.2 Chapter 6 - Performance metrics supplementary results

Chapter 6 investigated the potential effectiveness of reducing electric bills for households with EVs connected to a microgrid that also provides vehicle-to-grid (V2G) services for short term operation reserve (STOR).

Figure B.4 shows a comparison of the results of EBI, similarly to self-suffiency ratio (SSR), column 1 shows that depending on the tariff there is a slight difference between the weeks of the year for PV penetration rates from 1-50%. In column 2 shows a noticeable difference between each week of the year. Here, the scenarios with P2P perform better than those for which P2P is not allowed. *Setting two* shows a significant advantage compared to *Setting one*. The Summer - S2 week scores the highest in most tariffs and microgrid configurations, but there are some exceptions where Spring - S1 scores the highest, for example, column 2 row 5 (51-100% PV penetration rates and All tariffs scenario).

Figure B.5 shows a comparison of the maximum power load of the grid. The Agile tariff in column 1 shows that the maximum power load in most weeks is over 350 and column 2 shows a similar behaviour, with a few exceptions during Spring - S1 and Summer - S2. Agile Go shows a similar behaviour in column 1 and column 2, where the power load is between 275 and 370 kW in column 1 and column 2 showing the same exceptions during the Spring - S1 and Summer - S2. This is true for all case studies and microgrid configurations, regardless of whether P2P is used and the setting. E7 tariff max power load is between 225 and 350 kW when PV penetration rates are between 0-50% and for higher rates, 51-100%, this tariff shows lower max power loads, Summer - S2 being the lowest in some case studies. The flat tariff shows a more varied range of maximum power load in columns 1 and 2, with values ranging from around 0 kW during Summer - S2 with P2P and *Setting two*, to close to 300 kW during the Autumn - S5 week. The All tariffs scenario has very close max power loads across the six weeks in column 1 and a more significant difference between weeks in column 2. Here, values range from 200 to 330 kW with a lower PV penetration rates and a higher PV penetration rates from 100 kW to over 300 kW. These high peak demand values can be mainly due to EVs taking advantage of low electricity prices during the day to charge enough energy in advance for travel,

supply to the house when prices are high, and / or provide STOR.

Figure B.6 shows a comparison of the energy imported from the grid. Columns 1 and 2 show that weeks with fewer sunlight during the year depend more on drawing energy from the grid. Here, Autumn - S5 and Winter - S6 draw more energy compared to the other weeks, especially the Summer - S2 week which is the one that results in lower total energy imported from the grid. The total energy imported from the grid is between close to 0 kW and up to more than 8,000 kWh depending on the tariff used, showing that traditional tariffs such as E7 and Flat tariffs are less dependent on the grid with high PV penetration rates present. Also, as expected, having higher PV penetration rates significantly reduces the amount of energy imported from the grid; this is further reduced when P2P is present, particularly when *Setting two* is used. However, the energy imported from the grid can also be affected depending on the STOR events and the number of events during the week. As mentioned above, ST_2 is the case study in which more energy is drawn from the grid due to having six events during the week compared to the other scenarios that only have three events during the week and similar PV penetration rates.

B.1.3 Chapter 6 - Short Term Operating Reserve (STOR) Performance supplementary results

Figures B.7 and B.8 show the ST_1 and ST_2 case studies and their STOR events for the six different weeks of the year using using the Agile Go tariff with 90% PV penetration rate, P2P and *Setting two*.

Each of these figures shows the total number of EVs available throughout the week and the number of EVs that provide energy for STOR. In addition, each graph includes the highest number of EVs that provides energy for STOR identified by a horizontal brown dashed line, as well as the lowest number of EVs identified by the horizontal magenta dashed line.

Here, the STOR events were chosen at random at do not happened at the same time for each week, compared to ST_3 and ST_4. In the case of ST_1, there are only three events at random during the week inside of the committed windows of each season that that week cover, as explained in section 6.1.3. Similarly, ST_2 shows STOR events chosen at random, but in this case, there are six STOR events per

week.

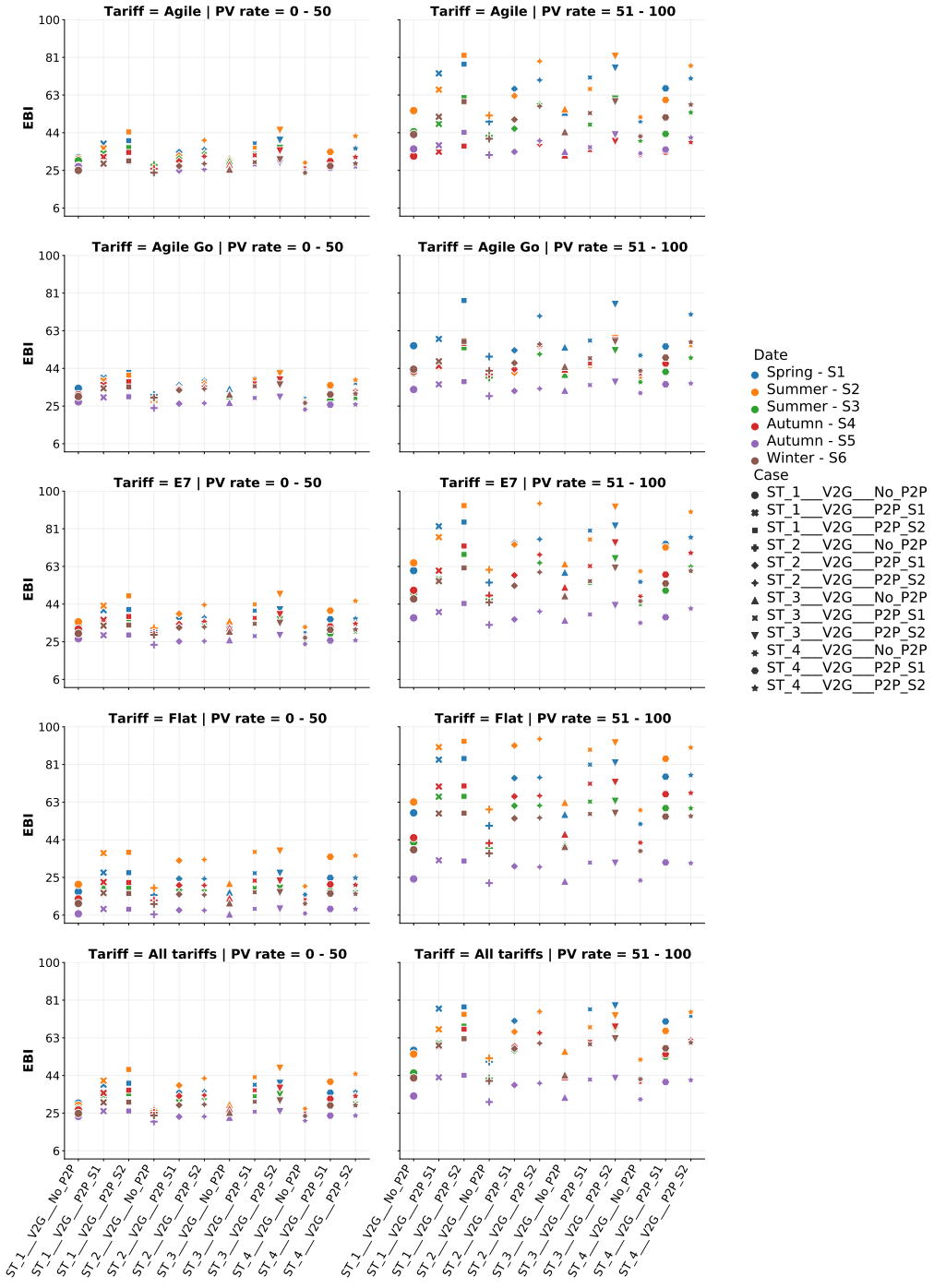

Figure B.4: Comparison of the different short term operation reserve case studies energy balance index values for the six representative weeks of the year, the five tariff scenarios and all microgrid configurations explored in this chapter. The left column contains the average values from 0% to 50% PV penetration rates and the right column contains the average values from 51% to 100% PV penetration rates.

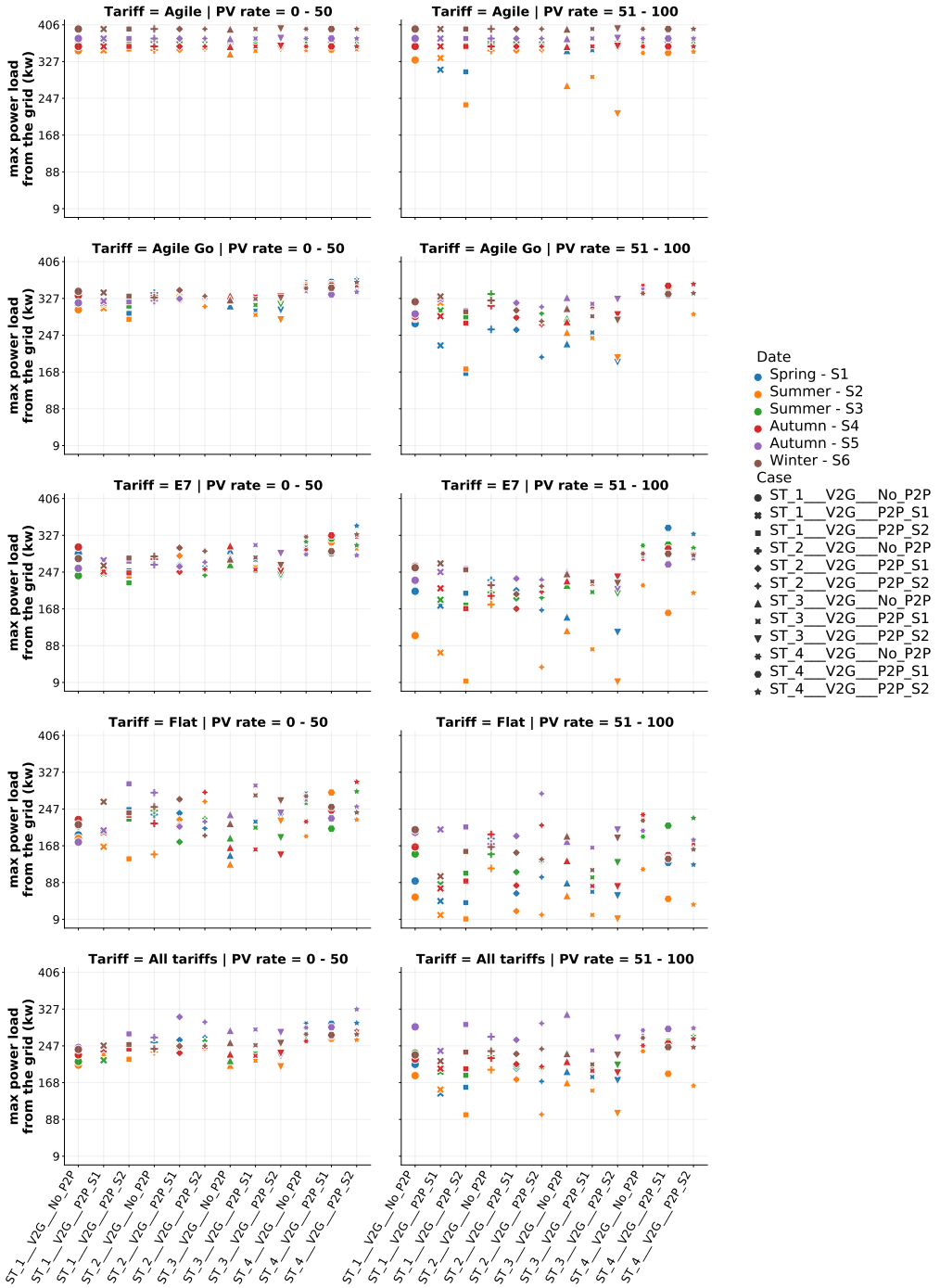

Figure B.5: Max power load from the grid for the six representative weeks of the year, the five tariff scenarios and all microgrid configurations explored in this chapter. The left column contains the average values from 0% to 50% PV penetration rates and the right column contains the average values from 51% to 100% PV penetration rates.

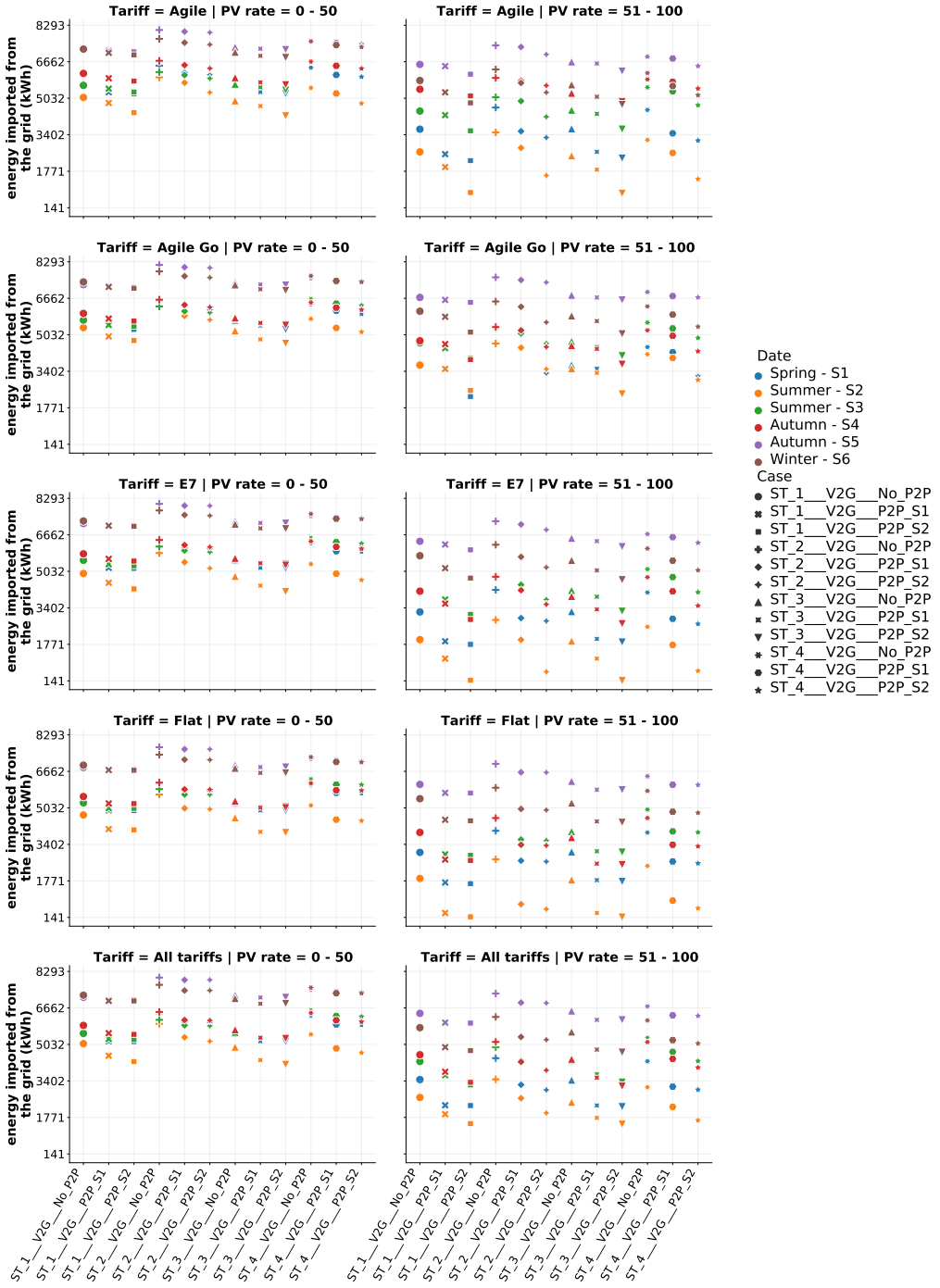

Figure B.6: Energy imported from the grid for the six representative weeks of the year, the five tariff scenarios and all microgrid configurations explored in this chapter. The left column contains the average values from 0% to 50% PV penetration rates and the right column contains the average values from 51% to 100% PV penetration rates.

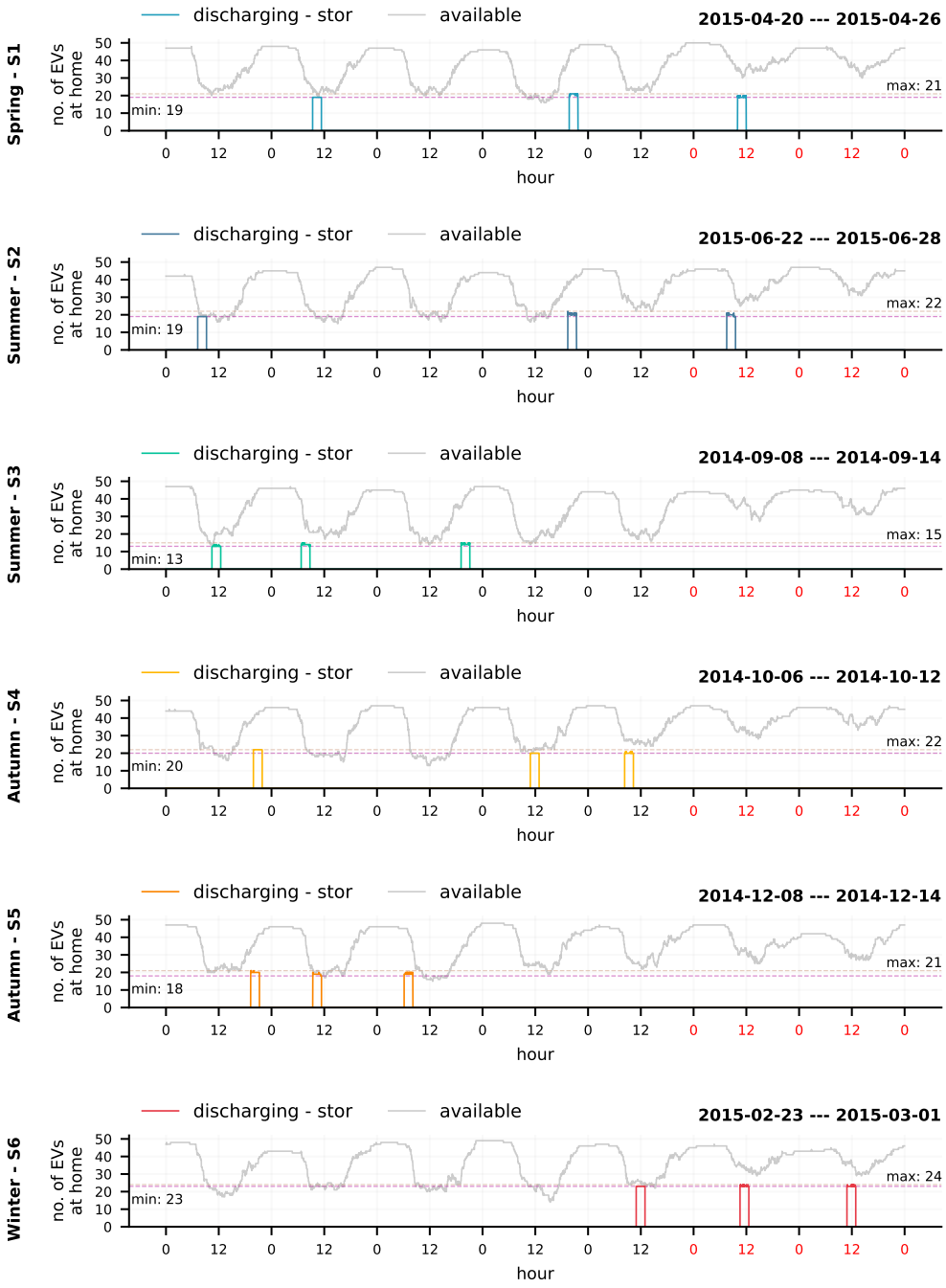

Figure B.7: STOR events in the case study *ST_1* for the six representative weeks of the year using the Agile Go tariff with 90% PV penetration rate, P2P and *Setting two*. Here, the number of EVs available at home during each week and the number of EVs that are discharging energy to provide STOR. Here, the black *X-axis* labels denote data from Monday to Friday, and the red labels, data from Saturday to Sunday.

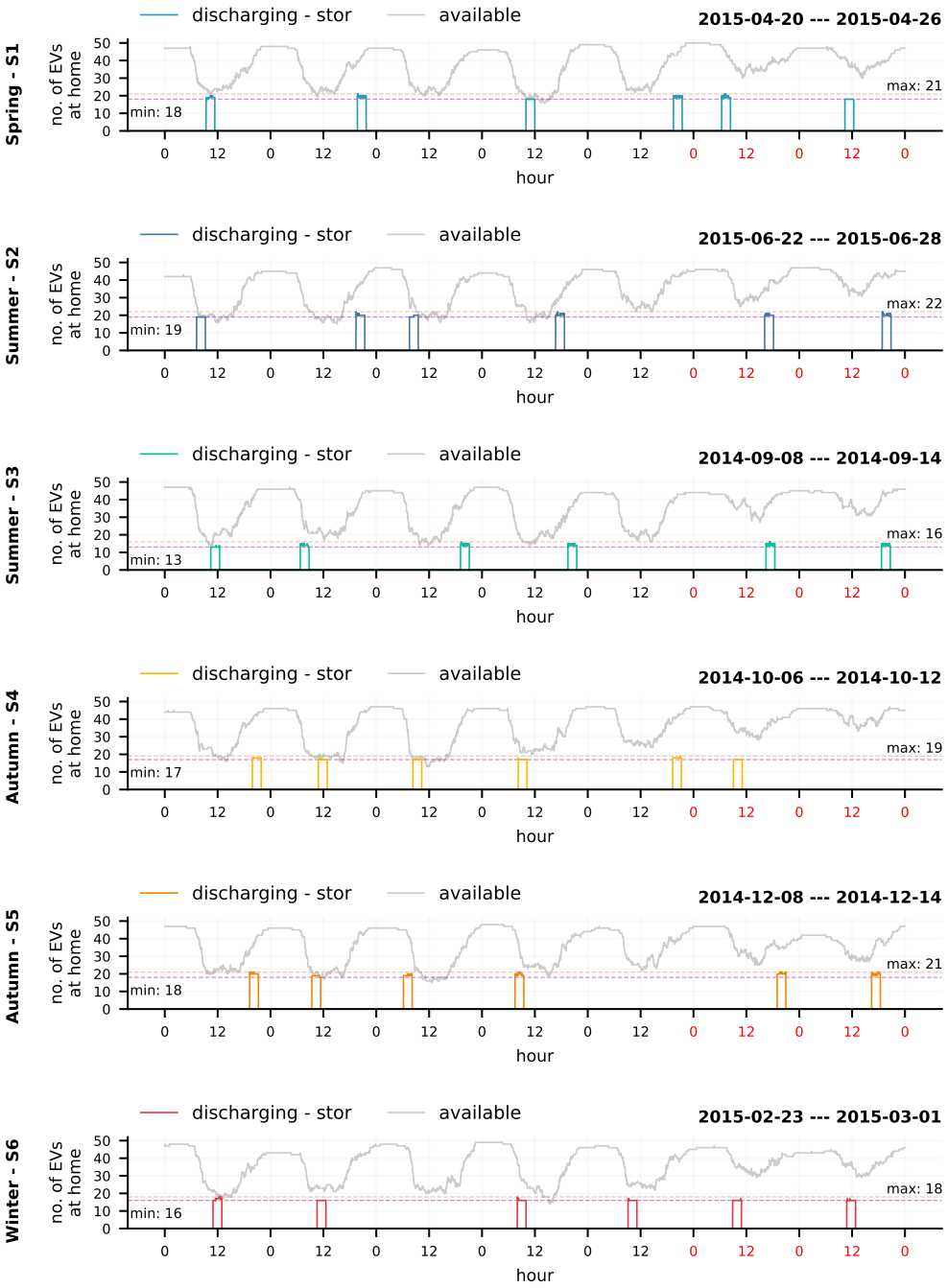

Figure B.8: STOR events in the case study *ST_2* for the six representative weeks of the year using the Agile Go tariff with 90% PV penetration rate, P2P and *Setting two*. Here, the number of EVs available at home during each week and the number of EVs that are discharging energy to provide STOR. Here, the black *X-axis* labels denote data from Monday to Friday, and the red labels, data from Saturday to Sunday.

B.1.4 Chapter 7 - supplementary results

Chapter 7 focused on investigating the maximum amount of state of charge (SOC) that can be held in all EVs within a microgrid during a week for the possibility of providing restoration services (formerly known as black start services). This was done by introducing payment mechanism that aims to encourage EVs to increase the amount of SOC throughout the week.

Figure B.9 shows a comparison of the results of EBI, similar to SSR, in columns 1 and 2, the three case studies show a similar behaviour. Using P2P with *Setting two* produces the best results for both smart charging (V1G) and V2H compared to not using P2P or using *Setting one*. More traditional energy tariffs such as E7 and Flat tariff show almost similar performance with PV penetration rates of 51-100%. All tariffs similar to each other with PV penetration rates of 0-50%. Spring - S1 week returns the highest values with PV penetration rates of 51-100% and Summer - S2 week with PV penetration rates of 0-50%.

The EBI values present the same pattern as the SSR where in all three case studies the results are not too far from each other,with the case study BS_3 being the ones with slightly higher results from the three case studies. This metric tends to peak with lower PV penetration rates due to the way it is calculated, penalising exports as well as imports, and as seen in figures 7.1 and 7.2 that most of the surplus energy is exported to the grid instead of being used for self-consumption or shared among participants within the microgrid.

Figure B.10 shows a comparison of the maximum power load of the grid. Similarly to chapter 6, the Agile tariff shows the highest power loads regardless of PV penetration rates . This can be caused by a sudden reduction in electricity cost that leads all EVs to charge at the same time. Maximum peak loads range from 8 to 404 kW, where higher PV penetration rates tend to reduce this value depending on the tariff used. The lowest peak loads are produced by the Flat tariff followed by the All tariffs scenario. Using V1G shows the highest peak demand compared to suing V2H because energy is consumed from the grid only to provide enough energy for travel purposes.

Having V2H significantly reduces peak demands when having P2P allowed with

Setting two and higher PV penetration rates. In general, higher PV penetration rates reduce peak demand depending on the energy tariff used compared to not allowing P2P. Traditional tariffs manage to reduce the peak to as low as 8 kW with 51-100% PV penetration rates. Spring - S1 and Summer - S2 are the weeks with lower peak demands of the four weeks of the year explored. Furthermore, as with other metrics, users may be inclined to charge as much energy as possible during certain times of the day with low electricity prices to increase the amount of SOC at the end of the week.

Figure B.11 shows a comparison of the energy imported from the grid. Similarly to chapter 6, columns 1 and 2 show that weeks with fewer sunlight during the year depend more on the energy being drawn from the grid. Here, Autumn - S5 and Winter - S6 draw more energy compared to the other weeks, especially the Summer - S2 week, which results in lower total energy imported from the grid. The total imported energy ranges from 104 to 6,200 kWh with the Agile tariff being the one that results in the mos energy imported from the grid and more traditional tariffs with the lowest imported energy from the grid. P2P using the *Setting two* shows the lowest amount of energy imported from the grid in the three case studies when combined with V2H due to the ability to store energy from solar surplus and then use it later during the day. Higher PV penetration rates result in lower dependence of the grid.

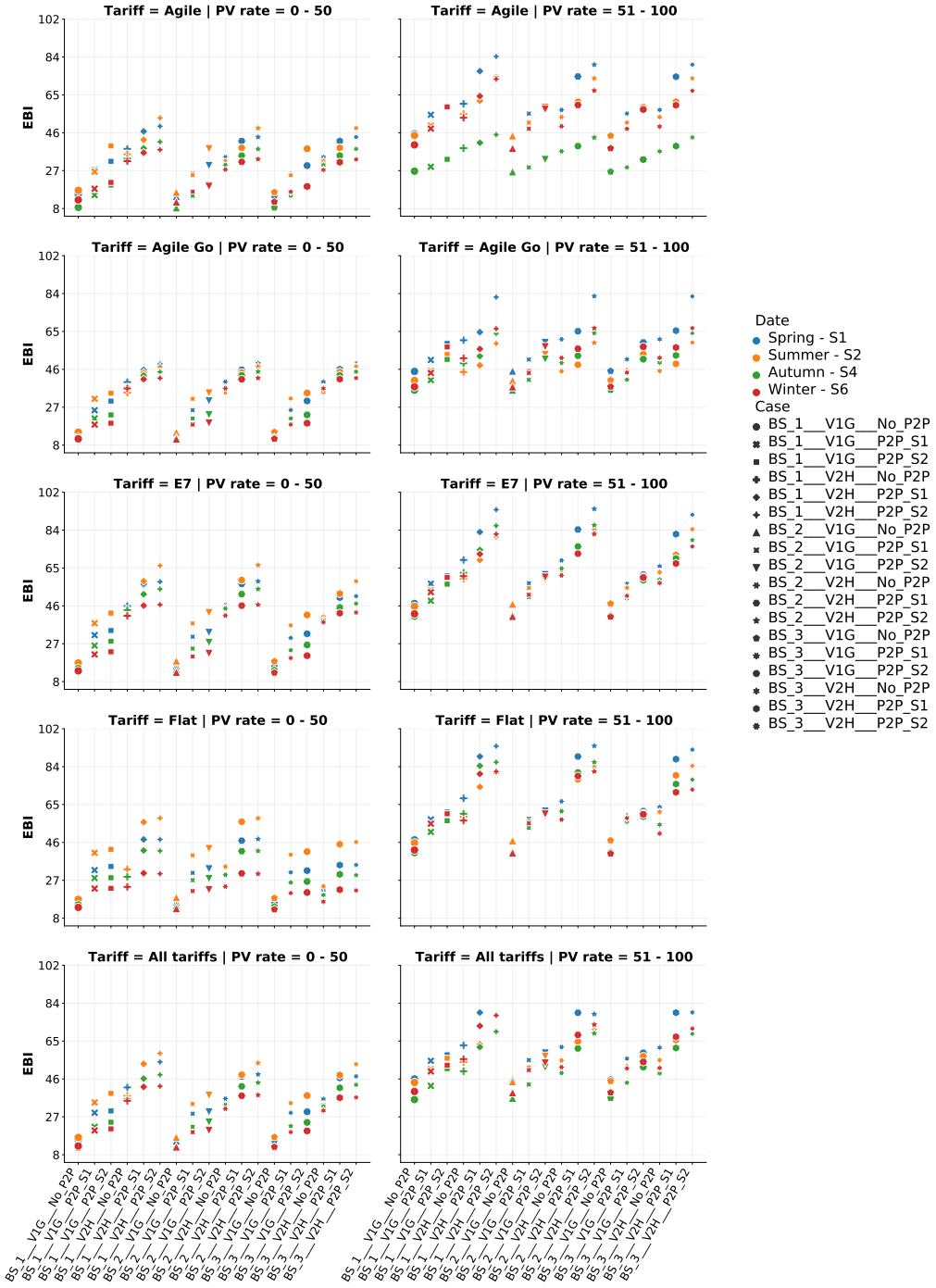

Figure B.9: Energy balance index values for the four representative weeks of the year, the five tariff scenarios and all microgrid configurations explored in this chapter. The left column contains the average values from 0% to 50% PV penetration rates and the right column contains the average values from 51% to 100% PV penetration rates.

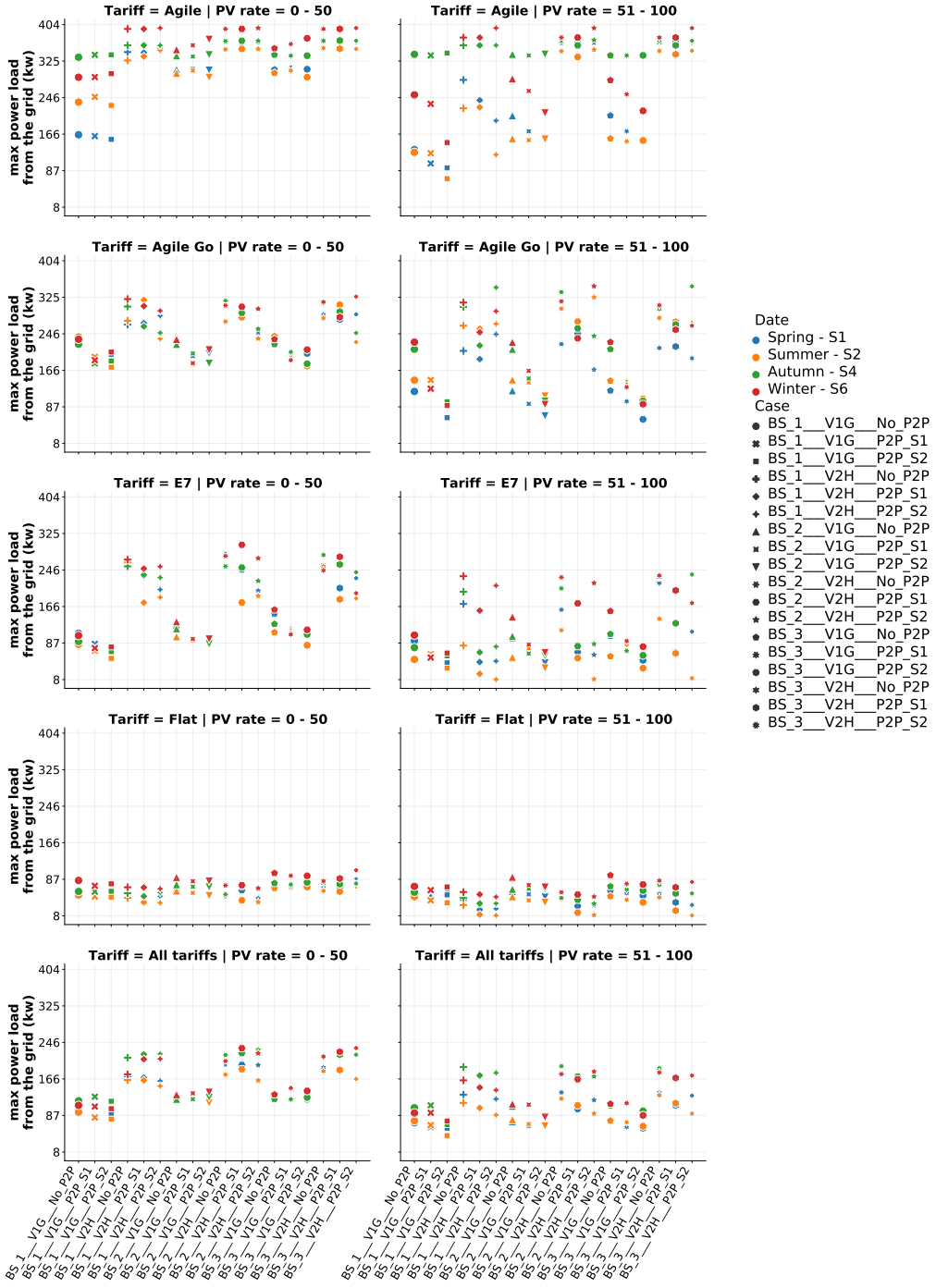

Figure B.10: Max power load from the grid for the four representative weeks of the year, the five tariff scenarios and all microgrid configurations explored in this chapter. The left column contains the average values from 0% to 50% PV penetration rates and the right column contains the average values from 51% to 100% PV penetration rates.

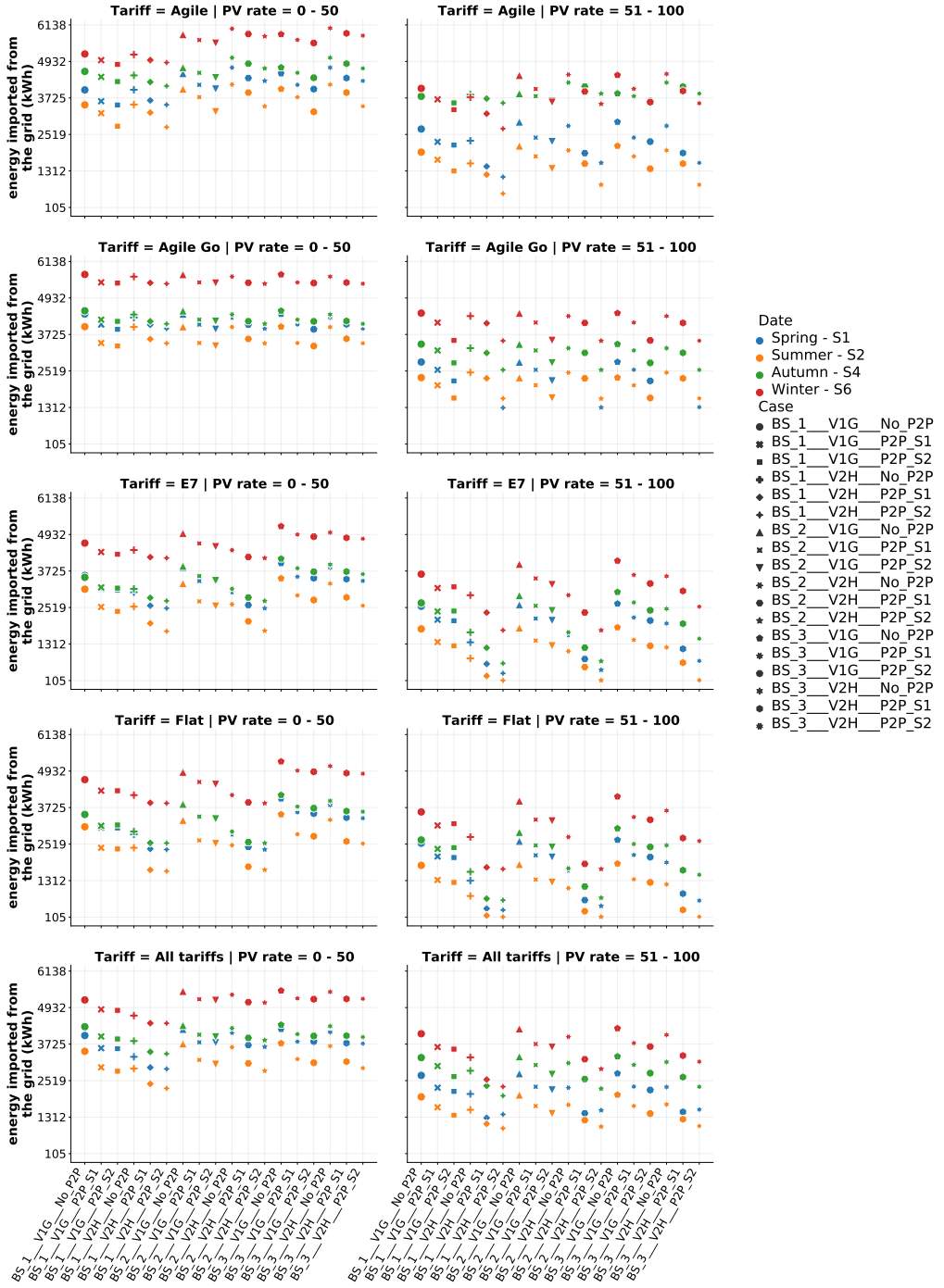

Figure B.11: Energy imported from the grid for the four representative weeks of the year, the five tariff scenarios and all microgrid configurations explored in this chapter. The left column contains the average values from 0% to 50% PV penetration rates and the right column contains the average values from 51% to 100% PV penetration rates.

References

[1] UK Government. Transitioning to zero emission cars and vans: 2035 delivery plan. Technical report, HM Government, 2020.

[2] Department for Business Energy & Industrial Strategy. UK becomes first major economy to pass net zero emissions law - GOV.UK, 2019. URL https://www.gov.uk/government/news/uk-becomes-first-major-economy-to-pass-net-zero-emissions-law.

[3] Department for Business Energy and Industrial Strategy. 2018 UK greenhouse gas emissions, provisional figures. Technical Report March, National Statistics, 2019. URL https://assets.publishing.service.gov.uk/government/uploads/system/uploads/attachment_data/file/790626/2018-provisional-emissions-statistics-report.pdf.

[4] National Grid. Future Energy Scenarios. Technical Report July, National Grid ESO, 2019.

[5] Energy Technologies Institute. Smarter Charging – A UK transition to low carbon vehicles: Summary report. Technical report, EIT, 2019.

[6] John Bates and David Leibling. Spaced Out Perspectives on parking policy. Technical Report July, RAC Foundation, 2012. URL http://www.racfoundation.org/assets/rac_foundation/content/downloadables/spaced_out-bates_leibling-jul12.pdf.

[7] Henrik Lund and Willett Kempton. Integration of renewable energy into the transport and electricity sectors through V2G. *Energy Policy*, 36(9):3578–3587, 2008. ISSN 1898794X. doi: 10.12693/APhysPolA.118.825.

[8] Cenex, Element Energy Limited, Catapult, Nissan, Moixa, Western Power, and National Grid ESO. Vehicle to Grid Britain. Technical report, Element Energy, 2019. URL https://es.catapult.org.uk/report/vehicle-to-grid-britain/.

[9] University of Delaware. Vehicle-to-Grid — V2G, 2011. URL http://www1.udel.edu/V2G/index.html.

[10] Benjamin K. Sovacool, Jonn Axsen, and Willett Kempton. The Future Promise of Vehicle-to-Grid (V2G) Integration: A Sociotechnical Review and Research Agenda. *Annual Review of Environment and Resources*, 42(1): 377–406, 2017. ISSN 1543-5938. doi: 10.1146/annurev-environ-030117-020220. URL http://www.annualreviews.org/doi/10.1146/annurev-environ-030117-020220.

[11] Luke Morgan, Dani Strickland, and Laurence Chittock. Impact of driver behaviour on availability of electric vehicle stored energy for STOR. *Proceedings of the Universities Power Engineering Conference*, pages 1–6, 2014. doi: 10.1109/UPEC.2014.6934595.

[12] National Grid ESO. Black Start from Non-Traditional Generation Technologies. Technical Report June, National Grid ESO, 2019. URL https://www.nationalgrideso.com/document/148201/download.

[13] National Grid ESO. What is the Distributed ReStart project? — National Grid ESO, 2018. URL https://www.nationalgrideso.com/future-energy/projects/distributed-restart.

[14] Ruchi Gupta, Alejandro Pena-Bello, Kai Nino Streicher, Cattia Roduner, David Thöni, Martin Kumar Patel, and David Parra. Spatial analysis of distribution grid capacity and costs to enable massive deployment of PV, electric mobility and electric heating. *Applied Energy*, 287:116504, 4 2021. ISSN 0306-2619. doi: 10.1016/J.APENERGY.2021.116504.

[15] Konstantin Turitsyn, Petr Šulc, Scott Backhaus, and Michael Chertkov. Options for control of reactive power by distributed photovoltaic genera-

tors. *Proceedings of the IEEE*, 99(6):1063–1073, 2011. ISSN 00189219. doi: 10.1109/JPROC.2011.2116750.

[16] Andrew Keane and Mark O'Malley. Optimal allocation of embedded generation on distribution networks. *IEEE Transactions on Power Systems*, 20(3): 1640–1646, 8 2005. ISSN 08858950. doi: 10.1109/TPWRS.2005.852115.

[17] Peter Palensky and Dietmar Dietrich. Demand side management: Demand response, intelligent energy systems, and smart loads. *IEEE Transactions on Industrial Informatics*, 7(3):381–388, 8 2011. ISSN 15513203. doi: 10.1109/TII.2011.2158841.

[18] UK Government. Feed-in Tariff statistics - GOV.UK, 2021. URL https://www.gov.uk/government/collections/feed-in-tariff-statistics.

[19] Matt Reynolds. The Energy Crisis Is Pushing Solar Adoption—for Those Who Can Pay — WIRED UK, 2022. URL https://www.wired.co.uk/article/uk-energy-crisis-solar.

[20] IRENA. Peer-to-peer electricity trading: Innovation Landscape Brief. Technical report, IRENA, 2020. URL www.irena.org.

[21] Jillian Ambrose. UK plans to bring forward ban on fossil fuel vehicles to 2030, 2020. URL https://www.theguardian.com/environment/2020/sep/21/uk-plans-to-bring-forward-ban-on-fossil-fuel-vehicles-to-2030.

[22] Roger Harrabin. Ban on new petrol and diesel cars in UK from 2030 under PM's green plan, 2020. URL https://www.bbc.co.uk/news/science-environment-54981425.

[23] National Grid. Future Energy Scenarios: System Operator. Technical Report July, National Grid, 2018.

[24] Ofgem. Implications of the transition to Electric Vehicles. Technical report, OFGEM, 2018. URL https://www.ofgem.gov.uk/ofgem-publications/136142.

[25] Katarina Knezović, Mattia Marinelli, Antonio Zecchino, Peter Bach Andersen, and Chresten Traeholt. Supporting involvement of electric vehicles in distri-

bution grids: Lowering the barriers for a proactive integration. *Energy*, 134: 458–468, 2017. ISSN 03605442. doi: 10.1016/j.energy.2017.06.075.

[26] Wallbox. The Benefits Of Smart Charging For Planet, Grid & People, 2019. URL https://blog.wallbox.com/en/benefits-of-smart-charging/.

[27] HM Government and Department for Transport. Electric Vehicle Smart Charging. Technical Report July, HM Government, 2019. URL https://www.gov.uk/government/consultations/electric-vehicle-smart-charging.

[28] David Dallinger, Schubert Gerda, and Martin Wietschel. Integration of intermittent renewable power supply using grid-connected vehicles - A 2030 case study for California and Germany. *Applied Energy*, 104:666–682, 2013. ISSN 03062619. doi: 10.1016/j.apenergy.2012.10.065. URL http://dx.doi.org/10.1016/j.apenergy.2012.10.065.

[29] Kristien Clement-Nyns, Edwin Haesen, Student Member, and Johan Driesen. The impact of charging plug-in hybrid electric vehicles on residential distribution transformers. *IEEE Transactions on Power Systems*, 25(1):371–380, 2010.

[30] Kristien Clement-Nyns, Edwin Haesen, and Johan Driesen. The impact of vehicle-to-grid on the distribution grid. *Electric Power Systems Research*, 81 (1):185–192, 2011. ISSN 03787796. doi: 10.1016/j.epsr.2010.08.007. URL http://dx.doi.org/10.1016/j.epsr.2010.08.007.

[31] Francis Mwasilu, Jackson John Justo, Eun-kyung Kyung Kim, Ton Duc Do, and Jin-woo Woo Jung. Electric vehicles and smart grid interaction: A review on vehicle to grid and renewable energy sources integration. *Renewable and Sustainable Energy Reviews*, 34:501–516, 2014. ISSN 13640321. doi: 10.1016/j.rser.2014.03.031. URL http://dx.doi.org/10.1016/j.rser.2014.03.031.

[32] Franziska Schmalfuß, Claudia Mair, Susen Döbelt, Bettina Kämpfe, Ramona Wüstemann, Josef F. Krems, and Andreas Keinath. User responses to a smart charging system in Germany: Battery electric vehicle driver motivation, attitudes and acceptance. *Energy Research and Social Science*, 9:

60–71, 2015. ISSN 22146296. doi: 10.1016/j.erss.2015.08.019. URL http://dx.doi.org/10.1016/j.erss.2015.08.019.

[33] Baocheng Wang, Yafei Hu, Yu Xiao, and Yi Li. An EV charging scheduling mechanism based on price negotiation. *Future Internet*, 10(5), 2018. ISSN 19995903. doi: 10.3390/fi10050040.

[34] Christian Will and Alexander Schuller. Understanding user acceptance factors of electric vehicle smart charging. *Transportation Research Part C: Emerging Technologies*, 71:198–214, 2016. ISSN 0968090X. doi: 10.1016/j.trc.2016.07.006. URL http://dx.doi.org/10.1016/j.trc.2016.07.006.

[35] Kang Miao Tan, Vigna K. Ramachandaramurthy, and Jia Ying Yong. Integration of electric vehicles in smart grid: A review on vehicle to grid technologies and optimization techniques. *Renewable and Sustainable Energy Reviews*, 53:720–732, 2016. ISSN 18790690. doi: 10.1016/j.rser.2015.09.012. URL http://dx.doi.org/10.1016/j.rser.2015.09.012.

[36] Energy.gov. Reducing Pollution with Electric Vehicles — Department of Energy, 2019. URL https://www.energy.gov/eere/electricvehicles/reducing-pollution-electric-vehicles.

[37] Jong Roul Woo, Hyunhong Choi, and Joongha Ahn. Well-to-wheel analysis of greenhouse gas emissions for electric vehicles based on electricity generation mix: A global perspective. *Transportation Research Part D: Transport and Environment*, 51:340–350, 2017. ISSN 13619209. doi: 10.1016/j.trd.2017.01.005. URL http://dx.doi.org/10.1016/j.trd.2017.01.005.

[38] Cenex. Answering the preliminary questions for V2G, 7 2018. URL https://www.cenex.co.uk/app/uploads/2019/10/V2G-Market-Study-FINAL-LCV-Edition-with-QR-Code.pdf.

[39] Benjamin K. Sovacool, Lance Noel, Jonn Axsen, and Willett Kempton. The neglected social dimensions to a vehicle-to-grid (V2G) transition: A critical and systematic review. *Environmental Research Letters*, 13(1), 2018. ISSN 17489326. doi: 10.1088/1748-9326/aa9c6d.

[40] Institution of Mechanical Engineers. Engineering the UK Electricity Gap. Technical report, IEM, 2016.

[41] Destine Gay, Tom Rogers, and Rebekah Shirley. Small island developing states and their suitability for electric vehicles and vehicle-to-grid services. *Utilities Policy*, 55(February):69–78, 2018. ISSN 09571787. doi: 10.1016/j.jup.2018.09.006. URL https://doi.org/10.1016/j.jup.2018.09.006.

[42] Dimitrios Thomas, Olivier Deblecker, and Christos S. Ioakimidis. Optimal operation of an energy management system for a grid-connected smart building considering photovoltaics' uncertainty and stochastic electric vehicles' driving schedule. *Applied Energy*, 210:1188–1206, 2018. ISSN 03062619. doi: 10.1016/j.apenergy.2017.07.035. URL https://doi.org/10.1016/j.apenergy.2017.07.035.

[43] Cenex. Vehicle-to-Grid (V2G) - Cenex, 2019. URL https://www.cenex.co.uk/energy/vehicle-to-grid/.

[44] Yuri R. Rodrigues, A. C. Zambroni de Souza, and P. F. Ribeiro. An inclusive methodology for Plug-in electrical vehicle operation with G2V and V2G in smart microgrid environments. *International Journal of Electrical Power and Energy Systems*, 102(March):312–323, 2018. ISSN 01420615. doi: 10.1016/j.ijepes.2018.04.037. URL https://doi.org/10.1016/j.ijepes.2018.04.037.

[45] Murat Yilmaz and Philip T. Krein. Review of the impact of vehicle-to-grid technologies on distribution systems and utility interfaces, 2013. ISSN 08858993. URL http://arc.aiaa.org/doi/10.2514/6.2002-109.

[46] Mahdi Kiaee, Andrew Cruden, and Suleiman Sharkh. Estimation of cost savings from participation of electric vehicles in vehicle to grid (V2G) schemes. *Journal of Modern Power Systems and Clean Energy*, 3(2):249–258, 2015. ISSN 21965420. doi: 10.1007/s40565-015-0130-2.

[47] Matthieu Dubarry, Arnaud Devie, and Katherine McKenzie. Durability and reliability of electric vehicle batteries under electric utility grid operations: Bidirectional charging impact analysis. *Journal of Power Sources*, 358:39–

49, 2017. ISSN 03787753. doi: 10.1016/j.jpowsour.2017.05.015. URL http://dx.doi.org/10.1016/j.jpowsour.2017.05.015.

[48] Pratt David. V2G found to improve the lifetime of electric vehicle batteries — Current News, 2017. URL https://www.current-news.co.uk/news/v2g-found-to-improve-the-lifetime-of-electric-vehicle-batteries.

[49] Kotub Uddin, Matthieu Dubarry, and Mark B. Glick. The viability of vehicle-to-grid operations from a battery technology and policy perspective. *Energy Policy*, 113(November 2017):342–347, 2018. ISSN 03014215. doi: 10.1016/j.enpol.2017.11.015. URL https://doi.org/10.1016/j.enpol.2017.11.015.

[50] Rodica Loisel, Guzay Pasaoglu, and Christian Thiel. Large-scale deployment of electric vehicles in Germany by 2030: An analysis of grid-to-vehicle and vehicle-to-grid concepts. *Energy Policy*, 65(2014):432–443, 2014. ISSN 03014215. doi: 10.1016/j.enpol.2013.10.029. URL http://dx.doi.org/10.1016/j.enpol.2013.10.029.

[51] Mart Van der Kam and Wilfried Van Sark. Smart charging of electric vehicles with photovoltaic power and vehicle-to-grid technology in a microgrid; a case study. *Applied Energy*, 152:20–30, 2015. ISSN 03062619. doi: 10.1016/j.apenergy.2015.04.092. URL http://dx.doi.org/10.1016/j.apenergy.2015.04.092.

[52] Energy UK. Ancillary services report 2017. Technical Report April, Energy UK, 2017. URL http://www.energy-uk.org.uk/publication.html?task=file.download&id=6138.

[53] National Grid ESO. What is the ESO and what does it do? — National Grid ESO, 2019. URL https://www.nationalgrideso.com/about-us/what-eso-and-what-does-it-do.

[54] National Grid ESO. Demand side response (DSR) — National Grid ESO, 2019. URL https://www.nationalgrideso.com/balancing-services/demand-side-response-dsr.

[55] National Grid ESO. Frequency response services — National Grid ESO, 2019. URL https://www.nationalgrideso.com/balancing-services/frequency-response-services.

[56] National Grid ESO. Reserve services — National Grid ESO, 2019. URL https://www.nationalgrideso.com/balancing-services/reserve-services.

[57] National Grid ESO. System security services — National Grid ESO, 2019. URL https://www.nationalgrideso.com/balancing-services/system-security-services.

[58] Statnett. Fast Frequency Reserves 2018-pilot for raske frekvensreserver. Technical report, Statnett, 2018. URL https://www.statnett.no/contentassets/250c2da4dd564f269ac0679424fdfcfc/evaluering-av-raske-frekvensreserver.pdf.

[59] TheNewMotion. The Future of EV Charging with V2X Technology, 2019. URL https://newmotion.com/the-future-of-ev-charging-with-v2x-technology.

[60] Octopus Energy. Agile Octopus: A consumer-led shift to a low carbon future. Technical report, Octopus Energy, 2018. URL https://octoenergy-production-media.s3.amazonaws.com/documents/agile-report.pdf.

[61] Chunlin Guo and Ching Chuen Chan. Analysis method and utilization mechanism of the overall value of EV charging. *Energy Conversion and Management*, 89:420–426, 2015. ISSN 01968904. doi: 10.1016/j.enconman.2014.10.016. URL http://dx.doi.org/10.1016/j.enconman.2014.10.016.

[62] Michael Wolinetz, Jonn Axsen, Jotham Peters, and Curran Crawford. Simulating the value of electric-vehicle-grid integration using a behaviourally realistic model. *Nature Energy*, 3(2):132–139, 2018. ISSN 20587546. doi: 10.1038/s41560-017-0077-9. URL http://dx.doi.org/10.1038/s41560-017-0077-9.

[63] Jonathan Coignard, Samveg Saxena, Jeffery Greenblatt, and Dai Wang. Clean vehicles as an enabler for a clean electricity grid. *Environmental Research Letters*, 13(5):054031, 2018. ISSN 17489326. doi: 10.1088/1748-9326/aabe97.

[64] Soon-Jeong Lee, Yun-Sik Oh, Bo-Seok Sim, Min-Sung Kim, and Chul-Hwan Kim. Analysis of peak shaving effect of demand power using Vehicle to Grid system in distribution system. *Journal of International Council on Electrical Engineering*, 7(1):198–204, 2017. ISSN 2234-8972. doi: 10.1080/22348972.2017.1324275. URL https://www.tandfonline.com/doi/full/10.1080/22348972.2017.1324275.

[65] Justin D.K. K Bishop, Colin J. Axon, David Bonilla, and David Banister. Estimating the grid payments necessary to compensate additional costs to prospective electric vehicle owners who provide vehicle-to-grid ancillary services. *Energy*, 94:715–727, 2016. ISSN 03605442. doi: 10.1016/j.energy.2015.11.029. URL http://dx.doi.org/10.1016/j.energy.2015.11.029.

[66] Zhenpo Wang and Shuo Wang. Grid power peak shaving and valley filling using vehicle-to-grid systems. *IEEE Transactions on Power Delivery*, 28(3): 1822–1829, 2013. ISSN 08858977. doi: 10.1109/TPWRD.2013.2264497.

[67] B. Aluisio, A. Conserva, M. Dicorato, G. Forte, and M. Trovato. Optimal operation planning of V2G-equipped Microgrid in the presence of EV aggregator. *Electric Power Systems Research*, 152:295–305, 2017. ISSN 03787796. doi: 10.1016/j.epsr.2017.07.015. URL http://dx.doi.org/10.1016/j.epsr.2017.07.015.

[68] Vivek Bhandari, Kaiyang Sun, and Frances Homans. The profitability of vehicle to grid for system participants - A case study from the Electricity Reliability Council of Texas. *Energy*, 153:278–286, 2018. ISSN 03605442. doi: 10.1016/j.energy.2018.04.038. URL https://doi.org/10.1016/j.energy.2018.04.038.

[69] Christos S. Ioakimidis, Dimitrios Thomas, Pawel Rycerski, and Konstantinos N. Genikomsakis. Peak shaving and valley filling of power consumption profile in non-residential buildings using an electric vehicle parking lot. *Energy*, 148:148–158, 2018. ISSN 03605442. doi: 10.1016/j.energy.2018.01.128. URL https://doi.org/10.1016/j.energy.2018.01.128.

[70] Yusuf A. Sha'aban, Augustine Ikpehai, Bamidele Adebisi, and Khaled M. Rabie. Bi-directional coordination of plug-in electric vehicles with economic

model predictive control. *Energies*, 10(10), 2017. ISSN 19961073. doi: 10.3390/en10101507.

[71] Linni Jian, Yanchong Zheng, Xinping Xiao, and C. C. Chan. Optimal scheduling for vehicle-to-grid operation with stochastic connection of plug-in electric vehicles to smart grid. *Applied Energy*, 146:150–161, 2015. ISSN 03062619. doi: 10.1016/j.apenergy.2015.02.030. URL http://dx.doi.org/10.1016/j.apenergy.2015.02.030.

[72] M. A. López, S. Martín, J. A. Aguado, and S. De La Torre. V2G strategies for congestion management in microgrids with high penetration of electric vehicles. *Electric Power Systems Research*, 104:28–34, 2013. ISSN 03787796. doi: 10.1016/j.epsr.2013.06.005. URL http://dx.doi.org/10.1016/j.epsr.2013.06.005.

[73] Chao Peng, Jianxiao Zou, and Lian Lian. Dispatching strategies of electric vehicles participating in frequency regulation on power grid: A review. *Renewable and Sustainable Energy Reviews*, 68(July 2016):147–152, 2017. ISSN 18790690. doi: 10.1016/j.rser.2016.09.133. URL http://dx.doi.org/10.1016/j.rser.2016.09.133.

[74] Sergejus Martinenas, Mattia Marinelli, Peter Bach Andersen, and Chresten Træholt. Implementation and demonstration of grid frequency support by V2G enabled electric vehicle. *Proceedings of the Universities Power Engineering Conference*, 2014. doi: 10.1109/UPEC.2014.6934760.

[75] Yutaka Ota, Haruhito Taniguchi, Jumpei Baba, and Akihiko Yokoyama. Implementation of autonomous distributed V2G to electric vehicle and DC charging system. *Electric Power Systems Research*, 120:177–183, 2015. ISSN 03787796. doi: 10.1016/j.epsr.2014.05.016. URL http://dx.doi.org/10.1016/j.epsr.2014.05.016.

[76] Jasna Tomić and Willett Kempton. Using fleets of electric-drive vehicles for grid support. *Journal of Power Sources*, 168(2):459–468, 2007. ISSN 03787753. doi: 10.1016/j.jpowsour.2007.03.010.

[77] Nicholas DeForest, Jason S. MacDonald, and Douglas R. Black. Day ahead optimization of an electric vehicle fleet providing ancillary services in the Los Angeles Air Force Base vehicle-to-grid demonstration. *Applied Energy*, 210: 987–1001, 2018. ISSN 03062619. doi: 10.1016/j.apenergy.2017.07.069. URL https://doi.org/10.1016/j.apenergy.2017.07.069.

[78] Albert Y.S. Lam, Ka Cheong Leung, and Victor O.K. Li. Capacity estimation for vehicle-to-grid frequency regulation services with smart charging mechanism. *IEEE Transactions on Smart Grid*, 7(1):156–166, 2016. ISSN 19493053. doi: 10.1109/TSG.2015.2436901.

[79] Tobias Brandt, Sebastian Wagner, and Dirk Neumann. Evaluating a business model for vehicle-grid integration: Evidence from Germany. *Transportation Research Part D: Transport and Environment*, 50:488–504, 2017. ISSN 13619209. doi: 10.1016/j.trd.2016.11.017. URL http://dx.doi.org/10.1016/j.trd.2016.11.017.

[80] Kotub Uddin, Tim Jackson, Widanalage D. Widanage, Gael Chouchelamane, Paul A. Jennings, and James Marco. On the possibility of extending the lifetime of lithium-ion batteries through optimal V2G facilitated by an integrated vehicle and smart-grid system. *Energy*, 133:710–722, 2017. ISSN 03605442. doi: 10.1016/j.energy.2017.04.116. URL http://dx.doi.org/10.1016/j.energy.2017.04.116.

[81] Dai Wang, Jonathan Coignard, Teng Zeng, Cong Zhang, and Samveg Saxena. Quantifying electric vehicle battery degradation from driving vs. vehicle-to-grid services. *Journal of Power Sources*, 332:193–203, 2016. ISSN 03787753. doi: 10.1016/j.jpowsour.2016.09.116. URL http://dx.doi.org/10.1016/j.jpowsour.2016.09.116.

[82] Hui Liu, Junjian Qi, Jianhui Wang, Peijie Li, Canbing Li, and Hua Wei. EV Dispatch Control for Supplementary Frequency Regulation Considering the Expectation of EV Owners. *IEEE Transactions on Smart Grid*, 9(4):3763–3772, 2018. ISSN 19493053. doi: 10.1109/TSG.2016.2641481.

[83] Siyamak Sarabi, Arnaud Davigny, Vincent Courtecuisse, Yann Riffonneau, and Benoît Robyns. Potential of vehicle-to-grid ancillary services considering the uncertainties in plug-in electric vehicle availability and service/localization limitations in distribution grids. *Applied Energy*, 171:523–540, 2016. ISSN 03062619. doi: 10.1016/j.apenergy.2016.03.064. URL http://dx.doi.org/10.1016/j.apenergy.2016.03.064.

[84] Jian Meng, Yunfei Mu, Hongjie Jia, Jianzhong Wu, Xiaodan Yu, and Bo Qu. Dynamic frequency response from electric vehicles considering travelling behavior in the Great Britain power system. *Applied Energy*, 162:966–979, 2016. ISSN 03062619. doi: 10.1016/j.apenergy.2015.10.159.

[85] Jonathan Donadee and Marija Ilić. Stochastic co-optimization of charging and frequency regulation by electric vehicles. *2012 North American Power Symposium, NAPS 2012*, 2012. doi: 10.1109/NAPS.2012.6336373.

[86] Rebecca Gough, Charles Dickerson, Paul Rowley, and Chris Walsh. Vehicle-to-grid feasibility: A techno-economic analysis of EV-based energy storage. *Applied Energy*, 192:12–23, 2017. ISSN 03062619. doi: 10.1016/j.apenergy.2017.01.102. URL http://dx.doi.org/10.1016/j.apenergy.2017.01.102.

[87] Justin D.K. Bishop, Colin J. Axon, David Bonilla, Martino Tran, David Banister, and Malcolm D. McCulloch. Evaluating the impact of V2G services on the degradation of batteries in PHEV and EV. *Applied Energy*, 111: 206–218, 2013. ISSN 03062619. doi: 10.1016/j.apenergy.2013.04.094. URL http://dx.doi.org/10.1016/j.apenergy.2013.04.094.

[88] National Grid ESO. System security services — National Grid ESO, 2022. URL https://www.nationalgrideso.com/balancing-services/system-security-services.

[89] National Grid ESO. Future Energy Scenarios - 2020. Technical report, National Grid ESO, 7 2020.

[90] Yang Song, Pengcheng Li, Yuanliang Zhao, and Shuai Lu. Design and Integration of the Bi-directional Electric Vehicle Charger into the Microgrid as Emergency Power Supply. *2018 International Power Electronics Conference, IPEC-Niigata - ECCE Asia 2018*, pages 3698–3704, 10 2018. doi: 10.23919/IPEC.2018.8507385.

[91] Junbo Sun, Da Xie, Yucheng Lou, Minxia Yang, and Yu Zhang. Black-start scheme based on EV's intelligent integrated station. *POWERCON 2014 - 2014 International Conference on Power System Technology: Towards Green, Efficient and Smart Power System, Proceedings*, pages 3118–3123, 12 2014. doi: 10.1109/POWERCON.2014.6993609.

[92] Chao Long, Jianzhong Wu, Chenghua Zhang, Lee Thomas, Meng Cheng, and Nick Jenkins. Peer-to-peer energy trading in a community microgrid. *IEEE Power and Energy Society General Meeting*, 2018-January:1–5, 1 2018. ISSN 19449933. doi: 10.1109/PESGM.2017.8274546.

[93] Deloitte. Peer to peer energy trading — Future of Energy — Deloitte Netherlands, 2021. URL https://www2.deloitte.com/nl/nl/pages/energy-resources-industrials/articles/peer-to-peer-energy-trading.html.

[94] EDF Energy. Peer-to-peer-trading — R&D UK Blog — EDF, 2018. URL https://www.edfenergy.com/energywise/research-development-peer-to-peer-trading.

[95] Community Energy England. Peer to peer local energy trading — Community Energy England, 2020. URL https://communityenergyengland.org/how-to-pages/peer-to-peer-local-energy-trading.

[96] Chao Long, Yue Zhou, and Jianzhong Wu. A game theoretic approach for peer to peer energy trading. *Energy Procedia*, 159:454–459, 2 2019. ISSN 1876-6102. doi: 10.1016/J.EGYPRO.2018.12.075.

[97] David Vangulick, Bertrand Cornelusse, and Damien Ernst. Blockchain for Peer-to-Peer Energy Exchanges: Design and Recommendations. In *2018 Power Systems Computation Conference (PSCC)*, pages 1–7. IEEE, 6 2018.

ISBN 978-1-910963-10-4. doi: 10.23919/PSCC.2018.8443042. URL https://ieeexplore.ieee.org/document/8443042/.

[98] Thomas Morstyn and Malcolm D. McCulloch. Multiclass Energy Management for Peer-to-Peer Energy Trading Driven by Prosumer Preferences. *IEEE Transactions on Power Systems*, 34(5):4005–4014, 9 2019. ISSN 0885-8950. doi: 10.1109/TPWRS.2018.2834472. URL https://ieeexplore.ieee.org/document/8356100/.

[99] Zhenwei Guo, Pierre Pinson, Shibo Chen, Qinmin Yang, and Zaiyue Yang. Chance-Constrained Peer-to-Peer Joint Energy and Reserve Market Considering Renewable Generation Uncertainty. *IEEE Transactions on Smart Grid*, 12 (1):798–809, 1 2021. ISSN 1949-3053. doi: 10.1109/TSG.2020.3019603. URL https://ieeexplore.ieee.org/document/9178314/.

[100] Ni Wang, Ziyi Liu, Petra Heijnen, and Martijn Warnier. A peer-to-peer market mechanism incorporating multi-energy coupling and cooperative behaviors. *Applied Energy*, 311:118572, 4 2022. ISSN 0306-2619. doi: 10.1016/J.APENERGY.2022.118572.

[101] Jongbaek An, Minhyun Lee, Seungkeun Yeom, and Taehoon Hong. Determining the Peer-to-Peer electricity trading price and strategy for energy prosumers and consumers within a microgrid. *Applied Energy*, 261:114335, 3 2020. ISSN 0306-2619. doi: 10.1016/J.APENERGY.2019.114335.

[102] Nian Liu, Xinghuo Yu, Cheng Wang, Chaojie Li, Li Ma, and Jinyong Lei. Energy-Sharing Model With Price-Based Demand Response for Microgrids of Peer-to-Peer Prosumers. *IEEE Transactions on Power Systems*, 32(5):3569–3583, 9 2017. ISSN 0885-8950. doi: 10.1109/TPWRS.2017.2649558. URL http://ieeexplore.ieee.org/document/7809095/.

[103] Wayes Tushar, Tapan Kumar Saha, Chau Yuen, Thomas Morstyn, Malcolm D. McCulloch, H. Vincent Poor, and Kristin L. Wood. A motivational game-theoretic approach for peer-to-peer energy trading in the smart grid. *Applied Energy*, 243:10–20, 6 2019. ISSN 03062619. doi: 10.1016/j.apenergy.2019.03.111.

[104] Stefan Englberger, Archie C. Chapman, Wayes Tushar, Tariq Almomani, Stephen Snow, Rolf Witzmann, Andreas Jossen, and Holger Hesse. Evaluating the interdependency between peer-to-peer networks and energy storages: A techno-economic proof for prosumers. *Advances in Applied Energy*, 3:100059, 8 2021. ISSN 2666-7924. doi: 10.1016/J.ADAPEN.2021.100059.

[105] Timothy D. Hutty, Alejandro Pena-Bello, Siyuan Dong, David Parra, Rachael Rothman, and Solomon Brown. Peer-to-peer electricity trading as an enabler of increased PV and EV ownership. *Energy Conversion and Management*, 245: 114634, 10 2021. ISSN 0196-8904. doi: 10.1016/J.ENCONMAN.2021.114634.

[106] IBM Cloud Education. What is Machine Learning? - United Kingdom — IBM, 2020. URL https://www.ibm.com/uk-en/cloud/learn/machine-learning.

[107] Chris Wright. UK's drivers-first approach to vehicle-to-grid — Current News, 2018. URL https://www.current-news.co.uk/blogs/uks-drivers-first-approach-to-vehicle-to-grid.

[108] Rob Shipman, Rebecca Roberts, Julie Waldron, Sophie Naylor, James Pinchin, Lucelia Rodrigues, and Mark Gillott. We got the power: Predicting available capacity for vehicle-to-grid services using a deep recurrent neural network. *Energy*, 221:119813, 4 2021. ISSN 03605442. doi: 10.1016/j.energy.2021.119813. URL https://linkinghub.elsevier.com/retrieve/pii/S0360544221000621.

[109] Rob Shipman, Julie Waldron, Sophie Naylor, James Pinchin, Lucelia Rodrigues, and Mark Gillott. Where Will You Park? Predicting Vehicle Locations for Vehicle-to-Grid. *Energies 2020, Vol. 13, Page 1933*, 13(8):1933, 4 2020. ISSN 1996-1073. doi: 10.3390/EN13081933. URL https://www.mdpi.com/1996-1073/13/8/1933/htmhttps://www.mdpi.com/1996-1073/13/8/1933.

[110] H. Selcuk Nogay. Estimating the aggregated available capacity for vehicle to grid services using deep learning and Nonlinear Autoregressive Neural Network. *Sustainable Energy, Grids and Networks*, 29:100590, 3 2022. ISSN 23524677. doi: 10.1016/j.segan.2021.100590. URL https://linkinghub.elsevier.com/retrieve/pii/S2352467721001491.

[111] Connor Scott, Mominul Ahsan, and Alhussein Albarbar. Machine Learning Based Vehicle to Grid Strategy for Improving the Energy Performance of Public Buildings. *Sustainability 2021, Vol. 13, Page 4003*, 13(7):4003, 4 2021. ISSN 2071-1050. doi: 10.3390/SU13074003. URL https://www.mdpi.com/2071-1050/13/7/4003/htmhttps://www.mdpi.com/2071-1050/13/7/4003.

[112] Oliver Frendo, Nadine Gaertner, and Heiner Stuckenschmidt. Improving Smart Charging Prioritization by Predicting Electric Vehicle Departure Time. *IEEE Transactions on Intelligent Transportation Systems*, 22(10):6646–6653, 10 2021. ISSN 1524-9050. doi: 10.1109/TITS.2020.2988648. URL https://ieeexplore.ieee.org/document/9082829/.

[113] Penelope K. Jones, Ulrich Stimming, and Alpha A. Lee. Impedance-based forecasting of lithium-ion battery performance amid uneven usage. *Nature Communications*, 13(1), 8 2022. ISSN 20411723. doi: 10.1038/S41467-022-32422-W. URL https://www.cam.ac.uk/research/news/machine-learning-algorithm-predicts-how-to-get-the-most-out-of-electric-vehicle-batteries.

[114] Yu Wei Chung, Behnam Khaki, Tianyi Li, Chicheng Chu, and Rajit Gadh. Ensemble machine learning-based algorithm for electric vehicle user behavior prediction. *Applied Energy*, 254(April):113732, 2019. ISSN 03062619. doi: 10.1016/j.apenergy.2019.113732. URL https://doi.org/10.1016/j.apenergy.2019.113732.

[115] Yitong Shang, Hang Yu, Ziyun Shao, and Linni Jian. ISCP-Data: A Vehicle-to-grid Dataset For Commercial Center And Its Machine Learning Application. In *2021 IEEE 5th Conference on Energy Internet and Energy System Integration (EI2)*, pages 3246–3250. IEEE, 10 2021. ISBN 978-1-6654-3425-6. doi: 10.1109/EI252483.2021.9713203. URL https://ieeexplore.ieee.org/document/9713203/.

[116] Department for Business Energy & Industrial Strategy. Ensuring security of electricity supplies for winter 2022 to 2023 - GOV.UK, 2022. URL https://www.gov.uk/government/publications/ensuring-security-of-electricity-supplies-for-winter-2022-to-2023.

[117] Department for Business Energy & Industrial Strategy. Energy Emergencies Executive Committee: Interim Report. Technical report, UK Government, 2019. URL https://assets.publishing.service.gov.uk/government/uploads/system/uploads/attachment_data/file/836626/20191003_E3C_Interim_Report_into_GB_Power_Disruption.pdf.

[118] Financial Times. National Grid electricity blackout report points to failure at wind farm — Financial Times, 2019. URL https://www.ft.com/content/8b738eac-c024-11e9-89e2-41e555e96722.

[119] National Grid ESO. Black Start — National Grid ESO, 2019. URL https://www.nationalgrideso.com/balancing-services/system-security-services/black-start?technical-requirements.

[120] Entrepeneur Europe. How Machine Learning Is Changing the World - and Your Everyday Life, 2018. URL https://www.entrepreneur.com/article/312016.

[121] Department for Transport. National Travel Survey: 2020 - GOV.UK, 2020. URL https://www.gov.uk/government/statistics/national-travel-survey-2020/national-travel-survey-2020.

[122] Google. Generalization — Machine Learning — Google Developers, 2022. URL https://developers.google.com/machine-learning/crash-course/generalization/video-lecture.

[123] Department for Transport. National Travel Survey - GOV.UK, 2021. URL https://www.gov.uk/government/collections/national-travel-survey-statistics.

[124] Department for Transport. National Travel Survey 2021: Quality report - GOV.UK, 2022. URL https://www.gov.uk/government/statistics/national-travel-survey-2021/national-travel-survey-2021-quality-report.

[125] Python Software Foundation. Welcome to Python.org, 1991. URL https://www.python.org/.

[126] Pandas Dev Team. pandas - Python Data Analysis Library, 2010. URL https://pandas.pydata.org/.

[127] Charles R. Harris, K. Jarrod Millman, Stéfan J. Van der Walt, Ralf Gommers, Pauli Virtanen, David Cournapeau, Eric Wieser, Julian Taylor, Sebastian Berg, Nathaniel J. Smith, Robert Kern, Matti Picus, Stephan Hoyer, Marten H. Van Kerkwijk, Matthew Brett, Allan Haldane, Jaime Fernández del Río, Mark Wiebe, Pearu Peterson, Pierre Gérard-Marchant, Kevin Sheppard, Tyler Reddy, Warren Weckesser, Hameer Abbasi, Christoph Gohlke, and Travis E. Oliphant. Array programming with NumPy. *Nature 2020 585:7825*, 585(7825):357–362, 9 2020. ISSN 1476-4687. doi: 10.1038/s41586-020-2649-2. URL https://www.nature.com/articles/s41586-020-2649-2.

[128] Fabian Pedregosa, Gaël Varoquaux, Alexandre Gramfort, Vincent Michel, Bertrand Thirion, Olivier Grisel, Mathieu Blondel, Andreas Müller, Joel Nothman, Gilles Louppe, Peter Prettenhofer, Ron Weiss, Vincent Dubourg, Jake Vanderplas, Alexandre Passos, David Cournapeau, Matthieu Brucher, Matthieu Perrot, and Édouard Duchesnay. Scikit-learn: Machine Learning in Python. *Journal of Machine Learning Research*, 1 2012. URL https://arxiv.org/abs/1201.0490.

[129] Guolin Ke, Qi Meng, Thomas Finley, Taifeng Wang, Wei Chen, Weidong Ma, Qiwei Ye, and Tie Yan Liu. LightGBM: A highly efficient gradient boosting decision tree. *Advances in Neural Information Processing Systems*, 2017-Decem (Nips):3147–3155, 2017. ISSN 10495258.

[130] Aurelien Geron. *Hands-on Machine Learning with Scikit-Learn, Keras, and TensorFlow: Concepts, Tools, and Techniques to Build Intelligent Systems*. O'Reilly, 2nd edition, 2019.

[131] Microsoft. Welcome to LightGBM's documentation! — LightGBM 3.3.2 documentation, 2017. URL https://lightgbm.readthedocs.io/en/v3.3.2/index.html.

[132] Microsoft. LightGBM/Features.rst at master · microsoft/LightGBM, 2017. URL https://github.com/Microsoft/LightGBM/blob/master/docs/Features.rst#references.

[133] IBM Cloud Education. What is Overfitting? — IBM, 2020. URL https://www.ibm.com/topics/overfitting.

[134] Shachar Kaufman, Saharon Rosset, and Claudia Perlich. Leakage in data mining: Formulation, detection, and avoidance. *Proceedings of the ACM SIGKDD International Conference on Knowledge Discovery and Data Mining*, pages 556–563, 2011. doi: 10.1145/2020408.2020496. URL https://dl.acm.org/doi/10.1145/2020408.2020496.

[135] Scikit-learn Developer team. sklearn.preprocessing.MinMaxScaler — scikit-learn 1.1.2 documentation, 2021. URL https://scikit-learn.org/stable/modules/generated/sklearn.preprocessing.MinMaxScaler.html.

[136] Google Developers. Classification: Precision and Recall — Machine Learning — Google Developers, 7 2022. URL https://developers.google.com/machine-learning/crash-course/classification/precision-and-recall.

[137] Google Developers. Generalization — Machine Learning — Google Developers, 7 2022. URL https://developers.google.com/machine-learning/crash-course/generalization/video-lecture.

[138] Scikit-Learn Developers. sklearn.model_selection.RandomizedSearchCV — scikit-learn 1.1.2 documentation, 2022. URL https://scikit-learn.org/stable/modules/generated/sklearn.model_selection.RandomizedSearchCV.html.

[139] EA Technology. My Electric Avenue Summary Report, 2015. URL https://www.eatechnology.com/projects/my-electric-avenue/.

[140] Edward Barbour and Marta C. González. Projecting battery adoption in the prosumer era. *Applied Energy*, 215(August 2017):356–370, 2018. ISSN 03062619. doi: 10.1016/j.apenergy.2018.01.056. URL https://doi.org/10.1016/j.apenergy.2018.01.056.

[141] UK Power Networks. Smart Meter Energy Consumption Data in London Households - London Datastore, 2015. URL https://data.london.gov.uk/dataset/smartmeter-energy-use-data-in-london-households.

[142] UK Government. Energy consumption in the UK 2020 - GOV.UK, 2020. URL https://www.gov.uk/government/statistics/energy-consumption-in-the-uk-2020.

[143] C. Topping. Average Electricity Usage in the UK: How Many kWh Does Your Home Use? — OVO Energy, 2021. URL https://www.ovoenergy.com/guides/energy-guides/how-much-electricity-does-a-home-use.

[144] UK Power Networks. Photovoltaic Solar Panel Energy Generation data - London Datastore, 2017. URL https://data.london.gov.uk/dataset/photovoltaic--pv--solar-panel-energy-generation-data.

[145] Octopus Energy. Agile Octopus — Octopus Energy, 2019. URL https://octopus.energy/agile/.

[146] Octopus Energy. Outgoing Octopus — Octopus Energy, 2021. URL https://octopus.energy/outgoing/.

[147] Octopus Energy. All our tariffs — Octopus Energy, 2021. URL https://octopus.energy/tariffs/.

[148] Octopus Energy. Introducing Octopus Go, 2021. URL https://octopus.energy/go/.

[149] Zap-Map. How Much Does it Cost to Charge an Electric Car? — Vivint Solar, 2022. URL https://www.zap-map.com/tools/public-charging-calculator/.

[150] Pod Point. Cost of Charging an Electric Car — Pod Point, 2021. URL https://pod-point.com/guides/driver/cost-of-charging-electric-car.

[151] Gurobi. How do I improve the time to build my model? – Gurobi Help Center, 2023. URL https://support.gurobi.com/hc/en-us/articles/360013420111-How-do-I-improve-the-time-to-build-my-model-.

[152] Gurobi. General modeling tips to improve a formulation – Gurobi Help Center, 2023. URL https://support.gurobi.com/hc/en-us/articles/13793044538001-General-modeling-tips-to-improve-a-formulation.

[153] Donovan Aguilar-Dominguez, Alan Dunbar, and Solomon Brown. The electricity demand of an EV providing power via vehicle-to-home and its potential impact on the grid with different electricity price tariffs. In *Energy Reports*, volume 6, pages 132–141. Elsevier Ltd, 5 2020. doi: 10.1016/j.egyr.2020.03.007.

[154] Donovan Aguilar-Dominguez, Jude Ejeh, Alan D.F. Dunbar, and Solomon F. Brown. Machine learning approach for electric vehicle availability forecast to provide vehicle-to-home services. *Energy Reports*, 7:71–80, 2021. ISSN 23524847. doi: 10.1016/j.egyr.2021.02.053. URL https://doi.org/10.1016/j.egyr.2021.02.053.

[155] Donovan Aguilar-Dominguez, Jude Ejeh, Solomon Brown, and Alan Dunbar. Exploring the possibility to provide black start services by using vehicle-to-grid. *Energy Reports*, 8:74–82, 11 2022. ISSN 2352-4847. doi: 10.1016/J.EGYR.2022.06.111.

[156] Gurobi. Gurobi - The fastest solver, 2022. URL https://www.gurobi.com/.

[157] William E. Hart, Carl D. Laird, Jean-Paul Watson, David L. Woodruff, Gabriel A. Hackebeil, Bethany L. Nicholson, and John D. Siirola. *Pyomo – Optimization Modeling in Python*. Springer, second edition, 2017.

[158] Quasar. 07/01/2020 Wallbox Quasar — The first bidirectional charger for your home, 2020. URL https://wallbox.com/en_uk/quasar-dc-charger.

[159] Ridoy Das, Yue Wang, Ghanim Putrus, Richard Kotter, Mousa Marzband, Bert Herteleer, and Jos Warmerdam. Multi-objective techno-economic-environmental optimisation of electric vehicle for energy services. *Applied Energy*, 257(September 2019):113965, 2020. ISSN 03062619. doi: 10.1016/j.apenergy.2019.113965. URL https://doi.org/10.1016/j.apenergy.2019.113965.

[160] Abdurahman Yaldız, Tayfur Gökçek, İbrahim Şengör, and Ozan Erdinç. Optimal sizing and economic analysis of Photovoltaic distributed generation with Battery Energy Storage System considering peer-to-peer energy trading. *Sus-*

tainable Energy, Grids and Networks, 28:100540, 12 2021. ISSN 2352-4677. doi: 10.1016/J.SEGAN.2021.100540.

[161] Ni Wang, Ziyi Liu, Petra Heijnen, and Martijn Warnier. A peer-to-peer market mechanism incorporating multi-energy coupling and cooperative behaviors. *Applied Energy*, 311, 2022. ISSN 03062619. doi: 10.1016/j.apenergy.2022.118572.

[162] Rasmus Luthander, Joakim Widén, Daniel Nilsson, and Jenny Palm. Photovoltaic self-consumption in buildings: A review. *Applied Energy*, 142:80–94, 3 2015. ISSN 0306-2619. doi: 10.1016/J.APENERGY.2014.12.028.

[163] S. I. Sun, M. Kiaee, S. Norman, and R. G.A. Wills. Self-sufficiency ratio: an insufficient metric for domestic PV-battery systems? *Energy Procedia*, 151: 150–157, 10 2018. ISSN 1876-6102. doi: 10.1016/J.EGYPRO.2018.09.040.

[164] Yue Zhou, Jianzhong Wu, and Chao Long. Evaluation of peer-to-peer energy sharing mechanisms based on a multiagent simulation framework. *Applied Energy*, 222:993–1022, 7 2018. ISSN 0306-2619. doi: 10.1016/J.APENERGY.2018.02.089.

[165] Gurobi. Mixed-Integer Programming (MIP) – A Primer on the Basics - Gurobi Optimization, 2023. URL https://www.gurobi.com/resources/mixed-integer-programming-mip-a-primer-on-the-basics/.

[166] Gurobi Optimization. MIPGap, 2022. URL https://www.gurobi.com/documentation/9.5/refman/mipgap2.html.

[167] Antoine François, Quentin Cappart, and Louis-Martin Rousseau. How to Evaluate Machine Learning Approaches for Combinatorial Optimization: Application to the Travelling Salesman Problem, 2019. URL https://arxiv.org/abs/1909.13121.

[168] Eaton. Eaton xStorage Home Technical sheet 2019. Technical report, NIssan, 2019.

[169] Tesla. Powerwall — Tesla United Kingdom, 2020. URL https://www.tesla.com/en_gb/powerwall.

[170] EV Database. Nissan Leaf price and specifications - EV Database, 2021. URL https://ev-database.uk/car/1106/Nissan-Leaf.

[171] Matthias Miltenberger and Gurobi. Why does Gurobi perform differently on different machines? – Gurobi Help Center, 2022. URL https://support.gurobi.com/hc/en-us/articles/360045849232-Why-does-Gurobi-perform-differently-on-different-machines-.

[172] Bidan Zhang, Yang Du, Eng Gee Lim, Lin Jiang, and Ke Yan. Design and simulation of peer-to-peer energy trading framework with dynamic electricity price. *2019 29th Australasian Universities Power Engineering Conference, AUPEC 2019*, 11 2019. doi: 10.1109/AUPEC48547.2019.211948.

[173] Esteban A. Soto, Lisa B. Bosman, Ebisa Wollega, and Walter D. Leon-Salas. Peer-to-peer energy trading: A review of the literature. *Applied Energy*, 283: 116268, 2 2021. ISSN 0306-2619. doi: 10.1016/J.APENERGY.2020.116268.

[174] National Grid ESO. Short term operating reserve (STOR) — National Grid ESO, 2022. URL https://www.nationalgrideso.com/electricity-transmission/industry-information/balancing-services/reserve-services/short-term-operating-reserve.

[175] C. Weiller and A. Neely. Using electric vehicles for energy services: Industry perspectives. *Energy*, 77:194–200, 12 2014. ISSN 0360-5442. doi: 10.1016/J.ENERGY.2014.06.066.

[176] National Grid ESO. Demand Side Flexibility Annual Report 2019. Technical report, National Grid ESO, 2019. URL www.powerresponsive.com.